



**Design, Synthesis and Evaluation
of
Natural Product-Based Compound Collections**

Zur Erlangung des akademischen Grades eines
Doktors der Naturwissenschaften
(Dr. rer. nat.)
von der Fakultät Chemie
an der Technischen Universität Dortmund
angenommene

Dissertation

von
Diplom-Chemiker
Tobias J. Zimmermann
aus Riedlingen/Württemberg

Dekan: Prof. Dr. Heinz Rehage

1. Gutachter: Prof. Dr. Herbert Waldmann

2. Gutachter: Prof. Dr. Willem van Otterlo

Die vorliegende Arbeit entstand im Zeitraum von Juli 2008 bis Februar 2012 unter Anleitung von Prof. Dr. Herbert Waldmann an der Fakultät Chemie der Technischen Universität Dortmund und dem Max-Planck-Institut für molekulare Physiologie, Dortmund.

*Dedicated to Inga,
my family and friends for their support.*

“Science cannot solve the ultimate mystery of nature. And that is because, in the last analysis, we ourselves are a part of the mystery that we are trying to solve.”

Max Planck

Table of Contents

I	General Introduction.....	1
II	Theoretical Background	3
1	Biology-Oriented Synthesis (BIOS).....	3
1.1	Natural Products	3
1.2	Starting Points for BIOS in Chemical Space.....	5
1.3	BIOS of Compound Libraries.....	7
III	Tetrahydroisoquinolines (THIQs).....	11
1	Introduction.....	13
1.1	Tetrahydroisoquinolines (THIQs) in Nature.....	13
1.2	Noscapine Alkaloids	14
1.3	Microtubule Inhibition	17
2	Aims	20
3	Results and Discussion.....	22
3.1	Library Synthesis.....	22
3.2	Enantioselective Synthesis.....	31
3.3	Microtubule Inhibition	39
4	Summary and Conclusion.....	47
IV	Small Molecule Microarrays	49
1	Introduction.....	51
1.1	Small Molecule Microarray Technology	51
1.2	Glass Slide Preparation.....	53

Table of Contents

1.3	Gold Chip Preparation.....	55
1.4	Targeting Ras-Depalmitoylation	56
2	Aims	61
3	Results and Discussion.....	63
3.1	Array Validation and Optimization	63
3.2	Screening of NPDepo.....	66
3.3	Boron Compounds as APT1 and 2 Inhibitors.....	70
3.4	Identification of LYPLAL1 Inhibitors.....	81
4	Summary and Conclusion.....	86
V	Experimental Section	89
1	Assay Procedures.....	89
1.1	Enzymatic Assay Protocol for APT1 and APT2	89
1.2	Enzymatic Assay for LYPLAL1	92
2	Microarrays on Glass Slides	95
2.1	Preparation of Photo-Crosslinked Chemical Arrays.....	95
2.2	Screening of Microarray Slides.....	96
3	SPR Imaging	99
3.1	Preparation of Photo-Crosslinked Chemical Arrays.....	99
3.2	SPR Measurement.....	99
4	Immobilization of Small Molecules on Chemical Beads.....	99
5	Synthetic Procedures.....	101

Table of Contents

5.1	General	101
5.2	Synthesis	101
6	Tetrahydroisoquinoline Compound Library.....	166
VI	References.....	167
VII	Summary.....	179
VIII	Zusammenfassung.....	185
IX	Appendix	191
X	Curriculum Vitae.....	201

ACKNOWLEDGEMENTS

First of all I would like to express my sincere gratitude to Prof. Dr. Herbert Waldmann for his motivating supervision, helpful discussions, inspiring ideas and excellent guidance under a balanced mix of supervision and independence during this research work. I am very thankful for the opportunity to be part of the RIKEN - Max Planck Joint Research Center and therefore spent three challenging and very productive months in Japan. I also wish to express my gratitude to Dr. Christian Hedberg for various discussions, valuable input regarding all chemistry related questions and careful reading of my thesis.

I am most grateful to Prof. Dr. Willem van Otterlo for helpful advice, various suggestions, support for the tetrahydroisoquinoline project and his readiness to read and evaluate this thesis. Thank you for being part of my PhD committee.

In addition I want to thank Dr. Monika Wyszogrodzka for being part of my PhD defense.

I would like to acknowledge the people with whom I collaborated: Marco Bürger and Dr. Ingrid Vetter for a very fruitful collaboration on the structural biology aspects of the acyl protein thioesterases and related proteins (e.g. LYPLAL1) as well as Arthur T. Porfetye for his work on yeast APT1; Nancy E. Martinez for the smooth teamwork during the iterative cycles of synthesis and biological evaluation within the NET inhibition project; Dr. Sayantani Roy and Dr. Slava Ziegler for their work in the microtubule inhibition project; Dr. Marion Rusch and Dr. Robin Bon for their contribution to the APT1 project.

My time at the RIKEN Advanced Science Institute in Wako, Japan, was a very inspiring time that tremendously broadened my horizon. I want to especially thank Dr. Slava Ziegler who coordinated the exchange on behalf of the MPI and Prof. Dr. Hiroyuki Osada for being such a great host. I am grateful to Dr. Nobumoto Watanabe, Dr. Yasumitsu Kondoh, Motoko Uchida and Kaori Honda for their support and the nice working environment.

I would also like to thank the IMPRS-team; Christa Hornemann, Dr. Waltraud Hofmann-Goody and Prof. Dr. Martin Engelhard. It has been great to be part of the IMPRS. Many thanks for the financial support and all the encouragement. Further I want to acknowledge the financial support by the Fonds der Chemischen Industrie for a Kekulé PhD scholarship.

Thanks to the analytic team, Dr. Petra Janning, Andreas Brockmeyer, Evelyne Merten and Chantale Sevenich for all MS measurements.

Finally I would like to thank all colleagues of the chemical biology department for providing a nice working atmosphere. In particular I want to thank my past and present labmates of A3.11 that always made the lab a fun place to work: Dr. Sebastian Koch, Dr. Luc Eberhard, Nancy E. Martinez, Peter Schröder, Melanie Schwalfenberg and Federica Rosi.

Ac	Acetyl
ADIFAB	Acrylo Dated Intestinal Fatty Acid Binding Protein
APT1	Acyl Protein Thioesterase 1
APT2	Acyl Protein Thioesterase 2
aq.	aqueous
ar.	aromatic
Asp	Aspartate
BLAST	Basic Local Alignment Search Tool
Bn	Benzyl
Boc	<i>tert</i> -Butyl carboxycarbonyl
br	broad (NMR)
b.p.	boiling point
Bu	Butyl
c	concentration
CLL	Chronic Lymphocytic Leukemia
cpd	compound
δ	chemical shift in ppm (NMR)
d	doublet (NMR)
Da	Dalton
DALI	program for protein structure comparison
DAPI	4',6-Diamidino-2-phenylindole
DCM	Dichloromethane
DIBAL-H	Diisobutylaluminium hydride
DiFMU	6,8-Difluoro-4-methylumbelliferol
DiFMUA	6,8-Difluoro-4-methylumbelliferol acetate
DiFMUO	6,8-Difluoro-4-methylumbelliferyl octanoate
DIPEA	<i>N,N</i> -Diisopropylethylamine
DMAP	4-Dimethylaminopyridine
DMF	<i>N,N</i> -Dimethylformamide
DMSO	Dimethylsulfoxide
<i>ee</i>	enantiomeric excess
equiv	equivalent
ESI	Electrospray Ionization
Et	Ethyl
<i>et al.</i>	et alia (and others)
Et ₂ O	diethyl ether

EtOAc	Ethyl acetate
FITC	Fluorescein Isothiocyanate
g	gram(s)
GDP	Guanosine 5'-diphosphate
GTP	Guanosine 5'-triphosphate
GTPase	Guanosine 5'-triphosphatase
h	hour(s)
His	Histidine
HPLC	High Performance Liquid Chromatography
HRMS	High Resolution Mass Spectrometry
Hz	Hertz
IC ₅₀	half maximal inhibitory concentration
<i>J</i>	coupling constant
K _m	Michaelis-Menten constant
L	Liter(s)
LYPLAL1	Lysophospholipase-like 1
m	multiplet (NMR)
<i>m</i>	meta
Me	Methyl
MeCN	acetonitrile
MeOH	Methanol
m.p.	melting point
mg	milligram
m/z	mass to charge ratio (MS)
N	Normal (molar equivalents per liter)
<i>n</i> -BuLi	<i>n</i> -Butyllithium
n.d.	not determined
nM	nanomolar [concentration]
NMR	Nuclear magnetic resonance
<i>o</i>	ortho
OTf	triflate
<i>p</i>	para
PAMPA	Parallel Artificial Membrane Permeability Assay
PEG	Polyethylene Glycol
Ph	Phenyl
PNP	<i>p</i> -Nitrophenol

PNPA	<i>p</i> -Nitrophenyl acetate
PNPO	<i>p</i> -Nitrophenyl octanoate
PPT1	Palmitoylthioesterase 1
PSSC	Protein Structure Similarity Clustering
Pyr	Pyridine
q	quartet (NMR)
Ras	Rat sarcoma
R _f	Retention factor (TLC)
RT	Room Temperature (ca. 23 °C)
s	singlet (NMR)
Ser	Serine
t	triplet (NMR)
TBAF	Tetrabutylammonium fluoride
THF	Tetrahydrofuran
TIPS	Triisopropylsilyl
TLC	Thin Layer Chromatography
TMS	Trimethylsilyl
Ts	<i>p</i> -Toluenesulfonyl
Triflate	Trifluoromethane sulfonate
UV	Ultraviolet
V _{max}	maximum velocity

I General Introduction

Chemical space comprehends all theoretically possible small molecules, including those in biological systems. This space is huge, therefore, as of now only a tiny part of it has been explored. Yet, these explorations have greatly enhanced our understanding of biology, and have led to the development of many of today's drugs. The discovery of new bioactive molecules, facilitated by a deeper understanding of the nature of the regions of chemical space with relevance to biology, will advance our knowledge of biological processes and is thus likely to lead towards new strategies for the treatment of diseases.¹

Natural products however, constitute only a small fraction of the available chemical space; they are defined chemical entities that often display biological activity. During evolution, only a small fraction of available chemical space was explored by nature. The same applies to the targets of those natural products, mainly being polymers of simple chemical moieties such as amino acids and nucleic acids. Structural matching between protein binding site and ligand is a prerequisite for high-affinity interactions, thus the structural space of both proteins and their ligands has to be highly complementary. The fraction of chemical space used by natural products is possibly not the only region compatible with protein structural space, but the number and size of such regions within chemical space is likely to be limited. Therefore, space used by natural products is preferably enriched with bioactive structures and thus contains promising structural starting points in the search for bioactive entities aimed at the development of novel drugs.²

In chemical biology research, cell-permeable and selective small molecules – commonly referred to as chemical probes – are used to perturb protein function rapidly, reversibly and conditionally with temporal and quantitative control in the biological system of interest. By analysing these perturbations, conclusions about the studied biological system can be drawn.³ However, this powerful approach relies on the accessibility of appropriate small molecules that can be employed as chemical probes. On the venture for such probes, chemists often resort to systematic screenings of small molecule compound libraries that are built up from pure, individual, well-characterized molecules. Consequently, this screening process can only succeed if a high quality compound library with enriched biological activity is used and high-throughput screening technologies are available that allow a rapid, time- and cost-efficient screening and analysis process.⁴

As modern organic chemistry allows the synthesis of vast numbers of synthetic small molecules enormous combinatorial libraries have become accessible. In theory all parts of chemical space or

more precisely the ‘multi-dimensional descriptor space’ – defined as the total descriptor space that encompasses all possible small molecules – are reachable by modern synthetic techniques.¹ However, the success rate of such libraries derived from ‘random’ synthesis in biological screens turned out to be rather low as only a subfraction of chemical space is biologically relevant.⁵ Concepts focusing chemical synthesis on the biologically relevant areas in drug-like chemical space are of utmost interest for both academic and industrial research. Biology-oriented synthesis (BIOS) deals with this critical point and constitutes a theoretical concept for the design of small molecules on the basis of biologically relevant and prevalidated starting points in drug-like chemical space.⁴

In order to advance chemical biology research, not only the generation of biologically active molecules, but also the development of state of the art screening techniques is essential. Small molecule microarray technology constitutes a rapid ultra-high throughput screening technique in order to investigate small molecule protein interactions. Small molecules are immobilized on the surface of glass slides employing a concept of functional group independent immobilization by UV-triggered carbene insertion. Such glass arrays comprehend thousands of small molecules that simultaneously can be incubated with the protein of interest. After successive washing steps, compound-bound protein is visualized and thus reveals high affinity protein-small molecule interplay. Many successful examples of functional protein inhibitors highlight the potential of this inexpensive, time-efficient screening method.^{6,7}

This thesis is build around these two core paradigms of chemical biology research, namely, generation of biologically relevant small molecules - alkaloids of the class of tetrahydroisoquinolines - and application of small molecule microarray screening technology in order to identify modulators of pharmaceutically significant target proteins.

II Theoretical Background

1 Biology-Oriented Synthesis (BIOS)

1.1 *Natural Products*

Natural products have been a source of medicinal agents since ancient times in the treatment of diseases and pathological states and continue to be an abundant source of novel chemotypes and pharmacophores.^{8,9} From 2600 B.C. on, in Mesopotamia for example, oils of the cedar *Cedrus* species and the cypress *Cupressus sempervirens* were used, and are still used today, against a wide range of malaises as colds, parasitic infections and inflammation. Also the Egyptian, Chinese and Indian cultures helped to develop the medicinal treatments with the use of natural products in the B.C. era.¹⁰ In the ancient Western world, the Greeks contributed substantially to the rational development of the use of herbal drugs (~300 B.C.). During the Middle Ages, monasteries in countries like England, Ireland, France, and Germany preserved the remnants of this Western knowledge. At that time, the Arabs took over responsibility for the preservation of much of the Greco-Roman expertise, as well as for expanding it to include the use of their own resources, together with Chinese and Indian herbs.⁹ An important date for the development of modern medicine was the isolation of morphine (**1**) by Friedrich Sertürner.¹¹ Being the most abundant alkaloid in opium – the dried latex from the opium poppy *Papaver somniferum* - **1** was the first active ingredient purified from a plant source. Morphine (**1**) acts directly on the central nervous system (CNS) to relieve pain and is used in clinical medicine as benchmark for analgesics used to relieve pain. In 1827, **1** was first commercially sold by Merck. From that time on, the development of pharmaceutical drugs obtained from natural sources gained increasing importance.

Still today, many therapeutically useful compounds are based on natural products. Considering new chemical entities (NCE) approval, roughly about 50% of all small molecules over the last 30 years are related to natural products. This fact highlights the continuing role that natural products and structures derived from or related to natural products from all sources have played and continue to play in the development of the current therapeutic armamentarium of the physician.⁸

Over the years, natural product isolation ventures were not only limited to the plant kingdom but to all kingdoms of life. The alkaloids morphine (**1**) and quinine (**2**) were derived from plant sources, while daunomycin (**3**), mevastatin (**4**) and the macrolide zearalenone (**5**) were obtained from fungal and discodermolide (**6**) from marine sources (**Figure 1**).

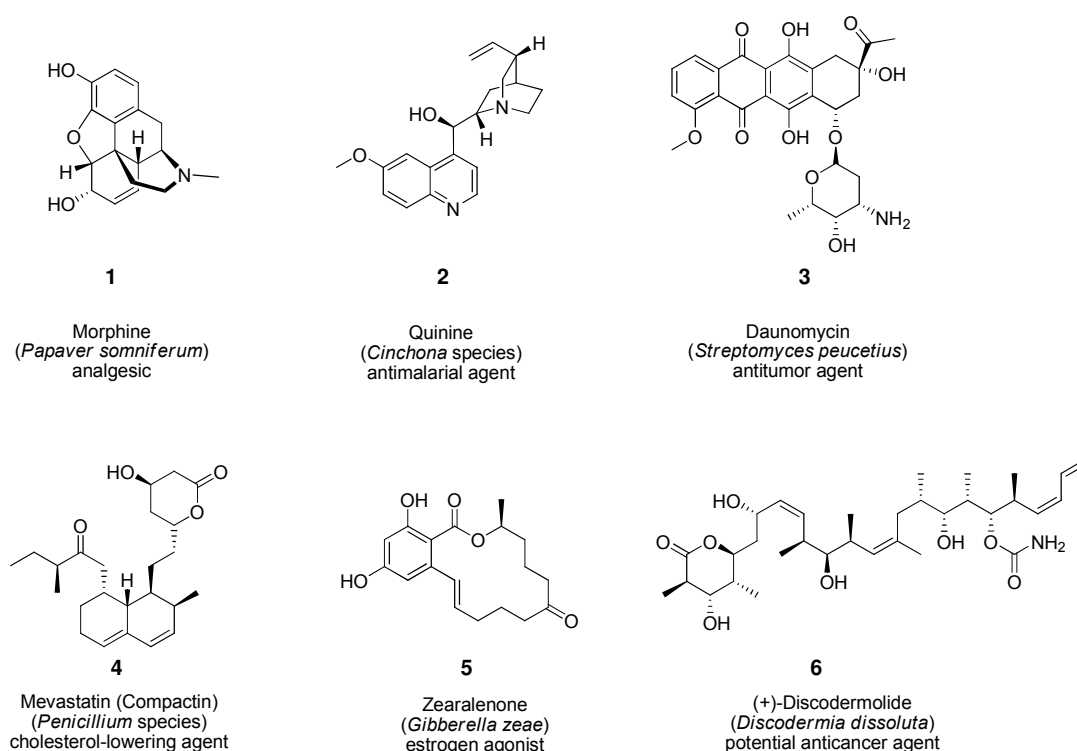


Figure 1: Examples of natural product structures, their origin and biological activities.

The quinoline alkaloid quinine (**2**) was isolated from the bark of *Cinchona* species in 1820 by the French pharmacists Caventou and Pelletier. They knew that the bark of these trees had been used for a long time in the Amazon region, especially for the treatment of fever. This usage found by indigenous groups was brought to Europe and it remained the antimalarial drug of choice until the 1940s.¹² According to tradition, the bitter taste of anti-malarial quinine led British colonials in India to mix it with gin, thereby creating the up to now very popular “gin & tonic” cocktail. The DNA intercalating agent daunomycin (**3**), extracted from *Streptomyces peucetius*, consists of a pigmented aglycone (daunomycinone) in glycoside linkage with an amino sugar (daunosamine) and is most commonly used to treat specific types of leukaemia.¹³ From the fungal source *Penicillium* species mevastatin (**4**), also known as compactin, was isolated and later on showed cholesterol-lowering properties.¹² Lastly, the classical benzolactone, the fungal metabolite zearalenone (**5**) was first isolated from the fungus *Gibberella zeae* in 1962 and reported having anabolic, estrogenic and antibacterial effects.¹⁴ It has been used to treat postmenopausal symptoms in women and was patented as oral contraceptive.¹⁵

Marine natural products provide a rich source of bioactivity that became gradually more available with the development of reliable diving technology within the last 40 years.¹⁶ Among these compounds discodermolide (**6**), isolated from the Caribbean sponge *Discodermia dissoluta*, exerted potent inhibition of tumour growth and has been the target of various total syntheses.^{17,18}

1.2 Starting Points for BIOS in Chemical Space

Natural product structures rise from the evolutionary generation of secondary metabolites that provides advantages for survival of the producing organisms. Surprisingly, only a very small fraction of the total possible number of small carbon-based compounds in chemical space has been generated by biosynthesis. Interestingly, this observation is also true for the protein targets of natural products. During evolution, out of all possible amino acid sequences in 'protein-space', nature has chosen only a minute fraction.¹⁹ Hence, the natural product space and the protein structure space utilized by nature are limited in size. In order to identify small molecules that bind to their protein target, the space defined by the proteins' ligand sensing cores and their ligands should be complementary. In the concept of biology-oriented synthesis (BIOS), natural product scaffolds encoding various biological activities are selected as biologically prevalidated starting points in chemical space for the development of small focused libraries with limited diversity. As a conceptually alternative approach to other library design concepts such as diversity-oriented synthesis (DOS),²⁰ BIOS allows to elucidate prior unknown links between the protein world and natural products such as predicted target proteins of a natural product-based library by bio- and cheminformatic methods.^{2,4,21-23}

By introducing a hierarchical classification, Waldmann and co-workers developed a suitable tool to visualize the chemical space populated by natural products, their scaffolds, cyclic frameworks and linkers. As most small molecule inhibitors and drugs are based on ring-systems, the focus of the structural classification of natural products (SCONP) was set on molecules containing cyclic structures. The resulting rigidification of the molecule backbone results in enhanced target affinity due to less entropy loss upon binding. Hence, scaffolds based on rings, linker chains and ring-based double bonds were isolated, following a set of defined rules from organic and medicinal chemistry to step-wise deconstruct the underlying natural product framework into smaller structures. This reductionistic approach resulted in a scaffold tree, in which each scaffold in the hierarchy represents a well defined chemical entity and substructure of the original natural product. Consequently, the scaffold tree allows relating more complex scaffolds to simpler frameworks and offers a tool to reduce molecular complexity from multiple annulated rings at the outer rims of the scaffold tree to monocyclic systems of the inner circle of the scaffold. The tree gives the possibility to categorize structural diversity in an intuitive and chemically meaningful way (**Figure 2**).^{4,24,25}

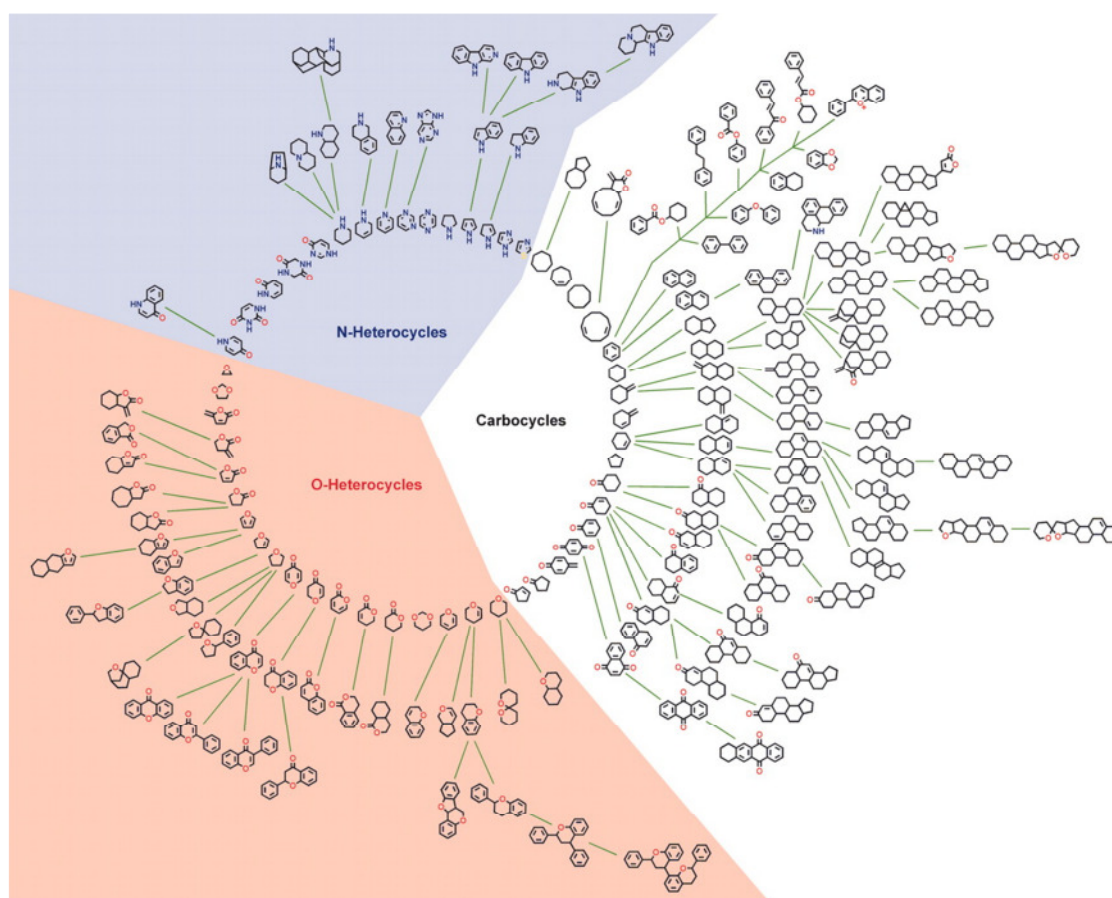


Figure 2: A scaffold tree generated in the structural classification of natural products (SCONP), where only scaffolds that represent at least 0.2% of the natural products described in the Dictionary of Natural Products (DNP) database have been sketched. Figure reproduced from the literature.⁴

The scaffold tree (**Figure 2**) can be classified in three classes – nitrogen heterocycles, carbocycles and oxygen heterocycles of which two to four ring systems are most common. The significance of the natural product tree lies on the one hand in its descriptive representation of biologically relevant scaffolds for the design of focused compound collections and on the other hand in the possibility of correlating different scaffold classes as performed during BIOS. Recently extensions for the identification of biologically relevant starting points in chemical space have been reported by scaffold tree generation using bioactivity data together with a process called ‘brachiation’ as intuitive guiding criteria for hierarchical scaffold selection. In analogy to the locomotion of primates along branches in trees, ‘brachiation’ describes moving from complex to simpler, but still similar, structures along lines of biological relevance.^{26,27} A program called Scaffold Hunter facilitates the complex cheminformatic analysis. It reads compound structures, bioactivity data and generates compound scaffolds, correlates them in a hierarchical tree-like arrangement, and annotates them with bioactivity.²⁶

According to the BIOS-concept, a given biologically active compound does not have to be resembled in detail to exert the same biological effect. Moreover only the underlying core scaffold has to be retained while the necessary substitution pattern and stereochemistry can be evolved using structure-activity studies. Various studies have shown the potential of this concept.^{4,21,28}

In analogy to the SCONP concept, that facilitates chemical space navigation, also protein space can be analysed in a similar fashion. During evolution only a limited set of amino acid sequences and protein folds have emerged, thus these structures containing binding sites or 'ligand-sensing cores' can be regarded as prevalidated by nature. A concept called Protein Structure Similarity Clustering (PSSC)^{21,25,29,30} allows to group proteins according to their ligand-sensing core topology. Enzymes are grouped into the same PSSC if they share structural similarity in the ligand-sensing core part of the overall domain. Proteins sharing structural similarity despite low sequence identity are therefore of special interest. If a ligand for one member of the cluster is known, the scaffold of this ligand can then be expected to be a prevalidated starting point for the synthesis of ligands for the other members of the protein cluster. Consequently, members of a library of synthesised derivatives based on the scaffold should target several members of the protein cluster. This concept has proven successful in many cases.³¹⁻³³

1.3 BIOS of Compound Libraries

The BIOS approach facilitates hit generation in two ways. On the one hand, it provides scaffolds prone to bind to the target protein and structurally simpler relatives as a starting point for small molecule compound collections. On the other hand, side chain diversity is the key to increase the probability of finding hits by matching the distinct interaction pattern of the target selectively. As protein binding pockets are shaped by the individual side chains of the amino acids, library synthesis of an identified scaffold is necessary for optimization of the distinct binding site. In the case of two nearly identical binding-sites with similar fold, one with negative charge and the other one with positive charge, a suitable small molecule inhibitor has to be adapted complementarily. Consequently the scaffold with the positively charged side chain would target the protein with a negatively charged pocket. This example highlights the importance of sufficient chemical diversity to match biological diversity on the search for potent protein ligands. In addition, BIOS can be used to generate target clusters that can be used to identify cross-inhibition and selectivity profiles from a very early stage on. Taking the BIOS approach as guideline and the SCONP tree as map of chemical space, the synthesis of focused libraries has yielded several successful inhibitors.⁴

As an example, polyketide-based natural products exert various biological activities. In order to extend chemical diversity available for polyketide synthesis, Maier and co-workers chose a

framework inspired by the classical benzolactone zearalenone (**5**) for a systematic replacement of the acetate building blocks during synthesis by propionate moieties (**Figure 3**). The so-called 'propionate scanning'³⁴ is a synthetic concept using biology-oriented synthesis for library design. The general idea of this concept is the use of a propionate building block instead of an acetate in polyacetate-based natural products. Propionate is thus incorporated in all possible (reasonable) positions. Due to the fact that acetate/propionate-polyketides are biologically validated, propionate scanning should lead to highly active natural product analogues. The additional hydrophobic methyl group reduces the conformational flexibility of the macrolactone and could for example detect hydrophobic holes within the binding domain. Both effects could increase binding affinity and selectivity. Indeed the concept of propionate scanning led to several new inhibitors with increased potency in comparison with the underlying zearalenone (**5**) core scaffold. The monopropionate analogue **7** turned out to be a quite potent ($IC_{50} = 210$ nM) and selective inhibitor of human carbonyl reductase 1 (CBR1).³⁴ CBR enzymes play a critical role in cancer therapy as CBR1 is involved in the metabolism of xenobiotics. Doxorubicin, a hydroxyl derivative of daunomycin (**3**), is a common chemotherapeutic DNA-interacting drug used to treat solid and hematopoietic tumors. Serious side effects include cardiac injury and chronic congestive heart failure. As CBR1 has been identified to catalyse the reduction of doxorubicin to the cardiotoxic metabolite doxorubicinol, CBR1 inhibition might constitute a promising means of ameliorating the side effects of doxorubicin in patients undergoing chemotherapy. Further studies indicate CBR1 inhibitors may enhance the effectiveness of anticancer anthracyclines by inhibiting metabolism.^{35,36} The potential of the propionate scanning approach is further highlighted by the two monopropionate analogues **8** and **9** that targeted Hsp90 with higher affinity than the classical inhibitor geldanamycin.^{37,38} Though it has to be pointed out that this concept is not suitable for the generation of large compound libraries as basically every product of the propionate scan has to be synthesised separately by means of total synthesis (**Figure 3**).

Over the years, Waldmann and co-workers have developed various BIOS examples - a few selected cases are shown in **Figure 3**. On the venture for phosphatase inhibitors, the screening of more than 300 chemically diverse natural products yielded yohimbine and ajmalicine – two structurally complex pentacyclic alkaloids – as moderate Cdc25A phosphatase inhibitors. SCONP analysis and brachiation along the line of pre-validation by nature led to the tetracyclic indolo[2,3-a]-quinolizidine, a scaffold frequently occurring in nature, e.g. in the antiviral natural product hirsutine (**10**). Library syntheses with focused diversity around the indoloquinolizidine scaffold yielded two compounds with IC_{50} values comparable with the corresponding natural product. By extending the screen to other phosphatases, structurally new inhibitors of the *Mycobacterium tuberculosis* phosphatase MtpB (**11**) could be identified.³⁹

Further MtpB inhibitors were found using the ajmaline (**12**) macroline framework as lead scaffold. Ajmaline (**12**), isolated from *Rauwolfia serpentine*, is an antiarrhythmic agent with the trade name Gilurytma[®]. In a focused library consisting of 100 compounds several new inhibitors of the *Mycobacterium tuberculosis* phosphatase MtpB were obtained (**13**).⁴⁰

Among the carbocycles a decalin-type core structure and quinoid or related aromatic side chain often are characterized by manifold biological properties. Based on the natural product and kinase inhibitor nakijiquinone A (**14**) a relatively small library of various decalines was synthesised leading to the identification of potent IGF1R, Tie-2, and VEGFR-3 inhibitors (**15**).^{41,42}

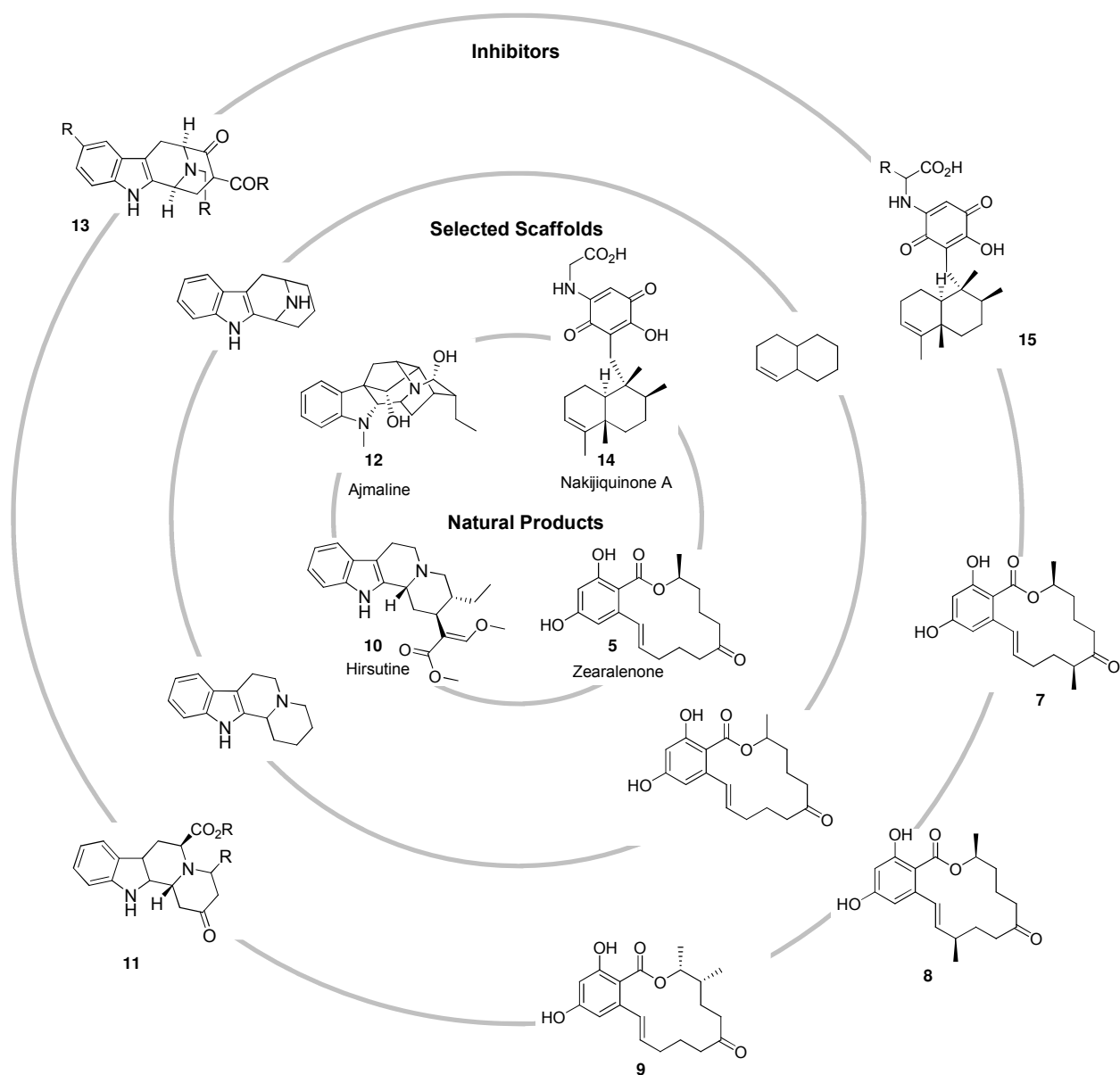


Figure 3: From natural products *via* SCONP and BIOS to focused libraries with high activity hit rates. The inner circle depicts the starting structure of the natural products, the middle circle their underlying scaffold, and the outer circle structures of biologically active small molecules identified from BIOS compound libraries generated on the basis of these scaffolds.

III Tetrahydroisoquinolines (THIQs)



1 Introduction

1.1 *Tetrahydroisoquinolines (THIQs) in Nature*

As early as 1804, the first known alkaloid and narcotic pain reliever morphine (**1**) was isolated by Friedrich Sertürner and named after the Greek god Morpheus, the creator of sleep and dreams in *Ovid*.^{11,43} The group of alkaloids constitutes an important class of low molecular weight nitrogen-containing natural products found mainly in plants, but also in microorganisms and animals. More than 27,000 different structures have been found, with 21,000 from plants. Alkaloids incorporate one or more nitrogen atoms and this usually confers basicity. Therefore the name alkaloid is in fact derived from alkali. Classification of alkaloids is conducted according to the nature of the nitrogen-containing structure (e.g. quinoline, isoquinoline **16**, tetrahydroisoquinoline **17**), though the structural complexity of some examples rapidly expands the number of subdivisions. The nitrogen atoms in alkaloids originate from an amino acid as well as the carbon skeleton that is also mainly retained intact in the alkaloid structure.⁴⁴ As secondary metabolites, alkaloids are thought to play a defensive role in the plant against herbivores and pathogens. Due to their potent biological activity, various alkaloids have been utilised as pharmaceuticals, stimulants, narcotics and poisons. Plant-derived alkaloids in clinical use involve the analgesics morphine (**1**) and codeine, the anti-neoplastic agent vinblastine (**29**), the gout suppressant colchicine (**30**), the muscle relaxant papaverine, and the sedative scopolamine. Other well known alkaloids of plant origin include caffeine, nicotine, and cocaine, and the synthetic *O*-diacetylated morphine derivative heroin.⁴³

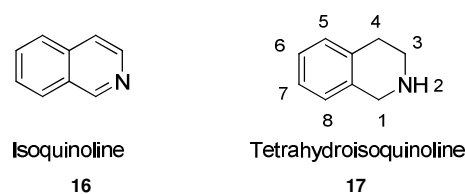


Figure 4: Core structures isoquinoline (**16**) and tetrahydroisoquinoline (**17**).

1,2,3,4-Tetrahydroisoquinolines (THIQs) are part of the isoquinoline alkaloids that constitute the largest group among the alkaloids. Their structural backbone is derived from isoquinoline (**16**) and tetrahydroisoquinoline (**17**). The tetrahydroisoquinoline (THIQ) class of alkaloids is of great interest to the synthetic, medicinal and natural products chemistry community. Due to the interesting biological activities displayed by THIQ-containing molecules many are used in pharmaceutical applications. Natural products with the underlying THIQ core scaffold range from rather simple 1-MeTHIQ (**18**) and carnegine (**19**) to complex structures with THIQs embedded like ecteinascidin 743 (**20**), a THIQ extracted from a marine tunicate.^{45,46} Examples of medically important THIQs

include **20**, which is in several anti-cancer clinical trials and 1-MeTHIQ (**18**), a simple compound with activity against endogenous Parkinson's disease.⁴⁷⁻⁴⁹

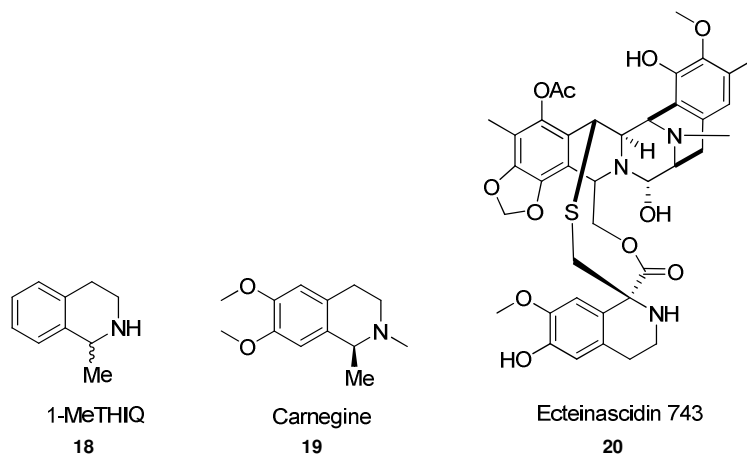


Figure 5: Prominent THIQ examples.

1.2 Noscapine Alkaloids

A prominent member of the THIQ-family is noscapine (**21**), constituting 1-10% of the alkaloid content of opium, and has been used as an oral anti-tussive agent with few side effects in humans.⁵⁰ In the last decade **21** has drawn a lot of interest due to its anti-cancer potential. Noscapine has been shown to bind stoichiometrically to tubulin, thus modulating microtubule polymerisation. It causes growth arrest of tumor cells in mitosis and induces apoptosis of tumor cells *in vivo*. The significant *in vivo* antitumor activity, coupled with its minimal toxicity, is probably derived from the weak interaction between noscapine and tubulin. Noscapine does not bind to tubulin as strongly as colchicine, but its interaction is adequate to arrest mitosis.^{51,50} The brominated analogue EM011 (**22**) is more potent than the natural product noscapine and achieved significant inhibition of hormone-refractory human prostate cancer. Mechanistically, *in vitro* data suggested that the antiproliferative and proapoptotic effects of EM011 (**22**) in human prostate cancer cell lines were through blocking of cell-cycle progression by impairing the formation of a bipolar spindle apparatus. The G2/M arrest was accompanied by activation of the mitotic checkpoint.^{52,53} Therefore, noscapine and its analogues are interesting lead compounds and noscapine is in clinical phase trials.⁵⁴

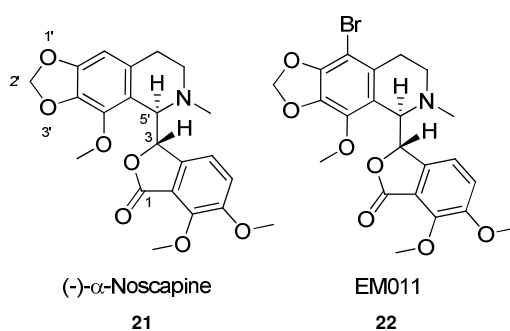


Figure 6: Structures of the natural product noscapine (**21**) and its closely related derivative EM011 (**22**).

Natural noscapine (α - or *erythro*-form) contains two stereogenic carbon centers: C-5' at the THIQ-ring and C-3 at the phthalide framework. Clinically used (-)- α -noscapine is obtained either by plant extraction or resolution of synthetic (\pm)- α -noscapine.⁵⁵ The first total synthesis of (\pm)- α -noscapine by constructing the C5'-C3 bond was already accomplished by Robinson and Perkins in 1911 (**Figure 7**). They could build up on the synthesis of cotarnine (**23**) from myristicine (**24**) by Salway⁵⁶ and obtained **21** via direct potassium carbonate-mediated condensation of cotarnine (**23**) with meconine (**25**), followed by resolution of the two resulting enantiomers.⁵⁷

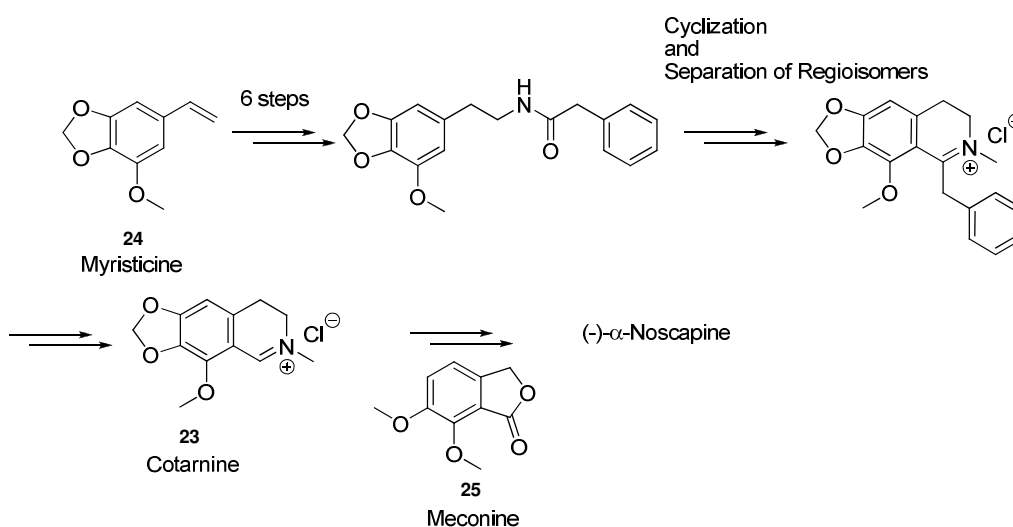


Figure 7: First total synthesis of noscapine by Robinson and Perkins in 1911.⁵⁷

In a recent approach – about 100 years after the first total synthesis – Ni *et al.* reported a blocking group-directed diastereoselective total synthesis of (\pm)- α -noscapine (**Figure 8**). In this synthesis bromine as removable blocking group on C-9' hinders the formation of the undesired regioisomer (C5'-C9' connection) upon Bischler-Napiralski cyclization of precursor **26**, that was synthesised

from amine **27** and meconine-3-carboxylic acid (**28**). In the last step, bromine is removed by reduction (H_2 , Raney Ni-W2).⁵⁵

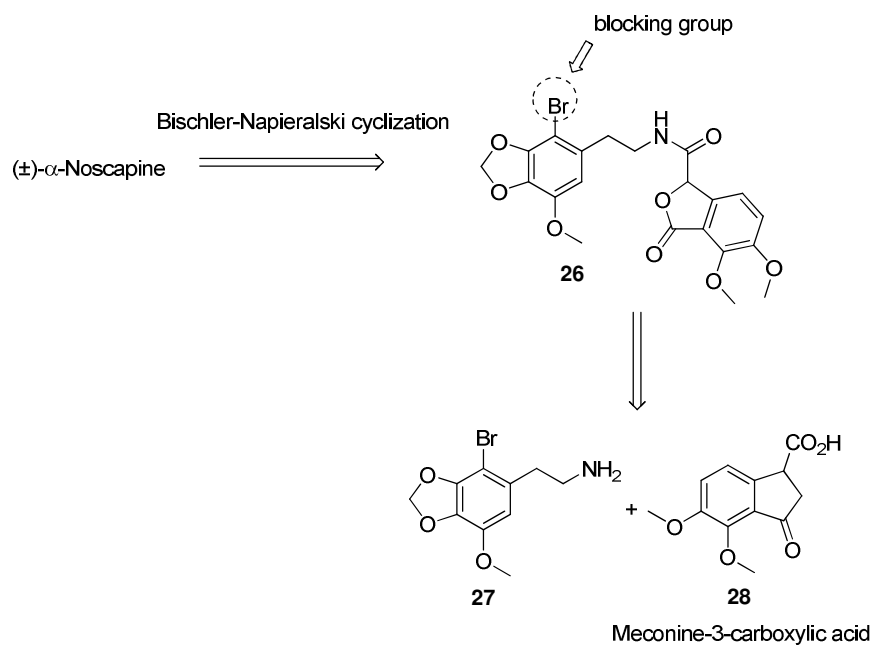


Figure 8: Synthesis of racemic noscapine *via* Bischler-Napieralski cyclization.⁵⁵

1.3 Microtubule Inhibition

Microtubules are dynamic filamentous cytoskeletal proteins composed of tubulin and are an important therapeutic target in tumour cells. Microtubule-binding agents have been part of anticancer therapy for decades and until the advent of targeted therapy, microtubules were the only alternative to DNA as a therapeutic target in cancer. In eukaryotic cells microtubules play key roles in cell proliferation, trafficking, signalling and migration. Along with actin microfilaments and intermediate filaments, microtubules form the cytoskeleton. In mammalian cells microtubules are present both in interphase cells and in dividing cells. In dividing cells, microtubules are highly dynamic and especially sensitive to therapeutic inhibitors. Hence compounds that alter microtubule function have proven to be highly active in patients with cancer.^{58,59}

The biological functions of microtubules in cells are determined and regulated in large part by their polymerisation dynamics. They are formed by the association of α - and β -tubulin heterodimers that are folded and unfolded by chaperones as a heterodimer complex. These heterodimers assemble head-to-tail into linear protofilaments that further polymerise to result in hollow microtubule cylinders.^{59,60}

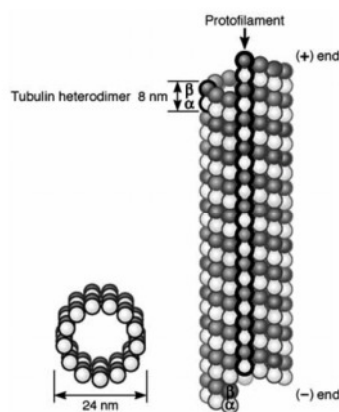


Figure 9: Microtubules are composed of $\alpha\beta$ -tubulin heterodimers that arrange head to tail into protofilaments. 13 protofilaments form a cylinder 24 nm in diameter. The end exposing the β -subunit is termed plus end and the end with the α -subunit exposed is named minus end. Figure reproduced from the literature.⁶⁰

During mitosis the cell's duplicated chromosomes are separated by mitotic spindle microtubules into two identical sets before cleavage of the cell into two daughter cells. The correct movements of the chromosomes and their proper segregation to daughter cells require extremely rapid microtubule-dynamics, rendering mitosis exquisitely sensitive to microtubule-targeting drugs.⁶⁰

Various chemically diverse compounds, generally originating from natural sources, bind to tubulin and/or microtubules, altering microtubule polymerisation and dynamics in diverse ways. Most likely plants and animals evolved these substances that mimic endogenous regulators of microtubule behaviour in order to avoid predation. Altering microtubule dynamics results in the activation of the spindle assembly checkpoint and thus induces a mitotic arrest.⁵⁸ The simplest classification divides these agents into two types: microtubule-destabilizing and -stabilizing agents, according to their effects on microtubule polymer mass at high concentrations. Destabilizing agents inhibit microtubule polymerisation when present at high concentrations and most of these agents bind in one of the two domains of tubulin; either the vinca domain (e.g. vinblastine **29**) or the colchicine (**30**) domain. Microtubule-stabilizing agents (e.g. paclitaxel **31**, discodermolide **6**) enhance microtubule polymerisation at high concentrations and bind to the same or to an overlapping taxoid-binding site on β -tubulin, which is located on the inside surface of the microtubule.^{61,58}

Taxol[®] (paclitaxel **31**) is used to treat several types of cancer (e.g. breast cancer) and was isolated from the bark of *Taxus brevifolia* in 1971. It was known that the bark of *Taxus* species was used by American tribes for the treatment of some noncancerous conditions.⁶² However, despite their clinical success, the efficacy of microtubule binding agents is often limited by the emergence of resistant tumour cells. One of the most studied mechanism is the multidrug resistance (MDR) phenotype that is associated with reduced drug accumulation because of drug efflux.⁶³ Therefore, novel microtubule binding agents are being investigated to offer more effective therapeutic options. One rationale for the continued development of novel agents is the potential of improving drug activity by exploiting the differences in mechanism of action.⁶⁴

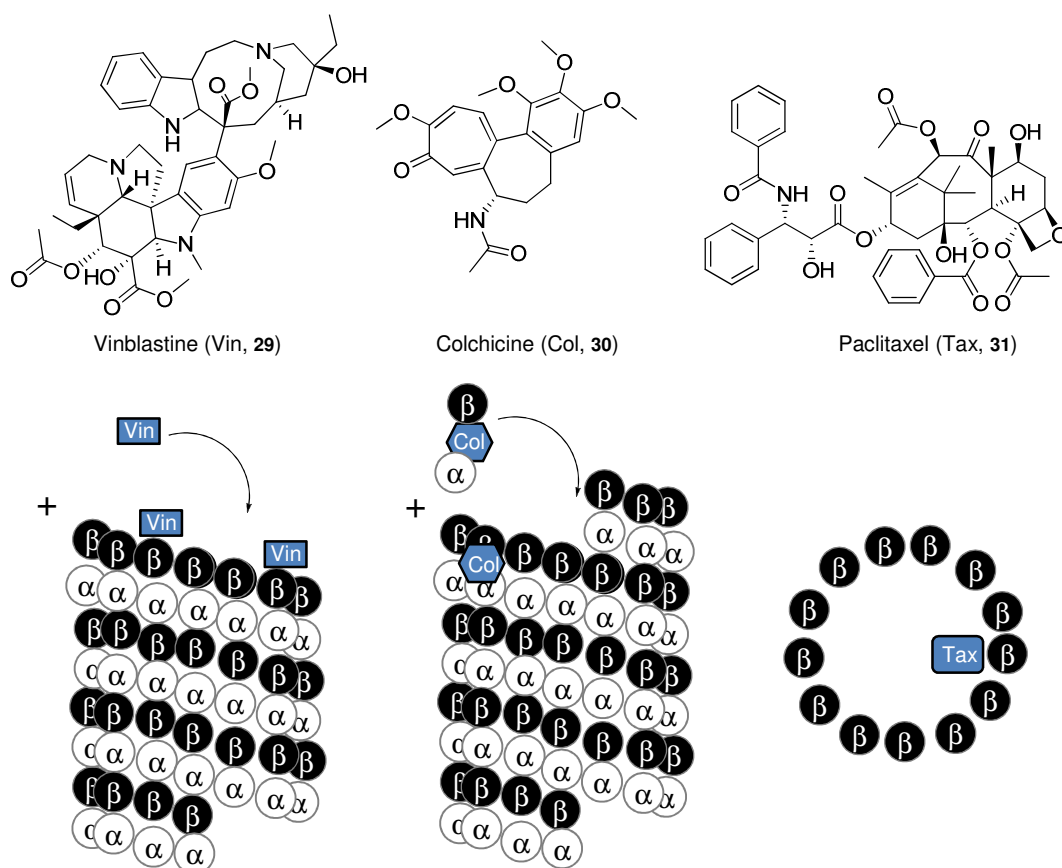


Figure 10: Structures and binding-sites of different microtubule-binders. Vinblastine (29, Vin) binds to the plus end of microtubules. Colchicine (30, Col) binds unpolymerised tubulin at the α/β -tubulin interface near the α -tubulin GTP-binding site and is then incorporated into microtubules. The binding of either 29 or 30 to the microtubule plus-end decreases microtubule dynamics. At higher concentrations, binding of these drugs along the length of microtubules disrupts lateral contacts between protofilaments, resulting in microtubule depolymerisation. Paclitaxel (Tax, 31) binds to the interior lumen of microtubules, resulting in decreased dynamics at low concentrations and microtubule bundling at higher concentrations.^{59,65}

2 Aims

Tetrahydroisoquinolines (THIQs) are an interesting class of compounds enriched with diverse bioactivities. The natural product noscapine (**21**) has shown potent effects in the treatment of cancers by modulating tubulin. Inspired by the underlying THIQ scaffold of the mentioned natural product, a focused library of THIQs was considered for synthesis.

The large group of benzyl isoquinoline alkaloids (e.g. norlaudanosine **32**) feature a benzyl group in α position to the nitrogen as they originate from the amino acid tyrosine. As due to biosynthetic pathways, substitution in the 1-position is quite frequent among tetrahydroisoquinoline natural products (**Figure 11**) and a certain degree of rigidity also seems to be beneficial, an alkyne function should be introduced in this position. This alkynylated THIQ core scaffold could now be decorated on the aromatic positions (R^1), the alkyne (R^2) or the nitrogen (R^3). According to the principles of BIOS, a limited set of compounds should be sufficient to explore chemical space and thereby aid in the detection of biologically active compounds. The library should then be evaluated towards modulating tubulin polymerisation.

Microtubule-binding agents have been part of anticancer therapy for decades and continue to be an important treatment option for various cancer types. Structurally new compounds are therefore of great value.

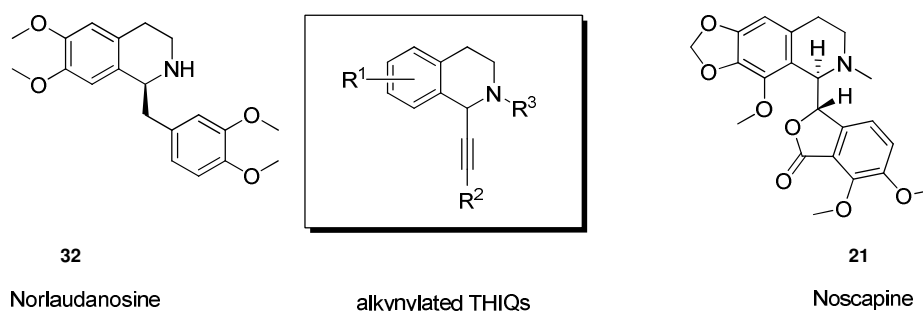


Figure 11: Outline for THIQ library.

More specifically, the library of alkynylated THIQs was outlined to consist of two conceptually different library parts: a *natural product inspired* (A) and *natural product derived* (B) part. In the latter case the cotarnine (**23**) core was chosen as prevalidated THIQ core that could be decorated by alkylation and optional quaternisation. Such compound collections obtained by means of modification of a given scaffold are referred to as *natural product derived*.²² If during synthesis the scaffold is built up, compound collections obtained by means of this approach are referred to as

natural product inspired. In this process different functional groups and substituents are introduced not necessarily at the sites of substitution found in the guiding natural product.²²

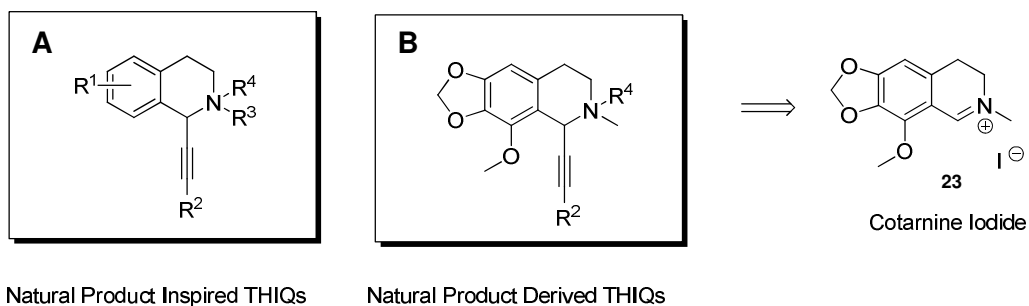


Figure 12: Library of alkynylated THIQs. The library consists of a natural product inspired part (A) and a natural product derived part (B) on the basis of the cotarnine (23) scaffold.

3 Results and Discussion

3.1 Library Synthesis

Readily accessible substituted phenylethylamines (**33**, **34**, **35**) were chosen as starting point. Reaction with ethyl chloroformate yielded the corresponding carbamates (**36**, **37**, **38**) and subsequent dehydrative cyclization (using P_2O_5 , $POCl_3$) led to the substituted 3,4-dihydroisoquinolin-1(2*H*)-ones (**39**, **40**, **41**).^{66,67} Deprotonation of these lactams with base (*n*-BuLi or NaH or DMAP/ Et_3N) and subsequent *N*-acylation with Boc_2O afforded *N*-Boc lactams (**42**, **43**, **44**, **45**) (Figure 13).

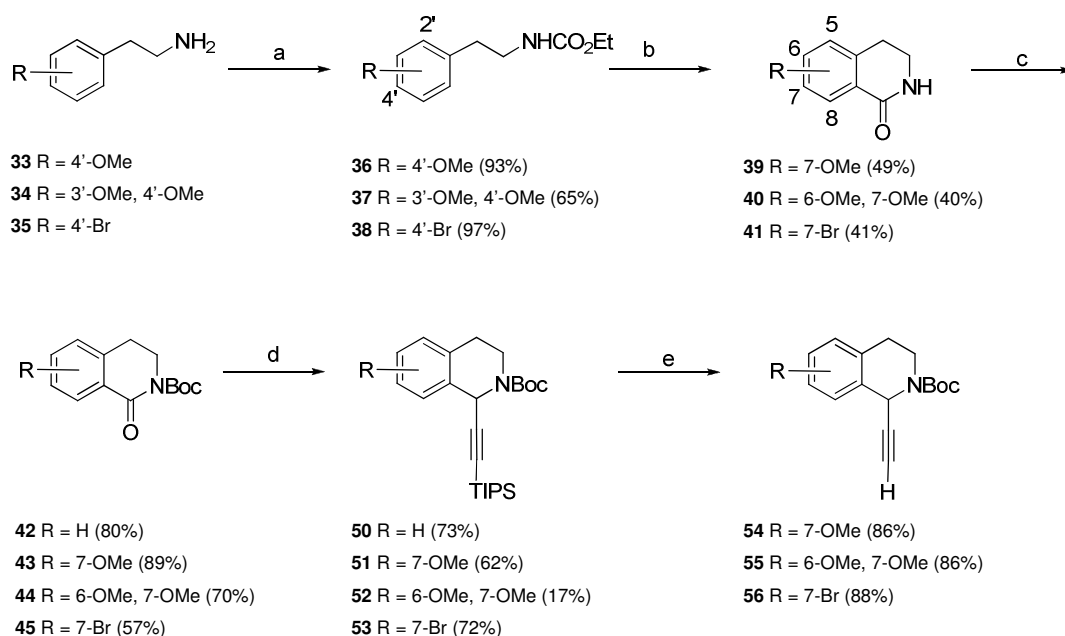


Figure 13: Synthesis of the protected core scaffold. a) ClO_2CET , Et_2O ; b) $P_2O_5/POCl_3$; c) 1. NaH or *n*-BuLi or DMAP/ Et_3N ; 2. Boc_2O ; d) 1. TIPS-acetylene, *n*-BuLi, $BF_3 \cdot Et_2O$, -78 °C, 2. DIBAL-H, e) TBAF, THF, 0 °C.

In 1983 Yamaguchi *et al.* described a one-pot alkylation protocol to access alkynyl azacycloalkanes by the coupling reaction of alkynyl boranes and aliphatic lactams.⁶⁸ Alkynyl boranes were generated *in situ* from lithium acetylide and boron trifluoride etherate in tetrahydrofuran at -78 °C and treated with the corresponding lactam. In all cases, the lactam was used as the *N*-alkylated derivative. The resulting adducts were then reacted with lithium aluminium hydride to afford alkynyl azacycloalkanes.⁶⁸ When adopting this protocol for the alkylation of the simple *N*-methylated aromatic lactam **46**, double alkylation (**47**) and only traces of the desired mono-alkynylated product **48** were observed (Figure 14). Only reducing the equivalents of the alkynyl borane resulted in the single-alkynylated product **48**, though in low yield.

In order to destabilize the proposed intermediate *N*-acyl iminium species (**49**), the methyl group of the lactam was exchanged for the electron withdrawing Boc-group (**42**, **43**, **44**, **45**) (**Figure 13**). Using the above described alkylation protocol and employing DIBAL-H as reducing agent yielded the desired alkynylated tetrahydroisoquinoline core scaffold (**50**, **51**, **52**, **53**). Yields indicated that this reaction strongly depends on the electronic properties of the lactam. While good yields could be obtained for simple (**50**) or moderately activated lactams (**51**, **53**), low yield was obtained for the rather electron rich dimethoxy-substituted lactam (**52**). Finally, TIPS-deprotection with tetrabutyl ammonium fluoride⁶⁹ yielded terminal alkynes (**54**, **55**, **56**), constituting a fundamental scaffold and starting point for further library expansion. Overall this alkylation procedure constitutes an efficient one-pot protocol to access alkynylated tetrahydroisoquinolines; especially secondary THIQs that are rather difficult to access otherwise can be synthesised *via* this route.

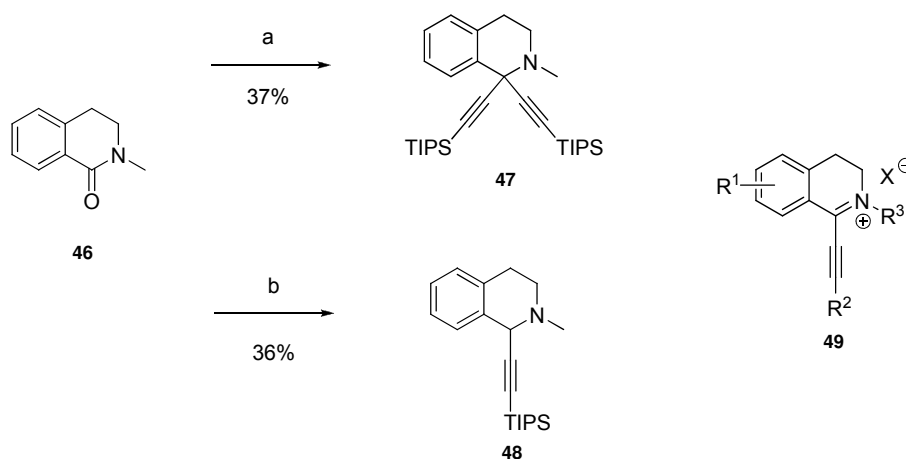


Figure 14: Lactam-alkynylation. a) 1. TIPS-acetylene (3 equiv.), *n*-BuLi, BF₃·Et₂O, -78 °C, 2. LiAlH₄, -78 to -10 °C; b) TIPS-acetylene (1 equiv.), *n*-BuLi, BF₃·Et₂O, -78 °C, 2. LiAlH₄, -78 to -10 °C.

Terminal alkynes open up a wide range of possible reactions for the decoration of the core scaffold and the design of a structurally diverse THIQ library (**Figure 15**). Sonogashira coupling⁷⁰ of terminal alkynes with assorted aryl iodides and subsequent acidolytic Boc deprotection led to secondary amines as the corresponding hydrochlorides (**73-90**). Furthermore, employing a protocol by Maier and co-workers,⁶⁹ Cu(I)-catalysed Huisgen [2+3] cycloaddition⁷¹ of terminal THIQ alkynes with various azides, followed by Boc deprotection afforded different triazoles (**64-72**). Of note is that a range of benzylic and phenylic azides reacted smoothly under these conditions (**Table 2**).

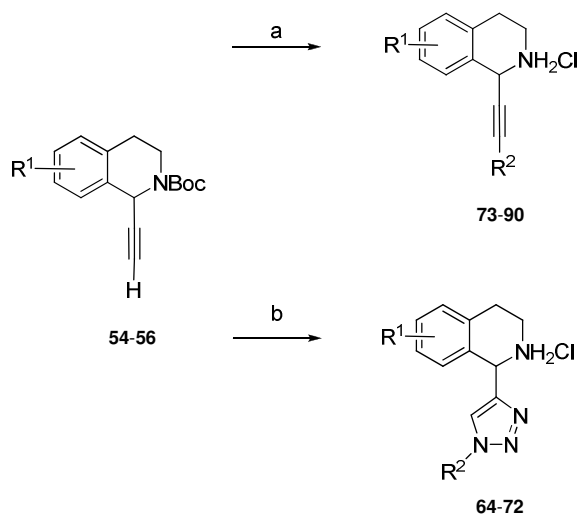


Figure 15: Decoration of terminal alkynes. a) (1) $\text{Pd}(\text{PPh}_3)_4$, CuI , Et_3N , THF , RT , R^1 , (2) HCl/MeOH ; b) (1) CuSO_4 , Na-ascorbate , $\text{EtOH}/\text{H}_2\text{O}$, R^2N_3 , (2) HCl/MeOH .

In general, the reaction of carbanion equivalents with imines constitutes a useful procedure for the formation of carbon-carbon bonds in the α position of a nitrogen atom. Consequently, the base-mediated alkylation of iminium-salts was explored as an alternative access to alkylnated THIQs. The necessary 3,4-dihydroisoquinolines (**57**⁷², **58**, **59**⁷³) were therefore readily accessible from either the corresponding lactam (**39**) or phenylethylamines (**60**, **34**) (**Figure 16**).

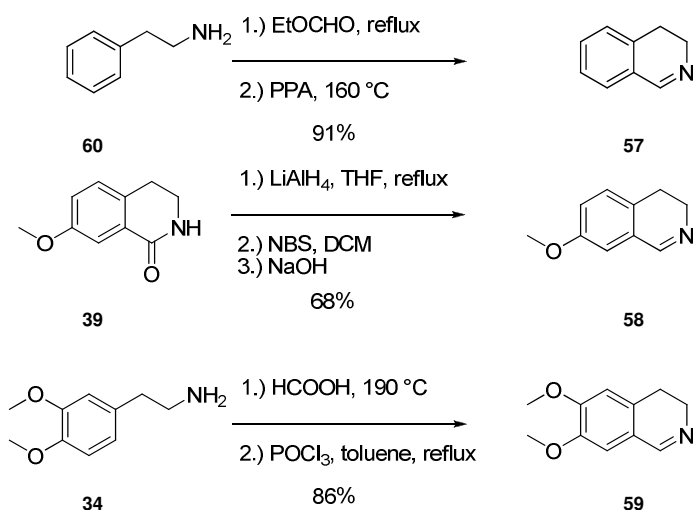


Figure 16: Synthesis of 3,4-dihydroisoquinolines. Reduction of lactam **39**, followed by oxidation resulted in **58**. Bischler-Napieralski cyclization yielded **57**⁷² and **59**⁷³.

In order to alkylnate the 3,4-dihydroisoquinolines in the α position of the nitrogen atom, an activation as iminium salt is necessary. While the use of *N*-methylated iminium salts is described in

literature quite frequently,⁷⁴ reagents that activate the imine by quaternisation and are subsequently readily removable are quite rare. In this respect, trimethylsilyl trifluoromethanesulphonate (TMS-OTf) appeared as optimal choice as it fulfilled these demands. The usefulness of trimethylsilyl triflate as a removable activating group in imine chemistry has initially been demonstrated by Holland and co-workers.⁷⁵

Using TMS-OTf as reagent gave iminium salts as heavy precipitates formed *in situ*. Subsequent alkynylation with acetylides and TMS-group removal upon aqueous work-up satisfyingly yielded alkynylated THIQs (**Figure 17**). This protocol constitutes a versatile alternative to the above described synthetic route *via* Sonogashira coupling. Especially, alkynylated THIQ cores that were challenging to obtain *via* lactam alkynylation could be synthesised more efficiently using the iminium route.

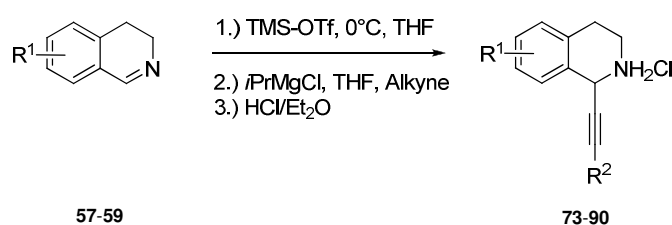


Figure 17: Alkynylation of TMS-iminium salts.

The compound library of alkynylated THIQs should not only consist of library members with secondary amines but also *N*-alkylated derivatives. As mentioned above, *N*-methylated iminium salts are used quite frequently for the installation of C-C bond in the α position of the nitrogen atom. Such *N*-methyl iminium salts were readily formed by refluxing the corresponding imines with methyl iodide to give air stable salts (**61**, **62**, **63**). In addition to the synthesised iminium salts, commercially available cotarnine (**23**) could also be derivatized by means of base-mediated alkynylation, opening access to a diverse set of *N*-methylated alkynylated THIQs with an underlying *natural product inspired* or *natural product derived* core. Further treatment of these tertiary amines with methyl iodide yielded the quaternised THIQs (**Figure 18**).

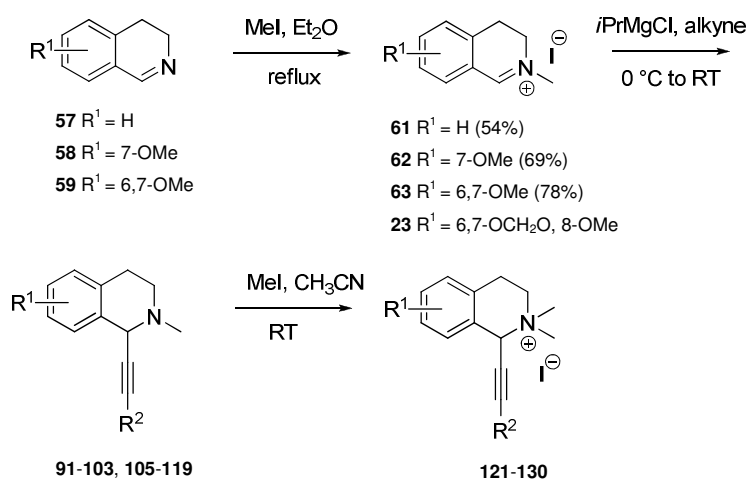
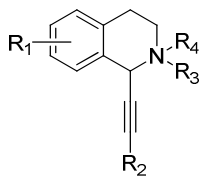


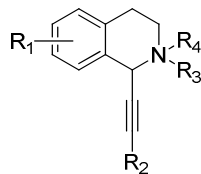
Figure 18: Synthesis of alkynylated *N*-methylated THIQs.

Table 1: Overview of synthesised THIQs via [3+2] cycloaddition. Yields over two steps from alkyne 54 using general procedure XI.

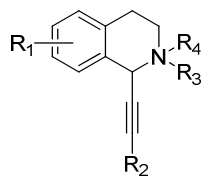
cpd	R	Yield [%]
64	Benzyl	64
65	<i>o</i> -Methoxyphenyl	63
66	<i>m</i> -Methoxyphenyl	54
67	<i>m</i> -Methoxybenzyl	71
68	<i>o</i> -Bromobenzyl	73
69	<i>m</i> -Bromobenzyl	75
70	<i>p</i> -Bromobenzyl	60
71	Pyridine-2-yl-methyl	64
72	(1,3-Benzodioxol-5-yl)methyl	75

Table 2: Overview of synthesised THIQs. ^A Synthesis *via* general procedure V: Sonogashira coupling and Boc-deprotection. ^B Synthesis *via* general procedure VI: alkylation of TMS-iminium salt.

cpd					
	R ¹	R ²	R ³	R ⁴	Yield [%]
73	H	<i>m</i> -Methoxyphenyl	H	H	16 ^B
74	7-OMe	H	H	H	99 ^B
75	7-OMe	Phenyl	H	H	41 ^B
76	7-OMe	<i>o</i> -Methoxyphenyl	H	H	43 ^B
77	7-OMe	<i>m</i> -Methoxyphenyl	H	H	95 ^A
78	7-OMe	<i>p</i> -Trifluoromethylphenyl	H	H	72 ^A
79	7-OMe	3-Thiophene	H	H	46 ^A
80	7-OMe	Pyridine-3-yl	H	H	46 ^A
81	6,7-OMe	H	H	H	47 ^B
82	6,7-OMe	Phenyl	H	H	35 ^B
83	6,7-OMe	<i>o</i> -Methoxyphenyl	H	H	10 ^B
84	6,7-OMe	<i>m</i> -Methoxyphenyl	H	H	90 ^B
85	6,7-OMe	<i>p</i> -Trifluoromethylphenyl	H	H	71 ^A
86	6,7-OMe	Thiophene-3-yl	H	H	68 ^B
87	6,7-OMe	<i>m</i> -Diethylene glycol monomethyl phenyl	H	H	16 ^B
88	Br	Phenyl	H	H	45 ^A
89	Br	<i>m</i> -Methoxyphenyl	H	H	32 ^A
90	Br	<i>p</i> -Trifluoromethylphenyl	H	H	59 ^A
91	H	Phenyl	Me	H	83
92	H	<i>o</i> -Methoxyphenyl	Me	H	73



cpd	R ¹	R ²	R ³	R ⁴	Yield [%]
93	H	<i>m</i> -Methoxyphenyl	Me	H	85
94	H	3-Thiophene	Me	H	99
95	7-OMe	H	Me	H	81
96	7-OMe	Phenyl	Me	H	99
97	7-OMe	<i>o</i> -Methoxyphenyl	Me	H	88
98	7-OMe	<i>m</i> -Methoxyphenyl	Me	H	71
99	7-OMe	3-Thiophene	Me	H	89
100	7-OMe	Pyridine-3-yl	Me	H	67
101	6,7-OMe	H	Me	H	61
102	6,7-OMe	Phenyl	Me	H	41
103	6,7-OMe	<i>o</i> -Methoxyphenyl	Me	H	89
104	6,7-OMe	<i>m</i> -Methoxyphenyl	Allyl	H	72
105	6,7-OMe	3-Thiophene	Me	H	40
106	6,7-OCH ₂ O, 8-OMe	H	Me	-	76
107	6,7-OCH ₂ O, 8-OMe	Phenyl	Me	-	95
108	6,7-OCH ₂ O, 8-OMe	<i>o</i> -Methoxyphenyl	Me	-	39
109	6,7-OCH ₂ O, 8-OMe	<i>m</i> -Methoxyphenyl	Me	-	99
110	6,7-OCH ₂ O, 8-OMe	<i>p</i> -Methoxyphenyl	Me	-	91
111	6,7-OCH ₂ O, 8-OMe	<i>p</i> -Trifluoromethylphenyl	Me	-	99
112	6,7-OCH ₂ O, 8-OMe	3-Thiophene	Me	-	74
113	6,7-OCH ₂ O, 8-OMe	Pyridine-3-yl	Me	-	23
114	6,7-OCH ₂ O, 8-OMe	Naphthalene-1-yl	Me	-	69



cpd	R ¹	R ²	R ³	R ⁴	Yield [%]
115	6,7-OCH ₂ O, 8-OMe	<i>o</i> -Chlorophenyl	Me	-	48
116	6,7-OCH ₂ O, 8-OMe	<i>m</i> -Chlorophenyl	Me	-	37
117	6,7-OCH ₂ O, 8-OMe	<i>m,m</i> -Dimethoxyphenyl	Me	-	13
118	6,7-OCH ₂ O, 8-OMe	<i>m</i> -Diethylene glycol monomethyl phenyl	Me	-	39
119	6,7-OCH ₂ O, 8-OMe	Cyclopropane	Me	-	16
120	6,7-OCH ₂ O, 8-OMe	CH ₂ O-(4-F-Ph)	Me	-	99
121	6,7-OCH ₂ O, 8-OMe	H	Me	Me	88
122	6,7-OCH ₂ O, 8-OMe	Phenyl	Me	Me	99
123	6,7-OCH ₂ O, 8-OMe	<i>m</i> -Methoxyphenyl	Me	Me	99
124	6,7-OCH ₂ O, 8-OMe	<i>p</i> -Methoxyphenyl	Me	Me	99
125	6,7-OCH ₂ O, 8-OMe	<i>p</i> -Trifluoromethylphenyl	Me	Me	99
126	6,7-OCH ₂ O, 8-OMe	Thiophene-3-yl	Me	Me	99
127	6,7-OCH ₂ O, 8-OMe	CH ₂ O-(4-F-Ph)	Me	Me	97
128	7-OMe	<i>o</i> -Methoxyphenyl	Me	Me	93
129	7-OMe	<i>m</i> -Methoxyphenyl	Me	Me	76
130	6,7-OMe	Phenyl	Me	Me	99

Especially for further structure-activity-relationship studies the reduction of the alkynylated THIQs was evaluated using Pd/C and H₂. Overall the alkyne reduction proved to proceed quite smoothly under mild conditions. Secondary THIQ **77**, tertiary THIQ **109** and propargylic tertiary THIQ **120** were readily converted into their reduced analogues (**131-133**) (**Table 3**).

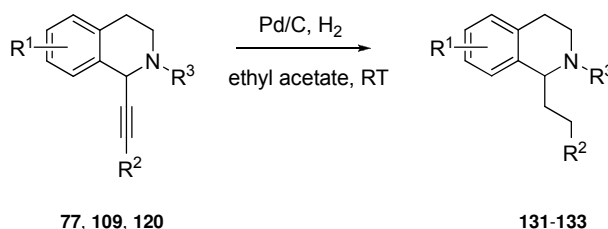


Table 3: Reduction of alkynylated THIQs.

cpd	R ¹	R ²	R ³	Yield [%]
131	7-OMe	<i>m</i> -Methoxyphenyl	H	95
132	6,7-OCH ₂ O, 8-OMe	<i>m</i> -Methoxyphenyl	Me	54
133	6,7-OCH ₂ O, 8-OMe	CH ₂ O-(4-F-Ph)	Me	91

Overall, efficient synthetic protocols were thus developed that allowed the implementation of a focused THIQ library that was subsequently used for biological studies (see section **III.3.3** Microtubule Inhibition).

3.2 Enantioselective Synthesis

In order to get access to enantiomerically pure or highly enantio-enriched analogues of alkynylated THIQs the addition of terminal alkynes to isolated alkyloisoquinoliniums (the natural product derivative cotarnine **23** was chosen as model substrate), catalysed by copper bromide and a chiral ligand, was investigated. Various chiral phosphine ligands were screened, like Josiphos derivatives (**Figure 20**), different BINAP analogs and QUINAP (**Figure 21**). While Josiphos derived ligands (**136-143**) resulted in almost no stereinduction, QuinoxP (**144**) and BINAP (**148**) led at least to an enantiomeric excess of 50%. The best ligand proved to be QUINAP⁷⁶ (**152**) resulting in quantitative yields and efficient stereinduction (*ee*: 98%) (**Table 4**).

Overall Josiphos derivatives (**Figure 20**) resulted in low stereinduction. Generally speaking most P,P-ligands (**140, 141, 143**) gave slight stereinduction while almost no induction could be observed for P,N-ligands (**137-139**). Remarkable was the effect of exchanging Josiphos' (**143**) phenyl-groups to cyclohexyl-groups (**142**) that resulted in extinguishing the slight stereinduction of Josiphos.

When comparing the stereinduction by BINAP derivatives and structurally related ligands (**147-150**) enantioselectivity dramatically decreased with increasing steric crowding and electron-rich substituents on the phosphorous atom from phenyl (**148**) to toluene (**149**), xylene (**150**) or trimethoxyphenyl (**147**). Most likely the catalytically active species of the CuBr/BINAP and CuBr/QUINAP system is a tetrahedral dinuclear copper(I) complex with bridging bromine counterions (**134, 135**) (**Figure 19**).^{77,78} Introducing more electron rich substituents on the phosphorus could stabilize the CuBr/ligand complex and steric crowding prevents substrate coordination, both effects could lead to a decrease in *ee*.

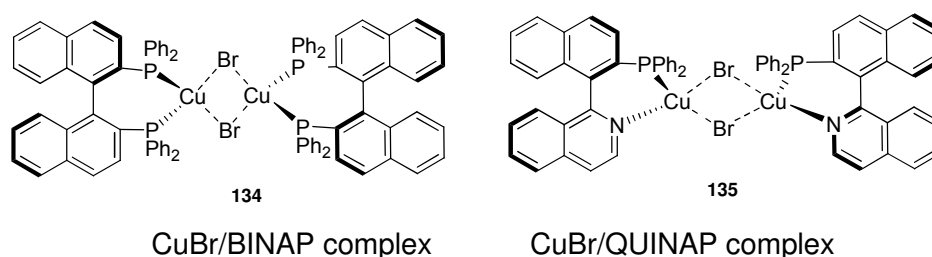


Figure 19: Proposed CuBr/BINAP and CuBr/QUINAP complexes.

Most beneficial proved to be the change from the bidentate P,P-ligand BINAP (**148**) to the less sterically demanding bidentate hemilabile P,N-ligand QUINAP (**152**). Probably the more labile nitrogen coordination facilitates the coordination of the iminium substrate and the following conversion.

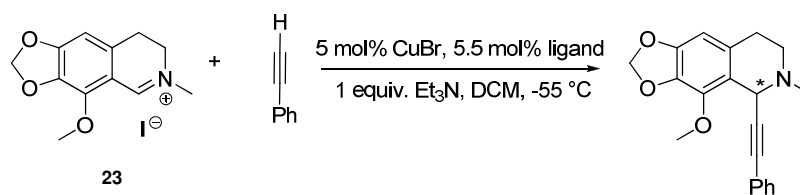


Table 4: Ligand Screening. Various different ligands were screened for the alkylation of cotarnine employing reaction conditions as published by Taylor and Schreiber.⁷⁶

Ligand	yield [%]	ee [%]
136	99	2
137	25	4
138	56	4
139	99	2
140	15	12
141	26	10
142	99	0
Josiphos (143)	42	10
(<i>R</i>)-QuinoxP (144)	99	50
145	41	6
(<i>R</i>)-Phanephos 146	99	18
147	52	8
(<i>R</i>)-BINAP (148)	99	50
(<i>R</i>)-TolBINAP (149)	73	16
(<i>R</i>)-XylBINAP (150)	61	22
(<i>R</i>)-MonoPhos (151)	53	4
(<i>S</i>)-QUINAP (152)	99	98

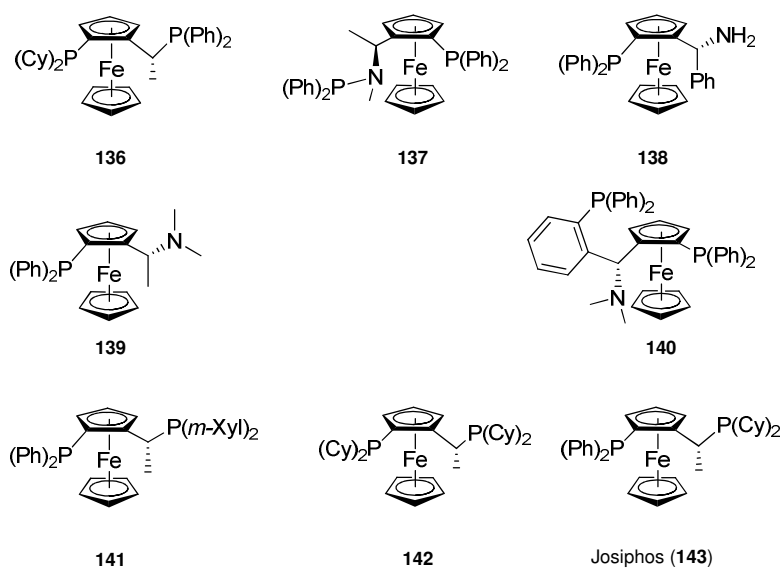


Figure 20: Josiphos derivatives.

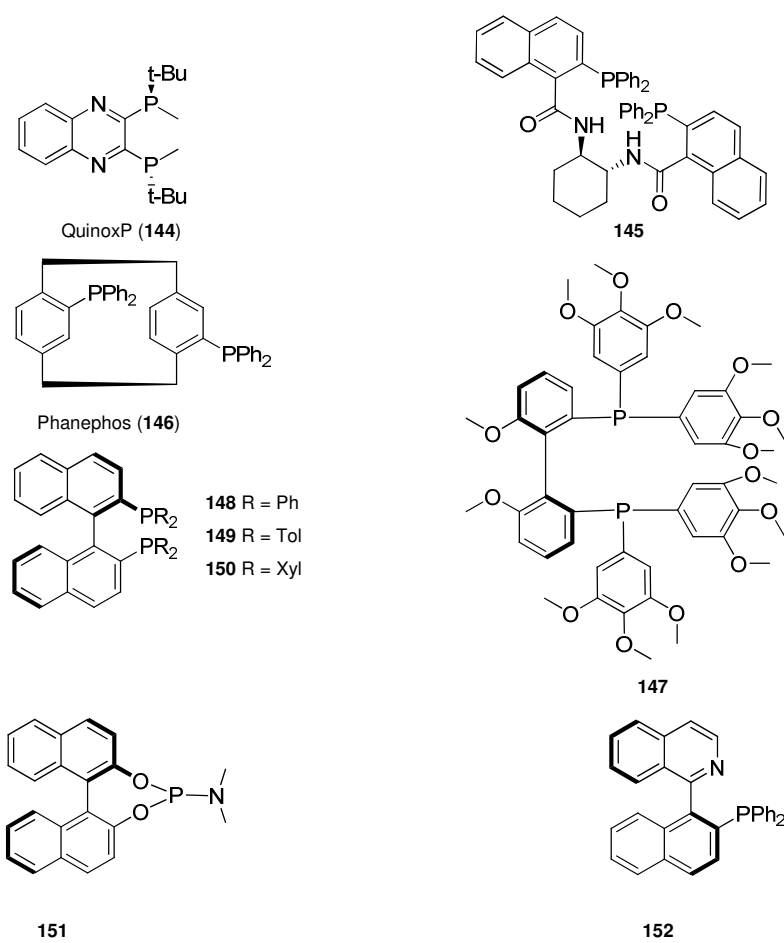


Figure 21: Assorted chiral ligands.

The QUINAP/CuBr system reported by Taylor and Schreiber gave the highest enantiomeric excess (**Table 4**). The absolute configuration of the major enantiomer was assigned by assuming that the stereochemical course of the reactions proceeds by analogy to the results of Taylor and Schreiber. They employed the CuBr/(*S*)-QUINAP alkynylation as key step for the synthesis of (*S*)-(-)-homolaudanosine, an isoquinoline-based natural product.⁷⁶

A possible mechanism could be proposed in analogy to reports by Knochel and coworkers (**Figure 22** and **Figure 23**).⁷⁷⁻⁷⁹ The chiral, dimeric copper(I) complex **135**⁷⁹ could coordinate an alkyne under formation of a side-on complex **153**. Base-mediated deprotonation results in an end-on copper-acetylide with a coordinated iminium ion **154**. The addition of the acetylide to the iminium ion within the coordination sphere of the chiral copper(I) complex **155** and the regeneration of the catalyst yields the chiral alkynylated THIQ **156** (**Figure 22**).

The postulated transition state **157** (**Figure 23**) could consist of two QUINAP molecules creating a chiral sphere that facilitates the side-on coordination of the iminium ion to the copper(I) center. The methoxy groups of the THIQ might in addition be involved in the copper chelation, especially the 8-OMe. Shown in **Figure 23** is a dimeric copper(I) complex consisting of two (*S*)-QUINAP molecules, end-on coordinated phenylacetylene and side-on coordinated cotarnine (**23**).

Different iminium species were used for the investigation of the CuBr/QUINAP catalysed alkynylation reaction (**Table 5**). The simple imine 7-methoxy-3,4-dihydroisoquinoline (**58**) (entry 1) could not be converted to the corresponding alkynylated product. Also *in situ* generated TMS-iminium salts (entry 2) did only result in recovered starting materials. This might be due to the rather labile TMS-group. Activation with a methyl or allyl group (entry 3 and 4) resulted in high to moderate *ee*. The rather bulky and electron withdrawing carboxybenzyl group (entry 5) gave low conversion without any enantioselectivity. The loss of selectivity might either be due to steric hindrance or to disfavoured side-on coordination of the imine caused by the electron withdrawing carbamate. Quite remarkable is the effect of the methoxy groups. While no methoxy group (entry 6) gave 83% *ee*, just the installation of one methoxy group in 8-position enhanced the selectivity to 99% *ee* (entry 7). This might be due to additional copper chelating effects and therefore enhanced stereinduction. In accordance with the proposed transition state (**Figure 23**) additional substituents on the aromatic iminium salt in 6- or 7-position do not cause steric crowding and are therefore tolerated (entry 8).

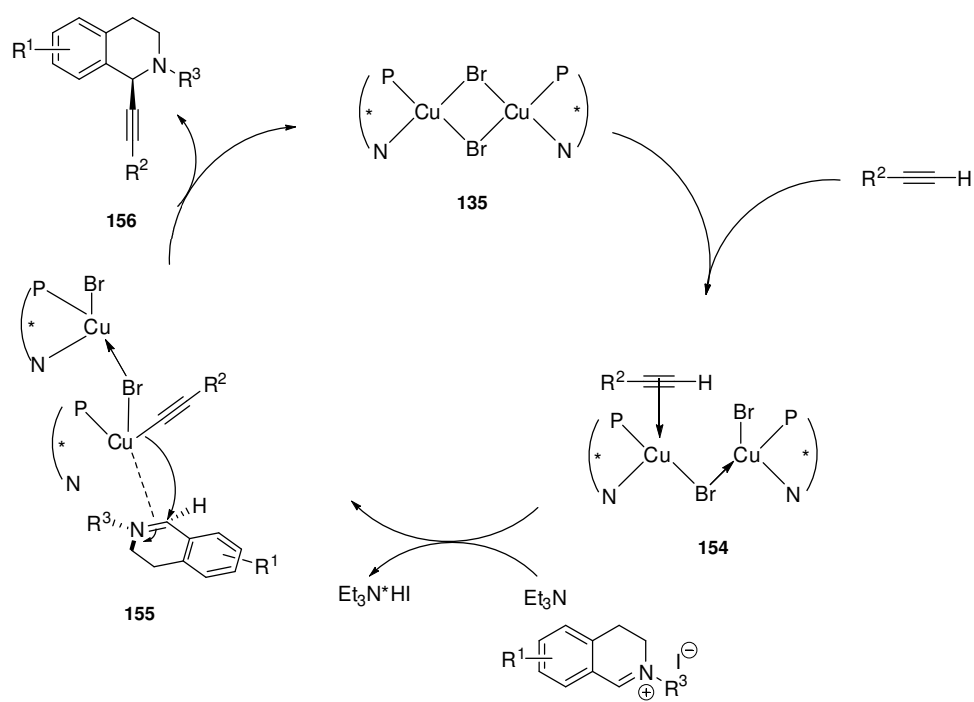


Figure 22: Postulated mechanism for CuBr/QUINAP catalyzed alkylation of tetrahydroisoquinoline iminium salts.

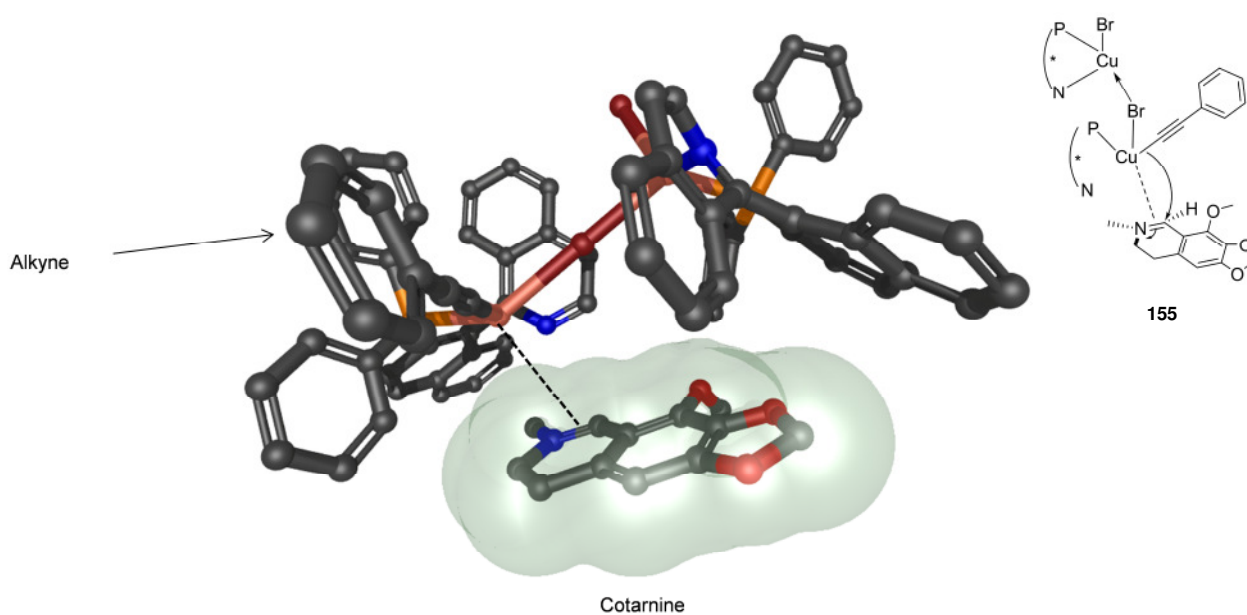


Figure 23: Postulated transition state of (S)-QUINAP/CuBr complex with end-on copper acetylide and side-on cotarnine coordination. Figure generated with Marvin Sketch⁸⁰ and Ball View.^{81,82}

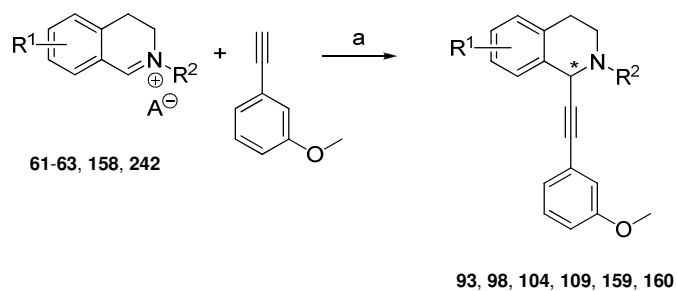


Table 5: CuBr-catalysed addition of 3-ethynylanisole to different iminium salts. a) 1 equiv Et₃N, DCM, -55 °C, 5 mol% CuBr, 5.5 mol% QUINAP. *prepared *in situ*.

entry	R ¹	R ²	cpd	yield [%]	ee [%]
1	7-OMe	-	-	-	-
2	7-OMe	TMS*	-	-	-
3	7-OMe	Me	98	99	91
4	6,7-OMe	Allyl	104	78	82
5	6,7-OMe	Carboxybenzyl*	159	34	0
6	H	Me	93	99	83
7	8-OMe	Me	160	99	99
8	6,7-OCH ₂ O, 8-OMe	Me	109	92	99

Various different alkynes were evaluated using the CuBr/QUINAP system. The system proved to give excellent *ee* values and viable yields of various substituted phenylacetylenes (**Table 6**, entries 1-4), as well as alkynes carrying a heterocyclic (**Table 6**, entry 5) or an aliphatic substituent (**Table 6**, entries 6, 8). For a more flexible propargylic ether the *ee* values decreased (**Table 6**, entry 7).

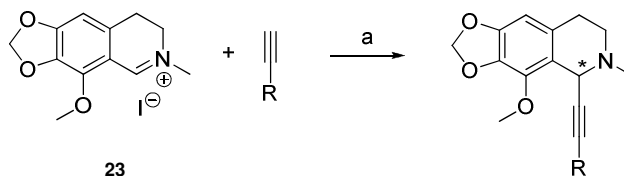


Table 6: CuBr-catalysed addition of terminal alkynes to cotarnine iodide 23. a) 1 equiv Et₃N, DCM, -55 °C, 5 mol% CuBr, 5.5 mol% (*S*)-QUINAP.

entry	R	cpd	yield [%]	<i>ee</i> [%]
1	Phenyl	107	99	98
2	<i>m</i> -Methoxyphenyl	109	92	99
3	<i>p</i> -Methoxyphenyl	110	88	99
4	<i>p</i> -Trifluoromethylphenyl	111	95	97
5	3-Thiophene	112	99	99
6	Cyclopropane	119	75	99
7	CH ₂ O-(4-F-Ph)	120	83	63
8	1-Cyclohexene	161	58	97

As the enantioselective alkylation with a flexible propargylic ether appeared to be challenging (**Table 6**, entry 7) a further ligand screening was performed. Ligands that gave stereinduction in the first screen were employed for the synthesis of **120**. However, none of the ligands resulted in improved yields or *ee* in comparison with the CuBr/QUINAP system (**Table 7**).

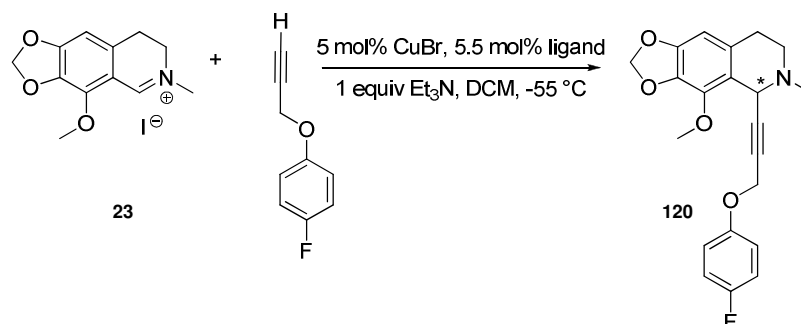


Table 7: Ligand Screening. Different ligands were screened for the alkylation of cotarnine using a propargylic alkyne under CuBr/QUINAP conditions.

Ligand	yield [%]	<i>ee</i> [%]
(<i>R</i>)-QuinoxP (144)	46	10
(<i>R</i>)-BINAP (148)	16	14
(<i>R</i>)-ToIBINAP (149)	40	4
(<i>R</i>)-XyIBINAP (150)	30	22
(<i>S</i>)-QUINAP (152)	83	63

In summary, a highly efficient enantioselective access to alkynylated tetrahydroisoquinolines could be established facilitating further structure-activity-relationship studies.

3.3 Microtubule Inhibition

Screening and further biological studies of the compounds synthesised as described in the previous chapters were performed by Dr. Sayantani Roy.

The synthesised THIQs were complemented by 6 commercial compounds (**322-327**, see **Appendix** for details) in order to give a library of 103 compounds (see experimental section for exact composition). According to their origin, compounds were clustered in three categories: (1) *natural product derived* THIQs were synthetic derivatives of the natural product noscapine (**21**), mainly obtained *via* alkylation of the iminium salt cotarnine (**23**); (2) *natural product inspired* THIQs exhibit a THIQ core that was built up synthetically; (3) fragments or building blocks (e.g. 6,7-dimethoxy-1,2,3,4-tetrahydroisoquinolinium chloride **162**) (**Figure 24**).

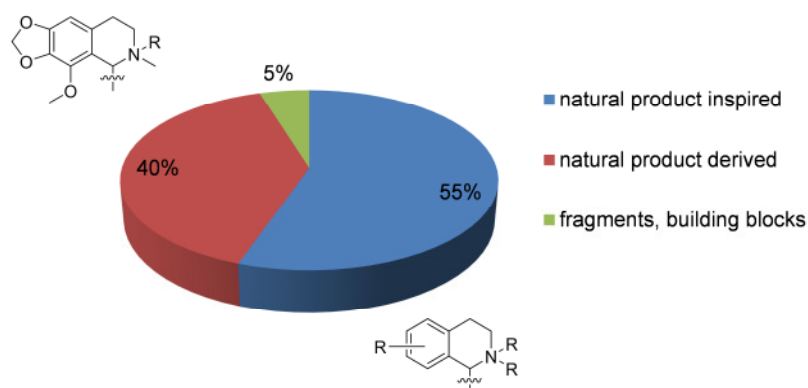
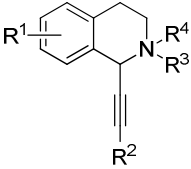


Figure 24: THIQ library tested on tubulin modulation. 103 THIQs were sorted according to their origin.

The described compound collection was screened at a concentration of 30 μM for phenotypic changes associated with microtubule cytoskeleton and mitotic arrest in BSC-1 and HeLa cells after treatment for 24h. Chromosomes were stained with DAPI and anti-tubulin antibody coupled to FITC (fluorescein isothiocyanate) was used to detect tubulin. From the 103 compounds tested, 7 compounds (including noscapine **21**) induced phenotypic changes, such as accumulation of round-shaped cells with condensed DNA, which are indicative of mitotic arrest. For the three compounds causing the strongest effects (**107**, **109**, **117**), both enantiomers were tested. While the (*S*)-enantiomer was inactive, the (*R*)-enantiomer proved to be the active component of the racemic mixture initially screened. The identified hit compounds clearly occupy a distinct niche within the THIQ library. Only *natural product derived* compounds, containing the noscapine THIQ core were found as actives. The best compound (*R*)-**109** features a phenyl acetylene function with one methoxy group in the *meta* position and (*R*)-configuration of the only stereocenter. Loss of the triple bond, aliphatic alkyne residues, bulky *meta* substituents or quaternisation of the nitrogen led to complete loss of activity (**Figure 25**).

Table 8: Structure-activity relationship (SAR) of selected THIQs in a phenotypic HeLa-cell based screen. HeLa-cells were incubated with 30 μ M compound for 24h and cells in mitotic arrest were counted. The percentage of mitotic versus normal cells was determined.

cpd						% of mitotic cells
	R ¹	R ²	R ³	R ⁴		
93	H	<i>m</i> -Methoxyphenyl	Me	H	7	
98	7-OMe	<i>m</i> -Methoxyphenyl	Me	H	4	
106	6,7-OCH ₂ O, 8-OMe	H	Me	H	4	
107	6,7-OCH ₂ O, 8-OMe	Phenyl	Me	H	65	
108	6,7-OCH ₂ O, 8-OMe	<i>o</i> -Methoxyphenyl	Me	H	26	
109	6,7-OCH ₂ O, 8-OMe	<i>m</i> -Methoxyphenyl	Me	H	67	
110	6,7-OCH ₂ O, 8-OMe	<i>p</i> -Methoxyphenyl	Me	H	11	
116	6,7-OCH ₂ O, 8-OMe	<i>m</i> -Chlorophenyl	Me	H	11	
117	6,7-OCH ₂ O, 8-OMe	<i>m,m</i> -Dimethoxyphenyl	Me	H	46	
122	6,7-OCH ₂ O, 8-OMe	Phenyl	Me	Me	4	
123	6,7-OCH ₂ O, 8-OMe	<i>m</i> -Methoxyphenyl	Me	Me	3	
Noscapine (21)					56	
DMSO					6	

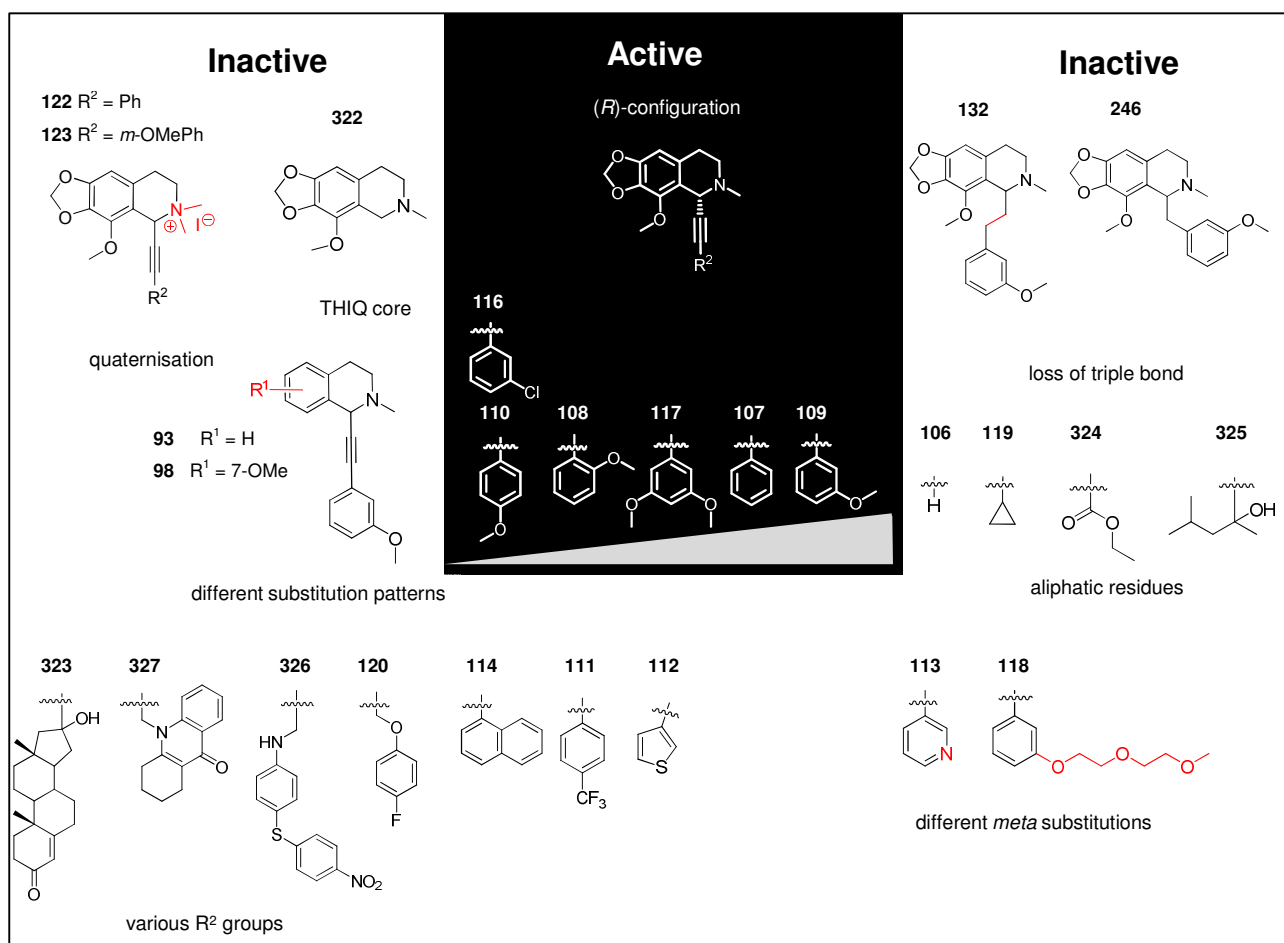


Figure 25: Structure-activity relationship for THIQs tested on HeLa cells. Compounds were ranked “active” if they significantly (more than 10% mitotic versus normal cells) increased mitotic arrest (see Table 8).

Screening efforts led to structurally simplified (one stereocenter versus two in the natural product) noscapine related microtubule inhibitors (**Figure 25**).

The identified hit compounds were subjected to concentration dependent measurements (30 μM , 15 μM , 7.5 μM) on HeLa and BSC-1 cells. As depicted in **Figure 26** a clear dose responsiveness was observed. The most potent compound (*R*)-**109** was compared to noscapine (**21**), that was known to arrest cells in mitosis. Treatment of HeLa and BSC-1 cells resulted in rounded cell shape with highly condensed DNA content, suggesting their arrest in mitosis. This phenotype was observed upon treatment of HeLa cells with (*R*)-**109** even at 7.5 μM , while noscapine appeared to be less potent at the same concentration (**Figure 26**). Comparable phenotypes were caused by incubation of BSC-1 cells with (*R*)-**109** and **21**. However, the consequences were less pronounced and higher concentrations of compound were required to cause comparable effects as in HeLa cells. Thus, as a general trend BSC-1 cells seemed to be less affected by (*R*)-**109** than HeLa cells (**Figure 26**).

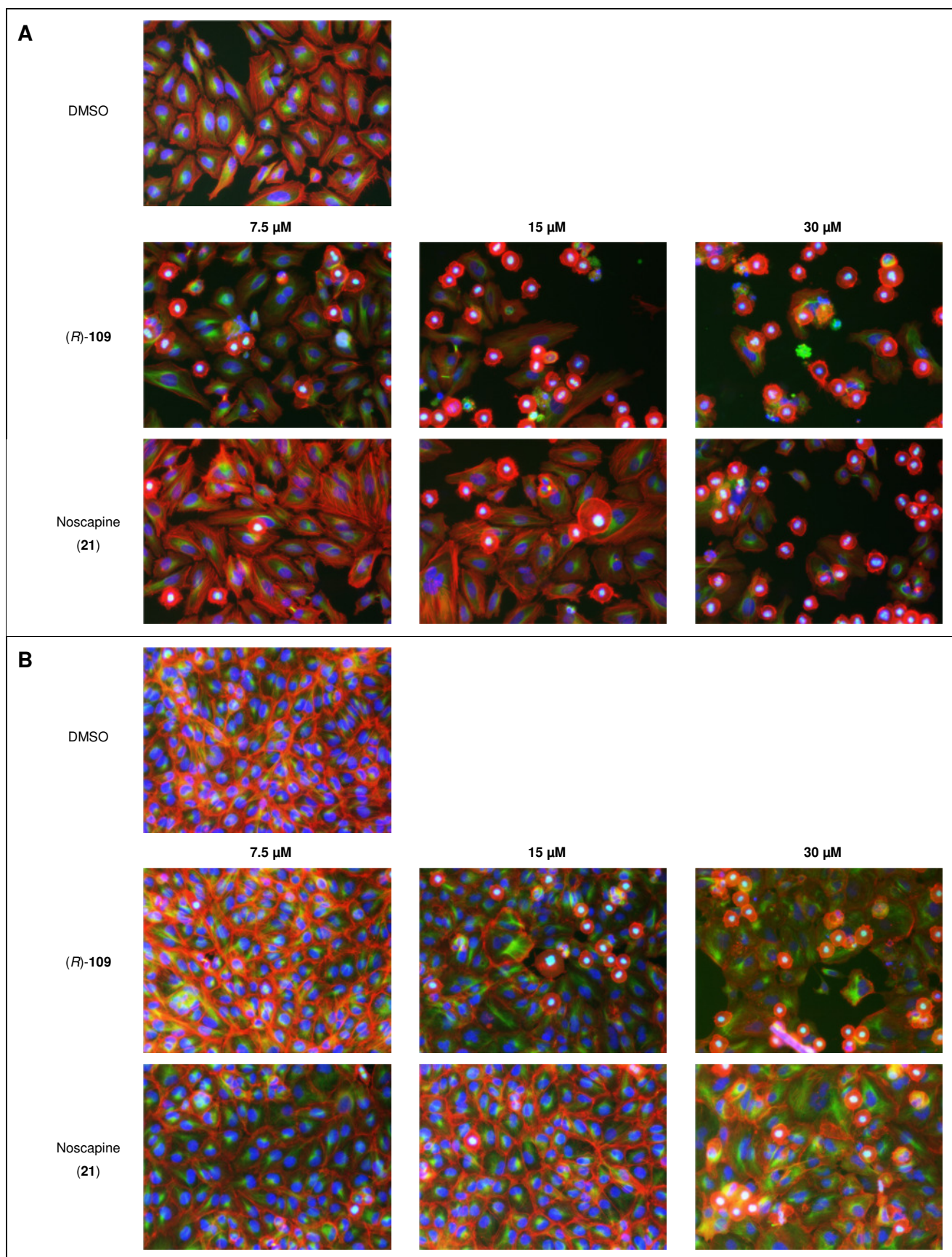


Figure 26: Influence of (*R*)-109 and 21 on A) HeLa and B) BSC-1 cells treated either with different concentrations of (*R*)-109 and 21 or 0.3% DMSO for 24h. Chromosomes were stained with DAPI and anti- α -tubulin-FITC antibody was used to detect tubulin.

As noscapine (**21**) is a known tubulin binder, experiments investigating the influences of the identified noscapine related alkynylated THIQs on *in vitro* tubulin polymerisation were performed. The polymerisation of isolated porcine tubulin was thus induced with GTP and monitored.⁸³ The anti-neoplastic agent nocodazole (**163**) is known to inhibit tubulin polymerisation strongly and is therefore frequently used in cell biology to synchronize cells. In this experiment **163** was consequently used as control for the inhibition of tubulin polymerisation. In comparison with the natural product **21** the synthesised compound (*R*)-**109** showed a much stronger inhibition of tubulin polymerisation (**Figure 27**).

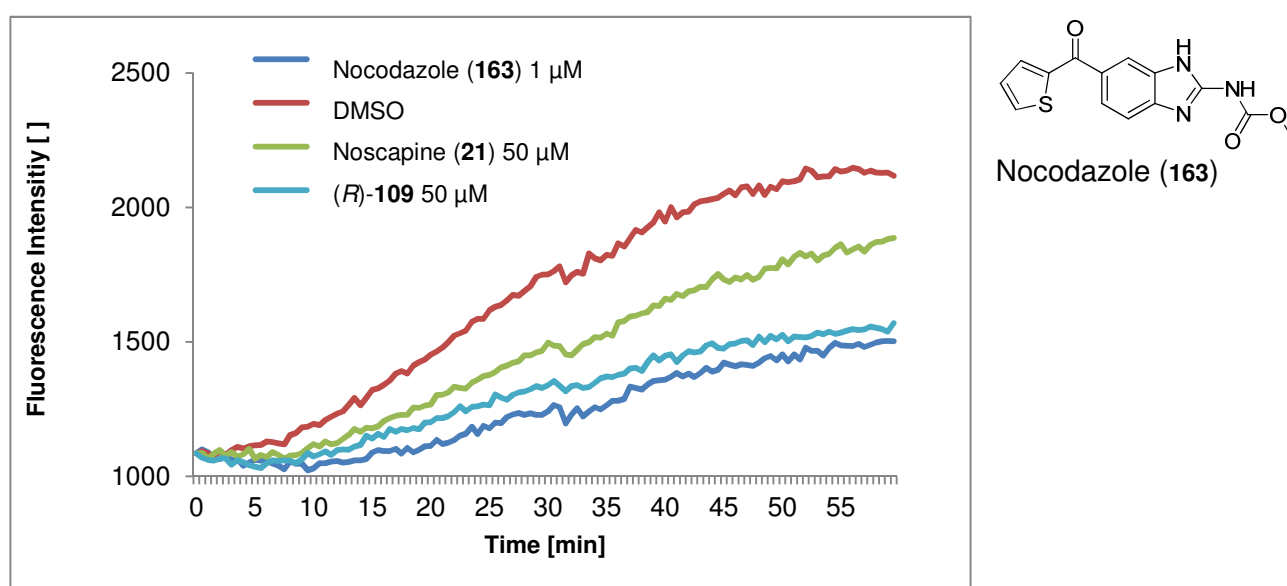


Figure 27: *In vitro* tubulin polymerisation assay. Tubulin polymerisation was monitored by fluorescence measurement at excitation/emission 370/460 nm. After tubulin polymerisation was induced with GTP, polymerisation was monitored by means of enhanced DAPI fluorescence upon binding to microtubules.

The most potent compounds were subjected to a microtubule re-growth assay. In this experiment the time-dependent microtubule re-polymerisation in BSC-1 cells upon re-warming after cold treatment is studied. When cells are cooled down microtubules depolymerise. Examining the time-dependent re-growth of microtubules upon re-warming with and without tubulin modulators is a widely accepted approach to elucidate a compound's impact on cells (**Figure 27**). In DMSO treated cells, microtubule-organizing centers (MTOCs) reappeared just 2 min after re-warming and the microtubule cytoskeleton had recovered after 10 min. In contrast (*R*)-**109** and **21** partially inhibited microtubule regrowth as up to 10 min and recovering after 15 min.

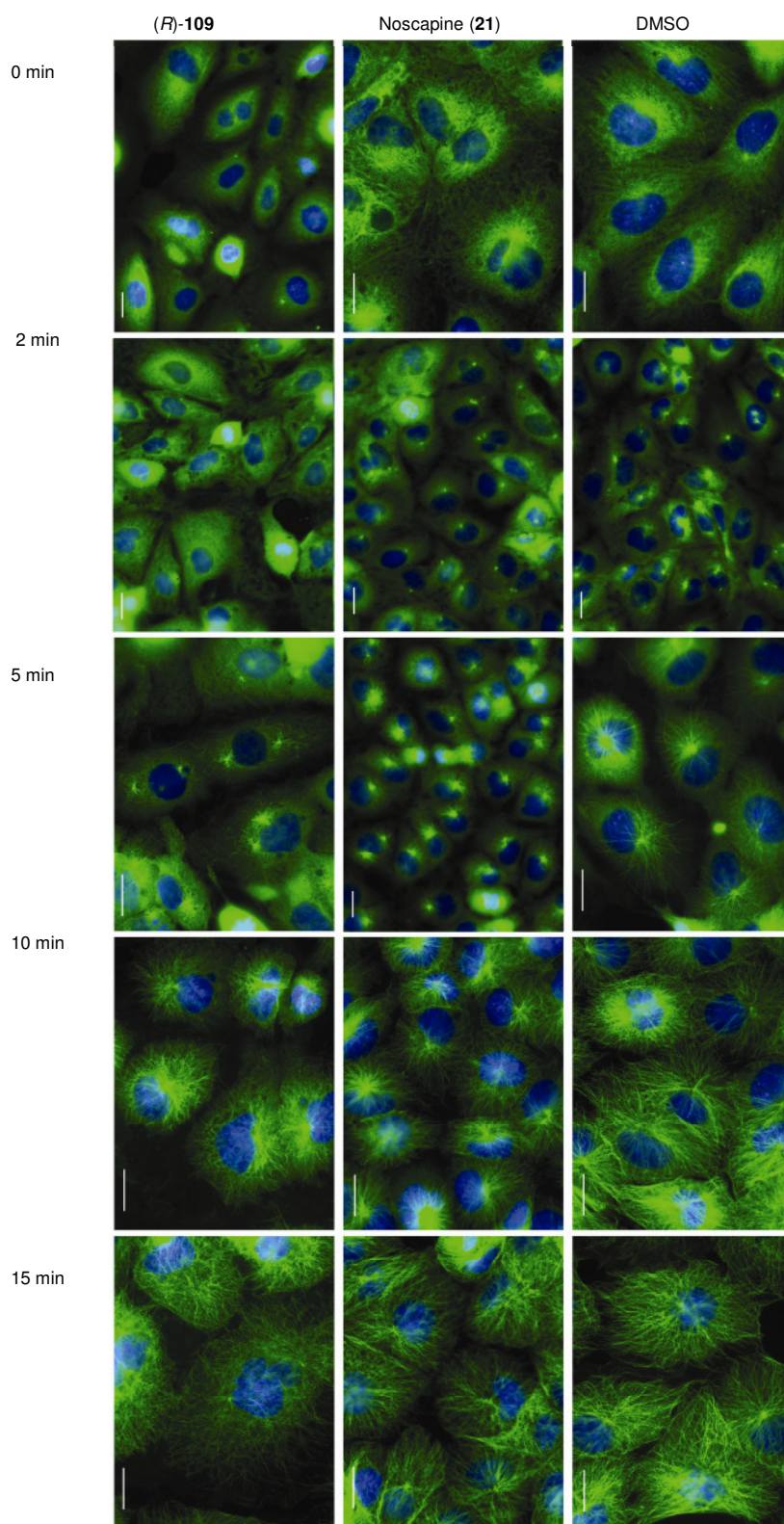


Figure 28: Re-growth of microtubules in BSC-1 cells. Cells were treated with 0.3% DMSO, 15 μM of each 21 and (R)-109. After cold treatment on ice and re-warming at 37 $^{\circ}\text{C}$ microtubule re-growth was studied at the given time points after fixation and staining. DNA was stained with DAPI (blue) and tubulin was detected using anti- α -tubulin antibody coupled to FITC and secondary antibody coupled to Alexa. Size bar: 20 μm .

Fluorescence activated cell sorting (FACS) of HeLa cells treated with (*R*)-**109** and stained for DNA with propidium iodide, confirmed the compounds' ability to efficiently arrest cells in the G2/M phase (A, **Figure 29**). Staining of cells with anti-PhosphoHistoneH3 antibody and propidium iodide revealed that at 15 μ M (*R*)-**109** 37% of the cells were in mitosis, while only 14% of mitotic cells were observed after treatment with parent compound noscapine (**21**) at the same concentration (B, **Figure 29**). In comparison DMSO treated cells showed 3% mitotic cells.

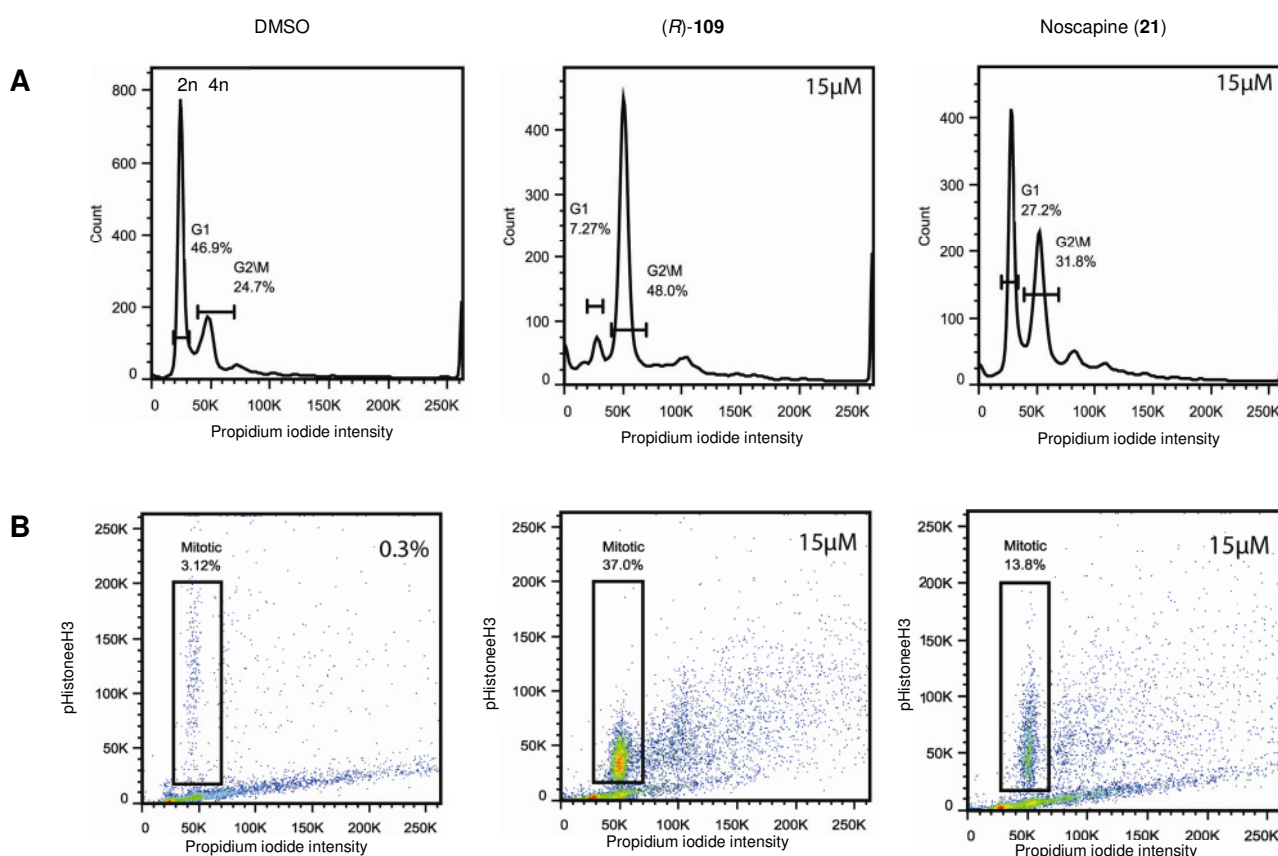


Figure 29: Cell cycle analysis of HeLa cells treated with (*R*)-**109** and noscapine (**21**). **A**) Cells were incubated for 24h with 15 μ M (*R*)-**109** and noscapine (**21**) and 0.3% DMSO as control prior to staining with propidium iodide and FACS. The percentage of cells in the G1 and G2/M phase is shown in the figure. **B**) FACS analysis to determine the amount of mitotic cells. Cells were treated with 15 μ M of (*R*)-**109**, noscapine (**21**) and anti-PhosphoHistoneH3 antibody (mitotic marker) overnight and stained with propidium iodide (PI) to measure the DNA content.

Although several efforts were made to determine the binding site for noscapine on tubulin, so far in literature there is no direct evidence for binding to the well-characterized colchicine and vinca sites.⁸⁴ For the brominated noscapine derivative, Br-noscapine (**22**), a binding to the colchicine site has been reported.⁸⁵

In order to explore the possible binding site of (*R*)-**109** on tubulin, competition experiments using colchicine (**30**) or the vinblastine (**29**) derivative BODIPY® FL-vinblastine were performed. The

fluorescence of both compounds increases significantly upon binding to tubulin. After preincubation of the two probes with tubulin, (*R*)-109 was added at different concentrations and the change in fluorescence upon replacement of the probes observed. In a control experiment known competitors (vincristine for the vinblastine binding site and nocodazole for the colchicine binding site) were added. However, similarly to noscapine, (*R*)-109 could neither displace colchicine nor vinblastine and therefore does not bind to one of these two well-characterized binding sites (**Figure 30**).

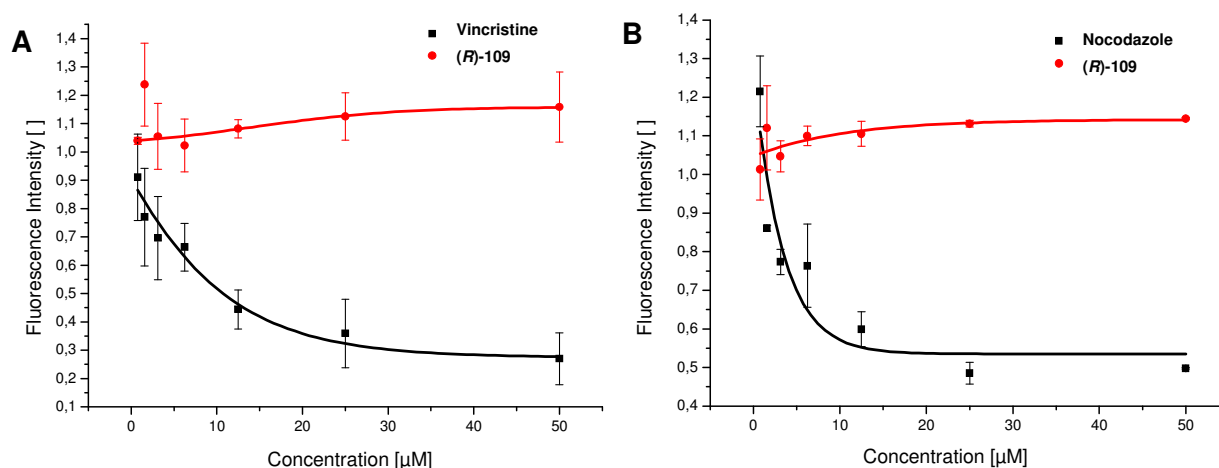


Figure 30: Competition experiments for binding site determination of (*R*)-109 on tubulin. A) Vinblastine competition assay using BODIPY® FL-vinblastine. The tubulin-vinblastine-test compound or tubulin-vinblastine-vincristine complex was formed by incubating 5 μ M tubulin with 5 μ M BODIPY-FL-vinblastine and different concentrations of (*R*)-109 or vincristine for 1h at RT. Fluorescence readings (ex/em 470/514 nm) were performed in black 96 well plates using SAFIRE II plate reader (Tecan, Grödig, Austria). Blank values were subtracted from all sample values. Values were normalized to the DMSO control. B) The tubulin-colchicine-test compound or tubulin-colchicine-nocodazole complex was formed by incubating 5 μ M tubulin with 50 μ M colchicine and different concentrations of (*R*)-109 or nocodazole for 1h at RT. Fluorescence readings (ex/em 365/435 nm) were performed in black 96 well plates using SAFIRE II plate reader. Blank values were subtracted from all sample values. Values were normalized to the DMSO control.

4 Summary and Conclusion

Using the principles of biology-oriented synthesis a library of alkynylated tetrahydroisoquinolines was synthesised. This library was based on the biologically prevalidated core scaffold of tetrahydroisoquinoline, a structural backbone occurring in various natural products of diverse origin, exerting numerous biological effects. This collection of THIQs was applied to the biological application of microtubule inhibition.

The designed library with limited structural diversity around the THIQ core consisted of two theoretically distinct parts. On the one side the natural product cotarnine, an *N*-methyl iminium salt, was readily alkynylated using various acetylides, thus resulting in a *natural product derived* collection of alkynylated THIQs. Further modifications included the quaternisation with methyl iodide or reduction of the triple bond. The second part of the library – *natural product inspired* – was built up from various phenylethylamines that were cyclized to result in the corresponding lactam. These lactams were then alkynylated using a modified protocol by Yamaguchi *et al.*⁶⁸ that yielded alkynylated THIQs. On the basis of the fully protected THIQ core various modifications were possible. Library generations however, focused on triazole derivatives generated by click chemistry and diverse alkynylated THIQs available *via* Sonogashira coupling. As the one-pot alkynylation reaction proved to be challenging, especially for electron rich dimethoxy lactams, an alternative approach *via* the alkynylation of TMS-triflate precipitated imines was developed. In most cases this approach resulted in enhanced yields for the synthesis of electron rich alkynylated THIQs. Together with the lactam alkynylation a very efficient methodology platform was established in order to access numerous secondary THIQs, that are challenging to obtain otherwise.

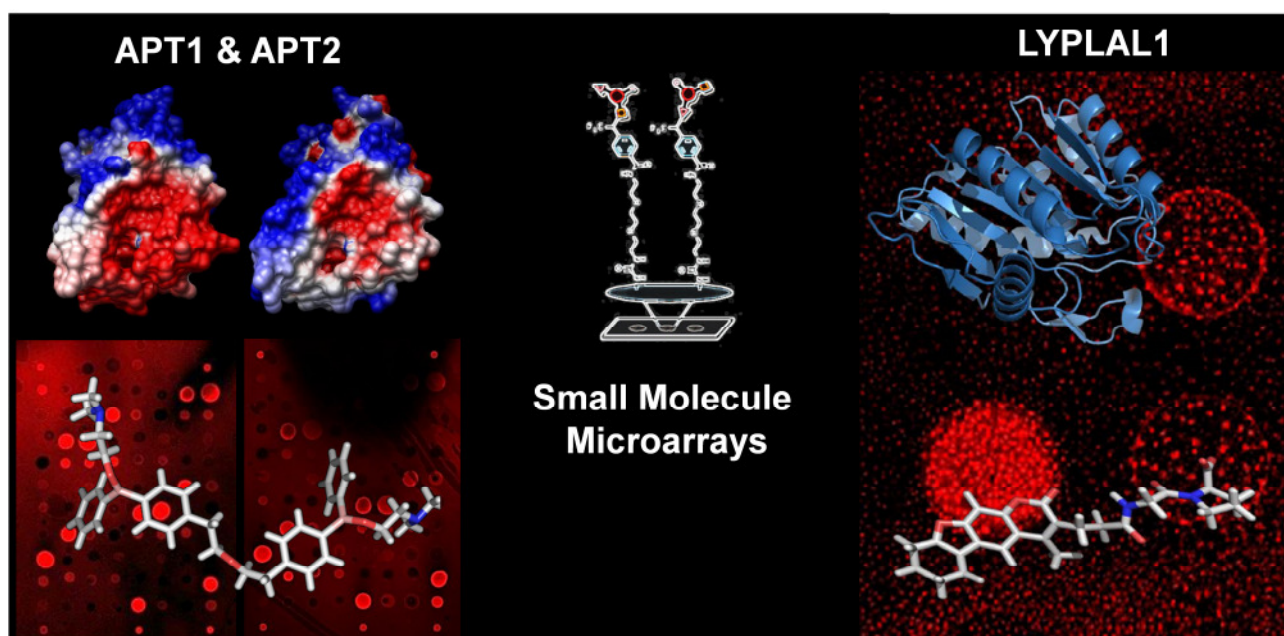
Further investigations concentrated on CuBr-catalysed enantioselective alkynylation reactions of iminium salts. Extensive ligand screening efforts led to a very efficient method giving high *ee* and almost quantitative yields. The absolute stereochemistry of the obtained alkynylated THIQs could be assigned in analogy to reports published by Taylor and Schreiber.⁷⁶

A library of 103 THIQs was tested in a phenotypic screen on cancer cell lines (HeLa and BSC-1) and led to the identification of small molecule microtubule inhibitors. Quite interestingly, only compounds closely related to the natural product noscapine were identified. In contrast to noscapine that contains two stereocenters, the identified compounds comprised only one stereocenter with the same (*R*)-stereochemistry at the carbon in the α position to the nitrogen. A clear structure activity relationship could be drawn, yielding compounds that were more potent than noscapine. As new microtubule inhibitors due to tumor resistance are in urgent need and

noscapine and its derivatives recently have drawn scientific interest due to favourable toxicity and superior *in vivo* activity, these structurally related, simplified small molecules could be of great interest.

The need for new suitable small molecules applicable as protein ligands lies at the heart of chemical biology. The BIOS approach is a tool to explore well-defined parts of drug-like chemical space. As natural products can be regarded as evolutionary pre-validated structures by nature, these scaffolds are used as guideline for the generation of chemical diversity. Being metabolites of plant, animal, fungal or bacterial origin, natural products were in contact with many proteins during their biosynthesis, and consequently have inherent potential to bind to proteins. In the search for molecules that interact with proteins, natural substances can therefore serve as a model. A hierarchical classification of known natural products allows to trace back complex natural products to their underlying core structures. The performed studies for the generation of a focused compound collection inspired by the natural product noscapine and its underlying THIQ-core prove the power of the BIOS concept to generate along the lines of biological prevalidation, high content small molecule libraries with exalted hit rates.

IV Small Molecule Microarrays



1 Introduction

1.1 Small Molecule Microarray Technology

The discovery of small molecule modulators of a protein of interest can enable not only the functional analysis of the protein but also the development of drugs targeting human disease related proteins. Within the past decade the development of high-throughput screening (HTS) methods using microarray technologies has led to major advances in modern chemical biology research. In a single step, thousands of biochemical interactions can be analysed simultaneously, diverse biomolecules including DNA/RNA and oligonucleotides, proteins, peptides, carbohydrates, small molecules, tissue and live cells.⁸⁶ Small molecule microarrays were first described by MacBeath *et al.* in 1999. In this approach small molecules containing carboxylic acid functions were immobilized on maleimide-derivatized glass slides.⁸⁷ In the following years various applications especially combining diversity-oriented-synthesis (DOS) strategies with consecutive compound immobilization were developed. However, a serious limitation to all of these approaches was that library members must possess some functional group that is able to react predictably and chemoselectively with another functional group on the substrate surface. Consequently, this technique is not suitable for high-throughput-immobilization of complex, synthesis intense, small molecules or isolated natural products.⁸⁶

Osada and co-workers therefore developed an approach towards “non-selective” and functional-group-independent immobilization using a photoinduced cross-linking reaction to anchor small molecules on glass slides^{88,7} or gold surfaces.⁸⁹ This approach relies on reactive carbene species generated from trifluoromethyl aryl diazirine upon UV irradiation. After spotting small molecules on glass or gold surfaces coated with diazirin-based photo-affinity linkers, covalent immobilization is initiated *via* UV irradiation. The *in-situ* generated carbene-species react with proximate small molecules in a functional-group-independent manner. With this method there is no need for the incorporation of certain reactive groups amongst library members and therefore it is especially suited for natural product derived compound libraries. Furthermore, this technique allows various facets of the immobilized compound to be exposed for interaction.⁷ Osada and co-workers could demonstrate that the immobilized small molecules retained their ability to interact with their binding protein by immobilization of small molecules with known protein binding partners and detection of their binding affinity.⁸⁹

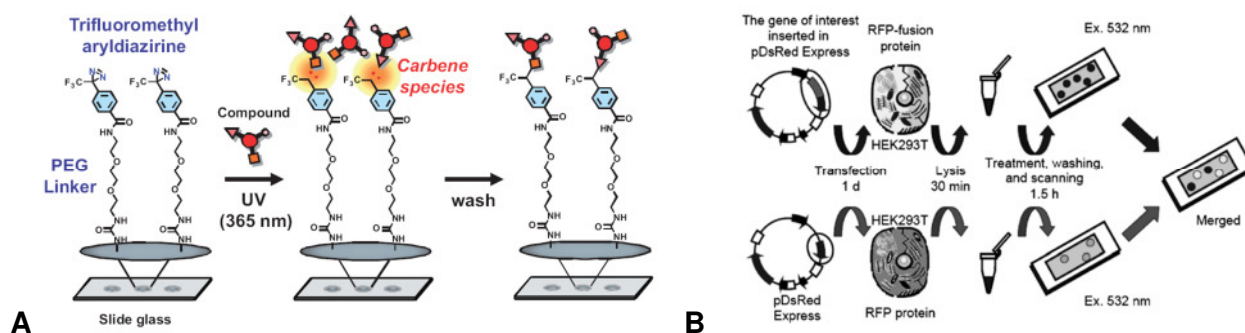


Figure 31: A) Trifluoromethyl aryl diazirine attached to a glass slide *via* PEG linker. UV irradiation generates reactive carbene species that react with small molecules in a “non-selective” manner, resulting in immobilization. B) Overview of a systematic chemical array screening method. Genes of interest are cloned and can be expressed as RFP-fused proteins in the mammalian cell line HEK293T. After transfection, cell lysates are prepared for incubation with glass slides. Hit compounds are detected *via* merged display analysis.^{90,6}

Further improvements to array screening using small molecules that were immobilized in a functional-group-independent manner allowed the screening of cell lysates. Protein lysates of cells that express the protein of interest fused with red fluorescent protein (RFP) can be used and merged display analysis with lysate from RFP-only expressing cells removes false positive signals (**Figure 1B**). For example, this technique was used to detect novel inhibitors of carbonic anhydrase II that could serve as antiglaucoma drugs.^{90,6}

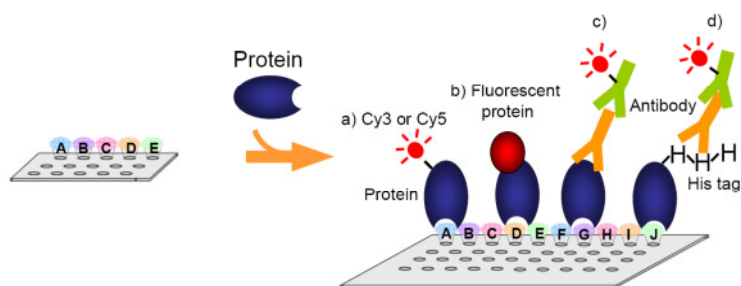


Figure 32: Different options for the detection of proteins bound to small molecule microarray. a) Cy3 or Cy5 labelled protein, b) target protein conjugated with fluorescent protein (e.g. mCherry), c) antibody detection of protein, d) antibody detection of protein-tag (e.g. His-tag, GST-tag).

For small molecule microarrays on glass slides, either fluorescently labelled or tagged proteins (e.g. His- or GST-tag) are essential. Furthermore, small molecule microarrays have to be washed and dried before scanning the fluorescence and relatively weak small molecule-protein interactions might be susceptible to the washing process. Therefore alternative platforms not requiring protein labeling and allowing *in-situ* observation of binding are of interest. Such methods could be used to supplement and validate primary screening using glass slides. Osada and co-workers successfully applied their photo-cross-linking protocol to Surface Plasmon Resonance imaging (SPR) of

immobilized small molecules on gold surfaces. Proteins that bind to the immobilized small molecules on the gold surface change the local index of refraction and therefore alter the resonance conditions of the surface plasmon waves. Such SPR binding assays can be performed under wet conditions in real time with untagged protein. This technique therefore constitutes an ideal supplement to glass slide array screening (**Figure 33**).^{89,91,92}

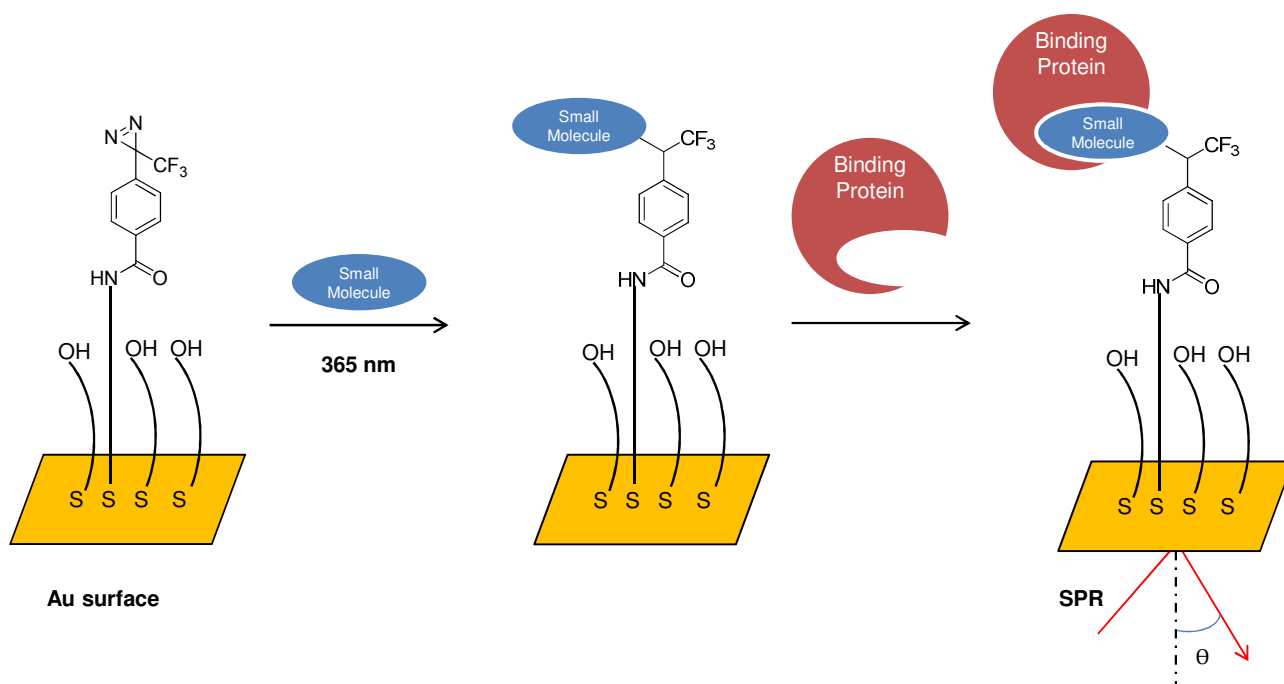


Figure 33: SPR imaging of immobilized small molecules on a gold surface.⁹³

1.2 Glass Slide Preparation

A major benefit of small molecule microarrays is the inexpensive preparation of array slides; however, precise microprinting technology needs to be available. Photo affinity linker-coated (PALC) glass slides were prepared by covalent attachment of photoaffinity linkers to an activated glass surface. Typically such a photoaffinity linker (PAL) consists of a UV sensitive head (e.g. trifluoromethyl aryl diazirine) and a flexible polyethylene glycol tail terminating with a functional amine group for covalent immobilization. **PAL1 (164)** and **PAL2 (165)** were synthesised from readily available trifluoromethyl aryl diazirine **166** and mono-protected diamine **167**. EDC-coupling and Boc-deprotection gave **164** and successive coupling with Fmoc-(Pro)₉-OSu followed by Fmoc-deprotection resulted in **165** (Linker synthesis was performed by K. Honda).

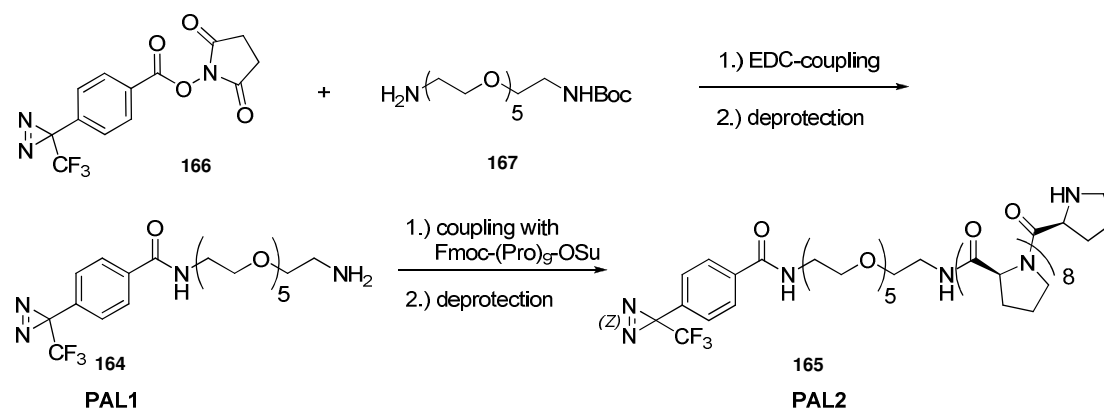


Figure 34: Synthesis of photoaffinity linker PAL1 (**164**) from trifluoromethyl aryldiazirine **166** and mono-protected bis-amine **167**. PAL2 (**165**) was synthesised from **164** via peptide coupling with Fmoc-(Pro)₉-OSu followed by deprotection.

In order to immobilize PEG-linkers, amine-coated (AC) glass slides were treated with *N,N*-disuccinimidyl carbonate (DSC) and base in order to give highly reactive *O*-succinimidyl carbamate-coated slides. Covalent attachment of photoaffinity linkers (PAL) containing amine groups (e.g. photoaffinity linker **PAL1** and **PAL2**, **Figure 34**) and blocking of free binding sites with ethanolamine gave photo affinity linker-coated (PALC) slides (**Figure 35**).⁷

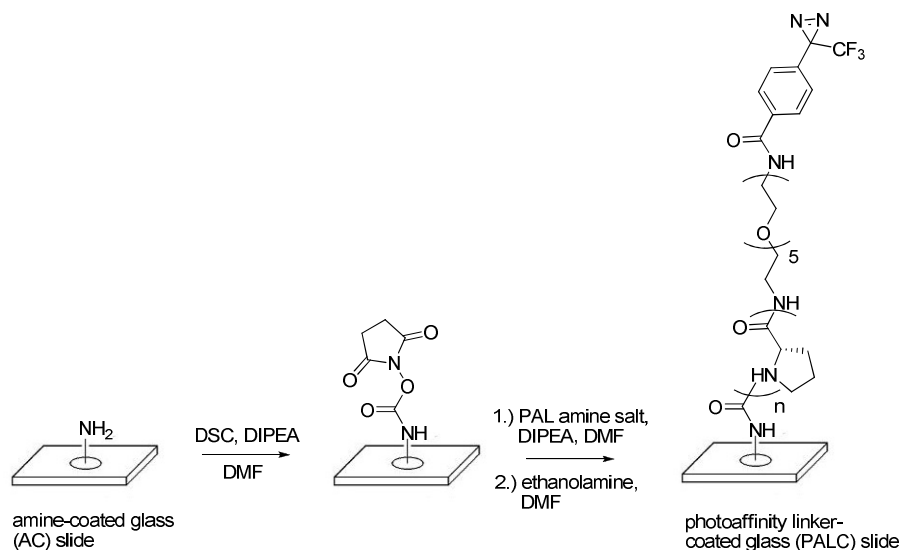


Figure 35: Preparation of PALC slides. PAL1 ($n = 0$), PAL2 ($n = 9$).

Using high-precision printing robots, compounds as DMSO stock solutions were spotted on the surface of PAL-coated slides. After the evaporation of the solvent, the slides were irradiated with UV light, followed by several washing steps. Typically 3,500 compounds were spotted in duplicates on a single glass slide.

1.3 Gold Chip Preparation

Self assembled monolayers (SAMs) on gold are commonly used for immobilizing organic molecules on gold surfaces, thus generating ordered and oriented layers. SAMs offer the opportunity to modify surfaces with controlled morphology and reactivity. Especially thiols have been extensively studied for SAM anchoring on gold surfaces.^{94,95}

In order to investigate small molecule protein interactions *via* SPR measurements, Osada and co-workers employed SAMs of alkanethiolate photoaffinity linkers on gold. Thus UV irradiation enabled functional-group-independent immobilization of small molecules on SPR chips.^{92,93} Synthesis of thiol photoaffinity linker (**PAL3**, **168**) was performed according to literature procedures from **PAL1** (**164**) and alcohol **169** (linker synthesis by K. Honda).⁹³ In order to improve the SPR-signal a mixture of **168** and dummy linker **170** was always used to prepare SAMs. After coating such an SPR chip with **PAL3**, compounds were spotted and immobilized using a similar protocol as for the preparation of glass slides.

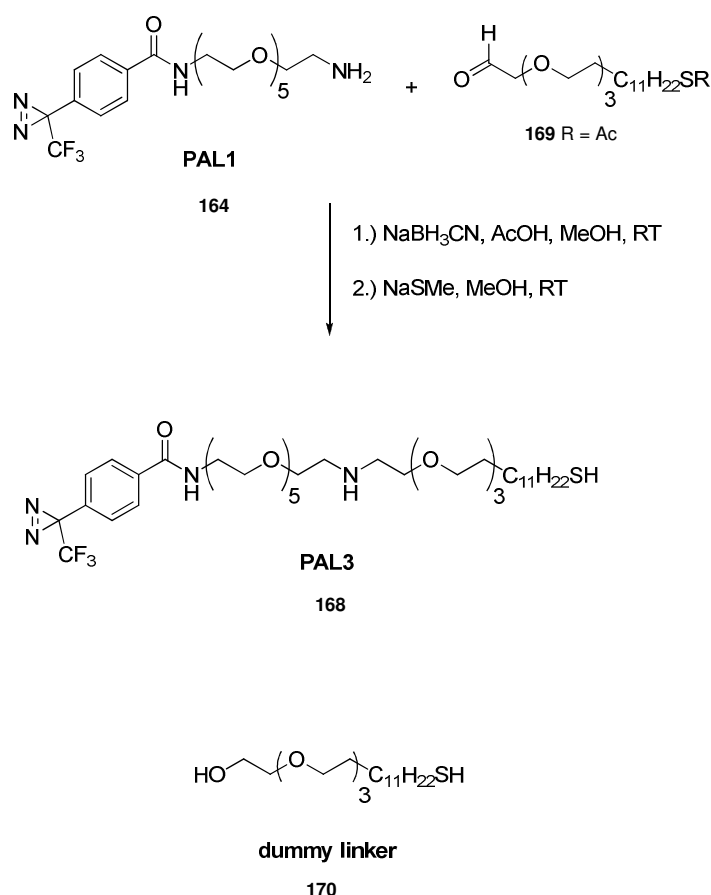


Figure 36: Synthesis of photoaffinity-thiol linker **PAL3** (**168**) from **PAL1** (**164**) and aldehyde **169**.⁹³

1.4 Targeting Ras-Depalmitoylation

The oncogene involved in the Harvey virus causing sarcoma tumor in rats was identified in the 1980s and therefore named H-Ras for Harvey rat sarcoma.^{96,97} Two additional oncogenic Ras isoforms were identified in Kirsten sarcoma viruses and in human Neuroblastoma and named respectively as K-Ras and N-Ras.^{96,98} The Ras subfamily comprising the H-Ras, N-Ras and K-Ras (K-Ras4A and K-Ras4B) proteins forms a group of 21 kDa GTP-regulated molecular switches cycling between a GDP-bound “OFF” and a GTP-bound “ON” state. Ras proteins bind GDP/GTP with high affinity and in the presence of a GTPase-activating protein (GAP) display high GTP-hydrolyzing activity.⁹⁹ Once activated, Ras proteins signal through various cell-signalling pathways involved in cell proliferation (e.g. MAPK).^{100,101} Oncogenic forms of Ras contain point mutations that incapacitate the proteins with respect to GTP hydrolysis.¹⁰² Consequently, the cycling of the switch is inhibited; Ras accumulates in the active form and contributes to tumor formation, due to constant signalling with subsequent gene expression in the nucleus. As many other genes involved in the Ras signal transduction pathway are also found as oncogenes in human or animal tumors, Ras itself and the Ras pathway are thus considered to be prime targets for antitumor therapy.⁹⁹ Indeed, Ras gene mutations occur in 20-30% of all cancers, with K-Ras most frequently mutated (~85%), followed by N-Ras (~15%) and H-Ras (<1%). Ras-mutations have a significant consequence, exemplified by K-Ras mutations found in 90% of all pancreatic cancers.¹⁰⁰

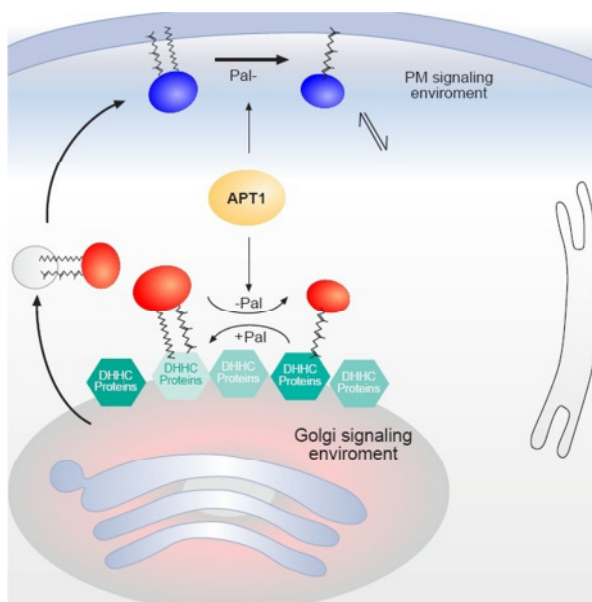


Figure 37: Schematic illustration of the dynamic processes that regulate the localization of Ras isoforms. The acylation/deacylation cycle maintains the specific plasma membrane/Golgi localization of palmitoylated H-Ras or N-Ras.¹⁰³

Members of the Ras superfamily have turned out to be precisely regulated in their cellular localization.¹⁰³ De- and re-palmitoylation,^{104,105} consisting of the reversible removal and attachment of palmitic acid from and to cysteines at the C-terminus of the H- and N-Ras GTPases, manage their membrane anchoring and thus maintain their specific subcellular localization and activity.^{106,107} The cycle of membrane tethering of Ras isoforms by palmitoylation on the Golgi, relocation to the plasma membrane by the secretory pathway and ubiquitous depalmitoylation counteracts unspecific distribution of H/N-Ras over all intracellular membranes by continuous redirection to the Golgi system.¹⁰³ This dynamic cycle accounts for the specific localization of palmitoylated Ras isoforms to the plasma membrane and Golgi apparatus and drives the rapid exchange of both protein pools.¹⁰⁷

Perturbation of the dynamic palmitoylation/depalmitoylation process might provide a new means for the modulation of local Ras activity with potential therapeutic relevance to unregulated signalling in tumors containing mutations in the Ras-encoding gene. Up to now, only three depalmitoylating enzymes have been described: protein palmitoylthioesterase-1 (PPT1), acyl protein thioesterase 1 (APT1) and acyl protein thioesterase 2 (APT2).

PPT1 was first isolated from bovine brain extract, later on also cloned and expressed.^{108,109} It was found important in lysosomal protein degradation by depalmitoylation¹¹⁰ exemplified by PPT1 mutations causing fatal lysosomal storage diseases such as infantile neuronal ceroid lipofuscinosis (INCL).^{111,112}

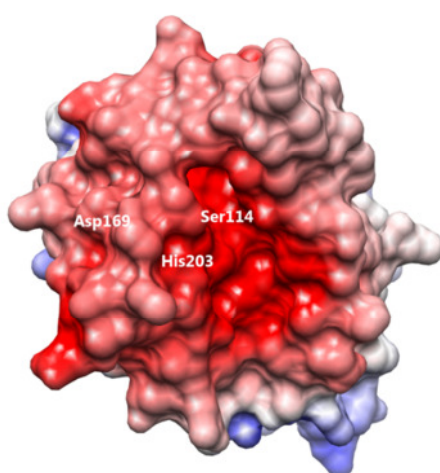


Figure 38: Crystal structure of hAPT1 (PDB-code: ifj2). View of the electrostatic surface potential of APT1. Positively charged regions are shown in blue and negative regions in red. Residues of the catalytic site: Ser114, Asp169, and His203.¹¹³

Human APT1 is a 25 kDa cytosolic¹¹⁴ protein that was originally described¹¹⁴ as a lysophospholipase (LYPLA1) involved in the hydrolysis of lysophospholipids.^{115,116} Lysophospholipids are detergent-

like intermediates of phospholipid metabolism, whose *in vivo* levels must be strictly regulated for proper cell function and survival.¹¹⁷ Recently LYPLA1 was identified as an enzyme with PLA₁ activity that is released from human platelets during blood clotting.¹¹⁸ As demonstrated by Duncan and Gilman, this protein preferentially employs thioacylated proteins as substrates and its name was therefore changed to acyl protein thioesterase 1 (hAPT1).¹¹⁴ In 2000, the crystal structure was solved displaying the tertiary fold of a typical α/β hydrolase with the catalytic site consisting of Ser114, His203 and Asp169, with Ser114 as the nucleophilic residue. hAPT1 shows a distinct negative surface potential surrounding its active site, which is a common feature among esterases and lipases to expulse negatively charged hydrolysis products like palmitic acid (**Figure 38**).¹¹³

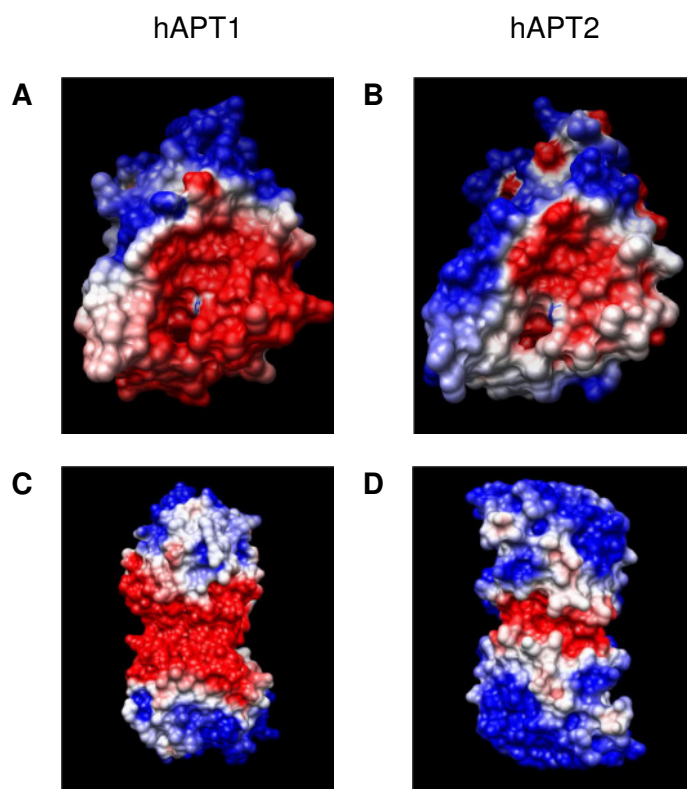


Figure 39: Surface potential of hAPT1 and hAPT2. A/B) Surface potential of hAPT1/hAPT2 monomer. C/D) Surface potential of hAPT1/hAPT2 dimer. Positively charged regions are shown in blue and negative regions in red (work by M. Bürger).

In addition, hAPT1 appears to be dimeric with its active site obstructed by the dimer interface, suggesting the requirement of enzyme dissociation to interact with its substrates. *In vitro* APT1 was found to depalmitoylate a variety of substrates like H-Ras, diverse heterotrimeric G protein α subunits, eNOs, RGS4, SNAP-23, Ghrelin and platelet proteins.^{114,119-123} It was described, therefore, as “the first *bona fide* player” in the regulated thioacylation of intracellular proteins.¹¹⁴ Results by Rocks *et al.*¹²⁴ suggested that no primary consensus sequence at the palmitoylation site of Ras is needed, as a farnesylated/palmitoylated protein with D-amino acids at the palmitoylation site resulted in the natural spatiotemporal pattern of Ras-localization. This finding raises the

question how a cytosolic protein like APT1 recognizes membrane-embedded thioesters and could explain the broad substrate tolerance of APT1 from soluble proteins like the eNOs to transmembrane proteins like SNAP-23.^{124,125} Yet, depalmitoylation does not occur without any discrimination as caveolin was not affected by APT1 in conditions used for eNOs deacylation.^{126,123}

Acyl protein thioesterase 2 (APT2) or lysophospholipase 2 (LYPLA2) was purified from pig stomach,¹²⁷ afterwards cloned and expressed.¹²⁸ With 66% sequence identity and especially a conserved catalytic triad hAPT2 is a close homologue of hAPT1. Like APT1, APT2 is dimeric with its catalytic site occluded by the dimer interface (**Figure 39**). The superimposition of the APT1 and APT2 crystal structure visualizes the similarity of the two proteins (**Figure 40**). However, the electrostatic potential reveals significant differences between the two proteins. In close proximity of their active sites, APT2 is substantially more hydrophobic than APT1 (**Figure 39**).

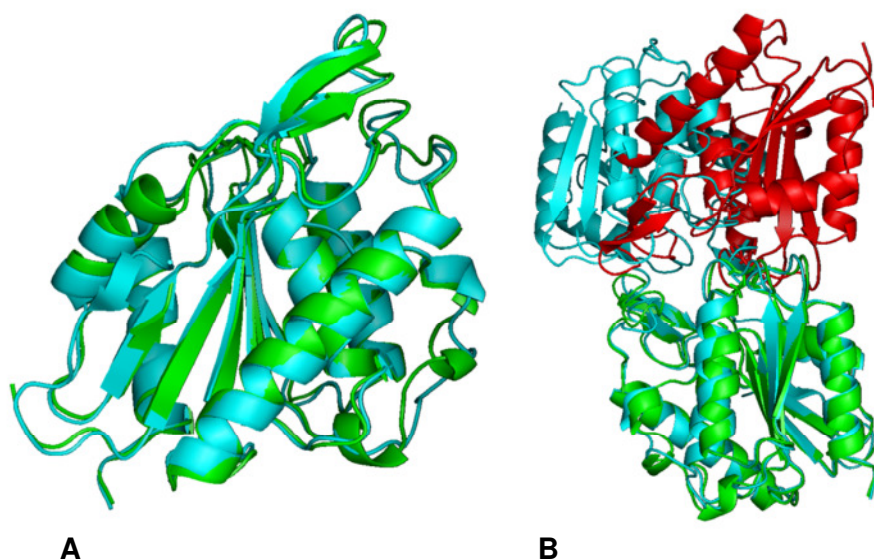


Figure 40: Superimposition of hAPT1 and hAPT2. A) Crystal structure overlay of APT1 and APT2 monomers. Green: hAPT2, blue: hAPT1. B) Crystal structure overlay of APT1 and APT2 dimers, with their catalytic site obstructed by the dimer interface. Green/red: hAPT2, blue: hAPT1 (work by M. Bürger).

Tomatis *et al.* observed increased depalmitoylation of GAP-43 (growth-associated protein 43) in APT2 overexpressing cells, indicating that APT2 may be involved in GAP-43 depalmitoylation, while no effect was perceived with cells overexpressing APT1. Furthermore, the authors suggest the involvement of APT2 in H-Ras depalmitoylation.¹²⁹ However, *in vivo* proof for the participation of APT2 in Ras depalmitoylation is still lacking.

Initially, based on a reverse chemical genetics approach, Waldmann and co-workers designed inhibitors antagonizing the biological function of APT1. As human H-Ras protein is a substrate for APT1 *in vitro*, inhibitors were designed to mimic the C-terminus of the natural protein. A

peptidomimetic benzodiazepinedione core was chosen as the underlying scaffold and equipped with a hydrolysis-stable sulfonamide to mimic the transient tetrahedral intermediate of thioester hydrolysis. However, no *in vivo* effects could be observed for this class of inhibitors.^{130,131}

In a more recent study, protein structure similarity clustering (PSSC)^{25,30} exploiting the highly conserved character of APT1,¹¹⁴ was used to develop APT1 inhibitors as chemical biology tools to investigate the role of APT1 and its relevance to Ras depalmitoylation. In analogy to the known gastric lipase inhibitor tetrahydrolipstatin a compound library was synthesised harbouring an electrophilic β -lactone core in order to trap the nucleophilic catalytic serine residue. Extensive screening efforts led to the development of potent inhibitors like palmostatin B (**171**) (**Figure 41**).

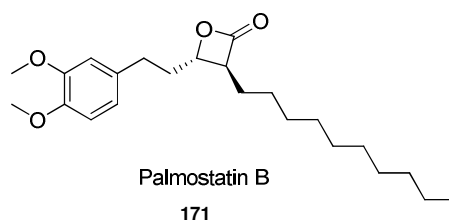


Figure 41: Structure of Palmostatin B (171). ($IC_{50} = 670$ nM). The IC_{50} value was obtained employing a colorimetric assay using 4-nitrophenyl octanoate (PNPO) as substrate (APT1: 75 nM, PNP: 600 μ M, 30 min inhibitor pre-incubation).¹³²

Dekker *et al.* could show that the inhibition of cellular thioesterase activity, which accounts for depalmitoylation, causes an entropy-driven loss of the precise steady-state localization of palmitoylated Ras proteins and, as a consequence, down-regulates rather than impairs the downstream signalling activity of oncogenic Ras. Additionally, after treatment of cells with palmostatin B (**171**), a partial phenotypic reversion was induced in H-RasG12V-transformed MDCK-F3 cells with restoration of E-cadherin expression at the cell-cell interfaces, while K-Ras transformed control cells were unaffected. The authors thus proposed APT1 inhibition as a potential strategy for the development of new anti-cancer drugs.¹³²

2 Aims

According to their amino acid sequence identities the human acyl protein thioesterases APT1, APT2 and the protein lysophospholipase-like 1 (LYPLAL1) belong to two different subclasses of the lysophospholipase family, which is in turn a subclass of the α/β hydrolases superfamily.¹³³ A BLAST (Basic Local Alignment Search Tool) search with LYPLAL1 finds acyl protein thioesterases as closest relatives. All three proteins possess a catalytic triad consisting of a serine, an aspartate and a histidine. The overlay of the crystal structures of the three proteins illustrates the very similar fold of the proteins (**Figure 42**). While APT1 has been identified as prime regulator of Ras palmitoylation,¹³² the biological function of APT2¹²⁸ (lysophospholipase II) and especially LYPLAL1 remain essentially unknown.

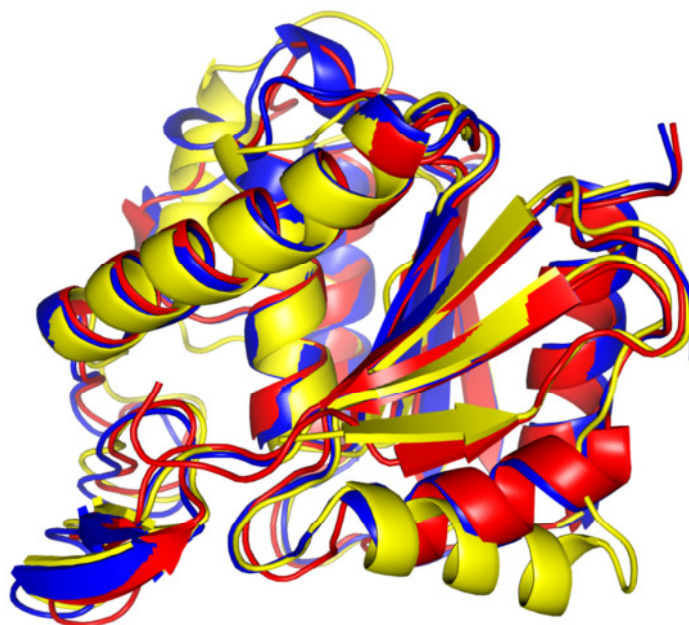


Figure 42: Superimposition of the crystal structures of hAPT1, hAPT2, and hLYPLAL1 (PDB code: 3U0V).¹³⁴ The structures are shown as cartoon representations. APT1 is colored in red, APT2 in blue, and LYPLAL1 in yellow (work by M. Bürger).

The tight relationship between the LYPLAL1 and APT1 families, the presence of the catalytic triad and the very similar fold of the proteins implicate a cellular function of LYPLAL1 comparable to APT1. However, LYPLAL1 was also suggested to act as a triglyceride lipase in adipose tissue;¹³⁵ some studies revealed a link between the *lyplal1* gene locus and the waist-hip ratio of study participants,^{136,137} others indicated an involvement in fat distribution¹³⁸ and non-alcoholic fatty liver disease.¹³⁹ So far, neither the biological function of LYPLAL1, nor any small molecule inhibitors for this protein have been investigated.

In summary, the three proteins APT1, APT2 and LYPLAL1 constitute an interesting group of proteins and small molecule inhibitors would provide a highly desirable tool box, both for chemical biology ventures as well as for medicinal purposes. Small molecule microarray screening of immobilized structurally diverse natural products and derivatives could provide a high-throughput chemical profiling of the three proteins by the means of finding small molecules that show high-affinity binding.

Chemical array screening should first be validated using known inhibitors (for APT1 and 2) and screening conditions optimized. Therefore a “validation array” (referred to as MPI array) had to be constructed containing known β -lactone inhibitors¹⁴⁰ (nanomolar inhibitors of APT1 and 2). Finally proteins were subjected to a structurally diverse library of compounds. As natural products portray a very prominent field in total chemical space, the chemical library “RIKEN Natural Products Depository (RIKEN NPDepo)” including approximately 13,000 compounds mainly consisting of secondary metabolites isolated from actinomycetes, fungi, plants and other organisms was chosen.¹⁴¹ Microarray screening was performed with tagged protein (GST-tag) and in order to validate screening results, SPR imaging was used to observe protein-ligand interaction with tag-free protein in real time. As follow-up experiments APT1 and APT2 binders were subjected to a biochemical functional analysis in an enzymatic test system. For LYPLAL1 such a test system had to be developed first.

3 Results and Discussion

Microarray experiments were performed at the RIKEN Advanced Science Institute in Wako, Japan under supervision of Prof. Dr. H. Osada with the help of Dr. Yasumitsu Kondoh, Kaori Honda and Motoko Uchida.

3.1 Array Validation and Optimization

In order to validate the array screening results, known inhibitors were included on the “MPI array” (about 500 compounds from the MPI Dortmund), that was used for the optimization of screening conditions. Palmostatin B (**171**)¹³² and four other second generation β -lactone inhibitors (**Figure 43**) were chosen as they are nanomolar inhibitors with equal potency for APT1 and 2.^{142,140}

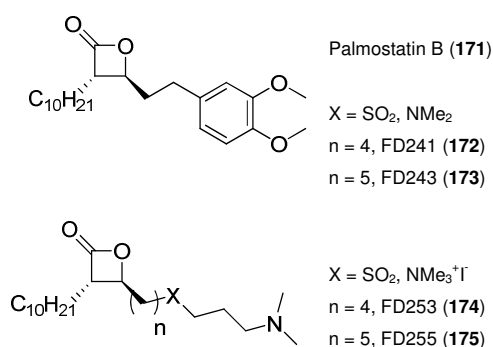


Figure 43: Palmostatin B and second generation β -lactone inhibitors.

For the first optimization round, standard PEG-slides (coated with **PAL1** linker, **164**) and two different APT1 protein concentrations, 5 nM (concentration of enzymatic APT1 assay) and 1 μ M were used for protein incubation. Two different incubation methods were examined; the cover slide method and the Agilent chamber incubation method. In the cover slide method the array slide was covered by a glass slide and incubated using 50 μ L of protein solution in buffer. In contrast, employing the chamber method, the array glass slide was covered by an Agilent Technologies Gasket slide using 500 μ L of protein solution. The covered array slide was then incubated in a special chamber that allowed the rotation of the slide.

Bound proteins were visualized by an antibody detection system. As GST labelled proteins were used throughout, firstly - after protein incubation and washing - array slides were treated with an anti-GST antibody from rabbit. As second antibody a species specific (anti-rabbit) Cy5 labelled antibody was used. Consequently protein bound to the small molecule microarray resulted in a

fluorescent signal (670 nm) after excitation at 650 nm (for a visualization of this detection method see **Figure 32d**).

The immobilized β -lactones (**Figure 43**) could be detected at either protein concentration, though the level of fluorescence was rather low in the case of 5 nM protein. Further, the influence of the used linker (**PAL2** linker, **165**) and the protein incubation method (Agilent chamber incubation) was evaluated, but none of the conditions led to further improvements. PEG-slides (**PAL1** linker, **164**) with cover slide incubation of APT1 (1 μ M) was selected as method of choice as it resulted in nicely analysable data with high signal-to-noise ratio. The same conditions were used for APT2 and LYPLAL1. As illustrated in **Figure 44** and **Figure 45**, β -lactone derivatives show almost equal binding affinity for APT1 and 2 on the chemical array. In order to compare the fluorescence signal of the three proteins, the signal was referenced to the glutathione signal. As immobilized glutathione binds to the GST-tag of the proteins its fluorescence therefore reflects a distinct signal for each protein and viable reference point. The equal potency of the β -lactone inhibitors for APT1 and 2¹⁴⁰ on the enzymatic level is also reflected in the fluorescent values of array binding affinity. The fluorescent values of LYPLAL1 show, in comparison to APT1 and 2, at least one order of magnitude lower affinity for the β -lactones. Very remarkably is the selectivity of Palmostatin B, which does not bind to LYPLAL1 at all. As demonstrated in this validation experiments, the chosen screening conditions are able to identify known inhibitors as potent protein binders. For further screening experiments these conditions were thus applied.

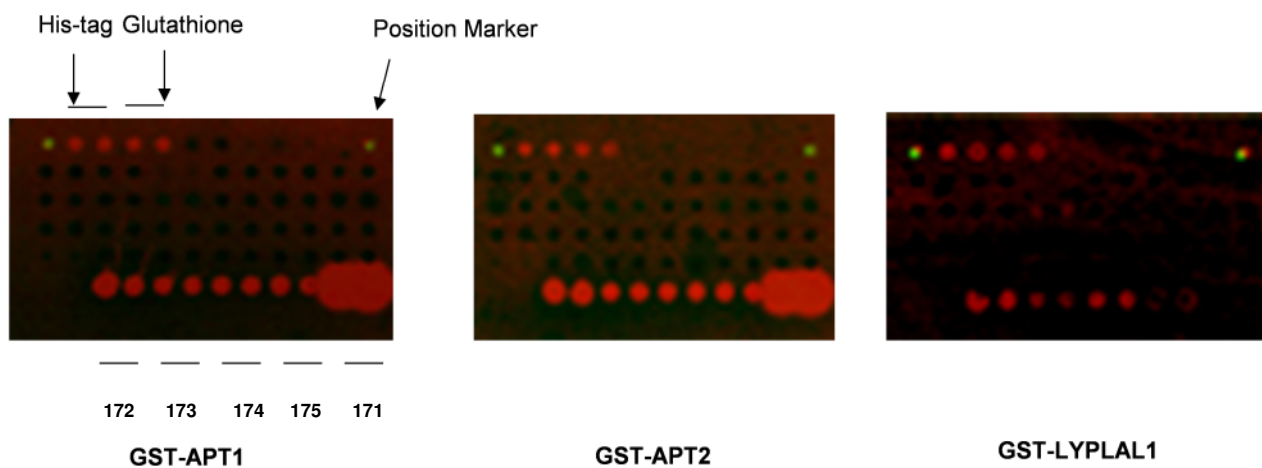


Figure 44: Picture of fluorescent spots at PMT-gain: 200. Compounds were spotted in double spots from left to right (172, 173, 174, 175, 171). After incubation with GST-protein, array slides were treated with anti-GST antibody from rabbit, followed by species specific (anti-rabbit) Cy5 labelled antibody. Cy5 labelled antibody was visualized by excitation at 650 nm and emission at 670 nm.

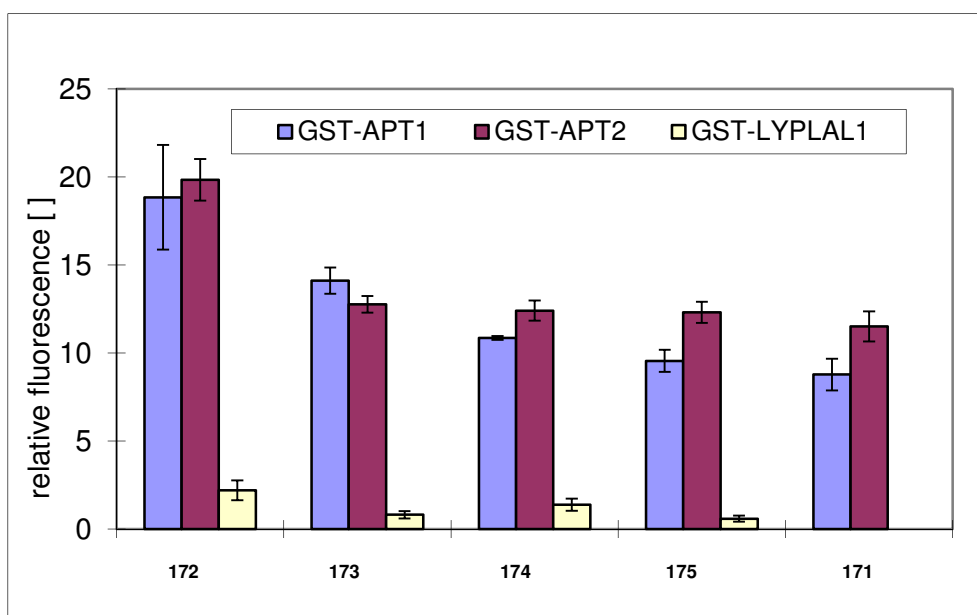


Figure 45: Comparison of GST-APT1, GST-APT2 and GST-LYPLAL1. Fluorescent values (fluorescence of Cy5 labelled antibody) were averaged from four spots on MPI array and referenced to Glutathione. Protein concentration: 1 μ M, PMT-gain: 200.

3.2 Screening of NPDepo

Compounds of RIKEN Natural Products Depository (NPDepo) were immobilized on **PAL1 (164)** coated glass slides in duplicates. In total, 12,356 compounds from NPDepo (slides A+B: 6,884; G+H: 5,472) were screened on the three GST-proteins using a GST-specific antibody for detection of bound protein.

After incubating the glass arrays with the corresponding protein, slides were successively treated with first (GST-specific) and secondary (species specific) Cy5 labelled antibodies. The dried slides were then scanned using a fluorescence scanner. For data analysis the fluorescence intensity of each spot was corrected by the local background and by a blank control. After analysis of the screening data, frequent hitters (showing binding affinity in more than 5% of the so far at RIKEN screened proteins) were removed. Data analysis revealed several hits. In order to fingerprint the chemical binding profile of the corresponding protein, all selected hit compounds from primary NPDepo screening were spotted on a single PALC-slide and binding of GST-protein was detected with an anti-GST and secondary antibody. Initial screening hits (from NPDepo slides A, B, G, H) were complemented by representative borinic acid derivatives (**176-180**) that were selected from 31 hits found on NPDepo slide F (compounds from RIKEN Brain Science Institute¹⁴³) and three boronic acids (**190-192**) with known micromolar APT1 inhibitory activity. As control compound glutathione was selected as it allows referencing the fluorescence intensity of each protein (fluorescence was set to 1000). The fingerprint of the three proteins reflects the similarity of APT1 and 2 with almost identical binding profiles and LYPLAL1 with a distinctly different binding pattern (**Figure 46**).

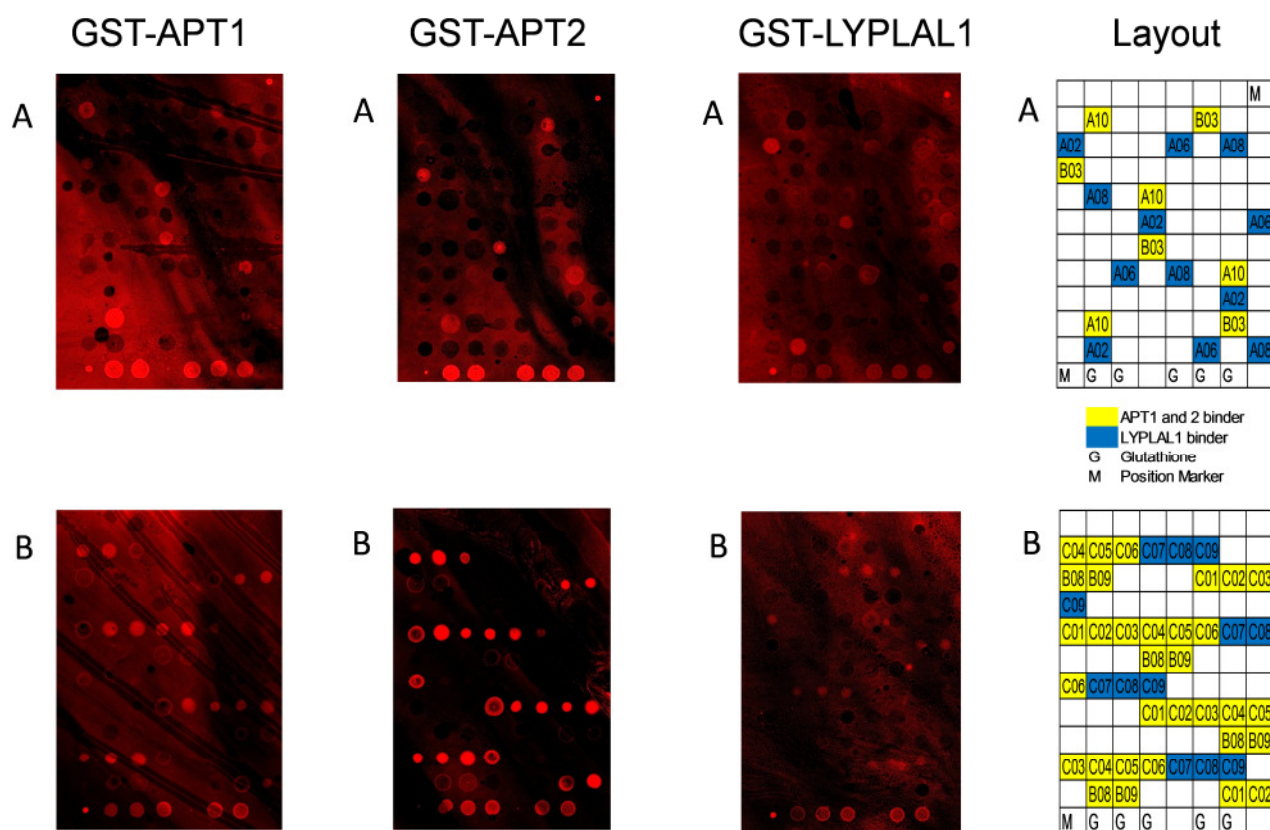


Figure 46: Comparison of GST-APT1, GST-APT2 and GST-LYPLAL1 binding profiles. Compounds were spotted on PALC-glass microarray in two different layouts (layout A and B). Protein concentration: 1 μ M, PMT-gain: 300.

As depicted in **Figure 47** various small molecules binding to GST-APT1 and GST-APT2 could be identified. Representatives of bis-borinic acids and bis-borinate esters bound APT1 and APT2 rather strongly (**176**, **177**, **178**, **179**, **180**). The pancreatic lipase inhibitor tetrahydrolipstatin (**181**) – a known obesity drug – that served as lead compound for the development of β -lactone APT1 inhibitors¹³² – was also identified with strong APT1 and 2 binding but minor LYPLAL1 binding (primary screen). Further microarray binders include **182**, nizatidine (**183**), **184** and analogues of the APT1 and 2 fluorescent substrates (**185**, **186**).

For LYPLAL1 a rather limited amount of compounds was detected on chemical array. In addition, the detected fluorescence was rather low. Nevertheless, besides pipemidic acid (**187**), **188**, 4,4'-[1,3-phenylenebis(oxy)]diphthalic acid (**189**), also three boronic acids (**190**, **191**, **192**), that were not detected with APT1 and 2, showed binding activity (**Figure 48**).

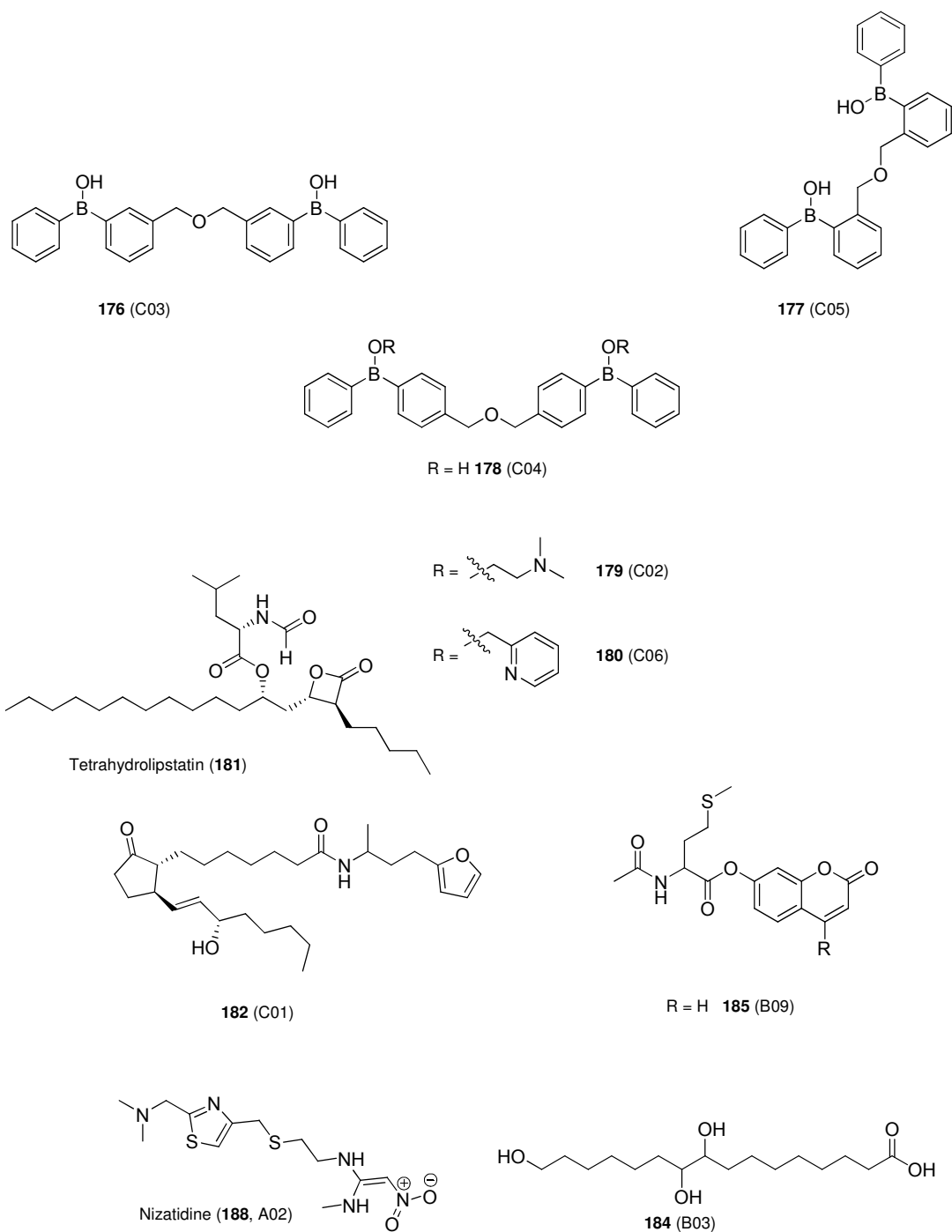


Figure 47: APT1 and APT2 binders. Small molecule binders of GST-APT1 and GST-APT2. Number in brackets indicates position on array.

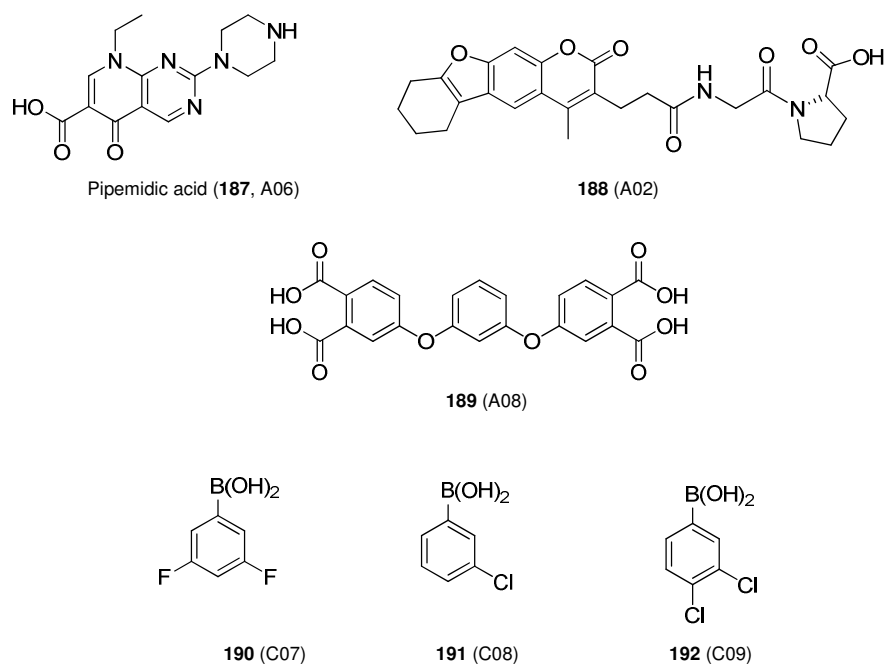


Figure 48: LYPLAL1 binders. Structures of small molecules binding to GST-LYPLAL1.

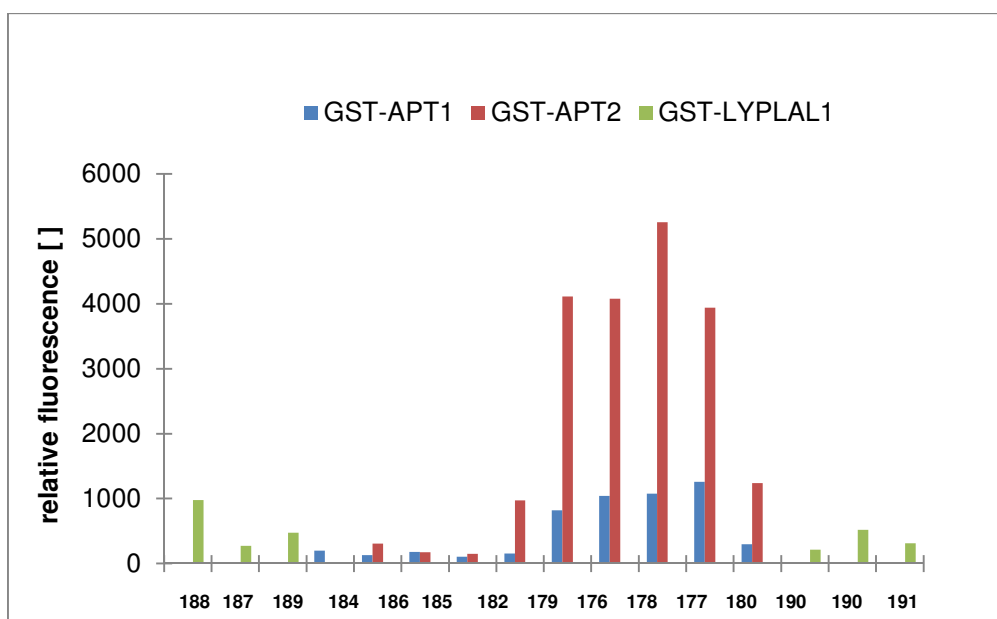


Figure 49: Binding profile of GST-proteins. Fluorescence values referenced to glutathione.

3.3 Boron Compounds as APT1 and 2 Inhibitors

Compounds that were detected upon small molecule microarray screening using GST-tagged proteins were also subjected to SPR-analysis with GST-free protein. SPR binding assays on gold chips can detect protein small molecule interaction in real time and therefore are often used to supplement and validate results from chemical arrays. All hits from the primary screen of NPDepo were printed with identical layout on glass array and SPR-chip to directly compare the two methods. **Figure 50** depicts the hit validation using SPR-analysis. The control compounds, the known β -lactone inhibitors palmostatin B (**171**), FD241 (**172**) and tetrahydrolipstatin (**181**) could as expected be confirmed as APT1 and APT2 binders in both microarray and SPR-analysis.

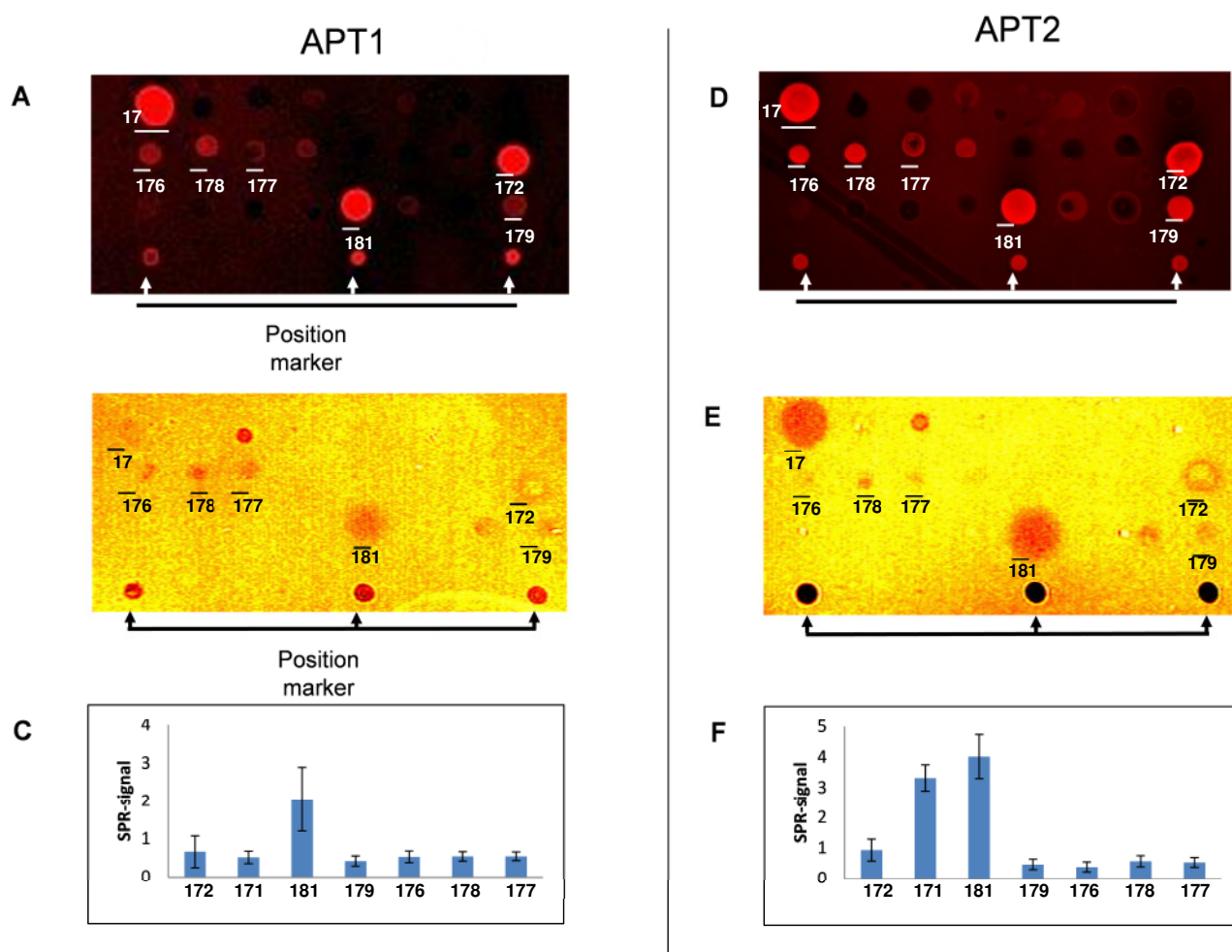


Figure 50: Validation of Microarray Hits using SPR-Analysis. A and D: Small molecule microarray data of GST-APT1 and GST-APT2. B and E: SPR-Analysis of APT1 and APT2. C and F: SPR-Signal of APT1 and APT2. Known β -lactone inhibitors 171, 172 and 181 were identified as APT1 and APT2 binders in both microarray and SPR-analysis. Bis-boron compounds (176-179) could also be confirmed upon SPR-analysis.

Out of the already limited number of APT1 and APT2 binders (**Figure 47**) an even smaller number of compounds could also be identified on SPR-chip. Interestingly, the bis-boron compounds (**176-179**) that already displayed rather strong binding signals on chemical array (see **Figure 50 A and D**) could likewise be detected on SPR-chip (see **Figure 50 B, C and E, F**). The detected bis-borinic acids and borinate esters (**176-179**) are cell penetrating¹⁴³ small molecules that were originally synthesised to inhibit store-operated calcium entry (SOCE), that is an important mechanism for replenishing intracellular calcium stores and sustaining calcium signalling.¹⁴³

In order to test if the small molecules identified upon microarray screening experiments impair the enzymatic activity of APT1 and APT2 a fluorometric assay detecting the release of 6,8-difluoro-4-methylumbelliferol (DiFMU) from 6,8-difluoro-4-methylumbelliferyl octanoate (DiFMUO) was applied. For APT1 the previously known conditions could be used (5 nM APT1, 15 μ M substrate),¹⁴⁰ but for APT2 the assay conditions had to be adapted due to the lower catalytic efficiency of APT2 towards the substrate (50 nM APT2, 15 μ M substrate) (**Table 9**).

Table 9: Kinetic data for human APT1 and APT2. Data determined in a fluorescent assay with DiFMUO as substrate. Protein concentration was chosen to be 5 nM (APT1) and 50 nM (APT2).

Kinetic Data	APT1	APT2
K_m [μ M]	6.1 ± 0.8	2.1 ± 0.6
v_{max} [nmol/s]	1.3 ± 0.05	0.7 ± 0.05
K_{cat} [s^{-1}]	0.26	0.014
K_{cat}/K_m [$s^{-1}mM^{-1}$]	43	6.7

All identified microarray APT1 and APT2 binders (**Figure 47**) were tested towards their inhibitory potency in the above described enzymatic assay at 50 μ M (note: out of the bis-boron compounds only **179** could be provided from RIKEN for biochemical studies). However, from these compounds only compound **179** did show an inhibitory effect at 50 μ M. Further measurements revealed an IC_{50} for both proteins in the low micromolar range (**Table 10**).

Table 10: IC₅₀ of APT1 and APT2 inhibitors.

compound	IC ₅₀ [nM] APT1	IC ₅₀ [nM] APT2
palmostatin B (171)	5.37 ± 0.38	19.58 ± 0.87
FD241 (172)	2.13 ± 0.13	36.74 ± 2.35
tetrahydrolipstatin (181)	549 ± 171	408 ± 211
179	3,300 ± 200	979 ± 58

In order to investigate the inhibition mode of **179**, Lineweaver-Burk analysis was performed. This is a double-reciprocal presentation of the Michaelis-Menten equation (**Equation 1**) where the reciprocal velocity of the reaction is plotted as a function of the reciprocal substrate concentration. The graph therefore intersects the x-axis at $-1/K_m$ (negative reciprocal Michaelis-Menten constant K_m) and the y-axis at $1/v_{max}$ (reciprocal maximal reaction velocity), which can be read directly from the graphical plot. In the competitive inhibition substrate and inhibitor compete for the active site of the enzyme. Therefore the affinity between substrate and enzyme at a certain inhibitor concentration appears to be lower and therefore K_m is higher while the maximum velocity does not change. In the double-reciprocal presentation competitive inhibition is consequently reflected in intersecting lines on the y-axis.

$$v = v_{max} \frac{[S]}{K_m + [S]}$$

v_{max} : maximal velocity

[S]: substrate concentration

K_m : Michaelis-Menten constant

Equation 1: The Michaelis-Menten equation

Equation 1 is converted to:

$$\frac{1}{v} = \frac{K_m + [S]}{v_{max}[S]} = \frac{K_m}{v_{max}} \frac{1}{[S]} + \frac{1}{v_{max}}$$

Equation 2: Linearized Michaelis Menten equation.

Lineweaver-Burk analysis of **179** on APT1 (**Figure 53**) and APT2 (**Figure 53**) revealed a competitive inhibition mode, the same mechanism already observed for other boron compounds that had been shown to inhibit β -hydrolases like porcine pancreatic lipase, presumably through complex formation with the active site serine residue.¹⁴⁴ Thus the K_i -values for **179** were determined to be $0.99 \pm 0.13 \mu\text{M}$ for APT1 and $0.73 \pm 0.20 \mu\text{M}$ for APT2 (**Table 11**). These values

are in the same magnitude as when calculated with non-linear curve fitting (APT1: $1.53 \pm 0.34 \mu\text{M}$ and APT2: $1.10 \pm 0.30 \mu\text{M}$). (Figure 51)

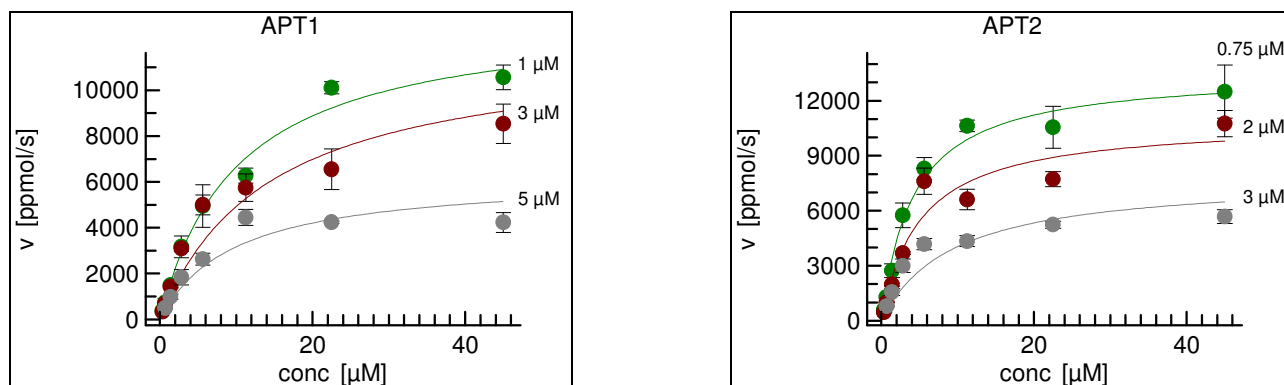


Figure 51: Non-linear curve fitting using different concentrations of compound 179.

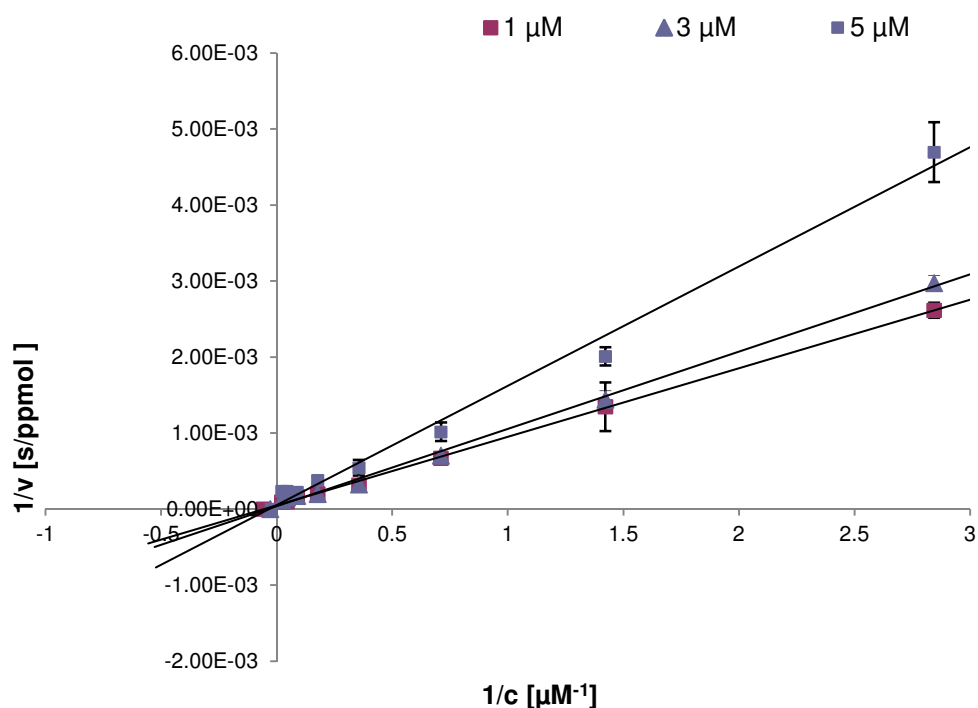


Figure 52: Lineweaver-Burk analysis of bis-boron compound 179 on APT1.

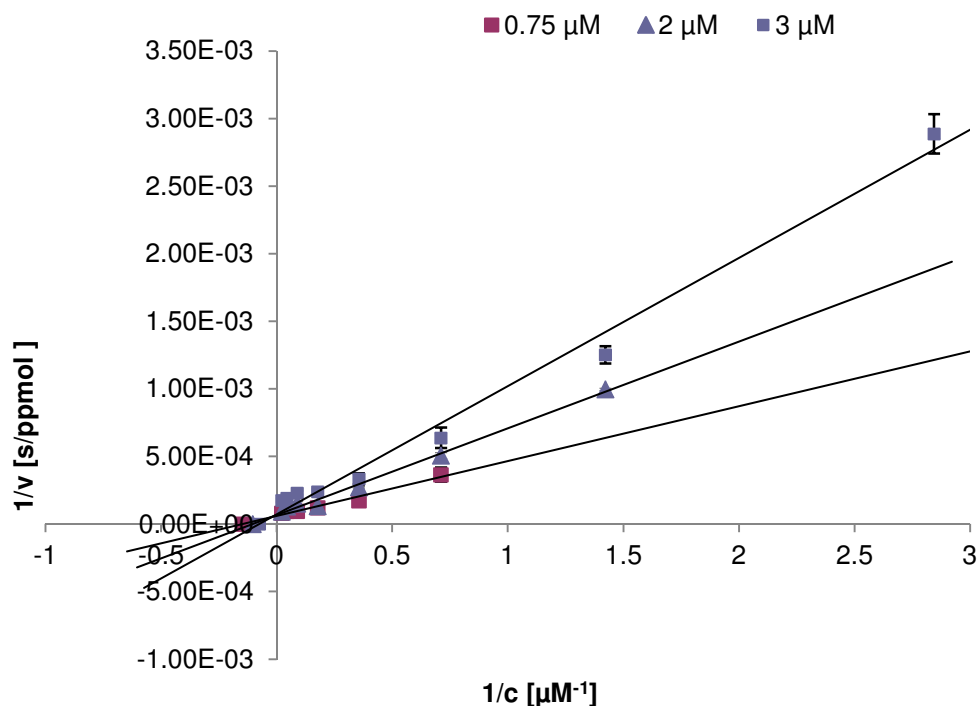


Figure 53: Lineweaver-Burk analysis of bis-boron compound 179 on APT2.

Table 11: Calculation of K_i .

APT1	K_M [μM]	K_i [μM]	mean K_i [μM]
1 μM	17.86	0.88	0.99 ± 0.13
3 μM	35.71	0.91	
5 μM	43.48	1.18	

APT2	K_M [μM]	K_i [μM]	mean K_i [μM]
0.75 μM	6.75	0.45	0.73 ± 0.20
2 μM	9.62	0.83	
3 μM	13.51	0.91	

Acyl Protein Thioesterase 1 (APT1) is an α/β -hydrolase¹¹³ containing an active serine in the catalytic site that was shown to be irreversibly targeted by β -lactones.¹³² Another way of reversibly trapping nucleophilic residues in enzyme catalytic sites and hence impairing the enzymatic function

involves the use of boronic acids. Boronic acids were reported to inhibit β -hydrolases like porcine pancreatic lipase. Garner reported that boronic acids are potent inhibitors of lipase action at substrate-water interfaces, presumably through complex formation with the active center serine.¹⁴⁴ A classical example for a boronic acid used in the clinic is the first approved proteasome inhibitor Bortezomib - a tripeptide where leucine contains a boronic acid function instead of a carboxylic acid function. The boron atom binds the catalytic site of the 26S proteasome with high affinity and specificity.¹⁴⁵ Inspired by the finding of bis-boron compound **179** as a low micromolar inhibitor of APT1 and APT2 various simple, sterically less demanding, small aliphatic and aromatic boronic acids were screened on APT1 using the fluorescent activity assay. Therefore, a set of simple aliphatic and aromatic boronic acids of commercial and synthetic origin (kindly provided by Prof. Dr. Dennis Hall) was assembled and screened on APT1.¹⁴⁰

As shown in **Table 13** phenyl boronic acids with electron withdrawing groups (e.g. **190**, **191** or **192**) and therefore increasing electrophilicity of the nucleophile trapping boron atom did show the most potent inhibition of APT1. Less electron rich unsubstituted phenyl boronic acid **202** did inhibit less, or in the case of bulky phenylboronic acids **203** and **204**, not at all. Testing the boronic acids on APT2 showed similar inhibition patterns as that for APT1. Some boronic acids even inhibited in the low nanomolar range (**192-194**).

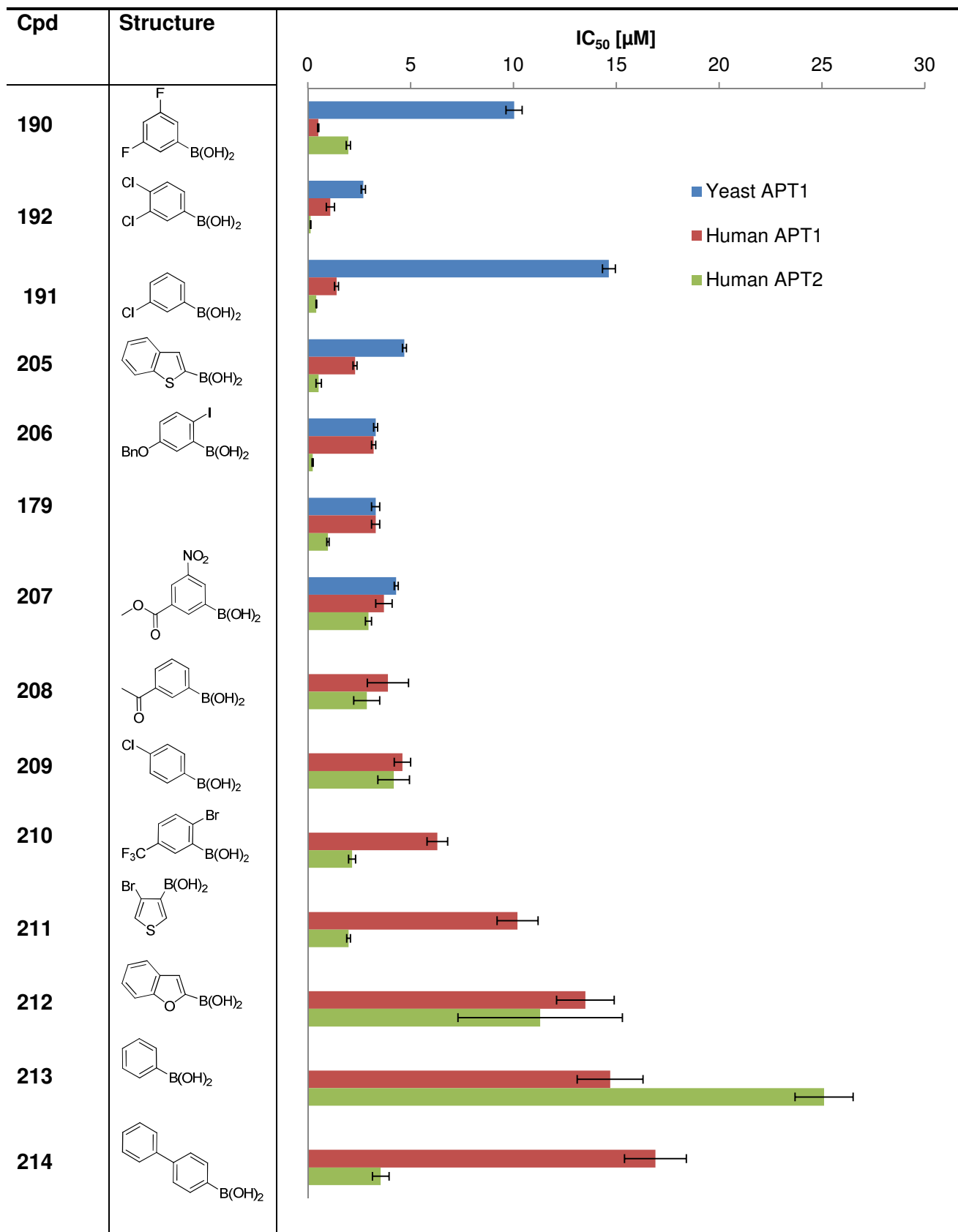
Table 12: Kinetic solubility, as determined by a direct LC/MS based measurement (assay well: 50 μ M). Cell permeability, as determined by a parallel artificial membrane permeability assay (PAMPA). Flux [%] denotes concentration (test well)/concentration (control well) \times 100. Data measured by the Lead Discovery Center, Dortmund.

compound	Solubility [μ M]	PAMPA flux [%]
190	42.3	64.5
191	37.6	60.7
192	32.0	20.6

Physicochemical studies, including parallel artificial membrane permeability assays (PAMPA)¹⁴⁶ revealed that boronic acids possess moderate (**192**) to excellent cell permeability (**190**, **191**) and favourable solubility properties (**Table 12**).

Table 13: IC₅₀ values for different phenylboronic acids.

Cpd	ID	Structure	IC ₅₀ [μM] APT1	IC ₅₀ [μM] APT2
190	BA4		0.51 ± 0.03	1.97 ± 0.10
192	BA23		1.1 ± 0.2	0.138 ± 0.013
191	BA22		1.4 ± 0.1	0.418 ± 0.013
193	BA13		2.3 ± 0.1	0.529 ± 0.133
194	BA74		3.2 ± 0.2	0.238 ± 0.025
195	BA37		3.7 ± 0.4	2.95 ± 0.15
196	BA14		3.9 ± 1.0	2.87 ± 0.63
197	BA05		4.6 ± 0.4	4.18 ± 0.77
198	BA36		6.3 ± 0.5	2.16 ± 0.17
199	BA62		10.2 ± 1.0	1.98 ± 0.09
200	BA49		13.5 ± 1.4	11.3 ± 4.0
201	BA03		14.7 ± 1.6	25.1 ± 1.41
202	BA16		16.9 ± 1.5	3.55 ± 0.40
203	BA35		> 50	> 50
204	BA29		> 50	> 50

Table 14: Graphical representation of IC₅₀ values for APT1, APT2 and selected yAPT1 values.

Although several APT inhibitors^{131,130,132,142,140} are known, no structural data elucidating the exact binding of the small molecule inhibitors has been obtained. Indeed, several attempts to obtain co-structures of APT1 with small molecule inhibitors (work by Marco Bürger) have not been successful and, so far, other groups did not present APT1 co-crystal structures either. These issues most likely originate from the solvent-inaccessible active site that is totally shielded by the dimer interface.¹⁴⁷ The venture for a suitable crystallographic model system for APT1 led Marco Bürger, Arthur T. Porfetye and Dr. Ingrid R. Vetter to the identification of APT1 from *Saccharomyces cerevisiae*, which possesses a completely accessible active site, but possesses a fold that is highly identical to its human relative. Furthermore, it could be demonstrated that yeast APT1 has comparable biochemical properties to human APT1 and is also able to depalmitoylate human N-Ras *in vitro* (shown by Dr. Kristina Görmer). Of interest is that boronic acids identified *via* enzymatic screening on human APT1 did inhibit yeast APT1 to comparable extent (significant aberrations for **190** and **191**). Arthur T. Porfetye succeeded in co-crystallizing the identified inhibitors with yAPT1, confirming the proposed mode of action.

Table 15: Comparison of yAPT1 and hAPT1. IC₅₀ data for the bis-boron compound 179, boronic acids 192, 194, 195, 193 were measured for both yAPT1 and hAPT1. Data for yAPT1 were obtained by Arthur T. Porfetye.

Compound	IC ₅₀ yAPT1 [μM]	IC ₅₀ hAPT1 [μM]
192	2.7 ± 0.1	1.1 ± 0.2
194	3.3 ± 0.1	3.2 ± 0.2
179	3.3 ± 0.2	3.3 ± 0.2
195	4.3 ± 0.1	3.7 ± 0.4
193	4.7 ± 0.1	2.3 ± 0.1

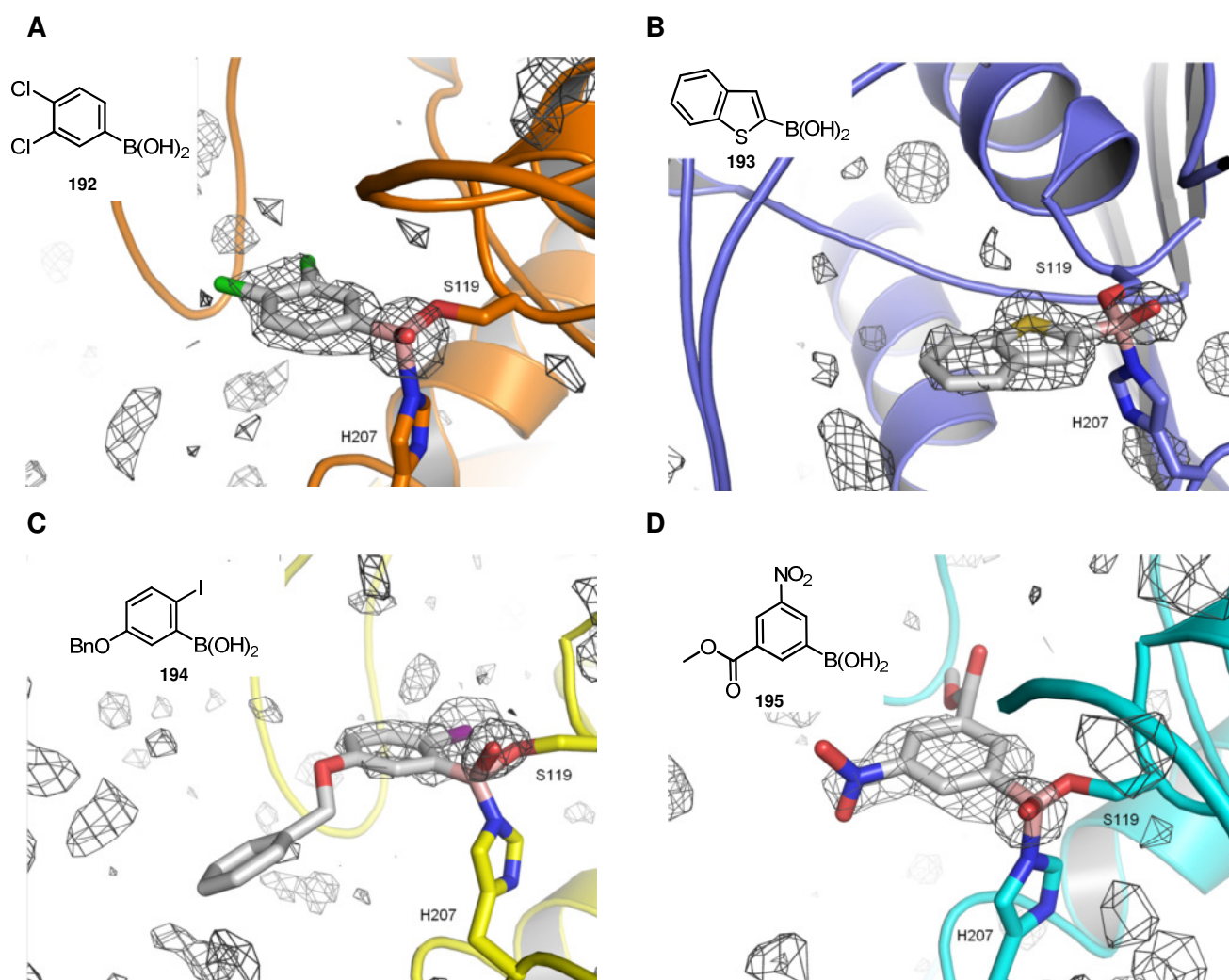


Figure 54: Crystal structures of yAPT1 with bound boronic acid. Resolution of SLS data sets: 193: 1.9 Å, 192: 1.85 Å, 195: 2.00 Å, 194: 1.75 Å (work by Arthur T. Porfetye).

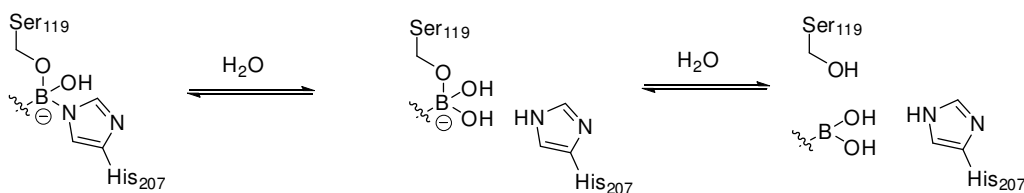


Figure 55: Proposed binding model for boronic acid inhibition.

According to the crystal structures (**Figure 54**) boronic acid inhibitors form a tetrahedral complex with serine 119 and histidine 207, thus inactivating the enzyme's active site. However, these enzyme-inhibitor complexes are in equilibrium with the free boronic acid (**Figure 55**). These compounds therefore constitute a class of covalent, but reversible, inhibitors. This feature renders boron compound very promising, as the known β -lactone APT1 and APT2 inhibitors that likewise covalently bind to the catalytic serine 119 are destroyed upon hydrolysis. Therefore, the inhibitory effect is diminished either by auto-hydrolysis of the β -lactones in aqueous media or by enzyme

hydrolysis, while for boron compounds such an inactivation does not take place. To further characterize these inhibitors, an *in vitro* inhibition assay was performed by Dr. Kristina Görmer using boron compound **179**, APT1 as a deacylating enzyme and palmitoylated N-Ras as a substrate. Briefly, after incubation of the inhibitor with N-Ras and APT1, the release of fatty acid was monitored with ADIFAB which in the presence of free fatty acid changes its fluorescent spectrum, thereby allowing the calculation of free palmitic acid.¹⁴⁸ Indeed, N-Ras depalmitoylation by APT1 was inhibited completely at 50 μM of **179**, indicating the potent *in vitro* inhibition of APT1. In an LDH-toxicity test none of the tested boron compounds did exert toxic effects at 50 μM or below. Furthermore, MDCK cells were subjected to boron compounds and the inhibition of downstream ERK-phosphorylation was checked. Compound **179** displayed a complete inhibition of ERK-phosphorylation at 30 and 15 μM (work by Nancy E. Martinez).

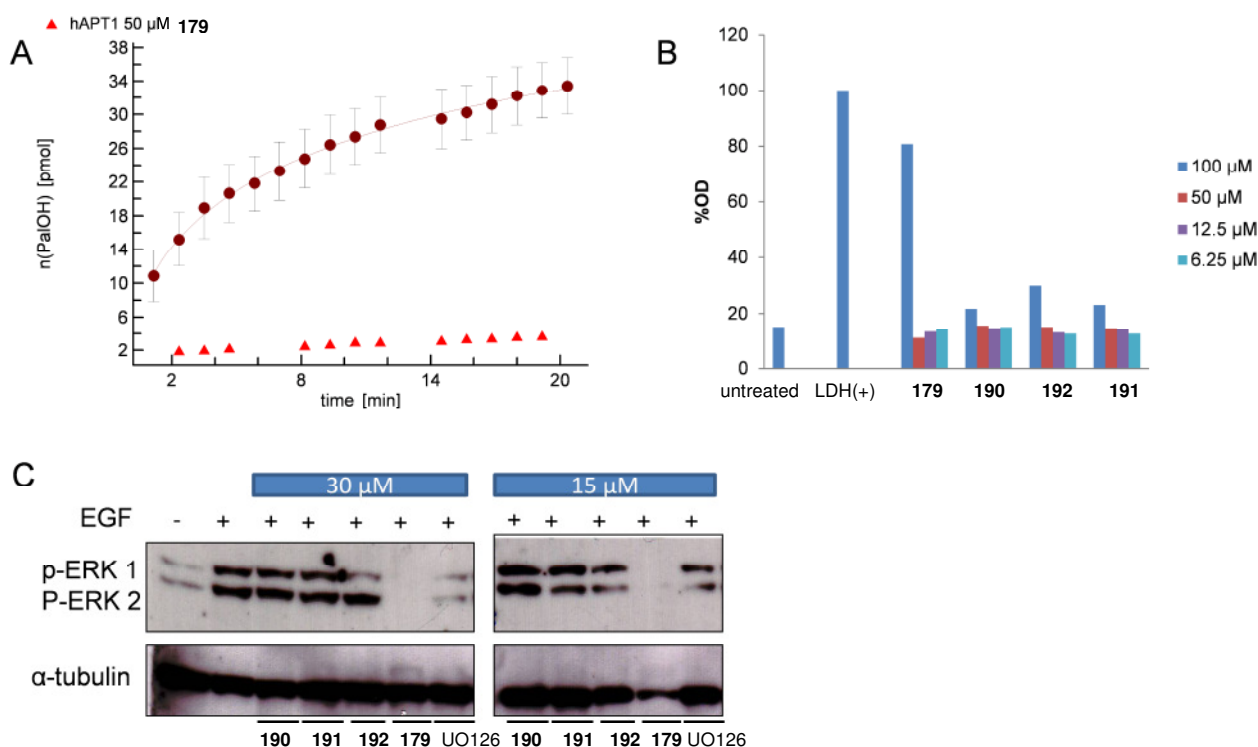


Figure 56: A: Amount of palmitic acid detected after incubation of N-Ras with APT1 (50 nM) and ADIFAB (200 nM) in absence (dark red) or in the presence of 50 μM 179 (light red) (work by Dr. Kristina Görmer). B: LDH-toxicity test for boron compounds 179, 190-192. C: ERK-phosphorylation blot of MDCK cells treated with 30 or 15 μM of boron compounds 179, 190-192 and control UO126 (work by Nancy E. Martinez).

In conclusion, by small molecule microarray screening a bis-boron compound could be identified that potently inhibited APT1 and APT2. Further experiments with simple phenyl boronic acids highlighted the potency of boron compounds to be non-toxic and effective APT1 and APT2 inhibitors.

3.4 Identification of LYPLAL1 Inhibitors

Regardless of the relatively low sequence identity of human lysophospholipase-like protein 1 (hLYPLAL1) of 33% to hAPT1 and hAPT2, LYPLAL1 is detected as the most similar fold in the protein database by a DALI search. Like APT1 and APT2, LYPLAL1 belongs to the protein superfamily of α/β hydrolases. The 1.72 Å crystal structure of human LYPLAL1¹³⁴ showed a typical α/β hydrolase fold with the classical catalytic triad of serine, aspartate and histidine. A structural feature of LYPLAL1 is that unlike acyl protein thioesterases, the hydrophobic tunnel that accommodates the lipid part of the substrate is closed. Therefore LYPLAL1 lacks the structural prerequisites for the delipidation of large substrates like palmitoylated proteins, as well as long chain lipid degradation in general. In fact, follow-up experiments in order to develop an enzymatic assay for LYPLAL1 confirmed that LYPLAL1 is neither able to hydrolyze long-chain esters (see below); nor to depalmitoylate N-Ras protein *in vitro*¹⁴⁸ so that a potential induced-fit mechanism is very unlikely. Besides the fact that LYPLAL1 exhibits a closed substrate tunnel two striking differences in comparison with APT1 and 2 are obvious: on the one hand the electrostatic surface potential around the active site shows distinct positive charge in the immediate vicinity of the catalytic serine (opposite charge as compared with APT1 and APT2) and on the other hand LYPLAL1 crystallizes as monomer. Hence, even though LYPLAL1 has the most similar folds to APT1 among all known PDB structures, the structure features an open, solvent-accessible active site reminiscent of α/β hydrolases that hydrolyze smaller substrates. The activity assays described in the following section confirmed this hypothesis.

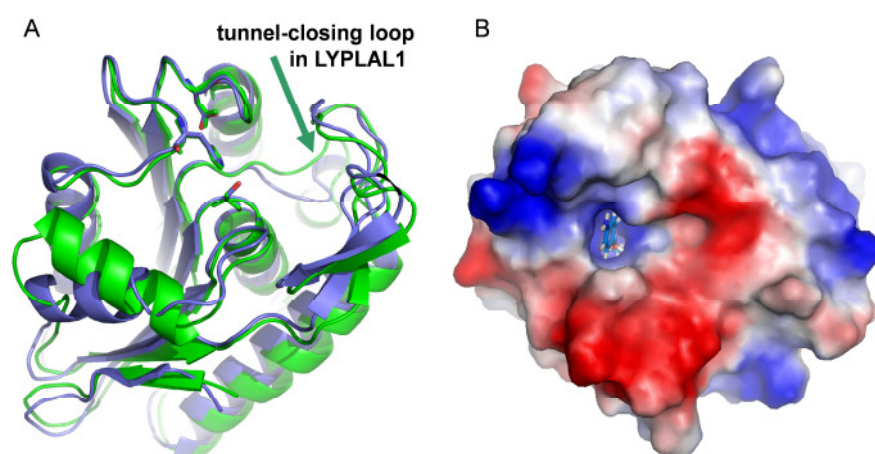


Figure 57: Crystal structure of LYPLAL1. A: Crystal structure of LYPLAL1 (green) superimposed on APT1 (blue). The tunnel-closing loop is highlighted by an arrow. **B:** 4-nitro-phenyl acetate docked into the active site of LYPLAL1. The surface is colored according to the electrostatic potential. Positively charged regions are shown in blue and negative regions in red.¹³⁴

In order to investigate whether the small molecules identified as LYPLAL1 binders on chemical array were capable to also inhibit the enzyme activity, an enzymatic assay had to be developed. So far no activity assay has been published and information about possible LYPLAL1 substrates was also rather vague. As LYPLAL1 was originally proposed to be a phospholipase, LYPLAL1 was subjected to activity tests for the four different types of phospholipases A₁, A₂, C and D (Invitrogen *EnzChek* phospholipase assays). However, as already implicated by the thorough analysis of the crystal structure, LYPLAL1 did not display measurable phospholipase activity. In addition commercial substrates sensing triacylglycerol lipase and lipase activity in general (**Table 17**, experimental section) did not result in any observable enzymatic activity. Consequently, in line with the knowledge from the crystallographic data various 4-nitrophenyl esters (**215**, **216**, **217**, **218**, **219**, **220**), differing in length were tested. 4-Nitrophenyl acetate (**215**, PNPA) turned out to be most efficiently hydrolyzed by LYPLAL1, confirming the already suspected preference for small substrates. Consistent with the shallow shape of the active site substrates with increasing chain length showed reduced activity. Interestingly, 4-nitrophenyl propionate (**216**) constituted an exception to that rule, and showed less hydrolysis than 4-nitrophenyl butyrate (**217**) by the enzyme.

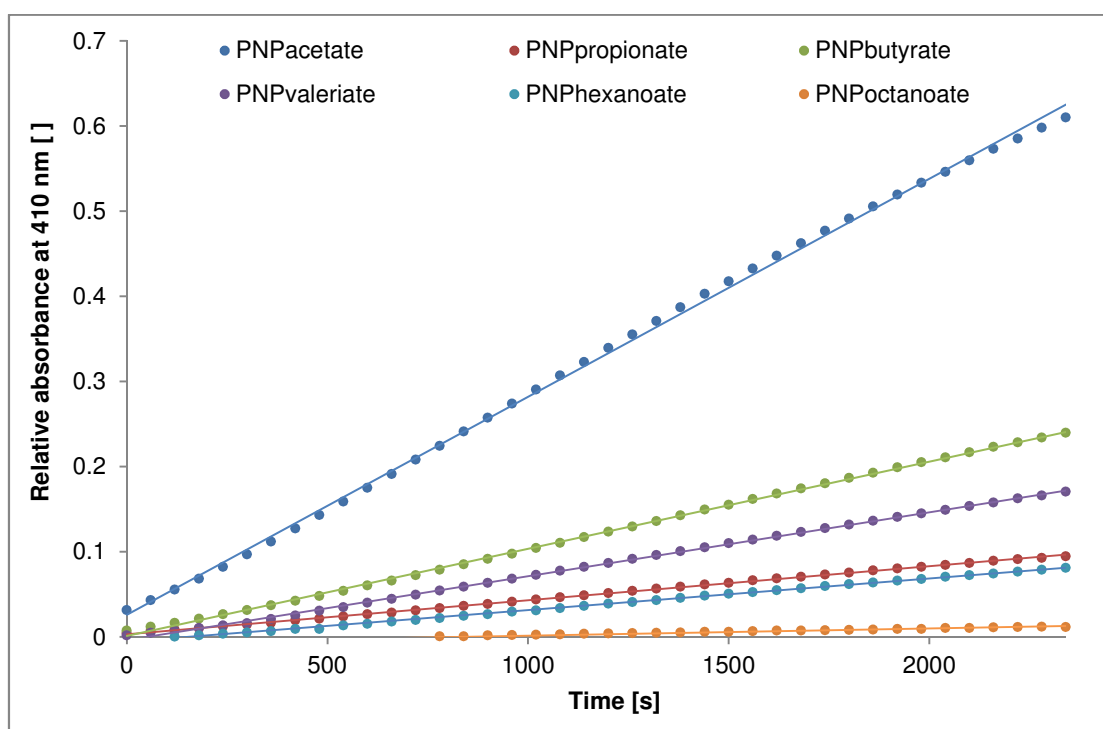


Figure 58: Hydrolysis of different 4-nitrophenyl esters by hLYPLAL1. Free 4-nitrophenol was detected by absorbance at 410 nm over a time period of 40 min. Measurements were carried out at 300 nM protein and 500 μ M substrate. Each data point represents the average value of three independent wells. Background caused by auto hydrolysis of the substrate was subtracted from the data.

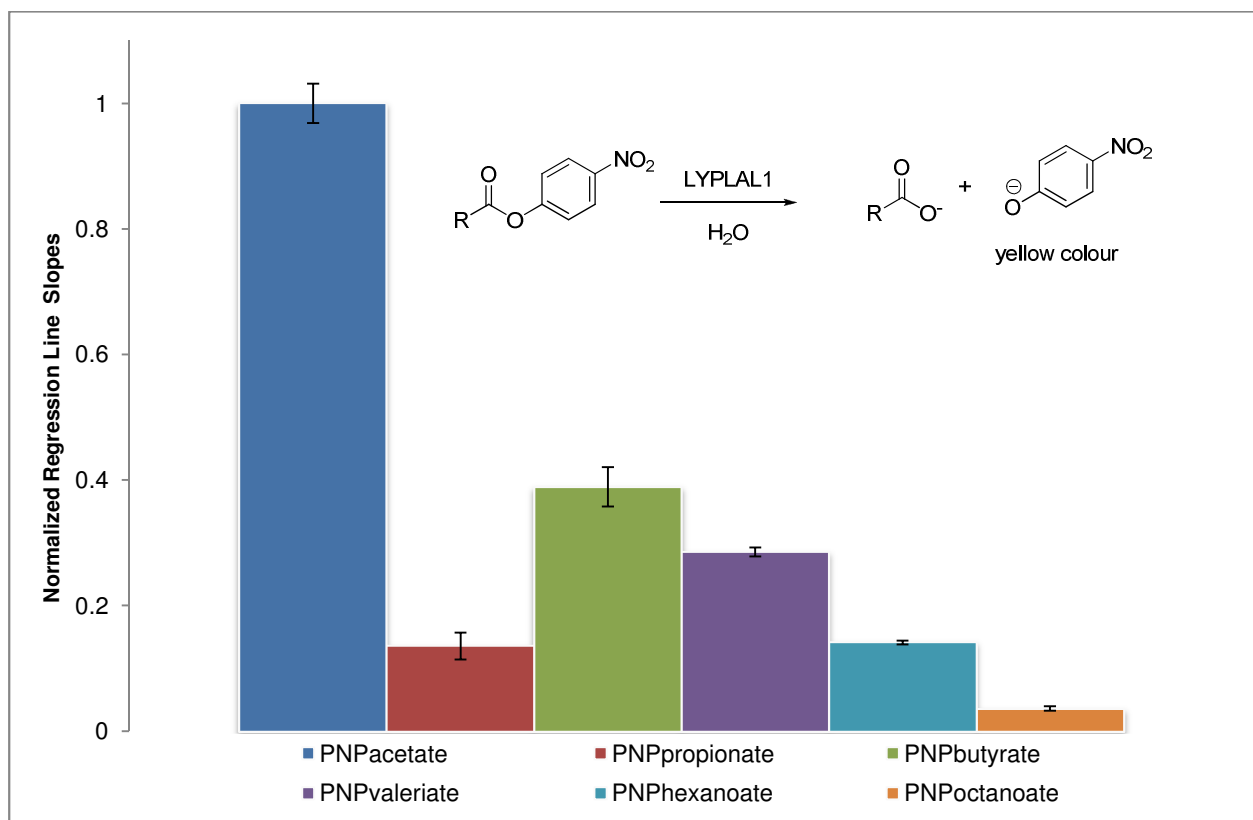


Figure 59: Normalized hydrolysis of different 4-nitrophenyl esters by hLYPLAL1. Regression line slopes of the above measurements were calculated and normalized against the slope of the most efficient substrate PNPA.

As the colorimetric PNPA-assay had to be performed using high concentrations of substrate (1.2 mM), a more sensitive assay employing lower substrate concentrations and therefore higher sensitivity was developed. PNPA (**215**) was substituted by 6,8-difluoro-4-methylumbelliferol acetate (**221**, DiFMUA) in the activity assay. DiFMUA was synthesised from literature known 6,8-difluoro-4-methylumbelliferol (**222**, DiFMU)^{149,142} (kindly provided by Dr. Marion Rusch) by way of acetylation with acetylchloride in 65% yield.

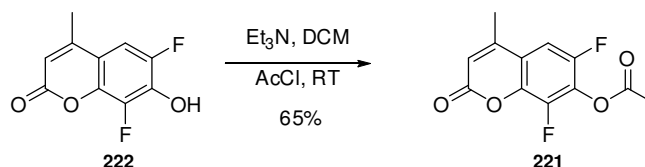
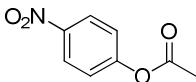
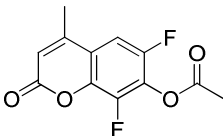


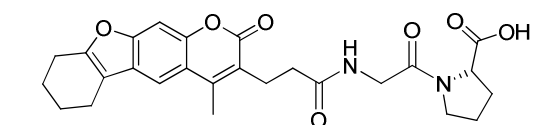
Figure 60: Synthesis of 6,8-difluoro-4-methylumbelliferol acetate (DiFMUA, **221**).

Michaelis-Menten kinetics showed that LYPLAL1 hydrolyzed DiFMUA (**221**) with the same catalytic efficiency (k_{cat}/K_m) as PNPA (**215**).

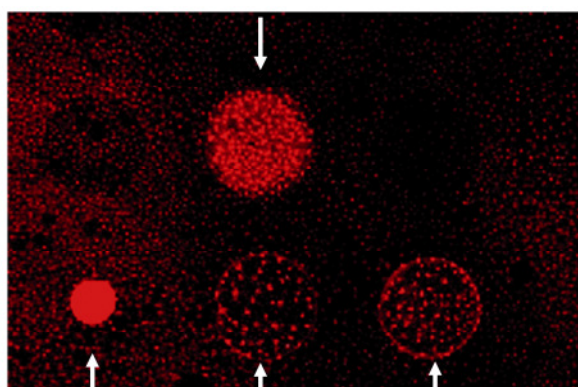
Table 16: Comparison of the two LYPLAL1 substrates PNPA (215) and DiFMUA (221).

Kinetic Data (300 nM LYPLAL1)	PNPA (215)	DiFMUA (221)
		
K_m [μM]	782 ± 130	12.6 ± 5.6
v_{max} [nmol/s]	168	2.72
$\frac{1}{2} v_{\text{max}}$ [nmol/s]	84	1.36
$K_{\text{cat}} = v_{\text{max}}/[E_0]$ [s^{-1}]	0.56	0.009
K_{cat}/K_m [$\text{s}^{-1}\text{mM}^{-1}$]	0.7	0.7
Assay conditions	1.2 mM	40 μM

A

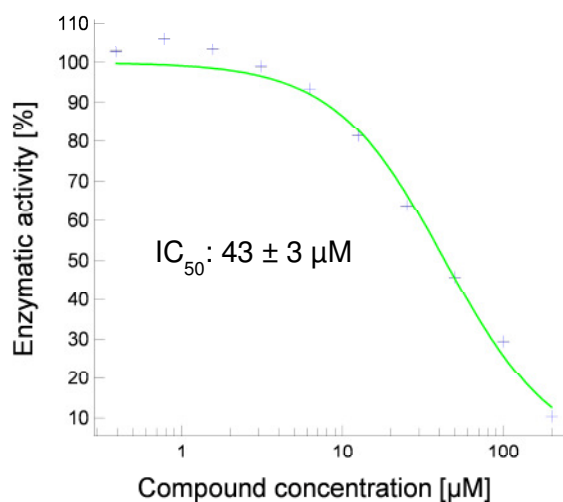


188

Position
marker

Glutathione

B

Figure 61: A) Microarray Analysis of LYPLAL1. Chemical array showing that compound 188 binds to GST-LYPLAL1. B) IC₅₀ value determination of LYPLAL1 inhibition by compound 188.

The analysis of the identified microarray binders for LYPLAL1 in the DiFMUA-assay resulted in one compound (**188**) with an IC_{50} below 50 μ M. Compound **188** is a successful example of microarray screening and constitutes a novel scaffold that could serve as starting point for the development of more potent inhibitors for LYPLAL1. Such inhibitors could help to elucidate the role of LYPLAL1 in obesity and be of interest for further pharmaceutical developments.

4 Summary and Conclusion

Small molecule microarray screening was evaluated as a technique to identify compounds binding to APT1, APT2 and LYPLAL1. All these proteins share high structural similarities and are members of the enzyme superfamily of the α/β -hydrolases. Using chemical array technology and known high-affinity inhibitors suitable conditions for microarray screening of thousands of natural products and natural product derivatives from RIKEN NPDepo could be found. After initial screening of NPDepo on the three GST-tagged proteins, hit compounds were selected and subjected to further validation efforts aiming to create a unique fingerprint binding profile for every protein. As already indicated by thorough analysis of the crystal structures of the proteins (structures were solved in the course of the project by Marco Bürger) the high similarity of APT1 and APT2 was also reflected in almost identical binding profiles, while LYPLAL1 interacted with completely different compounds. For follow-up experiments APT1/APT2 binders were investigated separately from LYPLAL1 binders.

Enzymatic screening of the identified APT1/APT2 binders did only reveal the compound class of bis-borinic esters and bis-borinate compounds. This rather low success rate of the screening of a compound library enriched with thousands of natural products, or derivatives thereof, at the same time points out the weak points of small molecule microarray screening. As only binding of a small molecule to the protein of interest is detected the proteins enzymatic activity is not necessarily perturbed. In the case of APT1 and APT2, microarray screening is maybe even less suitable due to the strong tendency of the proteins to form dimers. For further evaluation of microarray screening as tool to find inhibitors a monomeric model system like γ APT1 might be a valid strategy. However, microarray screening led to the identification of bis-boron compounds as potent APT1 and APT2 modulators not just on glass array and SPR-chip but also on the enzymatic level. The identified compound showed competitive behaviour towards the assay substrate, pointing out the potent effect of boron as the most important moiety of the molecule. In order to investigate the role of boron in more details, simple phenyl boronic acids were screened on the proteins revealing a potent inhibitory effect. Together with the crystallographic data obtained for co-crystals of boronic acids with monomeric γ APT1, that could be used as model system for human APT1, it could be concluded that the boron moiety is most likely involved in the blocking of the catalytic serine of APT1. Surprisingly, none of the boron compounds did show toxic effects on cells. For bis-boron compounds even potent *in vitro* and *in vivo* inhibition of the Erk pathway could be observed, that could be caused by APT1 and APT2 inhibition. However, further biological studies are needed.

The crystallographic analysis of LYPLAL1 combined with the results from biochemical substrate screening uncovered a rather unexpected substrate preference compared to the highly homologue APT1; namely LYPLAL1 has a shallow active site, whereas APT1 features a large hydrophobic tunnel that most likely accommodates the large lipid substituents of its natural substrates. In addition, it does neither cleave thioester bonds of prenylated N-Ras, nor exhibit any phospholipase activity in contradiction to initial assumptions.¹³⁵ An enzymatic assay was developed in order to investigate the potency of LYPLAL1 protein binders on chemical array to functionally inhibit the protein's enzymatic activity. During this study small nitrophenyl esters were found to be readily hydrolyzed. In substituting PNPA (**215**) by DiFMUA (**221**) the sensitivity of the assay could be improved without influencing the hydrolysis efficiency. This implicates that the fluorophore does not sterically obstruct the hydrolysis of the ester bond, or at least not more than the *p*-nitrophenyl group. Testing the identified microarray binders for their inhibition potential all binders showed inhibitory activity, with one small molecule showing an IC₅₀ below 50 μM and therefore constituting the first known LYPLAL1 inhibitor. This compound features a carboxyl group that could potentially interact with the positive patch in the active site. Using the identified compound as lead for further development of a high affinity inhibitor the investigation of the still unknown physiological role of LYPLAL1 could be uncovered, e.g. by applying the small molecule to adipocyte cell cultures or whole organisms.

In summary, small molecule microarray screening was used for the high-throughput determination of modulators for three human proteins of medical interest. Microarray screening constitutes a method with rather low hit rates as it completely relies on small molecule binding. Consequently, compounds with high affinity but, for example, fast off-rate are not detected in such a system, thus resulting in significant numbers of false negative results. Nevertheless, this screening technology benefits from its inexpensive and highly time-efficient realisation. During this study microarray screening results successfully led to the identification of structurally new inhibitors.

V Experimental Section

1 Assay Procedures

1.1 Enzymatic Assay Protocol for APT1 and APT2

Human acyl protein thioesterase 1 (APT1) was expressed and purified as described previously.¹¹³ APT2 was produced under the same conditions as already described for APT1, with the following changes: the apt2 gene (cDNA clone IRATp970G0114D, imaGenes, Berlin) was cloned into a pGEX expression vector by means of the Gateway system and modified to contain a PreScission protease recognition sequence between the apt2 and the gst gene. The construct was then expressed as GST-APT2 fusion protein in *E. coli* BL21 (DE3) Codon+ RIL cells at 20 °C for 16 hours. The fusion protein was loaded on a GSH column and APT2 was separated from GST by overnight incubation of the column with PreScission protease, and finally purified to homogeneity by gel filtration. Proteins were provided by Marco Bürger.

APT1-Assay¹⁴²

The enzymatic activity was determined by measuring the release of fluorescent 6,8-difluoro-4-methylumbelliferone (**222**, DiFMU) from 6,8-difluoro-4-methylumbelliferyl octanoate (**223**, DiFMUO) by APT1 hydrolysis using a Tecan Infinite M200 microplate reader in a 96 well format. The assay was performed in buffer containing 20 mM HEPES, 150 mM NaCl, which was titrated to pH 7.53-7.55 using 2 N HCl solution. The final enzyme concentration was 5 nM and the final substrate concentration was 15 μ M. In the assay, 30 μ L inhibitor solution (at varying concentrations) in buffer containing 0.01% (v/v) Triton-X100 was mixed with 50 μ L APT1 solution (10 nM) in buffer containing 0.01% (v/v) Triton-X100. The mixture was incubated for 20 min. at 37 °C. Subsequently, 20 μ L of a solution of **223** (75 μ M) in buffer containing 0.09% (v/v) Triton-X100 was added to the reaction mixture and after 2 min. lag time the formation of fluorescent DiFMU (**222**) was recorded ($\lambda_{\text{ex}} = 358$ nm, $\lambda_{\text{em}} = 455$ nm) over 40 min at 60 s intervals at 37 °C. The substrate solution was prepared by dissolving 2.43 mg of **223** in 100 μ L DMSO. Then, 900 μ L assay buffer containing 10% (v/v) Triton-X100 was added and the mixture was stirred vigorously (Vortex). The resulting mixture was added to 99 mL assay buffer to give a solution containing 100 μ M DiFMUO (**223**) and 0.09% (v/v) Triton-X100. During the incubation and in between measurements the reaction mixture was shaken. The reaction rate was determined by linear regression analyses ($r^2 \geq 0.98$) of the fluorescence emission increase over time. The background reaction rate with no enzyme present

was subtracted and the reaction rates were normalized to the reaction rate with no inhibitor present (100%).

APT2-Assay¹⁴⁰

As described for APT1, the enzyme activity was determined by measuring the release of fluorescent 6,8-difluoro-4-methylumbelliferone (**222**, DiFMU) from 6,8-difluoro-4-methylumbelliferyl octanoate (**223**, DiFMUO). The final enzyme concentration was 50 nM and the final substrate concentration 15 μ M. Besides that, the same protocol as for APT1 was followed.

Steady state enzyme kinetics (APT1 and APT2)

Parameters of steady state kinetics were measured at a final concentration of 5 nM APT1 and 50 nM APT2. Increase of fluorescence intensity at 358/455 nm (excitation/emission) with final DiFMUO (**223**) concentrations ranging from 45 μ M to 0.7 μ M in assay buffer were recorded at 37 °C over 40 min at 30 s intervals. The resulting fluorescence was referenced to a linear DiFMU fluorescence-concentration relationship.

K_m and v_{max} values for APT1 and APT2 were obtained by nonlinear least square fitting of Michaelis-Menten equation parameters to the data using XL Fit. The determined constants are for APT1: $K_m = 6.1 \pm 0.8 \mu\text{M}$ and $v_{max} = 1.3 \pm 0.05 \text{ nmol s}^{-1}$ and for APT2: $K_m = 2.1 \pm 0.6 \mu\text{M}$ and $v_{max} = 0.7 \pm 0.05 \text{ nmol s}^{-1}$ (**Figure 62**).

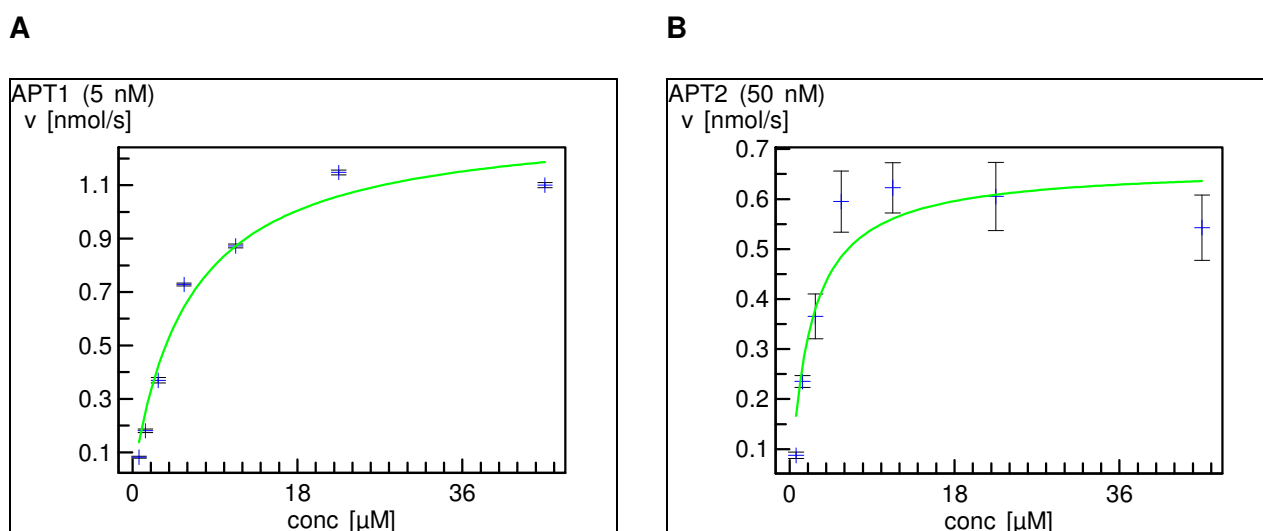


Figure 62: Michaelis-Menten plot for DiFMUO hydrolysis. The solid line represents the fitted Michaelis-Menten equation with the given constants. **A)** 5 nM APT1; $K_m = 6.1 \pm 0.8 \mu\text{M}$ and $v_{\text{max}} = 1,300 \pm 45 \text{ pmol s}^{-1}$. **B)** 50 nM APT2; $K_m = 2.1 \pm 0.6 \mu\text{M}$ and $v_{\text{max}} = 700 \pm 5 \text{ pmol s}^{-1}$.

From the v_{max} value and the enzyme concentration (APT1: 5 nM, APT2: 50 nM) the turnover number (K_{cat}) for the 6,8-difluoro-4-methylumbelliferyl octanoate (DiFMUO) hydrolysis by APT1/APT2 (APT1: 0.26 s^{-1} , APT2: 0.014 s^{-1}) and the enzyme efficiency (K_{cat}/K_m) were determined (APT1: $43 \text{ s}^{-1} \text{ mM}^{-1}$, APT2: $6.7 \text{ s}^{-1} \text{ mM}^{-1}$).

Concentration dependent inhibition of APT1/APT2 was measured using 10 different concentrations around the IC_{50} value resulting from two-fold dilution series. Reaction progress at every concentration of inhibitor was measured in triplicate. Linear regression analysis was performed with Microsoft Excel and IC_{50} values were calculated using 4-parameter logarithmic fits with XL Fit curve fitting software (www.idbs.com). Linear regression analysis was performed with Microsoft Excel and IC_{50} values were calculated using 4-parameter logarithmic fits with XL Fit curve fitting software (www.idbs.com) for Excel according to:

$$y = \frac{(A_1 - A_2)}{1 + (x/x_0)^p} + A_2$$

Equation 3: Equation used for IC_{50} evaluation.

y is the reaction rate at the inhibitor concentration x , A_1 is the minimum reaction rate (no enzyme present), A_2 the maximum reaction rate (no inhibitor present), p is the Hill-slope and x_0 is the IC_{50} . The fitted IC_{50} parameter represents the relative IC_{50} value, and is defined as the concentration giving a response half way between the fitted top (A_2) and bottom (A_1) of the curve.

1.2 Enzymatic Assay for LYPLAL1

Human *lyplal1* cDNA (imaGenes clone IRAUp969E0370D) was used as a template for PCR amplification. The *lyplal1* full-length gene was cloned into a pGEX 4T1 expression vector (GE Healthcare) by means of the Gateway system, with modified primer to encode a PreScission protease cleavage site immediately upstream to the *lyplal1* start codon, leaving the two amino acids GP preceding the N-terminal start methionine as cloning artifact. *E. coli* BL21 Codon +RIL cells were transformed using the cloned construct and the overexpressed LYPLAL1 was purified.¹³⁴ Protein was provided by Marco Bürger.

Substrate Screening

Different substrates were screened for their ability to be hydrolysed by LYPLAL1. Therefore different lipase substrates (**224-228**) in assay buffer (20 mM Hepes, 150 mM NaCl, pH 7.53-7.55, 0.01% (v/v) Triton-X100) were incubated at varying concentrations with different concentrations of LYPLAL1 and detected at the appropriate wavelengths. However no enzymatic activity could be observed. In addition EnzChek[®] Phospholipase kits A1, A2, C and D purchased from Invitrogen were used for the detection of LYPLAL1 phospholipase activity. However, LYPLAL1 did not exhibit phospholipase activity. Finally a series of various *p*-nitrophenol (PNP) esters (**216-220**) was subjected to LYPLAL1 hydrolysis. LYPLAL1 activity was determined by measuring the release of coloured *p*-nitrophenol (PNP) using a Tecan Infinite M200 microplate reader at 410 nm. The substrate screening was performed at 300 nM LYPLAL1 and 500 μ M of the PNP-ester in assay buffer. Parameters of steady state kinetics were measured at a final concentration of 300 nM LYPLAL1 using either a colorimetric (PNP-acetate, **215**) or fluorimetric detection (6,8-difluoro-4-methylumbelliferyl acetate, DiFMUA, **221**). In the colorimetric assay, the release of yellow PNP from **215** with final concentrations ranging from 2400 μ M to 37.5 μ M in assay buffer was monitored by recording the increase of absorbance at 410 nm at 37 °C over 40 min at 30 s intervals. The resulting absorbance was referenced to a linear PNP absorbance-concentration relationship. In the fluorimetric assay, the increase of fluorescence intensity at 358/455 nm (excitation/emission) with final DiFMUA (**221**) concentrations ranging from 60 μ M to 0.94 μ M in assay buffer were recorded at 37 °C over 40 min at 30 s intervals. The resulting fluorescence was referenced to a linear DiFMU fluorescence-concentration relationship. K_m and v_{max} values were obtained by nonlinear least square fitting of Michaelis-Menten equation parameters to the data using XL Fit. The determined constants were: PNPA-assay ($K_m = 782 \pm 130 \mu\text{M}$; $v_{max} = 168 \text{ nmol s}^{-1}$; $K_{cat} = 0.56 \text{ s}^{-1}$; $K_{cat}/K_m = 0.7 \text{ s}^{-1}\text{mM}^{-1}$) and DiFMUA-assay ($K_m = 12.6 \pm 5.6 \mu\text{M}$; $v_{max} = 2.72 \text{ nmol s}^{-1}$; $K_{cat} = 0.009 \text{ s}^{-1}$; $K_{cat}/K_m = 0.7 \text{ s}^{-1}\text{mM}^{-1}$).

Table 17: Substrates tested on LYPLAL1.

ID	Substrates
224	Resorufin oleate
223	6,8-Difluoro-4-methylumbelliferyl octanoate (DiFMUO)
225	4-(Trifluoromethyl)umbelliferyl oleate
226	8-Octanoyloxypyrene-1,3,6-trisulfonic acid
227	1,2-Dioleoyl-3-(pyren-1-yl)decanoyl- <i>rac</i> -glycerol
228	Dansyl-11-aminoundecanoic acid
229	Substrate for phospholipase A₁ : Glycerophosphoethanolamine derivative (dye-labelled at the acyl chain <i>sn</i> -1 position, quencher at the glycerophosphoethanolamine head group, non-cleavable ether linkage in the <i>sn</i> -2 position), full name: <i>N</i> -((6-(2,4-DNP)amino)hexanoyl)-1-(BODIPY [®] FL C5)-2-hexyl- <i>sn</i> -glycero-3-phosphoethanolamine
230	Substrate for phospholipase A₂ : Glycerophosphocholine derivative (red/green dye-labelled at the acyl chain <i>sn</i> -1 and <i>sn</i> -2 positions, non-cleavable ether linkage in the <i>sn</i> -1 position) full name: 1-O-(6-BODIPY [®] 558/568-amino)hexyl)-2-BODIPY [®] FL C5- <i>sn</i> -glycero-3-phosphocholine
231	Substrate for phospholipase C : Glycerophosphoethanolamine derivative (dye-labelled at the acyl chain <i>sn</i> -2 position, proprietary substrate)
232	Substrates for phospholipase D : Phosphatidylcholine, Cholin oxidase and Amplex Red [®]
215	4-nitrophenyl acetate ($v = 65.5 \pm 2.1$ nmol/s, $K_m = 782$ μ M, $k_{cat} = 0.56$ s ⁻¹ , $v_{max} = 168$ nmol/s)
216	4-nitrophenyl propionate ($v = 8.9 \pm 1.4$ nmol/s)
217	4-nitrophenyl butyrate ($v = 25.5 \pm 0.7$ nmol/s)
218	4-nitrophenyl valerate ($v = 18.7 \pm 0.5$ nmol/s)
219	4-nitrophenyl hexanoate ($v = 9.2 \pm 0.2$ nmol/s)
220	4-nitrophenyl octanoate ($v = 2.4 \pm 0.2$ nmol/s)

LYPLAL1 Assay¹³⁴

The enzyme activity was determined by measuring the release of fluorescent DIFMU (**222**) by LYPLAL1 hydrolysis of DiFMUA (**221**) in a Tecan Infinite M200 microplate reader in a 96 well format. The final enzyme concentration was 300 nM and the final substrate concentration was 40 μM . In the assay, 30 μL inhibitor solutions (at varying concentrations) in assay buffer were mixed with 20 μL LYPLAL1 solution (1.5 μM) in assay buffer. The mixture was incubated for 20 min at 37 $^{\circ}\text{C}$. Subsequently, 50 μL of a solution of **221** (80 μM) in assay buffer was added to the reaction mixture and after 2 min lag time the formation of fluorescent **222** was recorded ($\lambda_{\text{ex}} = 358 \text{ nm}$, $\lambda_{\text{em}} = 455 \text{ nm}$) over 40 min at 60 s intervals at 37 $^{\circ}\text{C}$. During the incubation and in between measurements the reaction mixture was shaken. The reaction rate was determined by linear regression analyses ($r^2 \geq 0.98$) of the fluorescence emission increase over time. The background reaction rate with no enzyme present was subtracted and the reaction rates were normalised to the reaction rate with no inhibitor present (100%).

Concentration dependent inhibition of LYPLAL1 was measured using 10 different concentrations around the IC_{50} value resulting from two-fold dilution series. Reaction progress at every concentration of inhibitor was measured in triplicate. Linear regression analysis was performed with Microsoft Excel and IC_{50} values were calculated using 4-parameter logarithmic fits with XL Fit curve fitting software (www.idbs.com). Linear regression analysis was performed with Microsoft Excel and IC_{50} values were calculated using 4-parameter logarithmic fits with XL Fit curve fitting software (www.idbs.com) for Excel according to **Equation 3**. The fitted IC_{50} parameter represents the relative IC_{50} value, and is defined as the concentration giving a response half way between the fitted top (A_2) and bottom (A_1) of the curve.

2 Microarrays on Glass Slides

2.1 Preparation of Photo-Crosslinked Chemical Arrays

The slides were prepared according to the literature.^{7,89} A solution of the compounds (dissolved in DMSO) was spotted onto PALC slides with a high-precision arrayer using a head with 16-micro-spotting pins. Then the slides were exposed to UV irradiation of 4 J/cm² at 365 nm using a CL-1000L UV crosslinker (UVP, CA). Slides were washed with DMSO, DMF, acetonitrile, THF, DCM, ethanol and MilliQ water (3 × 5 min in an ultrasonicator). Finally the slides were spin dried and stored at -20 °C until use. Compounds of NPDepo arrays were spotted with a 24 pin head at 2.5 mg/mL and compounds of the MPI array with a 16 pin head at 10 mM.

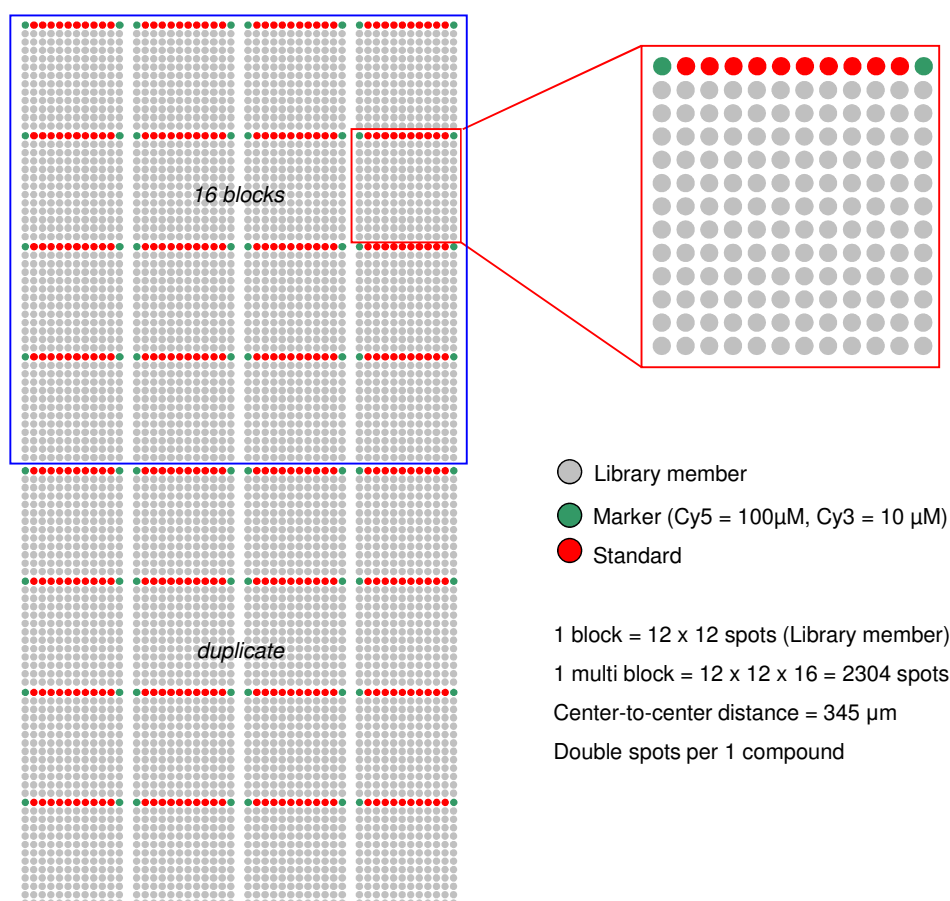


Figure 63: Layout of MPI-slide.

Compounds were spotted in blocks by 144 compounds. Whereas every block started with one row of standard compounds (most frequently used compounds on NPDepo arrays are shown in **Table 18**) and the corners of each block were marked by a position marker.

Table 18: Control compounds spotted on NPDepo-arrays and known binding partners.

Compound Name	Known binder(s)
Biotin	Streptavidin
Cyclosporine A	Cyclophilin A
Glutathione	Glutathion-S-transferase
His peptide	His antibody
FLAG peptide	FLAG antibody
SB203580	p38 MAP-kinase
MTX	Dihydrofolate hydrogenase (DHFR)
Staurosporine	Kinases

2.2 Screening of Microarray Slides

The same buffer as for the APT1 and 2 enzymatic assay was used (20 mM Hepes, 150 mM NaCl, pH = 7.53-7.55). The slides were incubated in buffer containing 1% skim milk for one hour at RT with gentle shaking, washed with buffer (3 × 5 min on shaker) and dried for 1 min using a spin dryer (Waken, model 2350, spindryer-mini). For protein and antibody incubation either cover slide or chamber method were used.

In the cover slide method the array slide was covered by a glass slide from Matsunami Glass Ind., Ltd. (micro cover glass, 24 × 60 mm) and incubated using 50 µL of protein solution in buffer containing 1% skim milk at 30 °C for 1 h. In the chamber method, the glass slide was covered by an Agilent Technologies Gasket slide using 500 µL of protein solution. The covered slide is incubated at 30 °C for 1 h in a hybridization oven using an Agilent G2534A Microarray Hybridization Chamber. Using chamber incubation, no spin drying of array slides after intermediate washing is necessary. Only after final wash, spin drying is essential.

Array slides were incubated with anti-GST antibody (rabbit IgG fraction, Invitrogen, 30 µg/mL) in buffer containing 1% skim milk at 30 °C for 1 h using one of the above mentioned incubation methods. This incubation was followed by another wash step (buffer: 3 × 5 min on shaker, spin dry: 1 min) and incubation with second antibody (Millipore, Gt X Rb IgG Cy5 anti-rabbit, 50 µg/mL) at 30 °C for 1 h. After the final wash step (assay buffer: 3 × 5 min on shaker, spin dry: 1 min) slides were scanned at 635 nm on a GenePix 4200AL microarray scanner (Molecular Devices). The fluorescence signals were quantified using GenePix 6.1 software with local background subtraction. From every slide two copies were used, one was treated with assay buffer containing 1% skim milk as control and the other one with GST labelled target protein in assay buffer containing 1% skim milk. The two resulting pictures were coloured green and red respectively

using Photoshop 5.5 software. Then, the colored figures were merged. The false positive signals caused by binding of ligands to antibody or by autofluorescent signals of the ligand itself were detected as yellow signals. For data analysis fluorescent signal for every compound in both multiblocks was corrected by the local background subtraction and the fluorescence intensity of the corresponding control slide (**Equation 4**).

$$\Delta I = I(\text{sample}) - I(\text{reference})$$

Equation 4: Calculation of fluorescence intensity.

For hit-analysis a relative ranking was used (**Equation 5**).

$$\Delta I = \bar{\Delta I} + n \cdot SD$$

relative ranking: $n \geq 1$: +; $n \geq 2$: ++; $n \geq 3$: +++

I: Fluorescence Intensity of compound spot

SD: standard deviation

$\bar{\Delta I}$: mean fluorescence intensity of all compound spots

Equation 5: Relative ranking of fluorescence.

The hits from screening of NPDepo slides (A, B, G, H) were complemented by known nanomolar APT1/APT2 inhibitors (β -lactones) and borinic acids, that were found upon screening of compounds from RIKEN BSI (array F). The chosen layout was spotted on two SPR chips (version A and B) on a single glass slide in order to compare glass array and SPR screening. While for SPR chips as position marker Sennoside B (frequent protein binder) was used, for glass slides a mixture of Cy5 and Cy3 was employed.

ID	Compound Name
A01	Leucomycin A1
A02	NPD2612
A03	NPD2826
A04	NPD3976
A05	NPD4355
A06	Pipemidic acid
A07	Spiramycin I
A08	4,4'-[1,3-phenylenebis(oxy)]diphthalic acid
A09	Captopril(CAP)
A10	Nizatidine(NIZ)
A11	NP214
A12	NP223
B01	NP275
B02	NP387
B03	NP513
B04	NPD3383
B05	NPD3397
B06	NPD3936
B07	NPD4020
B08	NPD6047
B09	NPD6048
B10	NPD7112
B11	NPD7330
B12	NPD8335
C01	NP558
C02	RBSI-B3003-C
C03	RBSI-B6057-5
C04	RBSI-B4045-26
C05	RBSI-B6055-4
C06	RBSI-B2133-C
C07	TZ-BA4
C08	TZ-BA22
C09	TZ-BA23
C10	FD241
C11	PalmB
C12	AGWI000564-1
D01	AGWI000566-1
D02	DMSO
M:	Sennoside B

Array version A

M	A01	A09	B05	A04	A12	C11	A07	B03	A02	A10	M
	A02	A10	B06	A05	B01	D02	A08	B04	A03	A11	D02
	A03	A11	C10	A06	B02	A01	A09	B05	A04	A12	B06
M	A04	A12	C11	A07	B03	A02	A10	B06	A05	B01	C10
	A05	B01	D02	A08	B04	A03	A11	C10	A06	B02	C11
	A06	B02	A01	A09	B05	A04	A12	C11	A07	B03	D02
	A07	B03	A02	A10	B06	A05	B01	D02	A08	B04	D02
M	A08	B04	A03	A11	C10	A06	B02	A01	A09	B05	M

M: Sennoside B (SPR chip), Cy3/Cy5 (glass slide)

D02: DMSO

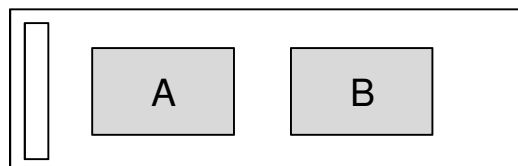
Array version B

M	B07	C03	C11	B10	C06	B05	C01	C09	B08	C04	M
	B08	C04	C12	B11	C07	D02	C02	C10	B09	C05	D02
	B09	C05	D01	B12	C08	B07	C03	C11	B10	C06	C12
	B10	C06	B05	C01	C09	B08	C04	C12	B11	C07	D01
M	B11	C07	D02	C02	C10	B09	C05	D01	B12	C08	B05
	B12	C08	B07	C03	C11	B10	C06	B05	C01	C09	D02
	C01	C09	B08	C04	C12	B11	C07	D02	C02	C10	D02
M	C02	C10	B09	C05	D01	B12	C08	B07	C03	C11	M

M: Sennoside B (SPR chip), Cy3/Cy5 (glass slide)

D02: DMSO

- Array version A
- Array version B
- SPR chip ver. A & B as positive control
- Array version A & B as negative control or marker



Arrangement on glass slide

Figure 64: Array layout for SPR chip and glass slides.

3 SPR Imaging

3.1 Preparation of Photo-Crosslinked Chemical Arrays

Gold-coated glass chips (TOYOBO, Japan) were incubated in ethanol containing photoaffinity linker **168** (0.1 mM) and dummy linker **170** for 12h. The chip was rinsed successively with ethanol and dried in air. DMSO solutions (10 mM) of small molecules were spotted on the gold-coated glass chip using an automated spotter (TOYOBO, Japan). After evaporation of DMSO chips were exposed to UV irradiation of 4 J/cm² at 365 nm using a CL-1000L UV crosslinker (UVP, CA). The chips were then washed with DMSO, water and ethanol, according to literature procedures.⁹²

3.2 SPR Measurement

The photo-cross-linked SPR chip was placed in an SPR imaging instrument (TOYOBO, Japan) and SPR signals were obtained in running buffer (10 mM Hepes, 150 mM NaCl, pH = 7.4). The running buffer and the protein samples were applied to the chip surface at 0.1 mL/min. After washing with running buffer, a solution of the corresponding protein (10 μM) was injected to the chip surface and incubated for 10 min. All SPR experiments were performed at 30 °C. SPR images and signal data were collected with an SPR analysis program (TOYOBO, Japan) and SPR difference images were constructed using a Scion Image (Scion, MD) program.

4 Immobilization of Small Molecules on Chemical Beads

In order to immobilize selected small molecules on chemical beads for further experiments like pull-down and target identification, photoaffinity linker-coated beads were prepared by covalent attachment of photoaffinity linkers to *N*-hydroxysuccinimide (NHS) activated sepharose beads. The photoaffinity linker was synthesised according to previous reports⁹³ from readily available mono-protected diamine (**233**) and trifluoromethyl aryldiazirine (**234**). EDC-coupling and Boc-deprotection resulted in photoaffinity linker **235** (synthesis performed by K. Honda). Before the immobilization of compounds their UV-stability (4 J/cm² at 365 nm) was confirmed by LC-MS analysis of UV irradiated sample and non-UV irradiated sample.

The following compounds were immobilized on chemical beads:

Microtubules project: **106** (negative control), (*R*)-**107**, (*R*)-**109**, **120** (negative control)

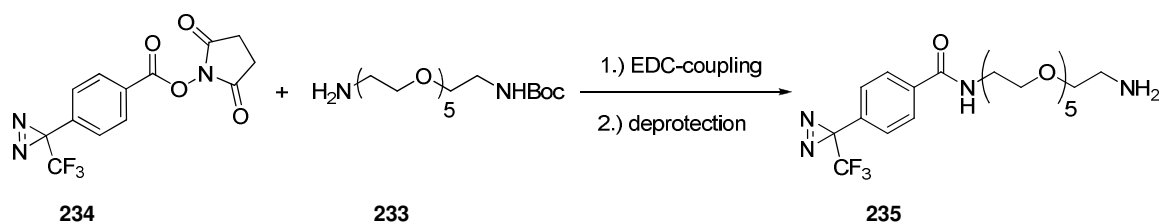


Figure 65: Synthesis of photoaffinity linker **235** from trifluoromethyl aryl diazirine **234** and mono-protected bis-amine **233**.

NHS-activated Sepharose 4 Fast Flow beads were obtained from GE Healthcare as suspension in 100% isopropanol. Compounds were immobilized to 15 nmol/ μ L bead suspension. Therefore 400 μ L of sepharose bead suspension was centrifuged at 1,500 rpm for 1 min and the supernatant discarded. Beads were washed (3 \times 400 μ L) with 1 mM HCl and 0.1 M NaHCO₃ in (1:1) dioxane/water (3 \times 400 μ L). Photoaffinity linker **235** (3 equiv.) was dissolved in 0.1 M NaHCO₃ in (1:1) dioxane/water (400 μ L) and beads were incubated for 2h at 37 °C in the linker solution with gentle rotation, followed by washing with 0.1 M NaHCO₃ in (1:1) dioxane/water (3 \times 400 μ L). In order to block residual binding sites, beads were treated with 1 M ethanolamine in Tris-HCl buffer (0.1 M, pH = 8.0) (1 mL) and incubated for 1h at 37 °C with gentle rotation.

Bead suspension was then transferred to a spin column (Scan Column) and washed with water (3 \times 400 μ L) followed by methanol (3 \times 400 μ L). Dry beads were then transferred to a glass vial and the compound added dissolved in methanol (400 μ L). Solvents were evaporated *in vacuo* and beads exposed to UV irradiation of 4 J/cm² at 365 nm using a CL-1000L UV crosslinker (UVP, CA). Beads were then transferred to a spin column with methanol followed by successive washing with methanol (15 \times 400 μ L) and PBS-buffer (3 \times 400 μ L). Finally beads were suspended in 1 mM NaN₃-PBS-buffer, pH = 7.4 (400 μ L) and stored at 4 °C.

5 Synthetic Procedures

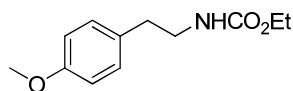
5.1 General

Unless otherwise noted, all reactions were performed in oven-dried glassware. Petroleum ether with a boiling range of 40–60 °C was used. Reactions were generally run under argon atmosphere. All commercially available compounds (Acros, Aldrich, Fluka, Merck, ABCR) were used without purification. Cotarnine iodide was purchased from ZereneX Molecule Ltd. Additional cotarnine derivatives were purchased from InterBioScreen Ltd. ¹H and ¹³C NMR: Varian Mercury 400 (¹H-, 400 MHz; ¹³C-, 101 MHz) or Bruker Avance DRX 500 (¹H-, 500 MHz; ¹³C-, 126 MHz) Varian Unity Inova 600 (¹H-, 600 MHz; ¹³C-, 126 MHz), spectra were recorded at 295 K; chemical shifts are calibrated to the residual proton and carbon resonance of the solvent: CDCl₃ (δH 7.26, δC 77.0 ppm), CD₃OD (δH 3.31, δC 49.0 ppm), DMSO-d₆ (δH 2.50, δC 39.5 ppm). Data are represented as follows: chemical shift (multiplicity [br = broad, s = singlet, d = doublet, t = triplet, q = quartet, m = multiplet], integration, coupling constants in Hz). Preparative chiral HPLC was conducted using a Dionex HPLC system (UltiMate 3000 preparative) with a Chiralpak® IC column (cellulose tris(3,5-dichlorophenylcarbamate) immobilized on 5 μm silica gel). Melting points: Büchi Melting Point B-450, uncorrected. HRMS (ESI): LTQ Orbitrap with flow injection (H₂O/MeCN = 1:1, 0.1% HCO₂H, flow rate: 250 μL/min) Flash chromatography: Acros silica gel 35–70 μm. Thin-layer chromatography: Merck silica gel 60 F₂₅₄ on aluminium plate. Optical rotations: Schmidt + Haensch Polartronic HH8, sodium D line (589 nm), c = g per 100 mL.

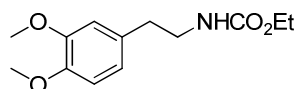
5.2 Synthesis

General procedure I: preparation of substituted phenethylcarbamates

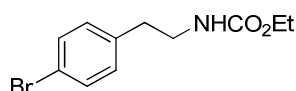
To a solution of phenylethylamine (1 equiv) and Hünigs base (1 equiv) in dry diethyl ether (40 mL) was added dropwise and under ice-cooling a solution of ethyl chloroformate (1 equiv) in diethyl ether (10 mL). A white precipitate formed immediately. After vigorous stirring for 2h at RT, the solution was filtered and the solvent was removed under reduced pressure. The colourless crystalline residue was redissolved in ether (50 mL) and extracted with water (50 mL), brine (50 mL) and dried with MgSO₄, filtered and evaporated to dryness.

Ethyl 4-methoxyphenethylcarbamate (36)

According to general procedure I, 4-methoxyphenethylamine **33** (4.84 mL, 33.0 mmol, 1 equiv) yielded **36** as a colourless solid (6.89 g, 93%). $R_f = 0.35$ (petroleum ether/ethyl acetate, 3:1); m. p. 49-50 °C; $^1\text{H-NMR}$ (400 MHz, CDCl_3): $\delta = 1.21$ (t, 3H, $J = 7.3$, OCH_2CH_3), 2.73 (t, 2H, $J = 6.8$, PhCH_2), 3.38 (m, 2H, CH_2NH), 3.77 (s, 3H, OMe), 4.08 (q, 2H, $J = 7.3$, OCH_2CH_3), 4.70 (br s, 1H, NH), 6.80 (d, 2H, $J = 8.5$, CH_{ar}), 7.09 (d, 2H, $J = 8.5$, CH_{ar}); $^{13}\text{C-NMR}$ (101 MHz, CDCl_3): $\delta = 14.6$ (OCH_2CH_3), 35.2 (PhCH_2), 42.2 (CH_2NH), 55.2 (OMe), 60.6 (OCH_2CH_3), 113.9 (2C, CH_{ar}), 129.6 (2C, CH_{ar}), 130.7 (C_q), 156.5 (CO), 158.2 ($\text{C}_q\text{-OMe}$); HRMS (ESI): $[\text{M}+\text{H}]^+$ calculated for $\text{C}_{12}\text{H}_{18}\text{O}_3\text{N}$ 224.12812, found 224.12807.

Ethyl 3,4-dimethoxyphenethylcarbamate (37)

According to general procedure I, 3,4-dimethoxyphenethylamine **34** (4.58 mL, 27.6 mmol, 1 equiv) yielded **37** as a yellow oil (4.52 g, 65%). $R_f = 0.43$ (petroleum ether/ethyl acetate, 1:1); $^1\text{H-NMR}$ (400 MHz, CDCl_3): $\delta = 1.31$ (t, 3H, $J = 7.3$, OCH_2CH_3), 2.67 (t, 2H, $J = 7.0$, PhCH_2), 3.30 (m, 2H, CH_2NH), 3.76 (s, 3H, OMe), 3.77 (s, 3H, OMe), 4.01 (q, 2H, $J = 7.3$, OCH_2CH_3), 4.89 (br s, 1H, NH), 6.65-6.63 (m, 2H, CH_{ar}), 6.70-6.73 (m, 1H, CH_{ar}); $^{13}\text{C-NMR}$ (101 MHz, CDCl_3): $\delta = 14.4$ (OCH_2CH_3), 35.4 (PhCH_2), 42.0 (CH_2NH), 55.5 (OMe), 55.6 (OMe), 60.3 (OCH_2CH_3), 111.0 (CH_{ar}), 111.6 (CH_{ar}), 120.4 (CH_{ar}), 131.1 (C_q), 147.3 ($\text{C}_q\text{-OMe}$), 148.6 ($\text{C}_q\text{-OMe}$), 156.4 (CO); HRMS (ESI): $[\text{M}+\text{H}]^+$ calculated for $\text{C}_{13}\text{H}_{20}\text{O}_4\text{N}$ 254.13868, found 254.13869.

Ethyl 4-bromophenethylcarbamate (38)

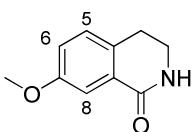
According to general procedure I, 4-bromophenethylamine **35** (3.88 mL, 25.0 mmol, 1 equiv) yielded **38** as a colourless solid (6.58 g, 97%). $R_f = 0.71$ (petroleum ether/ethyl acetate, 1:2); m.p. 77-78 °C; $^1\text{H-NMR}$ (400 MHz, CDCl_3): $\delta = 1.21$ (t, 3H, $J = 7.0$, OCH_2CH_3), 2.76 (t, 2H, $J = 6.8$,

PhCH₂), 3.40 (m, 2H, CH₂NH), 4.09 (q, 2H, *J* = 7.0, OCH₂CH₃), 4.62 (br s, 1H, NH), 7.06 (d, 2H, *J* = 8.0, CH_{ar}), 7.42 (d, 2H, *J* = 8.0, CH_{ar}); ¹³C-NMR (101 MHz, CDCl₃): δ = 14.6 (OCH₂CH₃), 35.6 (PhCH₂), 41.9 (CH₂NH), 60.8 (OCH₂CH₃), 120.3 (C_q-Br), 130.5 (2C, CH_{ar}), 131.6 (2C, CH_{ar}), 137.8 (C_q), 156.5 (CO); HRMS (ESI): [M+H]⁺ calculated for C₁₁H₁₅O₂NBr 272.02807, found 272.02841. Analytical data were in accordance with literature.¹⁵⁰

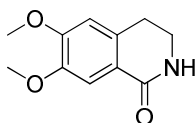
General procedure II: preparation of substituted dihydroisoquinolinones (GP2)

To a solution of the phenethylcarbamate (1 equiv) in POCl₃ (1 g starting material in 5 mL POCl₃) P₂O₅ (2 equiv) was added. The solution was heated to reflux for 2h. The reaction was quenched by slowly pouring into ice water (vigorous reaction!). The resulting mixture was basified with KOH and extracted with ethyl acetate. The combined organic phases were washed with water, brine and dried with MgSO₄, filtered and the solvent was evaporated *in vacuo*. The crude product was absorbed on silica gel and purified *via* flash chromatography.

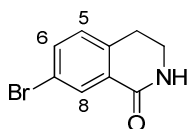
7-Methoxy-3,4-dihydroisoquinolin-1(2H)-one (39)



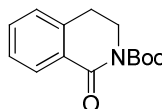
According to general procedure II, ethyl 4-methoxyphenethylcarbamate **36** (13.5 g, 60.5 mmol, 1 equiv) yielded **39** as a colourless solid (5.2 g, 49%). Flash chromatography (petroleum ether/ethyl acetate, 1:2). R_f = 0.39 (ethyl acetate); m.p. 113-114 °C; ¹H-NMR (400 MHz, CDCl₃): δ = 2.93 (t, 2H, *J* = 6.8, PhCH₂), 3.54 (dt, 2H, *J*₁ = 6.8, *J*₂ = 2.8, CH₂N), 3.84 (s, 3H, OMe), 5.98 (br s, 1H, NH), 7.00 (dd, 1H, *J*₁ = 8.3, *J*₂ = 3.0, 6-H), 7.12 (d, 1H, *J* = 8.3, 5-H), 7.58 (d, 1H, *J* = 3.0, 8-H); ¹³C-NMR (101 MHz, CDCl₃): δ = 26.9 (PhCH₂), 39.8 (CH₂N), 55.1 (OMe), 110.7 (CH_{ar}), 119.1 (CH_{ar}), 128.1 (CH_{ar}), 129.5 (C_q), 130.9 (C_q), 158.3 (C_q-OMe), 166.7 (CO); HRMS (ESI): [M+H]⁺ calculated for C₁₀H₁₂O₂N 178.08626, found 178.08603. Analytical data were in accordance with literature.¹⁵¹

6,7-Dimethoxy-3,4-dihydroisoquinolin-1(2H)-one (40)

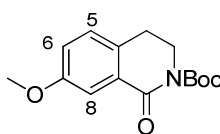
According to general procedure II, ethyl 3,4-dimethoxyphenethylcarbamate **37** (5.00 g, 19.7 mmol, 1 equiv) yielded **40** as a colourless solid (1.64 g, 40%). Flash chromatography (petroleum ether/ethyl acetate, 1:4). $R_f = 0.42$ (acetone); m.p. 169-171 °C; ^1H NMR (400 MHz, CDCl_3): $\delta = 2.82$ (t, 2H, $J = 6.8$, PhCH_2), 3.45-3.49 (m, 2H, CH_2N), 3.83 (s, 6H, OMe), 6.59 (s, 1H, CH_{ar}), 7.35 (br s, 1H, NH), 7.46 (s, 1H, CH_{ar}); ^{13}C -NMR (101 MHz, CDCl_3): $\delta = 27.7$ (PhCH_2), 40.1 (CH_2N), 55.8 (OMe), 55.8 (OMe), 109.4 (CH_{ar}), 109.7 (CH_{ar}), 121.2 (C_q), 132.5 (C_q), 147.6 ($\text{C}_q\text{-OMe}$), 151.8 ($\text{C}_q\text{-OMe}$), 166.6 (CO); HRMS (ESI): $[\text{M}+\text{H}]^+$ calculated for $\text{C}_{11}\text{H}_{14}\text{O}_3\text{N}$ 208.09682, found 208.09674. Analytical data were in accordance with literature.¹⁵²

7-Bromo-3,4-dihydroisoquinolin-1(2H)-one (41)

According to general procedure II, ethyl 4-bromophenethylcarbamate **38** (4.00 g, 14.7 mmol, 1 equiv) yielded **41** as a slightly yellow solid (1.37 g, 41%). Flash chromatography (petroleum ether/ethyl acetate, 1:2). $R_f = 0.36$ (petroleum ether/ethyl acetate, 1:3); m.p. 47-49 °C; ^1H -NMR (400 MHz, CDCl_3): $\delta = 2.91$ (t, 2H, $J = 6.5$, PhCH_2), 3.54 (dt, 2H, $J_1 = 6.5$, $J_2 = 3.0$, CH_2N), 7.08 (d, 1H, $J = 8.0$, 5-H), 7.52 (dd, 1H, $J_1 = 8.0$, $J_2 = 2.3$, 6-H), 7.68 (br s, 1H, NH), 8.15 (d, 1H, $J = 2.3$, 8-H); ^{13}C -NMR (101 MHz, CDCl_3): $\delta = 27.6$ (PhCH_2), 39.8 (CH_2N), 120.8 ($\text{C}_q\text{-Br}$), 129.0 (CH_{ar}), 130.6 (C_q), 130.7 (CH_{ar}), 134.9 (CH_{ar}), 137.6 (C_q), 165.5 (CO); HRMS (ESI): $[\text{M}+\text{H}]^+$ calculated for $\text{C}_9\text{H}_9\text{BrNO}$ 225.98620, found 225.98636.

***tert*-Butyl 1-oxo-3,4-dihydroisoquinoline-2(1*H*)-carboxylate (42)**

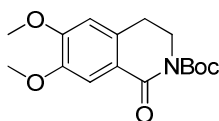
A solution of 3,4-dihydroisoquinolin-1(2*H*)-one⁶⁶ (0.89 g, 6.05 mmol, 1 equiv) in anhydrous THF (18 mL) was cooled to -78 °C and *n*-butyllithium (1.6 M in hexane, 3.80 mL, 3.40 mmol, 1 equiv) was added dropwise. After 30 min a solution of di-*tert*-butyl dicarbonate (1.32 g, 6.05 mmol, 1 equiv) in THF (3 mL) was added dropwise, and the reaction mixture was stirred at -78 °C until the reaction was complete as monitored *via* TLC (3h). The reaction was quenched with saturated aq. NH_4Cl and the organic phase extracted with diethyl ether (3 \times 50 mL), dried with MgSO_4 , filtered and the solvents were evaporated *in vacuo* to give the crude product, which was purified *via* flash chromatography (petroleum ether/ethyl acetate, 9:1) to afford **42** as a colourless solid (1.20 g, 80%). $R_f = 0.29$ (petroleum ether/diethyl ether, 4:1); m.p. 69-71 °C; $^1\text{H-NMR}$ (400 MHz, CDCl_3): $\delta = 1.49$ (s, 9H, Boc- $(\text{CH}_3)_3$), 2.98-3.01 (m, 2H, PhCH_2), 3.97-4.00 (m, 2H, CH_2N), 7.19-7.21 (m, 1H, CH_{ar}), 7.32-7.36 (m, 1H, CH_{ar}), 7.44-7.48 (m, 1H, CH_{ar}), 8.15 (dd, 1H, $J_1 = 7.9$, $J_2 = 1.5$, CH_{ar}); $^{13}\text{C-NMR}$ (101 MHz, CDCl_3): $\delta = 28.0$ (Boc- $(\text{CH}_3)_3$), 28.2 (PhCH_2), 44.3 (CH_2N), 83.0 (Boc- C_q), 127.1 (CH_{ar}), 129.2 (CH_{ar}), 128.5 (CH_{ar}), 132.7 (CH_{ar}), 139.4 (2C, C_q), 153.0 (Boc-CO), 163.8 (CO); HRMS (ESI): $[\text{M}+\text{H}]^+$ calculated for $\text{C}_{14}\text{H}_{18}\text{O}_3\text{N}$ 248.12812, found 248.12824.

***tert*-Butyl 7-methoxy-1-oxo-3,4-dihydroisoquinoline-2(1*H*)-carboxylate (43)**

A solution of 7-methoxy-3,4-dihydroisoquinolin-1(2*H*)-one (**39**) (50 mg, 28.0 mmol, 1 equiv) in THF (4 mL) was cooled to 0 °C and NaH (60% oil suspension, 12.4 mg, 31.0 mmol, 1.1 equiv) was added portion wise. The reaction mixture was stirred for 1h at this temperature and a solution of di-*tert*-butyl dicarbonate (62 mg, 28.0 mmol, 1 equiv) in THF (1 mL) was added dropwise. The reaction mixture was warmed to RT overnight. Water was added and the aqueous phase was extracted with diethyl ether (3 \times 30 mL). The combined organic fractions were washed with brine (30 mL), dried with MgSO_4 , filtered and the solvents were removed *in vacuo*. Flash chromatography (petroleum ether/diethyl ether, 4:1) yielded **43** as a colourless oil (70 mg, 89%). $R_f = 0.45$ (petroleum ether/ethyl acetate, 4:1); $^1\text{H-NMR}$ (400 MHz, CDCl_3): $\delta = 1.49$ (s, 9H, Boc-

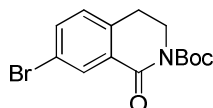
(CH_3)₃), 2.82 (t, 2H, $J = 6.3$, PhCH_2), 3.71 (s, 3H, OMe), 3.84-3.87 (m, 2H, CH_2N), 6.91 (dd, 1H, $J_1 = 8.3$, $J_2 = 2.8$, 6-H), 7.00 (d, 1H, $J = 8.3$, 5-H), 7.55 (d, 1H, $J = 2.8$, 8-H); ^{13}C -NMR (101 MHz, CDCl_3): $\delta = 27.1$ (PhCH_2), 27.8 (Boc-(CH_3)₃), 44.5 (CH_2N), 55.1 (OMe), 82.8 (Boc- C_q), 111.9 (CH_{ar}), 120.4 (CH_{ar}), 128.1 (CH_{ar}), 129.8 (C_q), 131.6 (C_q), 152.9 (Boc-CO), 158.4 (C_q -OMe), 163.6 (CO); HRMS (ESI): $[\text{M}+\text{H}]^+$ calculated for $\text{C}_{15}\text{H}_{20}\text{O}_4\text{N}$ 278.13868, found 278.13881.

***tert*-Butyl 6,7-dimethoxy-1-oxo-3,4-dihydroisoquinoline-2-carboxylate (44)**



To a 0.5 M solution of **40** (76 mg, 0.37 mmol, 1 equiv) in DCM was added triethylamine (102 μL , 0.73 mmol, 2 equiv), 4-dimethylaminopyridine (160 mg, 0.73 mmol, 2 equiv) and di-*tert*-butyl dicarbonate (160 mg, 0.73 mmol, 2 equiv), and the mixture was stirred at RT overnight. The solvents were evaporated *in vacuo*. Column purification (petroleum ether/ethyl acetate, 3:1) yielded **44** as a colourless solid (79 mg, 70%). $R_f = 0.33$ (petroleum ether/ethyl acetate, 2:1); m.p. 116-119 $^\circ\text{C}$; ^1H -NMR (400 MHz, CDCl_3): $\delta = 1.54$ (s, 9H, Boc-(CH_3)₃), 2.89 (t, 2H, $J = 6.3$, PhCH_2), 3.86 (s, 3H, OMe), 3.88 (s, 3H, OMe), 3.92-3.95 (m, 2H, CH_2N), 6.60 (s, 1H, CH_{ar}), 7.60 (s, 1H, CH_{ar}); ^{13}C -NMR (101 MHz, CDCl_3): $\delta = 27.9$ (PhCH_2), 28.0 (Boc-(CH_3)₃), 44.6 (CH_2N), 55.9 (OMe), 82.9 (Boc- C_q), 109.0 (CH_{ar}), 111.1 (CH_{ar}), 121.6 (C_q), 133.8 (C_q), 148.0 (C_q), 152.8 (C_q), 153.3 (Boc-CO), 163.8 (CO); HRMS (ESI): $[\text{M}+\text{H}]^+$ calculated for $\text{C}_{16}\text{H}_{22}\text{O}_5\text{N}$ 308.14965, found 308.14925. Analytical data were in accordance with literature.¹⁵³

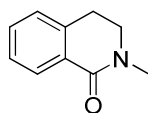
***tert*-Butyl 7-bromo-1-oxo-3,4-dihydroisoquinoline-2(1*H*)-carboxylate (45)**



To a 0.5 M solution of **41** (176 mg, 0.78 mmol, 1 equiv) in DCM was added triethylamine (114 μL , 0.82 mmol, 1.05 equiv), 4-dimethylaminopyridine (100 mg, 0.82 mmol, 1.05 equiv) and di-*tert*-butyl dicarbonate (178 mg, 0.82 mmol, 1.05 equiv), and the mixture was stirred at RT overnight. The solvents were evaporated *in vacuo*. Column purification (petroleum ether/diethyl ether, 4:1) yielded **45** as a yellow solid (146 mg, 57%). $R_f = 0.50$ (petroleum ether/ethyl acetate, 4:1); m.p. 97-99 $^\circ\text{C}$; ^1H -NMR (400 MHz, CDCl_3): $\delta = 1.53$ (s, 9H, Boc-(CH_3)₃), 2.92 (t, 2H, $J = 6.1$, PhCH_2), 3.91-3.94 (m, 2H, CH_2N), 7.06 (d, 1H, $J = 8.0$, 5-H), 7.50-7.52 (m, 1H, 6-H), 8.21-8.22 (m, 1H, 8-H); ^{13}C -NMR

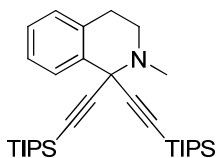
(101 MHz, CDCl₃): δ = 27.7 (PhCH₂), 27.9 (Boc-(CH₃)₃), 44.1 (CH₂N), 83.3 (Boc-C_q), 120.9 (C_q-Br), 128.8 (CH_{ar}), 130.9 (C_q), 132.2 (CH_{ar}), 135.5 (CH_{ar}), 138.1 (C_q), 152.6 (Boc-CO), 162.4 (CO); HRMS (ESI): [M+H]⁺ calculated for C₁₄H₁₇O₃NBr 326.03863, found 326.03879.

2-Methyl-3,4-dihydroisoquinolin-1(2H)-one (46)



To a solution of 3,4-dihydroisoquinolin-1(2H)-one⁶⁶ (0.21 g, 1.42 mmol, 1 equiv) in anhydrous DMF (15 mL), sodium hydride (60% oil suspension; 60 mg, 1.49 mmol, 1.05 equiv) was added, the suspension stirred for 30 min at RT and methyl iodide (90 μ L, 1.49 mmol; 1.05 equiv) was added dropwise to yield a clear solution immediately. The reaction mixture was stirred at RT overnight. The reaction was quenched by adding water (40 mL) and the aqueous phase was extracted with ethyl acetate (3 \times 20 mL). The combined organic fractions were dried with MgSO₄, filtered and the solvent evaporated *in vacuo* to give the crude product, which was purified *via* flash chromatography (petroleum ether/ethyl acetate, 2:1) to afford **46** as a slightly yellow oil (146 mg, 64%). R_f = 0.38 (petroleum ether/ethyl acetate, 1:2); ¹H-NMR (400 MHz, CDCl₃): δ = 2.84-2.87 (m, 2H, PhCH₂), 3.01 (s, 3H, NCH₃), 3.40-3.43 (m, 2H, CH₂N), 7.02-7.04 (m, 1H, CH_{ar}), 7.17-7.29 (m, 2H, CH_{ar}), 7.95-7.97 (m, 1H, CH_{ar}); ¹³C-NMR (101 MHz, CDCl₃): δ = 27.5 (PhCH₂), 34.8 (NCH₃), 47.7 (CH₂N), 126.6 (2C, CH_{ar}), 127.6 (CH_{ar}), 129.0 (C_q), 131.2 (CH_{ar}), 137.7 (C_q), 164.4 (CO); HRMS (ESI): [M+H]⁺ calculated for C₁₀H₁₂ON 162.09134, found 162.09100.

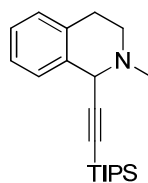
2-Methyl-1,1-bis[(triisopropylsilyl)ethynyl]-1,2,3,4-tetrahydroisoquinoline (47)



By analogy to the literature⁶⁸ to a solution of TIPS-acetylene (270 μ L, 1.21 mmol, 3 equiv) in THF (1.5 mL) at -78 °C a solution of *n*-butyllithium (1.6 M in hexane, 0.76 mL, 1.21 mmol, 3 equiv) was added dropwise. After 10 min stirring, boron trifluoride etherate (0.33 mL, 1.21 mmol, 3 equiv) was added and stirring was continued for 10 min. Then a solution of **46** (75 mg, 0.47 mmol, 1 equiv) in THF (1 mL) was added to react for 30 min at that temperature. The reaction mixture was treated with lithium aluminiumhydride (18.5 mg, 0.49 mmol, 1.05 equiv) elevating the temperature to -10

°C over 2h. The reaction was quenched by adding a small amount of ethanol and the aluminium salts were precipitated by adding a saturated aqueous solution of sodium sulfate (5 mL). The water layer was extracted with diethyl ether (3 × 50 mL), the combined organic layers were washed with brine, dried with MgSO₄, filtered and the solvents were evaporated under reduced pressure. Flash chromatography (petroleum ether/ethyl acetate, 12:1) yielded **47** as a colourless oil (56 mg, 37%). R_f = 0.40 (petroleum ether/ethyl acetate, 19:1); ¹H-NMR (400 MHz, CDCl₃): δ = 1.05 (s, 42H, TIPS-CH(CH₃)₂), 2.71 (s, 3H, NCH₃), 2.89-2.90 (m, 4H, PhCH, CH₂N), 7.02-7.04 (m, 1H, CH_{ar}), 7.12-7.19 (m, 2H, CH_{ar}), 7.73-7.76 (m, 1H, CH_{ar}); ¹³C-NMR (101 MHz, CDCl₃): δ = 11.3 (TIPS-CH(CH₃)₂), 18.6 (TIPS-CH(CH₃)₂), 28.7 (PhCH₂), 41.2 (NCH₃), 47.6 (CH₂N), 58.5 (C_q), 85.6 (C_q alkyne), 106.2 (C_q alkyne), 125.8 (CH_{ar}), 127.0 (CH_{ar}), 128.4 (CH_{ar}), 128.5 (CH_{ar}), 133.4 (C_q), 137.3 (C_q); HRMS (ESI): [M+H]⁺ calculated for C₃₂H₅₄NSi₂ 508.37893, found 508.37807.

2-Methyl-1-[(triisopropylsilyl)ethynyl]-1,2,3,4-tetrahydroisoquinoline (**48**)



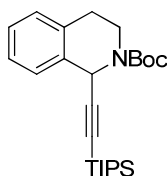
By analogy to the literature⁶⁸ to a solution of TIPS-acetylene (108 μL, 0.49 mmol, 1.05 equiv) in THF (1.5 mL) at -78 °C a solution of *n*-butyllithium (1.6 M in hexane, 0.31 mL, 0.49 mmol, 1.05 equiv) was added dropwise. After 10 min stirring, boron trifluoride etherate (0.13 mL, 0.49 mmol, 1.05 equiv) was added and stirring was continued for 10 min. A solution of **46** (75 mg, 0.47 mmol, 1 equiv) in THF (1 mL) was added and stirring was continued for 30 min at that temperature. The reaction mixture was treated with lithium aluminiumhydride (18.5 mg, 0.49 mmol, 1.05 equiv) elevating the temperature to -10 °C over 2h. The reaction was quenched by adding a small amount of ethanol and the aluminium salts were precipitated by adding a saturated aq. solution of sodium sulfate (5 mL). The water layer was extracted with diethyl ether (3 × 50 mL), the combined organic layers were washed with brine, dried with MgSO₄, filtered and the solvents were evaporated *in vacuo*. Flash chromatography (petroleum ether/ethyl acetate, 12:1) yielded **47** as a colourless oil (56 mg, 37%). Flash chromatography (petroleum ether/ethyl acetate, 12:1) yielded **56** mg (37%) of the target compound as a colourless oil. R_f = 0.29 (petroleum ether/diethyl ether, 4:1); ¹H-NMR (400 MHz, CDCl₃): δ = 1.04 (s, 21H, TIPS-CH(CH₃)₂), 2.57 (s, 3H, NCH₃), 2.64-2.99 (m, 4H, PhCH₂, CH₂N), 4.52 (s, 1H, CH), 7.07-7.09 (m, 1H, CH_{ar}), 7.13-7.15 (m, 2H, CH_{ar}), 7.30-7.32 (m, 1H, CH_{ar}); ¹³C-NMR (101 MHz, CDCl₃): δ = 11.2 (TIPS-CH(CH₃)₂), 18.6 (TIPS-CH(CH₃)₂), 28.8 (PhCH₂), 43.6 (NCH₃), 48.6 (CH₂N), 57.2 (CH), 86.8 (C_q alkyne), 105.4 (C_q alkyne), 125.7 (CH_{ar}),

126.7 (CH_{ar}), 127.5 (CH_{ar}), 128.7 (CH_{ar}), 133.2 (C_{q}), 135.3 (C_{q}); HRMS (ESI): $[\text{M}+\text{H}]^+$ calculated for $\text{C}_{21}\text{H}_{34}\text{NSi}$ 328.24550, found 328.24517.

General procedure III: preparation of alkynylated tetrahydroisoquinolines

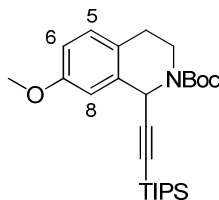
By analogy to the literature⁶⁸ to a solution of TIPS-acetylene (3 equiv) in THF (1.5 mL) at $-78\text{ }^{\circ}\text{C}$ a solution of *n*-butyllithium (1.6 M in hexane, 3 equiv) was added dropwise. After 10 min stirring, boron trifluoride etherate (0.13 mL, 0.49 mmol, 1.05 equiv) was added and stirring was continued for 10 min. Then a solution of the corresponding lactam (1 equiv) in THF (1 mL) was added and stirring was continued for 30 min at that temperature. The excess alkynyl borane was quenched by addition of ethanol (2.5 equiv). The reaction mixture was treated with diisobutylaluminium hydride solution (1 M in toluene, 2.7 equiv), stirred for 1 h at $-78\text{ }^{\circ}\text{C}$ and then 1 h at $-10\text{ }^{\circ}\text{C}$. The reaction was quenched by adding a saturated aqueous solution of Rochelle's salt (5 mL) and allowed to warm to RT overnight. The water layer was extracted with diethyl ether (3 \times 50 mL), the combined organic layers were washed with brine, dried with MgSO_4 , filtered and the solvents were evaporated *in vacuo*.

***tert*-Butyl 1-[(triisopropylsilyl)ethynyl]-3,4-dihydroisoquinoline-2(1*H*)-carboxylate (50)**



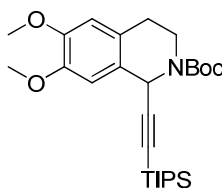
According to general procedure III, lactam **42** (200 mg, 0.81 mmol, 1 equiv) yielded **50** as a colourless oil (245 mg, 73%). Flash chromatography (petroleum ether/ethyl acetate, 49:1). $R_f = 0.43$ (petroleum ether/ethyl acetate, 19:1); $^1\text{H-NMR}$ (400 MHz, CDCl_3): $\delta = 1.03$ (s, 21H, TIPS- $\text{CH}(\text{CH}_3)_2$), 1.51 (s, 9H, Boc- $(\text{CH}_3)_3$), 2.73-2.77 (m, 1H, PhCH), 2.86-2.96 (m, 1H, PhCH), 3.23-3.36 (m, 1H, CHN), 4.06-4.30 (m, 1H, CHN), 5.77-5.95 (m, 1H, CH), 7.08-7.19 (m, 3H, CH_{ar}), 7.29-7.31 (m, 1H, CH_{ar}); $^{13}\text{C-NMR}$ (101 MHz, CDCl_3): $\delta = 11.1$ (TIPS- $\text{CH}(\text{CH}_3)_2$), 18.5 (TIPS- $\text{CH}(\text{CH}_3)_2$), 28.4 (Boc- $(\text{CH}_3)_3$), 28.6 (Ph CH_2), 37.7 (CH_2N), 47.7 (CH), 80.3 (C_{q} alkyne), 83.3 (Boc- C_{q}), 107.1 (C_{q} alkyne), 126.2 (CH_{ar}), 126.9 (CH_{ar}), 127.5 (CH_{ar}), 128.9 (CH_{ar}), 133.9 (C_{q}), 146.5 (C_{q}), 154.2 (Boc-CO); HRMS (ESI): $[\text{M}+\text{H}]^+$ calculated for $\text{C}_{20}\text{H}_{40}\text{O}_2\text{NSi}$ 414.28222, found 414.28228.

***tert*-Butyl 7-methoxy-1-[(triisopropylsilyl)ethynyl]-3,4-dihydroisoquinoline-2(1*H*)-carboxylate (51)**

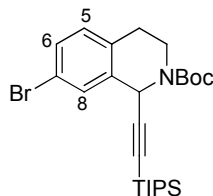


According to general procedure III, lactam **43** (285 mg, 1.03 mmol, 1 equiv) yielded **51** as a colourless oil (282 mg, 62%). Flash chromatography (petroleum ether/ethyl acetate, 49:1). $R_f = 0.47$ (petroleum ether/ethyl acetate, 9:1); $^1\text{H-NMR}$ (400 MHz, CDCl_3): $\delta = 1.02$ (s, 21H, TIPS- $\text{CH}(\text{CH}_3)_2$), 1.49 (s, 9H, Boc- $(\text{CH}_3)_3$), 2.65-2.71 (m, 1H, PhCH), 2.80-2.88 (m, 1H, PhCH), 3.31-3.17 (m, 1H, CHN) 3.76 (s, 3H, OMe), 4.16-4.29 (m, 1H, CHN), 5.75-5.91 (m, 1H, CH), 6.75 (dd, 1H, $J_1 = 8.4$, $J_2 = 2.5$, 6-H), 6.84 (s, 1H, 8-H), 7.00 (d, 1H, $J = 8.4$, 5-H); $^{13}\text{C-NMR}$ (101 MHz, CDCl_3): $\delta = 11.1$ (TIPS- $\text{CH}(\text{CH}_3)_2$), 18.5 (TIPS- $\text{CH}(\text{CH}_3)_2$), 27.8 (Ph CH_2), 28.3 (Boc- $(\text{CH}_3)_3$), 37.9 (CH_2N), 47.8 (CH), 55.2 (OMe), 80.3 (C_q), 83.0 (Boc- C_q), 107.0 (C_q alkyne), 111.4 (CH_{ar}), 114.2 (CH_{ar}), 126.0 (C_q), 129.8 (CH_{ar}), 135.0 (C_q), 154.2 (Boc-CO), 157.9 (C_q -OMe); HRMS (ESI): $[\text{M}+\text{H}]^+$ calculated for $\text{C}_{26}\text{H}_{42}\text{O}_3\text{NSi}$ 444.29285, found 444.29308.

***tert*-Butyl 6,7-dimethoxy-1-[(triisopropylsilyl)ethynyl]-3,4-dihydroisoquinoline-2(1*H*)-carboxylate (52)**



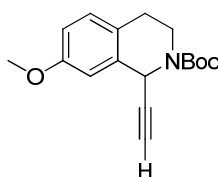
According to general procedure III, lactam **44** (79 mg, 0.26 mmol, 1 equiv) yielded **52** as a colourless oil (21 mg, 17%). Flash chromatography (petroleum ether/ethyl acetate, 9:1). $R_f = 0.33$ (petroleum ether/ethyl acetate, 3:1); $^1\text{H-NMR}$ (400 MHz, CDCl_3): $\delta = 0.97$ (s, 21H, TIPS- $\text{CH}(\text{CH}_3)_2$), 1.46 (s, 9H, Boc- $(\text{CH}_3)_3$), 2.57-2.61 (m, 1H, PhCH), 2.77-2.85 (m, 1H, PhCH), 3.09-3.19 (m, 1H, CHN), 3.80 (s, 6H, OMe), 4.19-4.28 (m, 1H, CHN), 5.66-5.82 (m, 1H, CH), 6.53 (s, 1H, CH_{ar}), 6.76 (s, 1H, CH_{ar}); $^{13}\text{C-NMR}$ (101 MHz, CDCl_3): $\delta = 10.9$ (TIPS- $\text{CH}(\text{CH}_3)_2$), 18.4 (TIPS- $\text{CH}(\text{CH}_3)_2$), 28.1 (Ph CH_2), 28.2 (Boc- $(\text{CH}_3)_3$), 37.5 (CH_2N), 47.2 (CH), 55.6 (2C, OMe), 80.2 (C_q), 82.8 (Boc- C_q), 94.7 (C_q), 107.2 (C_q), 109.8 (CH_{ar}), 111.0 (CH_{ar}), 125.7 (C_q), 147.5 (C_q -OMe), 147.8 (C_q -OMe), 154.2 (Boc-CO); HRMS (ESI): $[\text{M}+\text{H}]^+$ calculated for $\text{C}_{27}\text{H}_{44}\text{O}_4\text{NSi}$ 474.30341, found 474.30283.

***tert*-Butyl 7-bromo-1-[(triisopropylsilyl)ethynyl]-3,4-dihydroisoquinoline-2(1*H*)-carboxylate (53)**

According to general procedure III, lactam **45** (145 mg, 0.44 mmol, 1 equiv) yielded **53** as a colourless oil (158 mg, 72%) of the target compound. Flash chromatography (petroleum ether/ethyl acetate, 49:1). $R_f = 0.46$ (petroleum ether/ethyl acetate, 9:1); $^1\text{H-NMR}$ (400 MHz, CDCl_3): $\delta = 1.01$ (s, 21H, TIPS- $\text{CH}(\text{CH}_3)_2$), 1.49 (s, 9H, Boc- $(\text{CH}_3)_3$), 2.69-2.73 (m, 1H, PhCH), 2.80-2.88 (m, 1H, PhCH), 3.28-3.38 (m, 1H, CHN), 4.08-4.21 (m, 1H, CHN), 5.73-5.92 (m, 1H, CH), 6.97 (d, 1H, $J = 8.4$, 5-H), 7.27 (dd, 1H, $J_1 = 8.5$, $J_2 = 1.8$, 6-H), 7.44 (s, 1H, 8-H); $^{13}\text{C-NMR}$ (101 MHz, CDCl_3): $\delta = 11.0$ (TIPS- $\text{CH}(\text{CH}_3)_2$), 18.5 (TIPS- $\text{CH}(\text{CH}_3)_2$), 28.1 (Ph CH_2), 28.3 (Boc- $(\text{CH}_3)_3$), 37.4 (CH_2N), 47.2 (CH), 80.5 (C_q), 84.1 (Boc- C_q), 106.2 (C_q alkyne), 119.7 (C_q -Br), 130.1 (CH_{ar}), 130.3 (CH_{ar}), 130.5 (CH_{ar}), 132.8 (C_q), 136.3 (C_q), 154.0 (Boc-CO); HRMS (ESI): $[\text{M}+\text{H}]^+$ calculated for $\text{C}_{25}\text{H}_{39}\text{O}_2\text{NBrSi}$ 492.19280, found 492.19232.

General procedure IV: TIPS-deprotection

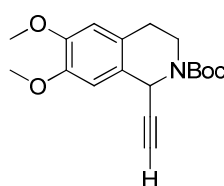
To a solution of TIPS-protected alkynylated tetrahydroisoquinoline in THF (5 mL) at 0 °C was added a solution of tetra-*n*-butylammonium fluoride (1 M in THF, 1.1 equiv) dropwise. The reaction mixture was stirred at RT for 20 min, after which saturated NaHCO_3 solution was added and the aqueous phase was extracted with diethyl ether (3 \times 30 mL). The combined organic fractions were washed with brine, dried with MgSO_4 , filtered and the solvent was removed *in vacuo*. Flash chromatography yielded the desired alkyne.

***tert*-Butyl 1-ethynyl-7-methoxy-3,4-dihydroisoquinoline-2(1*H*)-carboxylate (54)**

According to general procedure IV, TIPS-protected alkynylated tetrahydroisoquinoline **51** (563 mg, 1.27 mmol, 1 equiv) yielded **54** as a colourless oil (313 mg, 86%). Flash chromatography

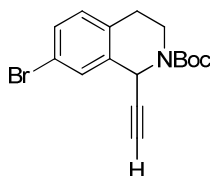
(petroleum ether/ethyl acetate, 9:1). $R_f = 0.34$; $^1\text{H-NMR}$ (400 MHz, CDCl_3): $\delta = 1.49$ (s, 9H, Boc- $(\text{CH}_3)_3$), 2.31 (d, 1H, $J = 2.5$, CH alkyne), 2.67-2.72 (m, 1H, PhCH), 2.81-2.89 (m, 1H, PhCH), 3.18-3.47 (m, 1H, CHN), 3.79 (s, 3H, OMe), 4.00-4.30 (m, 1H, CHN), 5.74-5.94 (m, 1H, CH), 6.76-6.82 (m, 2H, CH_{ar}), 7.04 (d, 1H, $J = 8.5$, CH_{ar}); $^{13}\text{C-NMR}$ (101 MHz, CDCl_3): $\delta = 27.6$ (Ph CH_2), 28.4 (Boc- $(\text{CH}_3)_3$), 38.7 (CH_2N), 46.5 (CH), 55.3 (OMe), 70.9 (CH alkyne), 80.5 (C_q), 83.2 (Boc- C_q), 111.8 (CH_{ar}), 114.1 (CH_{ar}), 126.0 (C_q), 130.0 (CH_{ar}), 134.7 (C_q), 154.1 (Boc-CO), 158.1 (C_q -OMe); HRMS (ESI): $[\text{M}+\text{H}]^+$ calculated for $\text{C}_{17}\text{H}_{22}\text{O}_3\text{N}$ 288.15942, found 288.15955.

***tert*-Butyl 1-ethynyl-6,7-dimethoxy-3,4-dihydroisoquinoline-2-carboxylate (55)**

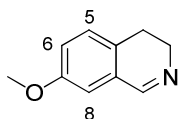


According to general procedure IV, TIPS-protected alkynylated tetrahydroisoquinoline **52** (144 mg, 0.30 mmol, 1 equiv) yielded **55** as a colourless oil (83 mg, 86%). Flash chromatography (petroleum ether/ethyl acetate, 9:1). $R_f = 0.46$ (petroleum ether/ethyl acetate, 2:1); $^1\text{H-NMR}$ (400 MHz, CDCl_3): $\delta = 1.48$ (s, 9H, Boc- $(\text{CH}_3)_3$), 2.31 (d, 1H, $J = 2.4$, CH alkyne), 2.61-2.66 (m, 1H, PhCH), 2.80-2.88 (m, 1H, PhCH), 3.18-3.40 (m, 1H, CHN), 3.82 (s, 3H, OMe), 3.85 (s, 3H, OMe), 4.05-4.29 (m, 1H, CHN), 5.67-5.87 (m, 1H, CH), 6.57 (s, 1H, CH_{ar}), 6.74 (s, 1H, CH_{ar}); $^{13}\text{C-NMR}$ (101 MHz, CDCl_3): $\delta = 27.9$ (Ph CH_2), 28.3 (Boc- $(\text{CH}_3)_3$), 39.0 (CH_2N), 45.6 (CH), 70.8 (CH alkyne), 80.4 (C_q), 83.3 (Boc- C_q), 109.8 (CH_{ar}), 111.4 (CH_{ar}), 125.4 (C_q), 135.7 (C_q), 154.1 (Boc-CO); HRMS (ESI): $[\text{M}+\text{H}]^+$ calculated for $\text{C}_{18}\text{H}_{24}\text{O}_4\text{N}$ 318.16998, found 318.17012.

Alternatively **55** could also be synthesised from **81**. To a solution of the free amine **81** (96 mg, 0.44 mmol, 1 equiv) in DCM (7 mL) triethylamine (123 μL , 0.88 mmol, 2 equiv), 4-dimethylaminopyridine (108 mg, 0.88 mmol, 2 equiv) and di-*tert*-butyl dicarbonate (193 mg, 0.88 mmol, 2 equiv) were added. The mixture was stirred at RT overnight. The solvents were evaporated *in vacuo*. Flash chromatography afforded **55** as a colourless oil (75 mg, 53%).

***tert*-Butyl 1-ethynyl-7-bromo-3,4-dihydroisoquinoline-2(1*H*)-carboxylate (**56**)**

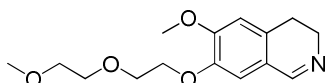
According to general procedure IV, TIPS-protected alkynylated tetrahydroisoquinoline **53** (266 mg, 0.54 mmol, 1 equiv) yielded **56** as a colourless solid (159 mg, 88%). Flash chromatography (petroleum ether/ethyl acetate, 9:1). $R_f = 0.40$; m.p. 129-130 °C; $^1\text{H-NMR}$ (400 MHz, CDCl_3): $\delta = 1.48$ (s, 9H, Boc- $(\text{CH}_3)_3$), 2.33 (d, 1H, $J = 2.5$, CH alkyne), 2.68-2.74 (m, 1H, PhCH), 2.80-2.88 (m, 1H, PhCH), 3.15-3.40 (m, 1H, CHN), 4.05-4.29 (m, 1H, CHN), 5.74-5.93 (m, 1H, CH), 6.99 (d, 1H, $J = 8.0$, CH_{ar}), 7.30 (dd, 1H, $J_1 = 8.0$, $J_2 = 1.8$, CH_{ar}), 7.43 (d, 1H, $J_2 = 1.8$, CH_{ar}); $^{13}\text{C-NMR}$ (101 MHz, CDCl_3): $\delta = 27.9$ (PhCH_2), 28.3 (Boc- $(\text{CH}_3)_3$), 38.1 (CH_2N), 45.9 (CH), 71.6 (CH alkyne), 80.8 (C_q), 82.5 (Boc- C_q), 119.9 ($\text{C}_q\text{-Br}$), 130.2 (CH_{ar}), 130.4 (CH_{ar}), 130.7 (CH_{ar}), 132.9 (C_q), 135.6 (C_q), 154.0 (Boc-CO); HRMS (ESI): $[\text{M}+\text{H}]^+$ calculated for $\text{C}_{16}\text{H}_{19}\text{O}_2\text{NBr}$ 336.05937, found 336.05960.

7-Methoxy-3,4-dihydroisoquinoline (58**)**

A solution of lithium aluminium hydride in THF (1 M, 13.0 mmol, 14.7 mL, 1.3 equiv) was slowly added to a solution of 7-methoxy-3,4-dihydroisoquinolin-1(2*H*)-one **39** (2.00 g, 10.0 mmol, 1 equiv) in anhydrous THF (50 mL). The mixture was heated to reflux for 2h and subsequently quenched by sequential addition of water (20 mL) and 3 N NaOH (20 mL). The reaction mixture was filtered and the residue was washed with acetone (2 × 50 mL) and diethyl ether (2 × 50 mL). The combined organic/aqueous mixture was concentrated to 1/3 of the volume under reduced pressure and acidified using 3 N HCl. The mixture was washed with diethyl ether (2 × 30 mL) and basified with solid KOH. The basic aqueous fraction was extracted with diethyl ether (5 × 50 mL). The combined organic fractions were washed with brine (30 mL), dried with MgSO_4 , filtered and the solvents were removed *in vacuo* to give 1.4 g (8.6 mmol). Without further purification the residue was dissolved in DCM (45 mL) and *N*-bromosuccinimide (1.68 g, 9.4 mmol, 1.1 equiv) was added portion wise over 20 min. After the addition was complete, the mixture was allowed to react for 30 min. Aq. NaOH (15 mL of a 30% aqueous solution) was added and stirring was continued for 1h at RT. The organic layer was separated, washed with water (20 mL) and the product was extracted with 4N

HCl (2 × 20 mL). The combined acidic extracts were washed with DCM and basified (pH = 9) with concentrated ammonia solution and the aqueous phase was extracted with DCM. The combined organic fractions were washed with brine (30 mL), dried with MgSO₄, filtered and the solvents were removed *in vacuo* to give **58** as a yellow oil (1.10 g, 68%). R_f = 0.30 (dichloromethane/methanol, 19:1); ¹H-NMR (400 MHz, CDCl₃): δ = 2.68-2.72 (m, 2H, PhCH₂), 3.77-3.81 (m, 2H, CH₂N), 3.84 (s, 3H, OMe), 6.85 (d, 1H, J = 2.5, 8-H), 6.95 (dd, 1H, J₁ = 8.2, J₂ = 2.5, 6-H), 7.09 (d, J = 8.2, 5-H), 8.33 (s, 1H, H-imine); ¹³C-NMR (101 MHz, CDCl₃): δ = 23.9 (PhCH₂), 47.6 (CH₂N), 55.1 (OMe), 112.0 (CH_{ar}), 116.4 (CH_{ar}), 127.9 (C_q), 128.0 (CH_{ar}), 128.8 (C_q), 158.4 (C_q-OMe), 159.9 (C-imine); HRMS (ESI): [M+H]⁺ calculated for C₁₀H₁₂ON 162.09134, found 162.09140.

6-Methoxy-7-[2-(2-methoxyethoxy)ethoxy]-3,4-dihydroisoquinoline (**236**)



To a solution of 7-hydroxy-6-methoxy-3,4-dihydroisoquinoline **319** (120 mg, 0.68 mmol, 1 equiv) in DMF (10 mL) was added tosyl-alcohol **239** (290 mg, 1.06 mmol, 1.56 equiv), Cs₂CO₃ (196 mg, 1.02 mmol, 1.50 equiv) and KI (22.5 mg, 0.14 mmol, 0.2 equiv). The reaction was stirred at 70 °C for 2d. The solvents were evaporated *in vacuo*. The residue was diluted with water, extracted with DCM and the combined organic fractions washed with saturated aq. Na₂CO₃ and brine, before being dried with MgSO₄ and the solvents were evaporated *in vacuo*. The residue was purified by flash chromatography (gradient from 3% to 8% of MeOH/DCM) to give **236** as a slightly yellow oil (123 mg, 65%). R_f = 0.33 (10% MeOH/DCM); ¹H-NMR (400 MHz, CDCl₃): δ = 2.65 (t, 2H, PhCH₂), 3.34 (s, 3H, OMe), 3.52-3.54 (m, 2H, CH₂), 3.67-3.71 (m, 4H, CH₂), 3.83-3.85 (m, 5H, OMe, CH₂), 4.16 (t, 2H, J = 5.1, CH₂), 6.63 (s, 1H, CH_{ar}), 6.86 (s, 1H, CH_{ar}), 8.19 (s, 1H, CH-imine); ¹³C-NMR (101 MHz, CDCl₃): δ = 24.7 (PhCH₂), 46.9 (CH₂N), 55.9 (OMe), 58.9 (OMe), 69.9 (CH₂), 69.6 (CH₂), 70.7 (CH₂), 71.9 (CH₂), 110.7 (CH_{ar}), 113.5 (CH_{ar}), 121.2 (C_q), 130.5 (C_q), 147.0 (C_q), 152.2 (C_q), 159.7 (CH-imine); HRMS (ESI): [M+H]⁺ calculated for C₁₅H₂₂O₄N 280.15433, found 280.15443.

General procedure V: preparation of alkylnylated tetrahydroisoquinolines via Sonogashira coupling

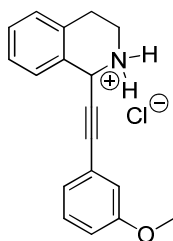
To a solution of the corresponding alkyne (1 equiv) and aryl iodide (1.2 equiv) in THF (50 mg alkyne in 3 mL), copper(I) iodide (0.1 equiv) and triethylamine (2 equiv) were added and the resulting mixture was degassed for 30 min. Tetrakis(triphenylphosphine)palladium(0) (0.05 equiv) was added and the reaction mixture was stirred overnight at RT. The solvents were removed *in vacuo*,

and the residue was purified by flash chromatography. The resulting material was subsequently dissolved in 5% HCl in methanol (1 mL) and stirred overnight. The solvents were removed *in vacuo* and the residue was washed several times with petroleum ether and diethyl ether to give the desired target compound.

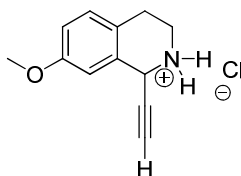
General procedure VI: preparation of alkynylated tetrahydroisoquinolines via imine alkynylation

A solution of the corresponding 3,4-dihydroisoquinoline in THF (70 mg dihydroisoquinoline in 1 mL) was cooled to 0 °C, trimethylsilyl trifluoromethanesulfonate (1.05 equiv) was added dropwise and the reaction mixture was stirred for 2h. In a separate flask a solution of the acetylene (6 equiv) in THF (1 mL) was also cooled to 0 °C and isopropyl magnesium chloride (6 equiv) was added dropwise. After 10 min stirring this reaction mixture was transferred to the iminium salt/THF suspension. The resulting solution was stirred at 0 °C for 1h and then warmed to RT within 1h. The reaction was quenched by the addition of MeOH and the solvents were evaporated *in vacuo*. The residue was purified *via* flash chromatography.

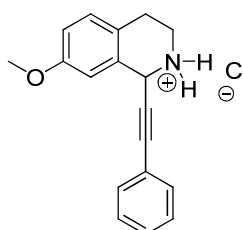
1-[(3-methoxyphenyl)ethynyl]-1,2,3,4-tetrahydroisoquinolinium chloride (73)



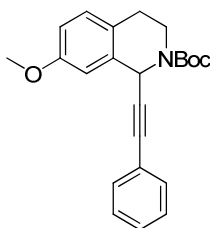
According to general procedure V, 3,4-dihydroisoquinoline⁷² yielded **73** as a slightly yellow solid (25 mg, 16%). m.p. 155-157 °C; $R_f = 0.32$ (petroleum ether/ethyl acetate, 1:2); $^1\text{H-NMR}$ (500 MHz, CD_3OD): $\delta = 3.14\text{-}3.25$ (m, 2H, PhCH_2), 3.43 (br s, 1H, NH), 3.56-3.61 (m, 1H, CHN), 3.70-3.75 (m, 1H, CHN), 3.78 (s, 3H, OMe), 5.80 (s, 1H, CH), 7.00 (dd, 1H, $J_1 = 8.4$, $J_2 = 2.7$, CH_{ar}) 7.04-7.05 (m, 1H, CH_{ar}), 7.09 (d, 1H, $J = 7.7$, CH_{ar}), 7.27-7.30 (m, 2H, CH_{ar}), 7.34-7.38 (m, 2H, CH_{ar}), 7.54-7.56 (m, 1H, CH_{ar}); $^{13}\text{C-NMR}$ (126 MHz, CD_3OD): $\delta = 25.9$ (PhCH_2), 41.3 (CH_2N), 48.8 (CH), 55.9 (OMe), 83.0 (C_q alkyne), 89.7 (C_q alkyne), 116.9 (CH_{ar}), 118.1 (CH_{ar}), 123.2 (C_q), 125.3 (CH_{ar}), 128.4 (CH_{ar}), 128.6 (CH_{ar}), 130.2 (CH_{ar}), 130.3 (CH_{ar}), 130.5 (C_q), 130.9 (CH_{ar}), 132.3 (C_q), 161.1 ($\text{C}_q\text{-OMe}$); HRMS (ESI): $[\text{M}+\text{H}]^+$ calculated for $\text{C}_{18}\text{H}_{18}\text{ON}$ 264.13829, found 264.13840.

1-Ethynyl-7-methoxy-1,2,3,4-tetrahydroisoquinolinium chloride (74)

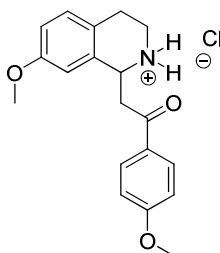
General procedure VI was modified as follows, dihydroisoquinoline **58** (70 mg, 0.43 mmol, 1 equiv) and ethynylmagnesium bromide (0.5 M in THF, 2.61 mL, 1.3 mmol, 3 equiv) yielded **74** as a slightly yellow wax (97 mg, 99%). $R_f = 0.30$ (ethylacetate); $^1\text{H-NMR}$ (400 MHz, CD_3OD): $\delta = 2.95$ - 3.07 (m, 2H, PhCH_2), 3.26 (br s, 1H, NH), 3.41 (s, 1H, CH alkyne), 3.43 - 3.49 (m, 1H, CHN), 3.54 - 3.63 (m, 1H, CHN), 3.74 (s, 3H, OMe), 5.48 (s, 1H, CH), 6.88 (d, 1H, $J = 8.0$, CH_{ar}), 6.94 (s, 1H, CH_{ar}), 7.13 (d, 1H, $J = 8.0$, CH_{ar}); $^{13}\text{C-NMR}$ (101 MHz, CD_3OD): $\delta = 25.0$ (PhCH_2), 41.4 (CH_2N), 48.4 (CH), 55.9 (OMe), 78.0 (C_q alkyne), 79.7 (C_q alkyne), 112.8 (CH_{ar}), 116.5 (CH_{ar}), 123.8 (2C_q), 130.9 (C_q), 131.4 (CH_{ar}), 160.1 (C_q - OMe); HRMS (ESI): $[\text{M}+\text{H}]^+$ calculated for $\text{C}_{12}\text{H}_{14}\text{ON}$ 188.10699, found 188.10690.

7-Methoxy-1-(phenylethynyl)-1,2,3,4-tetrahydroisoquinolinium chloride (75)

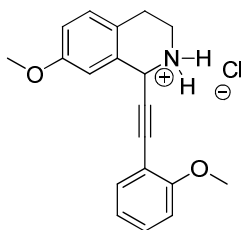
According to general procedure V and VI, **75** was obtained as a slightly yellow solid. (4 mg, 24% over 2 steps, general procedure V and 53 mg, 41%, general procedure VI). Preparative chiral HPLC of the free amine with a Chiralpak® IC column and 30% DCM/EtOH (100:2) in hexanes as eluent, a flow rate of 3 mL/min and detection at 254 nm delivered the two enantiomers. m.p. $50\text{ }^\circ\text{C}$ (decomposition); $R_f = 0.46$ (ethyl acetate); $^1\text{H-NMR}$ (400 MHz, CD_3OD): $\delta = 3.08$ - 3.14 (m, 2H, PhCH_2), 3.50 - 3.58 (m, 1H, CHN), 3.67 - 3.74 (m, 1H, CHN), 3.81 (s, 3H, OMe), 5.77 (s, 1H, CH), 6.96 (dd, 1H, $J_1 = 8.5$, $J_2 = 2.5$, CH_{ar}), 7.07 (d, 1H, $J = 2.5$, CH_{ar}), 7.21 (d, 1H, $J = 8.5$, CH_{ar}), 7.36 - 7.43 (m, 3H, CH_{ar}), 7.51 - 7.53 (m, 2H, CH_{ar}); $^{13}\text{C-NMR}$ (101 MHz, CD_3OD): $\delta = 25.2$ (PhCH_2), 41.4 (CH_2N), 49.23 (CH), 55.9 (OMe), 83.2 (C_q alkyne), 89.7 (C_q alkyne), 113.0 (CH_{ar}), 116.5 (CH_{ar}), 122.2 (C_q), 124.0 (C_q), 129.8 (2C , CH_{ar}), 130.8 (CH_{ar}), 131.5 (C_q), 131.5 (CH_{ar}), 133.0 (2C , CH_{ar}), 160.4 (C_q - OMe); HRMS (ESI): $[\text{M}+\text{H}]^+$ calculated for $\text{C}_{18}\text{H}_{18}\text{ON}$ 264.13829, found 264.13842.

***tert*-Butyl 7-methoxy-1-(phenylethynyl)-3,4-dihydroisoquinoline-2(1H)-carboxylate (237)**

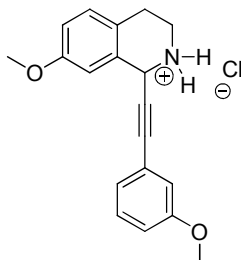
According to general procedure VI, **237** was obtained as a slightly brown oil (24 mg, 45% general procedure VI without Boc deprotection). Column purification (petroleum ether containing 2% ethyl acetate). $R_f = 0.34$ (petroleum ether/ethyl acetate, 9:1); $^1\text{H-NMR}$ (400 MHz, CD_3Cl_3): $\delta = 1.52$ (s, 9H, Boc- $(\text{CH}_3)_3$), 2.71-2.92 (m, 2H, PhCH_2), 3.32-3.50 (m, 1H, CHN), 3.80 (s, 3H, OMe), 4.05-4.26 (m, 1H, CHN), 6.05 (br s, 1H, CH), 6.79 (dd, 1H, $J_1 = 8.5$, $J_2 = 2.5$, CH_{ar}), 6.89 (d, 1H, $J = 2.5$, CH_{ar}), 7.06 (d, 1H, $J = 8.5$, CH_{ar}), 7.25-7.27 (m, 3H, CH_{ar}), 7.37-7.38 (m, 2H, CH_{ar}); $^{13}\text{C-NMR}$ (101 MHz, CD_3Cl_3): $\delta = 27.7$ (PhCH_2), 28.5 (Boc- $(\text{CH}_3)_3$), 38.4 (CH_2N), 46.9 (CH), 55.4 (OMe), 80.4 (C_q alkyne), 82.8 (C_q alkyne), 88.7 (Boc- C_q), 112.0 (CH_{ar}), 113.9 (CH_{ar}), 122.9 (C_q), 125.5 (C_q), 126.1 (C_q), 128.1 (2C, CH_{ar}), 129.9 (CH_{ar}), 131.8 (2C, CH_{ar}), 154.3 (Boc-CO), 160.4 (C_q -OMe); HRMS (ESI): $[\text{M}+\text{H}]^+$ calculated for $\text{C}_{23}\text{H}_{26}\text{O}_3\text{N}$ 364.19072, found 364.19092.

7-Methoxy-1-[2-(4-methoxyphenyl)-2-oxoethyl]-1,2,3,4-tetrahydroisoquinolinium chloride (238)

General procedure V was modified as follows, alkyne hydrolysis occurred upon Boc-deprotection using DCM/TFA (1:1), thus **238** was obtained as a brown solid (10 mg, 18% over two steps). m.p. 165-167 °C; $^1\text{H-NMR}$ (400 MHz, CD_3OD): $\delta = 3.03$ -3.10 (m, 2H, PhCH_2), 3.37-3.43 (m, 1H, CHN), 3.54-3.60 (m, 1H, CHN), 3.75 (s, 3H, OMe), 3.82-3.85 (m, 2H, CH_2), 3.88 (s, 3H, OMe), 5.10-5.12 (m, 1H, CH), 6.87-6.89 (m, 2H, CH_{ar}), 7.04 (d, 2H, $J = 9.0$, CH_{ar}), 7.17 (d, 1H, $J = 9.0$, CH_{ar}), 8.06 (d, 2H, $J = 9.0$, CH_{ar}); $^{13}\text{C-NMR}$ (101 MHz, CD_3OD): $\delta = 25.7$ (PhCH_2), 40.7 (CH_2N), 42.6 (CH_2), 52.9 (CH), 55.9 (OMe), 56.2 (OMe), 112.1 (CH_{ar}), 115.1 (CH_{ar}), 115.8 (CH_{ar}), 124.8 (C_q), 130.1 (C_q), 131.4 (CH_{ar}), 131.9 (CH_{ar}), 133.8 (C_q), 160.3 (C_q -OMe), 166.0 (C_q -OMe), 197.2 (CO); HRMS (ESI): $[\text{M}+\text{H}]^+$ calculated for $\text{C}_{19}\text{H}_{22}\text{O}_3\text{N}$ 312.15942, found 312.15954.

7-Methoxy-1-[(2-methoxyphenyl)ethynyl]-1,2,3,4-tetrahydroisoquinolinium chloride (76)

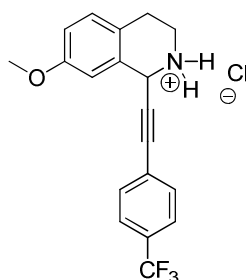
According to general procedure VI, **76** was obtained as a yellow solid (61 mg, 43%). m.p. 56-58 °C; $R_f = 0.34$ (petroleum ether/ethyl acetate, 1:2); $^1\text{H-NMR}$ (400 MHz, DMSO- d_6): $\delta = 2.97$ -3.06 (m, 2H, PhCH_2), 3.45-3.53 (m, 2H, CH_2N), 3.76 (s, 3H, OMe), 3.83 (s, 3H, OMe), 5.85 (s, 1H, CH), 6.94-6.99 (m, 2H, CH_{ar}), 7.06 (d, 1H, $J = 2.3$, CH_{ar}), 7.11 (d, 1H, $J = 8.5$, CH_{ar}), 7.20 (d, 1H, $J = 8.5$, CH_{ar}), 7.41-7.45 (m, 2H, CH_{ar}), 9.91 (br s, 1H, NH), 10.17 (br s, 1H, NH); $^{13}\text{C-NMR}$ (101 MHz, CD_3OD): $\delta = 24.1$ (PhCH_2), 40.2 (CH_2N), 48.3 (CH), 54.4 (OMe), 54.8 (OMe), 84.5 (C_q alkyne), 86.5 (C_q alkyne), 110.1 (C_q), 110.7 (CH_{ar}), 111.7 (CH_{ar}), 114.7 (CH_{ar}), 118.7 (C_q), 120.1 (CH_{ar}), 123.0 (C_q), 129.9 (CH_{ar}), 130.7 (CH_{ar}), 132.9 (CH_{ar}), 158.7 (C_q -OMe), 160.6 (C_q -OMe); HRMS (ESI): $[\text{M}+\text{H}]^+$ calculated for $\text{C}_{19}\text{H}_{20}\text{O}_2\text{N}$ 294.14886, found 294.14881.

7-Methoxy-1-[(3-methoxyphenyl)ethynyl]-1,2,3,4-tetrahydroisoquinolinium chloride (77)

According to general procedure V and VI, **77** was obtained as a slightly yellow solid (47 mg, 95% over 2 steps, general procedure V and 49 mg, 35%, general procedure VI). Preparative chiral HPLC of the free amine with a Chiralpak® IC column and 30% DCM/EtOH (100:2) in hexanes as eluent, a flow rate of 3 mL/min and detection at 254 nm delivered the two enantiomers. m.p. 166-168 °C; $R_f = 0.30$ (MeOH/DCM, 1:19); $^1\text{H-NMR}$ (400 MHz, CD_3OD): $\delta = 3.05$ -3.18 (m, 2H, PhCH_2), 3.52-3.58 (m, 1H, CHN), 3.67-3.74 (m, 1H, CHN), 3.78 (s, 3H, OMe), 3.80 (s, 3H, OMe), 5.77 (s, 1H, CH), 6.94-7.01 (m, 2H, CH_{ar}), 7.05-7.10 (m, 1H, CH_{ar}), 7.21 (d, 1H, $J = 8.5$, CH_{ar}), 7.27-7.31 (m, 1H, CH_{ar}); $^{13}\text{C-NMR}$ (101 MHz, CD_3OD): $\delta = 25.1$ (PhCH_2), 41.4 (CH_2N), 49.1 (CH), 55.9 (2C, OMe), 83.0 (C_q alkyne), 89.6 (C_q alkyne), 113.0 (CH_{ar}), 116.5 (CH_{ar}), 116.9 (CH_{ar}), 118.0 (CH_{ar}),

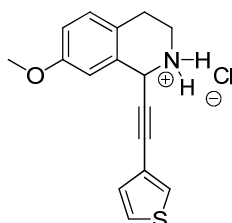
123.2 (C_q), 124.0 (C_q), 125.3 (CH_{ar}), 130.9 (CH_{ar}), 131.4 (C_q), 131.5 (CH_{ar}), 160.4 (C_q-OMe), 161.1 (C_q-OMe); HRMS (ESI): [M+H]⁺ calculated for C₁₉H₂₀O₂N 294.14886, found 294.14897.

7-Methoxy-1-([4-(trifluoromethyl)phenyl]ethynyl)-1,2,3,4-tetrahydroisoquinolinium chloride (78)



According to general procedure V, **78** was obtained as a slightly yellow solid (46 mg, 72% over 2 steps). m.p. 217-218 °C; ¹H-NMR (400 MHz, CD₃OD): δ = 3.07-3.20 (m, 2H, PhCH₂), 3.55-3.61 (m, 1H, CHN), 3.69-3.76 (m, 1H, CHN), 3.81 (s, 3H, OMe), 5.85 (s, 1H, CH), 6.96 (dd, J₁ = 8.5, J₂ = 2.5, 1H, CH_{ar}), 7.07 (d, 1H, J = 2.5, CH_{ar}), 7.22 (d, 1H, J = 2.5, CH_{ar}), 7.69-7.74 (m, 4H, CH_{ar}); ¹³C-NMR (101 MHz, CD₃OD): δ = 25.1 (PhCH₂), 41.4 (CH₂N), 48.4 (CH), 55.9 (OMe), 85.8 (C_q alkyne), 88.0 (C_q alkyne), 113.0 (CH_{ar}), 116.6 (CH_{ar}), 124.0 (C_q), 125.1 (q, J = 248, CF₃), 126.4 (C_q), 126.7 (q, 2C, J = 4, CH_{ar}), 131.0 (C_q), 131.6 (CH_{ar}), 132.2 (q, J = 32.0, C_q-CF₃), 133.6 (2C, CH_{ar}), 160.4 (C_q-OMe); HRMS (ESI): [M+H]⁺ calculated for C₁₉H₁₇ONF₃ 332.12568, found 332.12568.

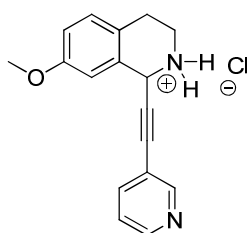
7-Methoxy-1-(thiophene-3-ylethynyl)-1,2,3,4-tetrahydroisoquinolinium chloride (79)



According to general procedure V and VI, **79** was obtained as a slightly yellow solid (25 mg, 46% over 2 steps, general procedure V and 44 mg, 33%, general procedure VI). m.p. 205-207 °C; R_f = 0.29 (petroleum ether/ethyl acetate, 1:2); ¹H-NMR (400 MHz, CD₃OD): δ = 3.06-3.13 (m, 2H, PhCH₂), 3.51-3.57 (m, 1H, CHN), 3.66-3.73 (m, 1H, CHN), 3.80 (s, 3H, OMe), 5.76 (s, 1H, CH), 6.95 (dd, 1H, J₁ = 8.3, J₂ = 2.8, CH_{ar}), 7.04-7.05 (m, 1H, CH_{ar}), 7.18-7.21 (m, 2H, CH_{ar}), 7.47 (dd,

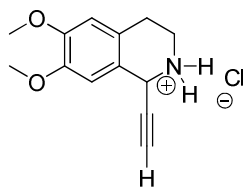
1H, $J_1 = 5.0$, $J_2 = 3.0$, CH_{ar}), 7.75 (dd, 1H, $J_1 = 3.0$, $J_2 = 1.0$, CH_{ar}); ^{13}C -NMR (101 MHz, CD_3OD): $\delta = 25.1$ ($PhCH_2$), 41.3 (CH_2N), 49.2 (CH), 55.9 (OMe), 82.8 (C_q alkyne), 85.1 (C_q alkyne), 113.0 (CH_{ar}), 116.5 (CH_{ar}), 121.2 (C_q), 124.0 (C_q), 127.5 (CH_{ar}), 130.7 (CH_{ar}), 131.4 (C_q), 131.5 (CH_{ar}), 132.3 (CH_{ar}), 160.3 (C_q -OMe); HRMS (ESI): $[M+H]^+$ calculated for $C_{16}H_{16}ONS$ 270.09471, found 270.09479.

7-Methoxy-1-(pyridine-3-ylethynyl)-1,2,3,4-tetrahydroisoquinolinium chloride (**80**)



According to general procedure V, **80** was obtained as a brown solid (12 mg, 46% over 2 steps). m.p. 139-140 °C; 1H -NMR (400 MHz, CD_3OD): $\delta = 3.12$ -3.16 (m, 2H, $PhCH_2$), 3.59-3.65 (m, 1H, CHN), 3.73-3.79 (m, 1H, CHN), 3.81 (s, 3H, OMe), 5.95 (s, 1H, CH), 6.97 (dd, 1H, $J_1 = 8.5$, $J_2 = 2.5$, CH_{ar}), 7.08 (d, 1H, $J = 2.5$, CH_{ar}), 7.23 (d, 1H, $J = 8.5$, CH_{ar}), 8.1 (dd, 1H, $J_1 = 8.0$, $J_2 = 5.5$, CH_{ar}), 8.73 (d, 1H, $J = 8.0$, CH_{ar}), 8.90 (d, 1H, $J = 5.5$, CH_{ar}), 9.14 (s, 1H, CH_{ar}); ^{13}C -NMR (101 MHz, CD_3OD): $\delta = 25.1$ ($PhCH_2$), 41.4 (CH_2N), 48.7 (CH), 56.0 (OMe), 82.7 (C_q alkyne), 90.8 (C_q alkyne), 113.2 (CH_{ar}), 116.7 (CH_{ar}), 123.2 (C_q), 124.1 (C_q), 128.5 (CH_{ar}), 130.2 (C_q), 131.7 (2C, CH_{ar}), 143.6 (CH_{ar}), 146.4 (CH_{ar}), 149.7 (CH_{ar}), 160.4 (C_q -OMe); HRMS (ESI): $[M+H]^+$ calculated for $C_{17}H_{17}ON_2$ 265.13354, found 265.13364.

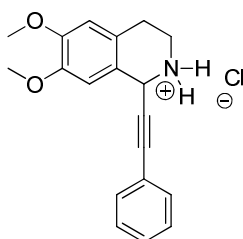
1-Ethynyl-6,7-dimethoxy-1,2,3,4-tetrahydroisoquinolinium chloride (**81**)



General procedure VI was modified as follows, dihydroisoquinoline **59** (70 mg, 0.37 mmol, 1 equiv) and ethynylmagnesium bromide (0.5 M in THF, 2.2 mL, 1.1 mmol, 3 equiv) yielded **81** as a slightly yellow solid (44 mg, 47%). m.p. 190 °C (decomposition); $R_f = 0.17$ (ethyl acetate); 1H -NMR (400 MHz, CD_3OD): $\delta = 2.92$ -3.06 (m, 2H, $PhCH_2$), 3.24 (br s, 1H, NH), 3.36 (s, 1H, H-alkyne), 3.39-3.45 (m, 1H, CHN), 3.51-3.60 (m, 1H, CH_2N), 3.68 (s, 6H, OMe), 5.32 (s, 1H, CH), 6.68 (s, 1H, CH_{ar}), 6.82 (s, 1H, CH_{ar}); ^{13}C -NMR (101 MHz, CD_3OD): $\delta = 24.1$ ($PhCH_2$), 39.9 (CH_2N), 46.8 (CH),

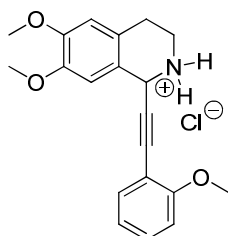
55.3 (2C, OMe), 76.9 (C_q alkyne), 78.2 (C_q alkyne), 109.7 (CH_{ar}), 111.5 (CH_{ar}), 120.3 (C_q), 123.1 (C_q), 148.4 (C_q-OMe), 149.7 (C_q-OMe); HRMS (ESI): [M+H]⁺ calculated for C₁₃H₁₆O₂N 218.11756, found 218.11753.

6,7-Dimethoxy-1-(phenylethynyl)-1,2,3,4-tetrahydroisoquinolinium chloride (**82**)



According to general procedure V and VI, **82** was obtained as a slightly yellow solid (6 mg, 15% over 2 steps, general procedure V and 57 mg, 35%, general procedure VI). Preparative chiral HPLC of the free amine with a Chiralpak® IC column and 60% DCM/EtOH (100:2) in hexanes as eluent, a flow rate of 3 mL/min and detection at 254 nm delivered the two enantiomers. m.p. 240 °C (decomposition); R_f = 0.25 (ethyl acetate); ¹H-NMR (400 MHz, CD₃OD): δ = 3.06-3.17 (m, 2H, PhCH₂), 3.51-3.58 (m, 1H, CHN), 3.68-3.74 (m, 1H, CHN), 3.83 (s, 3H, OMe), 3.84 (s, 3H, OMe), 5.71 (s, 1H, CH), 6.85 (s, 1H, CH_{ar}), 7.05 (s, 1H, CH_{ar}), 7.36-7.42 (m, 3H, CH_{ar}), 7.50-7.52 (m, 2H, CH_{ar}); ¹³C-NMR (101 MHz, CD₃OD): δ = 25.5 (PhCH₂), 41.2 (CH₂N), 48.2 (CH), 56.5 (OMe), 56.6 (OMe), 83.5 (C_q alkyne), 89.5 (C_q alkyne), 111.2 (CH_{ar}), 112.9 (CH_{ar}), 122.2 (C_q), 122.3 (C_q), 124.6 (C_q), 129.8 (CH_{ar}), 130.8 (CH_{ar}), 133.0 (CH_{ar}), 150.0 (C_q-OMe), 151.2 (C_q-OMe); HRMS (ESI): [M+H]⁺ calculated for C₁₉H₂₀O₂N 294.14886, found 294.14891.

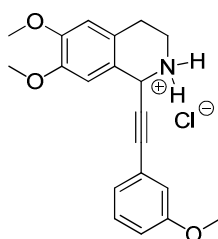
6,7-Dimethoxy-1-[(2-methoxyphenyl)ethynyl]-1,2,3,4-tetrahydroisoquinolinium chloride (**83**)



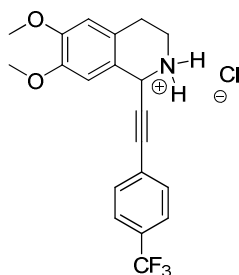
According to general procedure VI, **83** was obtained as a yellow wax (13 mg, 10%). R_f = 0.31 (8% MeOH/DCM); ¹H-NMR (600 MHz, CD₃OD): δ = 3.05-3.17 (m, 2H, PhCH₂), 3.43 (br s, 1H, NH), 3.49-3.55 (m, 1H, CHN), 3.67-3.74 (m, 1H, CHN), 3.83 (s, 3H, OMe), 3.84 (s, 3H, OMe), 3.85 (s, 3H, OMe), 5.68 (s, 1H, CH), 6.83 (s, 1H, CH_{ar}), 6.92-6.95 (m, 1H, CH_{ar}), 7.03 (d, 1H, J = 8.2, CH_{ar}),

7.11 (m, 1H, CH_{ar}), 7.37-7.42 (m, 2H, CH_{ar}); ^{13}C -NMR (151 MHz, CD_3OD): δ = 25.5 ($PhCH_2$), 41.4 (CH_2N), 48.2 (CH), 56.3 (OMe), 56.3 (OMe), 56.7 (OMe), 62.6 (C_q alkyne), 87.1 (C_q alkyne), 111.3 (C_q), 111.5 (CH_{ar}), 112.2 (CH_{ar}), 112.9 (CH_{ar}), 121.6 (CH_{ar}), 122.5 (C_q), 124.7 (C_q), 132.4 (CH_{ar}), 134.5 (CH_{ar}), 150.0 (C_q -OMe), 151.2 (C_q -OMe), 162.1 (C_q -OMe); HRMS (ESI): $[M+H]^+$ calculated for $C_{20}H_{22}O_3N$ 324.15942, found 324.15959.

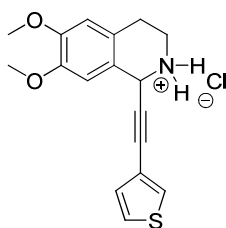
6,7-Dimethoxy-1-[(3-methoxyphenyl)ethynyl]-1,2,3,4-tetrahydroisoquinolinium chloride (**84**)



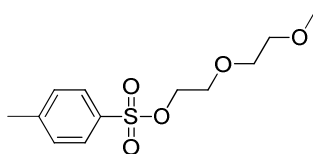
According to general procedure V and VI, **84** was obtained as a slightly yellow solid (6 mg, 31% over 2 steps, general procedure V and 119 mg, 90% general procedure VI). Preparative chiral HPLC of the free amine with a Chiralpak® IC column and 50% DCM/EtOH (100:2) in hexanes as eluent, a flow rate of 3 mL/min and detection at 254 nm delivered the two enantiomers. m.p. 180-182 °C; R_f = 0.36 (8% MeOH/DCM); 1H -NMR (400 MHz, CD_3OD): δ = 3.05-3.17 (m, 2H, $PhCH_2$), 3.51-3.57 (m, 1H, CHN), 3.68-3.74 (m, 1H, CHN), 3.78 (s, 3H, OMe), 3.84 (s, 6H, 2OMe), 5.70 (s, 1H, CH), 6.84 (s, 1H, CH_{ar}), 6.98-7.09 (m, 4H, CH_{ar}), 7.27-7.31 (m, 1H, CH_{ar}); ^{13}C -NMR (101 MHz, CD_3OD): δ = 25.5 ($PhCH_2$), 41.2 (CH_2N), 51.0 (CH), 55.9 (OMe), 56.6 (OMe), 83.2 (C_q alkyne), 89.5 (C_q alkyne), 111.2 (CH_{ar}), 112.9 (CH_{ar}), 116.8 (CH_{ar}), 118.1 (CH_{ar}), 122.2 (C_q), 123.3 (C_q), 124.6 (C_q), 125.3 (CH_{ar}), 131.0 (CH_{ar}), 150.1 (C_q -OMe), 151.3 (C_q -OMe), 161.1 (C_q -OMe); HRMS (ESI): $[M+H]^+$ calculated for $C_{20}H_{22}O_3N$ 324.15942, found 324.15950.

6,7-Dimethoxy-1-([4-(trifluoromethyl)phenyl]ethynyl)-1,2,3,4-tetrahydroisoquinolinium chloride (85)

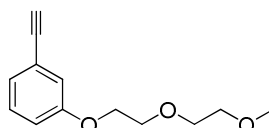
According to general procedure V, **85** was obtained as a slightly yellow solid (29 mg, 71% over 2 steps). m.p. 207-208 °C; $^1\text{H-NMR}$ (400 MHz, CD_3OD): δ = 3.11-3.18 (m, 2H, PhCH_2), 3.55-3.61 (m, 1H, CHN), 3.69-3.76 (m, 1H, CHN), 3.84 (s, 6H, OMe), 5.78 (s, 1H, CH), 6.86 (s, 1H, CH_{ar}), 7.05 (s, 1H, CH_{ar}), 7.68-7.73 (m, 4H, CH_{ar}); $^{13}\text{C-NMR}$ (101 MHz, CD_3OD): δ = 25.5 (PhCH_2), 41.1 (CH_2N), 48.4 (CH), 56.5 (OMe), 56.7 (OMe), 86.1 (C_q alkyne), 87.9 (C_q alkyne), 111.2 (CH_{ar}), 112.9 (CH_{ar}), 121.8 (C_q), 124.8 (C_q), 125.2 (q, J = 296, CF_3), 126.6 (2C, CH_{ar}), 132.2 (q, J = 32.0, $\text{C}_q\text{-CF}_3$), 133.6 (2C, CH_{ar}), 132.4 (C_q), 150.0 ($\text{C}_q\text{-OMe}$), 151.3 ($\text{C}_q\text{-OMe}$); HRMS (ESI): $[\text{M}+\text{H}]^+$ calculated for $\text{C}_{20}\text{H}_{19}\text{O}_2\text{NF}_3$ 362.13624, found 362.13629.

6,7-Dimethoxy-1-(thiophen-3-ylethynyl)-1,2,3,4-tetrahydroisoquinolinium chloride (86)

According to general procedure VI, **86** was obtained as a slightly yellow solid (83 mg, 68%). m.p. 190 °C (decomposition); R_f = 0.38 (8% MeOH/DCM); $^1\text{H-NMR}$ (400 MHz, DMSO-d_6): δ = 2.96-3.01 (m, 2H, PhCH_2), 3.43-3.49 (m, 2H, CH_2N), 3.74 (s, 3H, OMe), 3.75 (s, 3H, OMe), 5.72 (s, 1H, CH), 6.83 (s, 1H, CH_{ar}), 6.95 (s, 1H, CH_{ar}), 7.21 (dd, 1H, J_1 = 5.0, J_2 = 1.1, CH_{ar}), 7.65 (dd, 1H, J_1 = 5.0, J_2 = 2.8, CH_{ar}), 7.92 (dd, 1H, J_1 = 2.8, J_2 = 1.1, CH_{ar}), 9.94 (br s, 1H, NH), 10.20 (br s, 1H, NH); $^{13}\text{C-NMR}$ (101 MHz, CD_3OD): δ = 25.5 (PhCH_2), 41.1 (CH_2N), 48.9 (CH), 55.6 (OMe), 56.7 (OMe), 82.9 (C_q alkyne), 84.9 (C_q alkyne), 111.1 (CH_{ar}), 112.8 (CH_{ar}), 121.1 (C_q), 122.1 (C_q), 124.5 (C_q), 127.4 (CH_{ar}), 130.6 (CH_{ar}), 132.2 (CH_{ar}), 149.8 ($\text{C}_q\text{-OMe}$), 151.0 ($\text{C}_q\text{-OMe}$); HRMS (ESI): $[\text{M}+\text{H}]^+$ calculated for $\text{C}_{17}\text{H}_{18}\text{O}_2\text{NS}$ 300.10528, found 300.10528.

2-(2-Methoxyethoxy)ethyl tosylate (239)

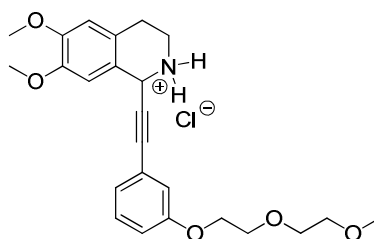
To a solution of 2-(2-methoxyethoxy)ethanol (0.75 mL, 6.3 mmol, 1.2 equiv) in pyridine (5 mL), tosyl chloride (1 g, 5.3 mmol, 1 equiv) was added under ice cooling. The mixture was stirred at RT for 2h. The mixture was diluted with water and extracted with ethyl acetate (3 × 30 mL). The combined organic fractions were washed with saturated aq. Na₂CO₃ solution and brine, dried with MgSO₄, filtered and the solvents were evaporated *in vacuo* to yield **239** as a colourless oil (1.1 g, 79%). R_f = 0.46 (petroleum ether/ethyl acetate, 1:1); ¹H-NMR (500 MHz, CDCl₃): δ = 2.39 (s, 3H, Tos-CH₃), 3.28-3.29 (m, 3H, OMe), 3.41-3.43 (m, 2H, CH₂), 3.51-3.52 (m, 2H, CH₂), 3.62-3.64 (m, 2H, CH₂), 4.10-4.12 (m, 2H, CH₂), 7.29 (d, 2H, *J* = 7.9, Tos-CH_{ar}), 7.73-7.75 (m, 2H, Tos-CH_{ar}); ¹³C-NMR (126 MHz, CDCl₃): δ = 21.4 (Tos-CH₃), 58.8 (OMe), 68.5 (CH₂), 69.1 (CH₂), 70.5 (CH₂), 71.6 (CH₂), 127.8 (2 Tos-CH_{ar}), 129.7 (2 Tos-CH_{ar}), 132.9 (Tos-C_q), 144.7 (Tos-C_q); HRMS (ESI): calculated for [M+H]⁺ C₁₂H₁₉O₅S 275.09477, found 275.09501.

1-Ethynyl-3-[2-(2-methoxyethoxy)ethoxy]benzene (240)

To a solution of 3-hydroxyphenylacetylene (0.3 mL, 2.75 mmol, 1 equiv) in DMF (10 mL) tosylate **239** (1.10 g, 4.13 mmol, 1.5 equiv), Cs₂CO₃ (0.8 g, 4.13 mmol, 1.5 equiv) and KI (91 mg, 0.55 mmol, 0.2 equiv) were added. The reaction mixture was stirred at 70 °C overnight. The solvents were evaporated *in vacuo*, the residue was dissolved in water and extracted with ethyl acetate (3 × 30 mL). The combined organic fractions were washed with brine, dried with MgSO₄ and the solvents were evaporated *in vacuo*. The residue was purified *via* flash chromatography (petroleum ether/ethyl acetate, 12:1) to give **241** as a colourless oil (441 mg, 73%). R_f = 0.46 (petroleum ether/ethyl acetate, 3:1); ¹H-NMR (500 MHz, CDCl₃): δ = 3.04 (s, 1H, CH alkyne), 3.36 (m, 3H, OMe), 3.54-3.56 (m, 2H, CH₂), 3.68-3.70 (m, 2H, CH₂), 3.81-3.83 (m, 2H, CH₂), 4.09-4.11 (m, 2H, CH₂), 6.90 (dd, *J*₁ = 8.2, *J*₂ = 2.5, CH_{ar}), 7.01 (br s, 1H, CH_{ar}), 7.06 (d, 1H, *J* = 7.3, CH_{ar}), 7.17-7.20 (m, 1H, CH_{ar}); ¹³C-NMR (126 MHz, CDCl₃): δ = 59.0 (OMe), 67.4 (CH₂), 69.6 (CH₂), 70.7 (CH₂), 71.9 (CH₂), 76.9 (CH alkyne), 83.4 (C_q alkyne), 115.9 (CH_{ar}), 117.7 (CH_{ar}), 123.0 (C_q), 124.7

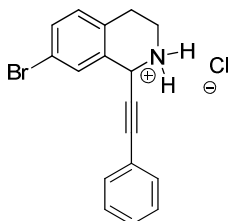
(CH_{ar}), 129.3 (CH_{ar}), 158.4 (C_q-O); HRMS (ESI): calculated for $[M+H]^+$ $C_{13}H_{17}O_3S$ 221.11722, found 221.11731.

6,7-dimethoxy-1-({3-[2-(2-methoxyethoxy)ethoxy]phenyl}ethynyl)-1,2,3,4-tetrahydroisoquinolinium chloride (87**)**



General procedure VI was modified as follows, dihydroisoquinoline **59** and alkyne **240** (3 equiv) yielded **87** as a slightly yellow solid (27 mg, 16%). m.p. 99-100 °C; R_f = 0.33 (MeOH/DCM, 1:10); 1H -NMR (600 MHz, CD_3OD): δ = 3.07-3.15 (m, 2H, $PhCH_2$), 3.34 (s, 3H, OMe), 3.52-3.57 (m, 3H, CHN , CH_2), 3.66-3.67 (m, 2H, CH_2), 3.69-3.73 (m, 1H, CHN), 3.79-3.82 (m, 2H, CH_2), 3.83 (s, 3H, OMe), 3.83 (s, 3H, OMe), 4.10-4.12 (m, 2H, CH_2), 5.71 (s, 1H, CH), 6.84 (s, 1H, CH_{ar}), 7.02 (dd, J_1 = 8.4, J_2 = 2.5, CH_{ar}), 7.03 (s, 1H, CH_{ar}), 7.07 (m, 1H, CH_{ar}), 7.09 (dd, J_1 = 7.6, J_2 = 0.9, CH_{ar}), 7.27-7.30 (m, 1H, CH_{ar}); ^{13}C -NMR (151 MHz, CD_3OD): δ = 25.5 ($PhCH_2$), 41.1 (CH_2N), 48.8 (CH), 56.5 (OMe), 56.7 (OMe), 68.8 (CH_2), 70.7 (CH_2), 71.5 (CH_2), 72.9 (CH_2), 83.3 (C_q alkyne), 89.4 (C_q alkyne), 111.3 (CH_{ar}), 112.9 (CH_{ar}), 117.5 (CH_{ar}), 118.8 (CH_{ar}), 122.2 (C_q), 123.3 (C_q), 124.7 (C_q), 125.5 (CH_{ar}), 131.0 (CH_{ar}), 150.1 (C_q-OMe), 151.3 (C_q-OMe), 160.3 (C_q-OMe); HRMS (ESI): $[M+H]^+$ calculated for $C_{24}H_{30}O_5N$ 412.21185, found 412.21136.

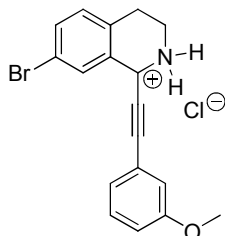
7-Bromo-1-(phenylethynyl)-1,2,3,4-tetrahydroisoquinolinium chloride (88**)**



According to general procedure V, **88** was obtained as a slightly yellow solid (13 mg, 45% over 2 steps). m.p. 223-224 °C; 1H -NMR (400 MHz, CD_3OD): δ = 3.09-3.21 (m, 2H, $PhCH_2$), 3.55-3.61 (m, 1H, CHN), 3.69-3.76 (m, 1H, CHN), 5.83 (s, 1H, CH), 7.24 (d, 1H, J = 8.2, CH_{ar}), 7.37-7.46 (m, 3H, CH_{ar}), 7.52-7.55 (m, 3H, CH_{ar}), 7.72 (s, 1H, CH_{ar}); ^{13}C -NMR (101 MHz, CD_3OD): δ = 25.5 ($PhCH_2$), 41.1 (CH_2N), 48.7 (CH), 82.6 (C_q alkyne), 90.3 (C_q alkyne), 121.9 (C_q), 122.0 (C_q), 129.8 (2C,

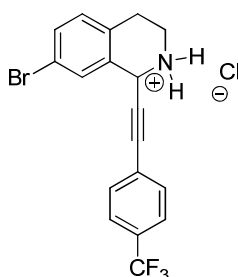
CH_{ar}), 131.2 (CH_{ar}), 131.7 (C_{q}), 132.3 (CH_{ar}), 132.8 (C_{q}), 133.0 (2C, CH_{ar}), 133.3 (CH_{ar}); HRMS (ESI): $[\text{M}+\text{H}]^+$ calculated for $\text{C}_{17}\text{H}_{15}\text{NBr}$ 312.03824, found 312.03865.

7-Bromo-1-[(3-methoxyphenyl)ethynyl]-1,2,3,4-tetrahydroisoquinolinium chloride (**89**)



According to general procedure V, **89** was obtained as a slightly yellow solid (15.3 mg, 32% over 2 steps). m.p. 195-196 °C; $^1\text{H-NMR}$ (400 MHz, CD_3OD): δ = 3.09-3.21 (m, 2H, PhCH_2), 3.55-3.61 (m, 1H, CHN), 3.69-3.76 (m, 1H, CHN), 3.79 (s, 3H, OMe), 5.82 (s, 1H, CH), 7.00-7.11 (m, 3H, CH_{ar}), 7.23-7.32 (m, 2H, CH_{ar}), 7.53 (dd, 1H, $J_1 = 8.2$, $J_2 = 1.6$, CH_{ar}), 7.71 (d, 1H, $J = 1.6$, CH_{ar}); $^{13}\text{C-NMR}$ (101 MHz, CD_3OD): δ = 25.5 (PhCH_2), 41.0 (CH_2N), 48.7 (CH), 55.9 (OMe), 82.4 (C_{q} alkyne), 90.2 (C_{q} alkyne), 117.1 (CH_{ar}), 118.1 (CH_{ar}), 121.8 (C_{q}), 123.0 (C_{q}), 125.4 (CH_{ar}), 130.9 (CH_{ar}), 131.2 (CH_{ar}), 131.7 (C_{q}), 132.3 (CH_{ar}), 132.8 (C_{q}), 133.3 (CH_{ar}), 161.1 (C_{q} -OMe); HRMS (ESI): $[\text{M}+\text{H}]^+$ calculated for $\text{C}_{18}\text{H}_{17}\text{ONBr}$ 342.04880, found 342.04920.

7-Bromo-1-[[4-(trifluoromethyl)phenyl]ethynyl]-1,2,3,4-tetrahydroisoquinolinium chloride (**90**)



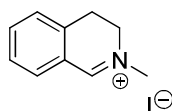
According to general procedure V, **90** was obtained as a slightly yellow solid (30 mg, 59% over 2 steps). m.p. 192-193 °C; $^1\text{H-NMR}$ (400 MHz, CD_3OD): δ = 3.10-3.24 (m, 2H, PhCH_2), 3.58-3.66 (m, 1H, CHN), 3.71-3.78 (m, 1H, CHN), 5.91 (s, 1H, CH), 7.25 (d, $J = 8.5$, 1H, CH_{ar}), 7.53 (dd, 1H, $J_1 = 8.5$, $J_2 = 1.8$, CH_{ar}), 7.70-7.75 (m, 5H, CH_{ar}); $^{13}\text{C-NMR}$ (101 MHz, CD_3OD): δ = 24.00 (PhCH_2), 39.5 (CH_2N), 46.9 (CH), 83.7 (C_{q} alkyne), 87.0 (C_{q} alkyne), 120.3 (C_{q}), 123.5 (q, $J = 228$, CF_3), 125.2 (q, 2C, $J = 4$, CH_{ar}), 129.7 (CH_{ar}), 130.3 (C_{q}), 130.5 (q, $J = 35.0$, C_{q} - CF_3), 130.9 (CH_{ar}), 131.0 (C_{q}),

131.9 (CH_{ar}), 132.1 (C_{q}), 132.2 (CH_{ar}); HRMS (ESI): $[\text{M}+\text{H}]^+$ calculated for $\text{C}_{18}\text{H}_{14}\text{NBrF}_3$ 380.02562, found 380.02656.

General procedure VII: preparation of methyl-3,4-dihydroisoquinolinium iodides

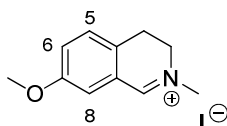
To a solution of the corresponding 3,4-dihydroisoquinoline (1 equiv) in diethyl ether (1 g starting material in 30 mL) methyl iodide (2 equiv) was added. The reaction mixture was refluxed overnight. The resulting yellow precipitate was filtered and washed with diethyl ether to give the desired target compound as air-stable salt.

2-Methyl-3,4-dihydroisoquinolinium iodide (61)

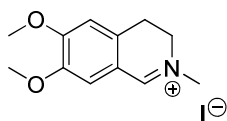


According to general procedure VII, 3,4-dihydroisoquinoline⁷² yielded iminium salt **61** as a yellow solid (1.10 g, 54%). m.p. 124-125 °C; $^1\text{H-NMR}$ (400 MHz, CD_3OD): δ = 3.11 (t, 2H, J = 8.2, PhCH_2), 3.82 (s, 3H, NCH_3), 4.10 (t, 2H, J = 8.2, CH_2N), 7.49-7.56 (m, 2H, CH_{ar}), 7.78-7.85 (m, 2H, CH_{ar}), 9.17 (s, 1H, CH imine); $^{13}\text{C-NMR}$ (101 MHz, CD_3OD): δ = 26.0 (PhCH_2), 48.4 (NCH_3), 51.4 (CH_2N), 126.1 (C_{q}), 129.5 (CH_{ar}), 129.5 (CH_{ar}), 134.7 (CH_{ar}), 137.6 (C_{q}), 139.1 (CH_{ar}), 168.5 (CH imine), HRMS (ESI): $[\text{M}]^+$ calculated for $\text{C}_{10}\text{H}_{12}\text{N}$ 146.09643, found 146.09622.

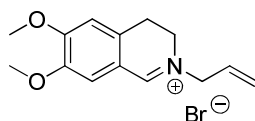
7-methoxy-2-methyl-3,4-dihydroisoquinolinium iodide (62)



According to general procedure VII, 7-methoxy-3,4-dihydroisoquinoline **58** yielded iminium salt **62** as a yellow solid (1.40 g, 69%). m.p. 161-163 °C; $^1\text{H-NMR}$ (400 MHz, CD_3OD): δ = 3.22 (t, 2H, J = 8.2, PhCH_2), 3.81 (br s, 3H, NCH_3), 3.81 (s, 3H, OMe), 4.05 (t, 2H, J = 8.2, CH_2N), 7.30 (dd, 1H, J_1 = 8.4, J_2 = 2.6, 6-H), 7.36-7.38 (m, 1H, 5-H), 7.41 (d, 1H, J = 2.6, 8-H), 9.20 (s, 1H, CH imine); $^{13}\text{C-NMR}$ (101 MHz, CD_3OD): δ = 25.2 (PhCH_2), 48.7 (NCH_3), 52.0 (CH_2N), 56.7 (OMe), 118.5 (CH_{ar}), 125.1 (CH_{ar}), 126.6 (C_{q}), 129.3 (C_{q}), 130.6 (CH_{ar}), 160.4 (CH imine), 168.0 ($\text{C}_{\text{q}}\text{-OMe}$); HRMS (ESI): $[\text{M}]^+$ calculated for $\text{C}_{11}\text{H}_{14}\text{ON}$ 176.10699, found 176.10660.

6,7-Dimethoxy-2-methyl-3,4-dihydroisoquinolinium iodide (63)

According to general procedure VII, 6,7-dimethoxy-3,4-dihydroisoquinoline **59**⁷³ yielded iminium salt **63** as a yellow solid (1.56 g, 78%). m.p. 200-201 °C; ¹H-NMR (400 MHz, CDCl₃): δ = 3.33 (t, 2H, *J* = 8.0, PhCH₂), 3.89 (s, 3H, NCH₃), 3.91 (s, 3H, OMe), 3.98 (s, 3H, OMe), 4.05 (t, 2H, *J* = 8.0, CH₂N), 6.86 (s, 1H, CH_{ar}), 7.59 (s, 1H, CH_{ar}), 9.74 (s, 1H, CH imine); ¹³C-NMR (101 MHz, CDCl₃): δ = 25.4 (PhCH₂), 47.8 (CH₂N), 50.2 (CH₂N), 56.7 (OMe), 56.8 (OMe), 110.8 (CH_{ar}), 115.4 (CH_{ar}), 117.0 (C_q), 131.8 (C_q), 148.7 (C_q-OMe), 157.3 (C_q-OMe), 164.6 (CH imine); HRMS (ESI): [M]⁺ calculated for C₁₂H₁₆O₂N 206.1190, found 206.11748. Analytical data according with literature.⁷⁶

2-Allyl-6,7-dimethoxy-3,4-dihydroisoquinolinium bromide (242)

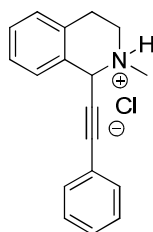
To a solution of 6,7-dimethoxy-3,4-dihydroisoquinoline **59**⁷³ (0.50 g, 2.61 mmol, 1 equiv) in diethyl ether (30 mL) allylbromide (0.53 mL, 5.23 mmol, 2 equiv) was added. The reaction mixture was refluxed overnight. The resulting yellow precipitate was filtered and washed with diethyl ether to give **243** as a yellow solid (0.52 g, 64%). m.p. 70-71 °C; ¹H-NMR (400 MHz, CD₃OD): δ = 3.23 (t, 2H, *J* = 8.3, PhCH₂), 3.78-3.83 (m, 1H, CHN), 3.89 (s, 3H, OMe), 3.95-3.96 (m, 1H, CHN), 3.99 (s, 3H, OMe), 4.58 (d, 2H, *J* = 6.5, CH₂N), 5.56-5.65 (m, 2H, CH₂ allyl), 6.02-6.11 (m, 1H, CH allyl), 7.12 (s, 1H, CH_{ar}), 7.40 (s, 1H, CH_{ar}), 8.92 (s, 1H, CH imine); ¹³C-NMR (101 MHz, CD₃OD): δ = 26.2 (PhCH₂), 48.8 (CH₂N), 56.8 (OMe), 57.3 (OMe), 63.1 (CH₂N), 112.3 (CH_{ar}), 116.4 (CH_{ar}), 118.4 (C_q), 124.3 (CH₂ allyl), 130.4 (CH allyl), 134.5 (C_q), 150.3 (C_q-OMe), 159.5 (C_q-OMe), 166.1 (CH imine); HRMS (ESI): [M]⁺ calculated for C₁₄H₁₈O₂N 232.13321, found 232.13319.

General procedure VIII: preparation of *N*-methylated alkynylated tetrahydroisoquinolines

A solution of the corresponding iminium salt (1 equiv) in THF (50 mg starting material in 1 mL) was cooled to 0 °C. In a separate flask the corresponding alkyne (6 equiv) in THF (0.5 mL) was also cooled to 0 °C and isopropyl magnesium chloride lithium chloride complex solution (1.3 M in THF, 6 equiv) was added dropwise. After 10 min stirring this reaction mixture was transferred to the

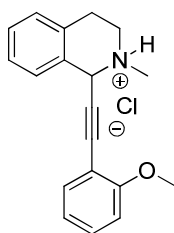
iminium salt suspension. The resulting solution was stirred at 0 °C for 1h and then warmed to RT within 1h. The reaction was quenched by the addition of methanol (0.5 mL) and the crude reaction mixture was purified by flash chromatography (cyclohexane/ethyl acetate, gradient from 0 to 100% ethyl acetate). Most of the amines were then converted to the corresponding HCl-salt by addition of HCl in diethyl ether (1 M).

2-Methyl-1-(phenylethynyl)-1,2,3,4-tetrahydroisoquinolinium chloride (91)

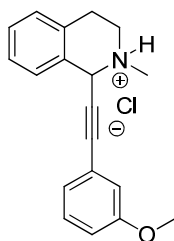


According to general procedure VIII, **91** was obtained as a yellow wax (43 mg, 83%). $R_f = 0.50$ (petroleum ether/ethyl acetate, 2:1); $^1\text{H-NMR}$ (400 MHz, CD_3OD): $\delta = 3.12\text{-}3.20$ (m, 5H, NCH_3 , PhCH_2), 3.65-3.84 (m, 2H, CH_2N), 5.85 (s, 1H, CH), 7.32-7.52 (m, 9H, CH_{ar}); $^{13}\text{C-NMR}$ (101 MHz, CD_3OD): $\delta = 26.3$ (PhCH_2), 42.0 (NCH_3), 48.7 (CH_2N), 58.4 (CH), 69.2 (C_q alkyne), 79.2 (C_q alkyne), 122.0 (C_q), 128.9 (CH_{ar}), 129.9 (3CH_{ar}), 130.4 (CH_{ar}), 130.5 (CH_{ar}), 131.1 (CH_{ar}), 131.4 (2C_q), 133.2 (CH_{ar}); HRMS (ESI): $[\text{M}+\text{H}]^+$ calculated for $\text{C}_{18}\text{H}_{18}\text{N}$ 248.14338, found 248.14341.

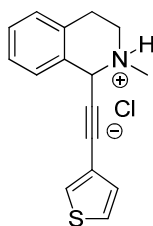
1-[(2-Methoxyphenyl)ethynyl]-2-methyl-1,2,3,4-tetrahydroisoquinolinium chloride (92)



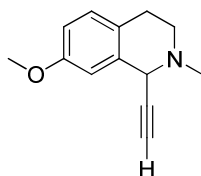
According to general procedure VIII, **92** was obtained as a slightly yellow wax (42 mg, 73%). $R_f = 0.49$ (petroleum ether/ethyl acetate, 1:1); $^1\text{H-NMR}$ (600 MHz, CD_3OD): $\delta = 3.11$ (s, 3H, NCH_3), 3.14-3.20 (m, 2H, PhCH_2), 3.49-3.53 (m, 1H, CHN), 3.72-3.77 (m, 1H, CHN), 3.80 (s, 3H, OMe), 5.68 (s, 1H, CH), 6.85-6.98 (m, 1H, CH_{ar}), 6.97 (d, 1H, $J = 8.5$, CH_{ar}), 7.24 (m, 1H, $J = 7.0$, CH_{ar}), 7.29-7.36 (m, 3H, CH_{ar}), 7.49-7.55 (m, 1H, CH_{ar}); $^{13}\text{C-NMR}$ (151 MHz, CD_3OD): $\delta = 26.1$ (PhCH_2), 41.8 (NCH_3), 49.3 (CH_2N), 56.4 (OMe), 59.0 (CH), 83.9 (C_q alkyne), 90.8 (C_q alkyne), 111.0 (C_q), 112.1 (CH_{ar}), 121.6 (CH_{ar}), 128.6 (CH_{ar}), 128.8 (CH_{ar}), 130.3 (4CH_{ar}), 132.6 (C_q), 134.3 (C_q); HRMS (ESI): $[\text{M}+\text{H}]^+$ calculated for $\text{C}_{19}\text{H}_{20}\text{ON}$ 278.15394, found 278.15392.

1-[(3-Methoxyphenyl)ethynyl]-2-methyl-1,2,3,4-tetrahydroisoquinolinium chloride (93)

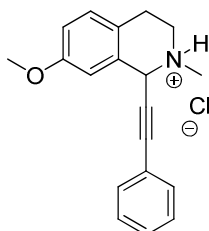
According to general procedure VIII, **93** was obtained as a slightly yellow wax (49 mg, 85%). General procedure XIII using (*S*)-QUINAP yielded (*S*)-(+)-**93** (31 mg, 99%). $[\alpha]_{\text{D}}^{20} = +39^{\circ}$ ($c = 1.0$, CH_2Cl_2); $R_f = 0.44$ (petroleum ether/ethyl acetate, 1:1); $^1\text{H-NMR}$ (600 MHz, CD_3OD): $\delta = 3.19\text{-}3.29$ (m, 5H, NCH_3 , PhCH_2), 3.60-3.70 (m, 1H, CHN), 3.78-3.90 (m, 3H, OMe, CHN), 5.85 (s, 1H, CH), 7.00 (d, 1H, $J = 7.9$, CH_{ar}), 7.06-7.10 (m, 2H, CH_{ar}), 7.27-7.33 (m, 2H, CH_{ar}), 7.36-7.38 (m, 2H, CH_{ar}), 7.51 (br s, 1H, CH_{ar}); $^{13}\text{C-NMR}$ (151 MHz, CDCl_3): $\delta = 26.9$ (PhCH_2), 48.9 (CH_2N), 55.8 (NCH_3), 55.9 (OMe), 55.9 (CH), 79.7 (C_q alkyne), 91.8 (C_q alkyne), 116.4 (CH_{ar}), 117.3 (CH_{ar}), 121.5 (C_q), 124.7 (CH_{ar}), 127.7 (CH_{ar}), 127.9 (CH_{ar}), 129.2 (CH_{ar}), 129.3 (CH_{ar}), 129.3 (CH_{ar}), 129.8 (2C_q); HRMS (ESI): $[\text{M}+\text{H}]^+$ calculated for $\text{C}_{19}\text{H}_{20}\text{ON}$ 278.15394, found 278.15426.

2-Methyl-1-(thien-3-ylethynyl)-1,2,3,4-tetrahydroisoquinolinium chloride (94)

According to general procedure VIII, **94** (TZ329) was obtained as a slightly brown solid (53 mg, 99%). m.p. 165-167 °C; $R_f = 0.44$ (petroleum ether/ethyl acetate, 2:1); $^1\text{H-NMR}$ (600 MHz, CD_3OD): $\delta = 3.17\text{-}3.19$ (m, 5H, NCH_3 , PhCH_2), 3.64-3.81 (m, 1H, CH_2N), 5.8 (s, 1H, CH), 7.19 (s, 1H, CH_{ar}), 7.30-7.31 (m, 1H, CH_{ar}), 7.34-7.39 (m, 2H, CH_{ar}), 7.45-7.65 (m, 2H, CH_{ar}), 7.78 (m, 1H, CH_{ar}); $^{13}\text{C-NMR}$ (151 MHz, CD_3OD): $\delta = 24.9$ (PhCH_2), 40.7 (NCH_3), 50.6 (CH_2N), 56.3 (CH), 81.3 (C_q alkyne), 85.5 (C_q alkyne), 119.7 (C_q), 126.4 (2CH_{ar}), 127.5 (CH_{ar}), 129.1 (C_q), 129.2 (C_q), 129.5 (2CH_{ar}), 130.2 (CH_{ar}), 131.6 (CH_{ar}); HRMS (ESI): $[\text{M}+\text{H}]^+$ calculated for $\text{C}_{16}\text{H}_{16}\text{NS}$ 254.09980, found 254.09998.

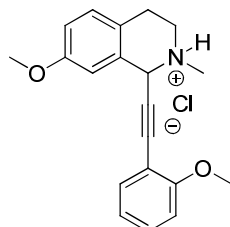
1-Ethynyl-7-methoxy-2-methyl-1,2,3,4-tetrahydroisoquinoline (95)

General procedure VII was modified as follows, iminium salt **62** and ethynylmagnesium bromide (0.5 M in THF, 1.98 mL, 1.0 mmol, 6 equiv) yielded **95** as a slightly yellow oil (27 mg, 81%). $R_f = 0.35$ (petroleum ether/ethyl acetate, 1:1); $^1\text{H-NMR}$ (400 MHz, CDCl_3): $\delta = 2.41$ (d, 1H, $J = 2.3$, CH alkyne), 2.54 (s, 3H, NCH_3), 2.62-2.67 (m, 1H, PhCH), 2.73-2.78 (m, 1H, PhCH), 2.84-2.96 (m, 2H, CH_2N), 3.76 (s, 3H, OMe), 4.45 (s, 1H, CH), 6.75 (dd, 1H, $J_1 = 8.5$, $J_2 = 2.7$, CH_{ar}), 6.81 (d, 1H, $J = 2.7$, CH_{ar}), 7.00 (d, 1H, $J = 8.4$, CH_{ar}); $^{13}\text{C-NMR}$ (101 MHz, CDCl_3): $\delta = 27.8$ (PhCH_2), 43.3 (NCH_3), 48.4 (CH_2N), 55.2 (OMe), 56.2 (CH), 74.1 (CH alkyne), 81.5 (C_q alkyne), 112.0 (CH_{ar}), 113.6 (CH_{ar}), 125.4 (C_q), 129.7 (CH_{ar}), 135.6 (C_q), 157.6 ($\text{C}_q\text{-OMe}$); HRMS (ESI): $[\text{M}+\text{H}]^+$ calculated for $\text{C}_{13}\text{H}_{16}\text{ON}$ 202.1226, found 202.1225.

7-Methoxy-2-methyl-1-(phenylethynyl)-1,2,3,4-tetrahydroisoquinolinium chloride (96)

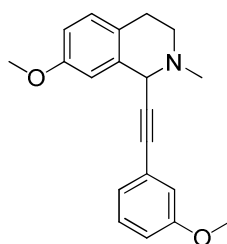
According to general procedure VIII, **96** was obtained as a colourless solid (52 mg, 99%). m.p. 164-166 °C; $R_f = 0.49$ (petroleum ether/ethyl acetate, 1:1); $^1\text{H-NMR}$ (600 MHz, CD_3OD): $\delta = 3.18$ -3.22 (m, 5H, NCH_3 , PhCH_2), 3.59-3.63 (m, 1H, CHN), 3.80-3.83 (m, 4H, OMe, CHN), 5.80 (s, 1H, CH), 6.97 (dd, 1H, $J_1 = 8.5$, $J_2 = 2.1$, CH_{ar}), 7.04 (br s, 1H, CH_{ar}), 7.20 (d, 1H, $J = 8.5$, CH_{ar}), 7.37-7.40 (m, 2H, CH_{ar}), 7.42-7.44 (m, 1H, CH_{ar}), 7.53 (d, 2H, $J = 7.6$, CH_{ar}); $^{13}\text{C-NMR}$ (151 MHz, CD_3OD): $\delta = 24.1$ (PhCH_2), 40.4 (NCH_3), 49.5 (CH_2N), 54.9 (OMe), 56.9 (CH), 80.3 (C_q alkyne), 89.8 (C_q alkyne), 112.2 (CH_{ar}), 115.7 (CH_{ar}), 121.9 (C_q), 128.7 (2C, CH_{ar}), 129.6 (CH_{ar}), 130.3 (C_q), 130.4 (CH_{ar}), 131.9 (2 CH_{ar}), 131.9 (C_q), 160.0 ($\text{C}_q\text{-OMe}$); HRMS (ESI): $[\text{M}+\text{H}]^+$ calculated for $\text{C}_{19}\text{H}_{20}\text{ON}$ 278.15394, found 278.15400.

7-Methoxy-1-[(2-methoxyphenyl)ethynyl]-2-methyl-1,2,3,4-tetrahydroisoquinolinium chloride (97)



According to general procedure VIII, **97** was obtained as a yellow solid (50 mg, 88%). m.p. 164-166 °C; $R_f = 0.40$ (petroleum ether/ethyl acetate, 1:1); $^1\text{H-NMR}$ (600 MHz, CD_3OD): $\delta = 3.10\text{-}3.21$ (m, 5H, NCH_3 , PhCH_2), 3.62-3.63 (m, 1H, CHN), 3.82-3.85 (m, 4H, OMe, CHN), 3.87 (s, 3H, OMe), 5.79 (s, 1H, CH), 6.91-6.96 (m, 2H, CH_{ar}), 7.04 (d, 1H, $J = 8.2$, CH_{ar}), 7.08-7.16 (m, 1H, CH_{ar}), 7.22 (d, 1H, $J = 8.2$, CH_{ar}), 7.39-7.44 (m, 2H, CH_{ar}); $^{13}\text{C-NMR}$ (151 MHz, CD_3OD): $\delta = 25.4$ (PhCH_2), 41.5 (NCH_3), 49.1 (CH_2N), 56.0 (OMe, CH), 56.0 (OMe), 69.1 (C_q alkyne), 87.7 (C_q alkyne), 111.0 (C_q), 112.1 (CH_{ar}), 113.4 (C_q), 116.8 (CH_{ar}), 121.7 (2C, CH_{ar}), 123.0 (C_q), 131.3 (CH_{ar}), 132.6 (CH_{ar}), 134.2 (CH_{ar}), 160.4 ($\text{C}_q\text{-OMe}$), 162.3 ($\text{C}_q\text{-OMe}$); HRMS (ESI): $[\text{M}+\text{H}]^+$ calculated for $\text{C}_{20}\text{H}_{22}\text{O}_2\text{N}$ 308.16451, found 308.16459.

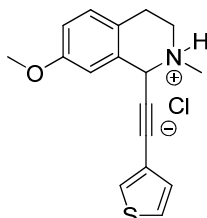
7-Methoxy-1-[(3-methoxyphenyl)ethynyl]-2-methyl-1,2,3,4-tetrahydroisoquinoline (98)



According to general procedure VIII, **98** was obtained as a yellow oil (72 mg, 71%). General procedure XIII using (*S*)-QUINAP yielded (*S*)-(-)-**98** (30 mg, 99%). $[\alpha]_{\text{D}}^{20} = -45^\circ$ ($c = 1.0$, CH_2Cl_2); $R_f = 0.42$ (petroleum ether/ethyl acetate, 1:1); $^1\text{H-NMR}$ (400 MHz, CDCl_3): $\delta = 2.62$ (s, 3H, NCH_3), 2.67-3.07 (m, 4H, PhCH_2 , CH_2N), 3.77 (s, 3H, OMe), 3.78 (s, 3H, OMe), 4.67 (s, 1H, CH), 6.77 (dd, 1H, $J_1 = 8.4$, $J_2 = 2.6$, CH_{ar}), 6.83 (ddd, 1H, $J_1 = 8.4$, $J_2 = 2.6$, $J_3 = 0.9$, CH_{ar}), 6.89 (d, 1H, $J = 2.6$, CH_{ar}), 6.94-6.95 (m, 1H, CH_{ar}), 7.01-7.04 (m, 2H, CH_{ar}), 7.16-7.20 (m, 1H, CH_{ar}); $^{13}\text{C-NMR}$ (101 MHz, CDCl_3): $\delta = 27.8$ (PhCH_2), 43.5 (NCH_3), 48.8 (CH_2N), 55.2 (OMe), 55.3 (OMe), 57.0 (CH), 86.2 (C_q alkyne), 87.0 (C_q alkyne), 112.3 (CH_{ar}), 113.4 (CH_{ar}), 114.6 (CH_{ar}), 116.5 (CH_{ar}), 123.0

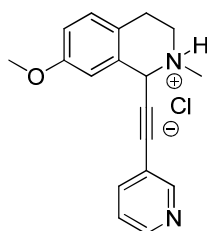
(C_q), 124.3 (CH_{ar}), 125.4 (C_q), 129.2 (CH_{ar}), 129.7 (CH_{ar}), 135.8 (C_q), 157.6 (C_q-OMe), 159.2 (C_q-OMe); HRMS (ESI): [M+H]⁺ calculated for C₂₀H₂₂O₂N 308.16451, found 308.16515.

7-Methoxy-2-methyl-1-(thien-3-ylethynyl)-1,2,3,4-tetrahydroisoquinolinium chloride (**99**)

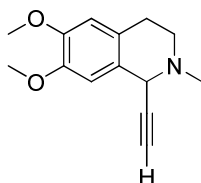


According to general procedure VIII, **99** was obtained as a colourless solid (47 mg, 89%). m.p. 166-168 °C; R_f = 0.46 (petroleum ether/ethyl acetate, 1:1); ¹H-NMR (600 MHz, CD₃OD): δ = 3.14-3.17 (m, 5H, NCH₃, PhCH₂), 3.57-3.59 (m, 1H, CHN), 3.76-3.79 (m, 4H, OMe, CHN), 5.76 (s, 1H, CH), 6.95 (d, 1H, J = 6.8, CH_{ar}), 7.01 (s, 1H, CH_{ar}), 7.19-7.21 (m, 2H, CH_{ar}), 7.45-7.46 (m, 1H, CH_{ar}), 7.77-7.78 (m, 1H, CH_{ar}); ¹³C-NMR (151 MHz, CD₃OD): δ = 25.4 (PhCH₂), 41.6 (NCH₃), 50.6 (CH₂N), 56.0 (OMe), 58.2 (CH), 81.1 (C_q alkyne), 87.5 (C_q alkyne), 113.1 (CH_{ar}), 116.8 (CH_{ar}), 120.9 (C_q), 123.0 (C_q), 127.5 (CH_{ar}), 130.7 (CH_{ar}), 131.4 (C_q), 131.4 (CH_{ar}), 132.6 (CH_{ar}), 160.3 (C_q-OMe); HRMS (ESI): [M+H]⁺ calculated for C₁₇H₁₈ONS 284.11036, found 284.11040.

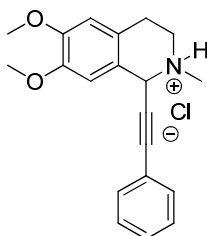
7-Methoxy-2-methyl-1-(pyridin-3-ylethynyl)-1,2,3,4-tetrahydroisoquinolinium chloride (**100**)



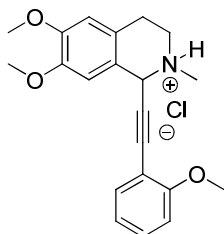
According to general procedure VIII, **100** was obtained as a brown solid (35 mg, 67%). m.p. 121-123 °C; R_f = 0.49 (ethyl acetate); ¹H-NMR (400 MHz, CDCl₃): δ = 2.92-3.01 (m, 4H, NCH₃, PhCH), 3.27-3.42 (m, 3H, PhCH, CH₂N), 3.79-3.85 (m, 3H, OMe), 5.23 (s, 1H, CH), 6.86 (s, 2H, CH_{ar}), 7.11 (s, 1H, CH_{ar}), 7.30 (s, 1H, CH_{ar}), 7.76 (s, 1H, CH_{ar}), 8.67-8.78 (m, 2H, CH_{ar}); ¹³C-NMR (101 MHz, CDCl₃): δ = 25.6 (PhCH₂), 42.2 (NCH₃), 48.9 (CH₂N), 55.6 (OMe), 56.2 (CH), 85.7 (C_q alkyne), 86.6 (C_q alkyne), 112.3 (CH_{ar}), 115.1 (CH_{ar}), 122.7 (2C_q), 123.4 (CH_{ar}), 130.2 (CH_{ar}), 131.1 (C_q), 139.2 (CH_{ar}), 149.5 (CH_{ar}), 152.5 (CH_{ar}), 158.4 (C_q-OMe); HRMS (ESI): [M+H]⁺ calculated for C₁₈H₁₉ON₂ 279.14919, found 279.14932.

1-Ethynyl-6,7-dimethoxy-2-methyl-1,2,3,4-tetrahydroisoquinoline (101)

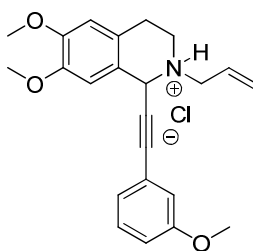
General procedure VII was modified as follows, iminium salt **63** and ethynylmagnesium bromide (0.5 M in THF, 1.80 mL, 0.90 mmol, 6 equiv) yielded **101** as a slightly yellow solid (21 mg, 61%). m.p. 95-97 °C; $R_f = 0.26$ (petroleum ether/ethyl acetate, 1:1); $^1\text{H-NMR}$ (400 MHz, CDCl_3): $\delta = 2.41$ (d, 1H, $J = 2.3$, CH alkyne), 2.54 (s, 3H, NCH_3), 2.64-2.78 (m, 2H, PhCH_2), 2.85-2.95 (m, 2H, CH_2N), 3.83 (s, 3H, OMe), 3.85 (s, 3H, OMe), 4.41 (s, 1H, CH), 6.57 (s, 1H, CH_{ar}), 6.74 (s, 1H, CH_{ar}); $^{13}\text{C-NMR}$ (101 MHz, CDCl_3): $\delta = 28.3$ (PhCH_2), 43.4 (NCH_3), 48.2 (CH_2N), 55.7 (CH), 56.2 (OMe), 55.9 (OMe), 74.0 (CH alkyne), 109.9 (CH_{ar}), 111.2 (CH_{ar}), 125.4 (C_q), 126.5 (C_q), 147.4 ($\text{C}_q\text{-OMe}$), 148.2 ($\text{C}_q\text{-OMe}$); HRMS (ESI): $[\text{M}+\text{H}]^+$ calculated for $\text{C}_{14}\text{H}_{18}\text{O}_2\text{N}$ 232.13321, found 232.13334.

6,7-Dimethoxy-2-methyl-1-(phenylethynyl)-1,2,3,4-tetrahydroisoquinolinium chloride (102)

According to general procedure VIII, **102** was obtained as a yellow solid (21 mg, 41%). m.p. 153-155 °C; $R_f = 0.41$ (petroleum ether/ethyl acetate, 1:2); $^1\text{H-NMR}$ (600 MHz, CD_3OD): $\delta = 3.16$ -3.18 (m, 5H, NCH_3 , PhCH_2), 3.58-3.60 (m, 1H, CHN), 3.79-3.81 (m, 1H, CHN), 3.82-3.83 (m, 6H, 2OMe), 5.71 (s, 1H, CH), 6.85 (s, 1H, CH_{ar}), 7.01 (s, 1H, CH_{ar}), 7.36-7.42 (m, 3H, CH_{ar}), 7.51-7.53 (m, 2H, CH_{ar}); $^{13}\text{C-NMR}$ (151 MHz, CD_3OD): $\delta = 25.7$ (PhCH_2), 41.5 (NCH_3), 50.9 (CH_2N), 56.5 (OMe), 56.7 (OMe), 57.8 (CH), 81.6 (C_q alkyne), 90.8 (C_q alkyne), 111.4 (CH_{ar}), 112.7 (CH_{ar}), 122.0 (C_q), 123.8 (C_q), 129.8 (CH_{ar}), 130.9 (CH_{ar}), 132.3 (C_q), 133.0 (CH_{ar}), 150.2 ($\text{C}_q\text{-OMe}$), 151.5 ($\text{C}_q\text{-OMe}$); HRMS (ESI): $[\text{M}+\text{H}]^+$ calculated for $\text{C}_{20}\text{H}_{22}\text{O}_2\text{N}$ 308.16451, found 308.16455.

6,7-Dimethoxy-1-[(2-methoxyphenyl)ethynyl]-2-methyl-1,2,3,4-tetrahydroisoquinolinium chloride (103)

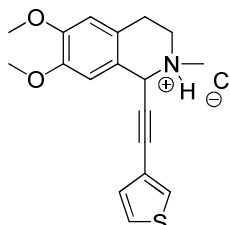
According to general procedure VIII, **103** was obtained as a yellow wax (50 mg, 89%). $R_f = 0.32$ (petroleum ether/ethyl acetate, 1:2); $^1\text{H-NMR}$ (400 MHz, CD_3OD): $\delta = 3.13\text{-}3.24$ (m, 5H, NCH_3 , PhCH_2), 3.39-3.65 (m, 2H, CH_2N), 3.81-3.83 (m, 9H, 3OMe), 5.71 (br s, 1H, CH), 6.82-7.14 (m, 4H, CH_{ar}), 7.37-7.55 (m, 2H, CH_{ar}); $^{13}\text{C-NMR}$ (126 MHz, CD_3OD): $\delta = 25.9$ (PhCH_2), 40.0 (NCH_3), 49.1 (CH_2N), 56.6, 56.7, 56.8 (3OMe, CH), 59.4 (C_q alkyne), 84.6 (C_q alkyne), 110.9 (CH_{ar}), 112.1 (CH_{ar}), 112.8 (CH_{ar}), 121.6 (CH_{ar}), 129.8 (CH_{ar}), 132.2 (C_q), 132.5 (C_q), 133.4 (CH_{ar}), 134.3 (C_q), 150.0 ($\text{C}_q\text{-OMe}$), 151.3 ($\text{C}_q\text{-OMe}$), 162.1 ($\text{C}_q\text{-OMe}$); HRMS (ESI): $[\text{M}+\text{H}]^+$ calculated for $\text{C}_{21}\text{H}_{23}\text{O}_3\text{N}$ 338.17502, found 338.17520.

2-Allyl-6,7-dimethoxy-1-[(3-methoxyphenyl)ethynyl]-1,2,3,4-tetrahydroisoquinolinium chloride (104)

According to general procedure VIII, **104** was obtained as a yellow solid (46 mg, 72%). General procedure XIII using (*R*)-QUINAP yielded (*R*)-(-)-**104** (25 mg, 78%). $[\alpha]_{\text{D}}^{20} = -18^\circ$ ($c = 0.3$, CH_2Cl_2); m.p. 133-135 °C; $R_f = 0.38$ (petroleum ether/ethyl acetate, 1:1); $^1\text{H-NMR}$ (500 MHz, CDCl_3): $\delta = 2.81\text{-}2.96$ (m, 1H, PhCH), 3.41-3.69 (m, 5H, PhCH , $2\text{CH}_2\text{N}$), 3.76 (s, 3H, OMe), 3.83 (s, 3H, OMe), 3.89 (s, 3H, OMe), 5.39 (s, 1H, CH), 5.61-5.66 (m, 2H, CH_2 allyl), 6.44 (s, 1H, CH allyl), 6.62-6.70 (m, 2H, CH_{ar}), 6.91-6.92 (m, 2H, CH_{ar}), 6.99-7.00 (m, 1H, CH_{ar}), 7.21-7.24 (m, 1H, CH_{ar}), 13.4 (s, 1H, NH); $^{13}\text{C-NMR}$ (126 MHz, CDCl_3): $\delta = 26.8$ (PhCH_2), 46.2 (CH_2N), 53.1 (CH_2N), 55.4 (OMe), 55.9 (OMe), 56.1 (OMe), 57.7 (CH), 79.7 (C_q alkyne), 91.4 (C_q alkyne), 109.8 (CH_{ar}), 111.1 (CH_{ar}), 115.9 (CH_{ar}), 117.1 (CH_{ar}), 120.8 (C_q), 121.4 (C_q), 122.5 (C_q), 124.4 (CH_{ar}), 125.9 (CH_2 allyl), 126.9

(CH_{ar}), 129.6 (CH allyl), 148.4 (C_q -OMe), 149.6 (C_q -OMe), 159.3 (C_q -OMe); HRMS (ESI): $[M+H]^+$ calculated for $C_{23}H_{26}O_3N$ 364.19072, found 364.19095.

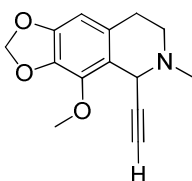
6,7-Dimethoxy-2-methyl-1-(thien-3-ylethynyl)-1,2,3,4-tetrahydroisoquinolinium chloride (**105**)



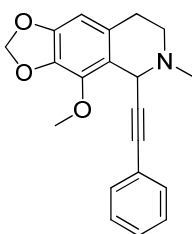
According to general procedure VIII, **105** was obtained as a slightly yellow solid (21 mg, 40%, general procedure VI). m.p. 155-157 °C; $R_f = 0.38$ (petroleum ether/ethyl acetate, 1:2); 1H -NMR (600 MHz, CD_3OD): $\delta = 3.15$ -3.20 (m, 5H, NCH_3 , $PhCH_2$), 3.55-3.60 (m, 1H, CHN), 3.78-3.80 (m, 1H, CHN), 3.81 (s, 3H, OMe), 3.83 (s, 3H, OMe), 5.70 (s, 1H, CH), 6.84 (s, 1H, CH_{ar}), 6.98 (s, 1H, CH_{ar}), 7.19 (d, 1H, $J = 4.7$, CH_{ar}), 7.45-7.47 (m, 1H, CH_{ar}), 7.77-7.78 (m, 1H, CH_{ar}); ^{13}C -NMR (151 MHz, CD_3OD): $\delta = 25.7$ ($PhCH_2$), 41.5 (NCH_3), 49.5 (CH_2N), 56.6 (OMe), 56.7 (OMe), 57.9 (CH), 79.3 (C_q alkyne), 87.6 (C_q alkyne), 111.4 (CH_{ar}), 112.7 (CH_{ar}), 120.9 (C_q), 122.0 (C_q), 123.7 (C_q), 127.5 (CH_{ar}), 130.7 (CH_{ar}), 132.7 (CH_{ar}), 150.1 (C_q -OMe), 151.5 (C_q -OMe); HRMS (ESI): $[M+H]^+$ calculated for $C_{18}H_{20}O_2NS$ 314.12093, found 314.12103.

General procedure IX: preparation of alkynylated cotarnine derivatives

A suspension of cotarnine iodide **23** (50 mg, 0.14 mmol, 1 equiv) in THF (1 mL) was cooled to 0 °C. In a separate flask the corresponding alkyne (0.43 mmol, 3 equiv) in THF (1.5 mL) was also cooled to 0 °C and isopropyl magnesium chloride lithium chloride complex solution (1.3 M in THF, 332 μ L, 0.43 mmol, 3 equiv) added dropwise. After 10 min stirring this reaction mixture was transferred to the cotarnine iodide suspension. The resulting solution was stirred at 0 °C for one hour and then warmed to RT within one hour. The reaction was quenched by the addition of saturated aq. $NaHCO_3$ solution and extracted with diethyl ether (3 \times 20 mL). The combined organic fractions were dried with $MgSO_4$, filtered and the solvent evaporated *in vacuo*. The residue was purified *via* flash chromatography. Most of the amines were then converted to the corresponding HCl-salt by addition of HCl in diethyl ether (1 M).

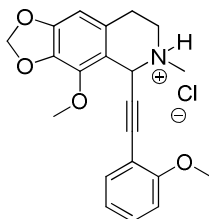
5-Ethynyl-4-methoxy-6-methyl-5,6,7,8-tetrahydro[1,3]dioxolo[4,5-g]isoquinoline (106)

General procedure IX was modified as follows, cotarnine iodide **23** and ethynylmagnesium bromide (0.5 M in THF, 0.86 mL, 0.43 mmol, 3 equiv) yielded **106** as a slightly yellow oil (27 mg, 76%). Flash chromatography (petroleum ether/ethyl acetate, 2:1). $R_f = 0.43$ (petroleum ether/ethyl acetate, 1:1); $^1\text{H-NMR}$ (400 MHz, CDCl_3): $\delta = 2.34$ (d, 1H, $J = 2.3$, CH alkyne), 2.51 (s, 3H, NCH_3), 2.58-2.70 (m, 2H, PhCH_2), 2.82-2.98 (m, 2H, CH_2N), 4.02 (s, 3H, OMe), 4.71 (s, 1H, CH), 5.86 (dd, 2H, $J_1 = 6.8$, $J_2 = 1.3$, O_2CH_2), 6.31 (s, 1H, CH_{ar}); $^{13}\text{C-NMR}$ (101 MHz, CDCl_3): $\delta = 28.7$ (PhCH_2), 42.9 (NCH_3), 46.4 (CH_2N), 50.5 (CH), 59.5 (OMe), 73.1 (CH alkyne), 80.8 (C_q alkyne), 100.7 (O_2CH_2), 102.9 (CH_{ar}), 120.6 (C_q), 127.4 (C_q), 134.3 (C_q), 139.7 (C_q), 148.4 (C_q); HRMS (ESI): $[\text{M}+\text{H}]^+$ calculated for $\text{C}_{14}\text{H}_{15}\text{O}_3\text{N}$ 246.11247, found 246.11244.

4-Methoxy-6-methyl-5-(phenylethynyl)-5,6,7,8-tetrahydro[1,3]dioxolo[4,5-g]isoquinoline (107)

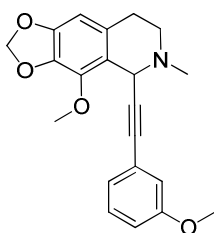
According to general procedure IX, **107** was obtained as a slightly yellow oil (44 mg, 95%). Flash chromatography (petroleum ether/ethyl acetate, 2:1). Preparative chiral HPLC with a Chiralpak® IC column and 30% DCM/EtOH (100:2) in hexanes as eluent, a flow rate of 4 mL/min and detection at 254 nm delivered, *S*-(-)-**107**, $[\alpha]_{\text{D}}^{20} = -110.5$ ($c = 1.0$, CH_2Cl_2) and *R*-(+)-**107**, $[\alpha]_{\text{D}}^{20} = +114.0^\circ$ ($c = 1.0$, CH_2Cl_2); $R_f = 0.40$ (petroleum ether/ethyl acetate, 1:1); $^1\text{H-NMR}$ (400 MHz, CDCl_3): $\delta = 2.86$ (s, 3H, NCH_3), 2.90-3.01 (m, 2H, PhCH_2), 3.20-3.30 (m, 2H, CH_2N), 4.32 (s, 3H, OMe), 5.21 (s, 1H, CH), 6.15 (d, 2H, $J = 2.0$, O_2CH_2), 6.61 (s, 1H, CH_{ar}), 7.52-7.54 (m, 3H, CH_{ar}), 7.66-7.69 (m, 2H, CH_{ar}); $^{13}\text{C-NMR}$ (101 MHz, CDCl_3): $\delta = 28.8$ (PhCH_2), 43.1 (NCH_3), 46.7 (CH_2N), 51.1 (CH), 59.6 (OMe), 85.6 (C_q alkyne), 86.8 (C_q alkyne), 100.7 (O_2CH_2), 103.0 (CH_{ar}), 121.2 (C_q), 123.4 (C_q), 127.4 (C_q), 127.8 (CH_{ar}), 128.1 (2C, CH_{ar}), 131.7 (2C, CH_{ar}), 134.5 (C_q), 139.9 (C_q), 148.4 (C_q); HRMS (ESI): $[\text{M}+\text{H}]^+$ calculated for $\text{C}_{20}\text{H}_{20}\text{O}_3\text{N}$ 322.14377, found 322.14380.

4-Methoxy-5-[(2-methoxyphenyl)ethynyl]-6-methyl-5,6,7,8-tetrahydro-[1,3]dioxolo[4,5-*g*]isoquinolin-6-ium chloride (108)



According to general procedure IX, **108** was obtained as a slightly yellow wax (22 mg, 39%). Flash chromatography (gradient from 0 to 100% ethyl acetate in cyclohexane). $R_f = 0.28$ (petroleum ether/ethyl acetate, 2:1); $^1\text{H-NMR}$ (400 MHz, CD_3OD): $\delta = 3.04\text{--}3.10$ (m, 1H, PhCH), 3.15 (s, 3H, NCH_3), 3.18–3.26 (m, 1H, PhCH), 3.55–3.60 (m, 1H, CHN), 3.68–3.81 (m, 1H, CHN), 3.85 (s, 3H, OMe), 4.10 (s, 3H, OMe), 5.72 (s, 1H, CH), 5.97 (s, 2H, O_2CH_2), 6.50 (s, 1H, CH_{ar}), 6.90–6.93 (m, 1H, CH_{ar}), 7.01–7.03 (m, 1H, CH_{ar}), 7.36–7.40 (m, 2H, CH_{ar}); $^{13}\text{C-NMR}$ (151 MHz, CD_3OD): $\delta = 26.9$ (PhCH_2), 42.0 (NCH_3), 48.9 (CH_2N), 54.0 (CH), 56.5 (OMe), 60.7 (OMe), 88.3 (C_q alkyne), 88.5 (C_q alkyne), 103.2 (O_2CH_2), 103.8 (CH_{ar}), 111.4 (C_q), 112.2 (CH_{ar}), 117.3 (C_q), 121.8 (CH_{ar}), 125.6 (C_q), 132.5 (CH_{ar}), 134.3 (CH_{ar}), 136.6 (C_q), 141.4 (C_q), 152.1 (C_q), 162.3 (C_q); HRMS (ESI): $[\text{M}+\text{H}]^+$ calculated for $\text{C}_{21}\text{H}_{22}\text{O}_4\text{N}$ 352.15433, found 352.15457.

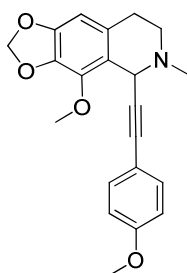
4-Methoxy-5-[(3-methoxyphenyl)ethynyl]-6-methyl-5,6,7,8-tetrahydro[1,3]dioxolo[4,5-*g*]isoquinoline (109)



According to general procedure IX, **109** was obtained as a slightly yellow oil (48 mg, 99%). General procedure XIII using (*R*)-QUINAP yielded (*R*)-(+)-**109** (25 mg, 99%), $[\alpha]_{\text{D}}^{20} = +70^\circ$ ($c = 1.0$, CH_2Cl_2). Flash chromatography (petroleum ether/ethyl acetate, 2:1). $R_f = 0.34$ (petroleum ether/ethyl acetate, 1:1); $^1\text{H-NMR}$ (400 MHz, CDCl_3): $\delta = 2.58$ (s, 3H, NCH_3), 2.62–2.76 (m, 2H, PhCH_2), 2.92–3.02 (m, 2H, CH_2N), 3.76 (s, 3H, OMe), 4.04 (s, 3H, OMe), 4.92 (s, 1H, CH), 5.87–5.88 (m, 2H, O_2CH_2), 6.33 (s, 1H, CH_{ar}), 6.80–6.83 (m, 1H, CH_{ar}), 6.92–6.93 (m, 1H, CH_{ar}), 6.98–7.01 (m, 1H, CH_{ar}), 7.14–7.18 (m, 1H, CH_{ar}); $^{13}\text{C-NMR}$ (101 MHz, CDCl_3): $\delta = 28.8$ (PhCH_2), 43.1

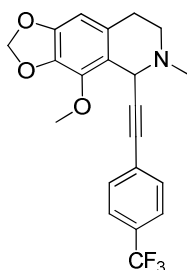
(NCH₃), 46.7 (CH₂N), 51.2 (CH), 55.2 (OMe), 59.6 (OMe), 85.5 (C_q alkyne), 86.8 (C_q alkyne), 100.7 (O₂CH₂), 103.0 (CH_{ar}), 114.2 (CH_{ar}), 116.7 (CH_{ar}), 121.2 (C_q), 124.3 (CH_{ar}), 124.4 (C_q), 127.5 (C_q), 129.1 (CH_{ar}), 134.5 (C_q), 139.9 (C_q), 148.3 (C_q), 159.2 (C_q); HRMS (ESI): [M+H]⁺ calculated for C₂₁H₂₂O₄N 352.15433, found 352.15433.

4-Methoxy-5-[(4-methoxyphenyl)ethynyl]-6-methyl-5,6,7,8-tetrahydro[1,3]dioxolo[4,5-g]isoquinoline (110)



According to general procedure IX, **110** was obtained as a slightly yellow oil (46 mg, 91%). Flash chromatography (petroleum ether/ethyl acetate, 2:1). R_f = 0.29 (petroleum ether/ethyl acetate, 1:1); ¹H-NMR (400 MHz, CDCl₃): δ = 2.57 (s, 3H, NCH₃), 2.61-2.73 (m, 2H, PhCH₂), 2.92-3.00 (m, 2H, CH₂N), 3.77 (s, 3H, OMe), 4.03 (s, 3H, OMe), 4.91 (s, 1H, CH), 5.86-5.87 (m, 2H, O₂CH₂), 6.32 (s, 1H, CH_{ar}), 6.76-6.80 (m, 2H, CH_{ar}), 7.31-7.34 (m, 2H, CH_{ar}); ¹³C-NMR (101 MHz, CDCl₃): δ = 28.7 (PhCH₂), 43.0 (NCH₃), 46.7 (CH₂N), 51.2 (CH), 55.2 (OMe), 59.6 (OMe), 85.2 (C_q alkyne), 85.4 (C_q alkyne), 100.7 (O₂CH₂), 103.0 (CH_{ar}), 113.7 (2C, CH_{ar}), 115.6 (C_q), 121.4 (C_q), 127.4 (C_q), 133.0 (2C, CH_{ar}), 134.6 (C_q), 139.9 (C_q), 148.3 (C_q), 159.2 (C_q); HRMS (ESI): [M+H]⁺ calculated for C₂₁H₂₂O₄N 352.15433, found 352.15433.

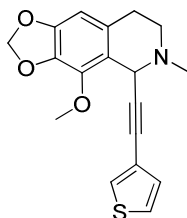
4-Methoxy-6-methyl-5-[[4-(trifluoromethyl)phenyl]ethynyl]-5,6,7,8-tetrahydro[1,3]dioxolo[4,5-g]isoquinoline (111)



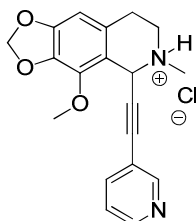
According to general procedure IX, **111** was obtained as a slightly yellow solid (56 mg, 99%). Flash chromatography (petroleum ether/ethyl acetate, 3:1). R_f = 0.43 (petroleum ether/ethyl acetate, 1:1);

m.p. 97-98 °C; $^1\text{H-NMR}$ (400 MHz, CDCl_3): δ = 2.58 (s, 3H, NCH_3), 2.63-2.76 (m, 2H, PhCH_2), 2.90-3.03 (m, 2H, CH_2N), 4.04 (s, 3H, OMe), 4.93 (s, 1H, CH), 5.87-5.88 (m, 2H, O_2CH_2), 6.34 (s, 1H, CH_{ar}), 7.47-7.52 (m, 4H, CH_{ar}); $^{13}\text{C-NMR}$ (101 MHz, CDCl_3): δ = 28.7 (PhCH_2), 43.1 (NCH_3), 46.8 (CH_2N), 51.2 (CH), 59.5 (OMe), 84.3 (C_q alkyne), 89.7 (C_q alkyne), 100.8 (O_2CH_2), 102.9 (CH_{ar}), 120.5 (C_q), 123.9 (q, J = 271, CF_3), 125.0 (q, 2C, J = 4.0, CH_{ar}), 127.2 (C_q), 127.5 (C_q), 129.5 (q, J = 32.0, $\text{C}_q\text{-CF}_3$), 131.9 (CH_{ar}), 134.4 (C_q), 139.8 (C_q), 148.4 (C_q); HRMS (ESI): $[\text{M}+\text{H}]^+$ calculated for $\text{C}_{21}\text{H}_{19}\text{O}_3\text{NF}_3$ 390.13201, found 390.13115.

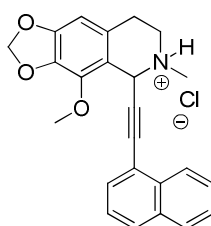
4-Methoxy-6-methyl-5-(thien-3-ylethynyl)-5,6,7,8-tetrahydro[1,3]dioxolo[4,5-g]isoquinoline (112)



According to general procedure IX, **112** was obtained as a slightly yellow solid (35 mg, 74%). Flash chromatography (petroleum ether/ethyl acetate, 3:1). R_f = 0.37 (petroleum ether/ethyl acetate, 1:1); m.p. 123-124 °C; $^1\text{H-NMR}$ (400 MHz, CDCl_3): δ = 2.56 (s, 3H, NCH_3), 2.61-2.75 (m, 2H, PhCH_2), 2.92-3.01 (m, 2H, CH_2N), 4.02 (s, 3H, OMe), 4.90 (s, 1H, CH), 5.87-5.88 (m, 2H, O_2CH_2), 6.33 (s, 1H, CH_{ar}), 7.06 (dd, 1H, J_1 = 5.0, J_2 = 1.3, CH_{ar}), 7.20 (dd, 1H, J_1 = 5.0, J_2 = 2.8, CH_{ar}), 7.36 (dd, 1H, J_1 = 2.8, J_2 = 1.3, CH_{ar}); $^{13}\text{C-NMR}$ (101 MHz, CDCl_3): δ = 28.7 (PhCH_2), 43.1 (NCH_3), 46.7 (CH_2N), 51.1 (CH), 59.6 (OMe), 80.5 (C_q alkyne), 86.3 (C_q alkyne), 100.7 (O_2CH_2), 102.9 (CH_{ar}), 121.1 (C_q), 122.3 (C_q), 124.9 (CH_{ar}), 127.4 (C_q), 128.1 (CH_{ar}), 130.1 (CH_{ar}), 134.5 (C_q), 139.9 (C_q), 148.3 (C_q); HRMS (ESI): $[\text{M}+\text{H}]^+$ calculated for $\text{C}_{18}\text{H}_{18}\text{O}_3\text{NS}$ 328.10029, found 328.10019.

4-Methoxy-6-methyl-5-(pyridin-3-ylethynyl)-5,6,7,8-tetrahydro-[1,3]dioxolo[4,5-g]isoquinolin-6-ium chloride (113)

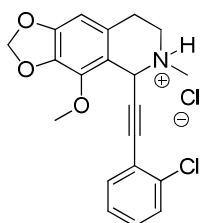
According to general procedure IX, **113** was obtained as a slightly yellow wax (12 mg, 23%). Flash chromatography (gradient from 0 to 100% ethyl acetate in cyclohexane). $R_f = 0.30$ (petroleum ether/ethyl acetate, 1:1); $^1\text{H-NMR}$ (400 MHz, CD_3OD): $\delta = 3.03\text{-}3.09$ (m, 1H, PhCH), 3.12 (s, 3H, NCH_3), 3.16-3.22 (m, 1H, PhCH), 3.52-3.57 (m, 1H, CHN), 3.68-3.76 (m, 1H, CHN), 4.11 (s, 3H, OMe), 5.74 (s, 1H, CH), 5.98 (s, 2H, O_2CH_2), 6.51 (s, 1H, CH_{ar}), 7.44-7.47 (m, 1H, CH_{ar}), 7.94-7.96 (m, 1H, CH_{ar}), 8.55-8.67 (m, 2H, CH_{ar}); $^{13}\text{C-NMR}$ (126 MHz, CD_3OD): $\delta = 24.6$ (PhCH_2), 41.3 (NCH_3), 47.8 (CH_2N), 51.3 (CH), 59.4 (OMe), 85.8 (C_q alkyne), 91.3 (C_q alkyne), 101.8 (O_2CH_2), 102.6 (CH_{ar}), 113.1 (C_q), 118.9 (C_q), 124.2 (CH_{ar}), 124.5 (C_q), 135.3 (C_q), 136.7 (C_q), 139.3 (CH_{ar}), 151.0 (CH_{ar}), 151.1 (C_q), 151.6 (CH_{ar}); HRMS (ESI): $[\text{M}+\text{H}]^+$ calculated for $\text{C}_{19}\text{H}_{19}\text{O}_3\text{N}_2$ 323.13902, found 323.13916.

4-Methoxy-6-methyl-5-(naphthalen-1-ylethynyl)-5,6,7,8-tetrahydro-[1,3]dioxolo[4,5-g]isoquinolin-6-ium chloride (114)

According to general procedure IX, **114** was obtained as a slightly yellow wax (38 mg, 69%). Flash chromatography (gradient from 0 to 100% ethyl acetate in cyclohexane). $R_f = 0.32$ (petroleum ether/ethyl acetate, 4:1); $^1\text{H-NMR}$ (600 MHz, CD_3OD): $\delta = 3.12\text{-}3.28$ (m, 5H, NCH_3 , PhCH_2), 3.61-3.66 (m, 1H, CHN), 3.81-3.86 (m, 1H, CHN), 4.15 (s, 3H, OMe), 5.90 (s, 1H, CH), 5.99 (s, 2H, O_2CH_2), 6.54 (s, 1H, CH_{ar}), 7.46-7.49 (m, 1H, CH_{ar}), 7.54-7.60 (m, 2H, CH_{ar}), 7.73-7.75 (m, 1H, CH_{ar}), 7.91-7.96 (m, 2H, CH_{ar}), 8.14-8.15 (m, 1H, CH_{ar}); $^{13}\text{C-NMR}$ (151 MHz, CD_3OD): $\delta = 25.6$ (PhCH_2), 40.4 (NCH_3), 48.7 (CH_2N), 52.2 (CH), 59.2 (OMe), 88.1 (C_q alkyne), 90.4 (C_q alkyne),

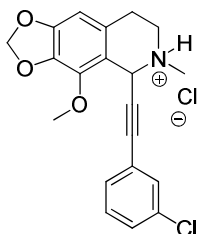
103.3 (O₂CH₂), 103.8 (CH_{ar}), 118.6 (C_q), 124.3 (C_q), 126.4 (CH_{ar}), 126.5 (CH_{ar}), 128.0 (CH_{ar}), 128.6 (CH_{ar}), 129.9 (CH_{ar}), 131.2 (C_q), 131.5 (CH_{ar}), 132.5 (CH_{ar}), 134.6 (C_q), 134.8 (C_q), 134.9 (C_q), 139.9 (C_q), 150.8 (C_q); HRMS (ESI): [M+H]⁺ calculated for C₂₄H₂₂O₃N 372.15942, found 372.15952.

5-[(2-Chlorophenyl)ethynyl]-4-methoxy-6-methyl-5,6,7,8-tetrahydro-[1,3]dioxolo[4,5-g]isoquinolin-6-ium chloride (115)



According to general procedure IX, **115** was obtained as a slightly yellow wax (27 mg, 48%). Flash chromatography (gradient from 0 to 100% ethyl acetate in cyclohexane). R_f = 0.44 (petroleum ether/ethyl acetate, 4:1); ¹H-NMR (400 MHz, CD₃OD): δ = 3.03-3.09 (m, 1H, PhCH), 3.15 (s, 3H, NCH₃), 3.18-3.26 (m, 1H, PhCH), 3.56-3.60 (m, 1H, CHN), 3.70-3.78 (m, 1H, CHN), 4.11 (s, 3H, OMe), 5.77 (s, 1H, CH), 5.97 (s, 2H, O₂CH₂), 6.49 (s, 1H, CH_{ar}), 7.29-7.33 (m, 1H, CH_{ar}), 7.37-7.41 (m, 1H, CH_{ar}), 7.46-7.48 (m, 1H, CH_{ar}) 7.55 (dd, 1H, J₁ = 7.8, J₂ = 1.5, CH_{ar}); ¹³C-NMR (101 MHz, CD₃OD): δ = 26.3 (PhCH₂), 41.8 (NCH₃), 48.6 (CH₂N), 53.2 (CH), 60.4 (OMe), 86.3 (C_q alkyne), 87.7 (C_q alkyne), 103.0 (O₂CH₂), 103.6 (CH_{ar}), 115.6 (CH_{ar}), 122.1 (CH_{ar}), 125.8 (CH_{ar}), 128.2 (CH_{ar}), 130.5 (C_q), 132.1 (C_q), 134.7 (C_q), 136.2 (C_q), 137.1 (C_q), 141.0 (C_q), 152.0 (C_q); HRMS (ESI): [M+H]⁺ calculated for C₂₀H₁₉O₃NCl 356.10480, found 356.10511.

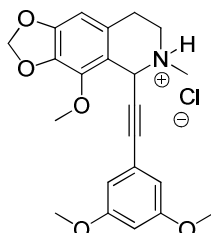
5-[(3-Chlorophenyl)ethynyl]-4-methoxy-6-methyl-5,6,7,8-tetrahydro-[1,3]dioxolo[4,5-g]isoquinolin-6-ium chloride (116)



According to general procedure IX, **116** was obtained as a slightly yellow wax (21 mg, 37%). Flash chromatography (gradient from 0 to 100% ethyl acetate in cyclohexane). R_f = 0.38 (petroleum

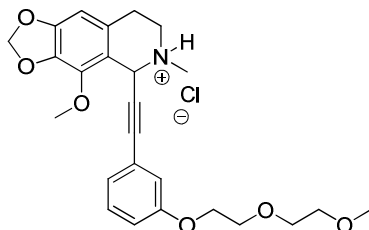
ether/ethyl acetate, 4:1); $^1\text{H-NMR}$ (600 MHz, CD_3OD): δ = 3.04-3.08 (m, 1H, PhCH), 3.10 (s, 3H, NCH_3), 3.16-3.22 (m, 1H, PhCH), 3.51-3.54 (m, 1H, CHN), 3.68-3.72 (m, 1H, CHN), 4.10 (s, 3H, OMe), 5.69 (s, 1H, CH), 5.97 (s, 2H, O_2CH_2), 6.50 (s, 1H, CH_{ar}), 7.34-7.37 (m, 1H, CH_{ar}), 7.41-7.44 (m, 2H, CH_{ar}), 7.51-7.52 (m, 1H, CH_{ar}); $^{13}\text{C-NMR}$ (151 MHz, CD_3OD): δ = 24.6 (PhCH_2), 40.4 (NCH_3), 47.5 (CH_2N), 53.1 (CH), 60.4 (OMe), 81.2 (C_q alkyne), 89.0 (C_q alkyne), 103.1 (O_2CH_2), 103.7 (CH_{ar}), 124.1 (C_q), 125.8 (C_q), 130.9 (CH_{ar}), 131.0 (C_q), 131.6 (CH_{ar}), 131.6 (CH_{ar}), 132.1 (CH_{ar}), 135.5 (C_q), 136.4 (C_q), 141.3 (C_q), 152.1 (C_q); HRMS (ESI): $[\text{M}+\text{H}]^+$ calculated for $\text{C}_{20}\text{H}_{19}\text{O}_3\text{NCl}$ 356.10480, found 356.10503.

5-[(3,5-dimethoxyphenyl)ethynyl]-4-methoxy-6-methyl-5,6,7,8-tetrahydro-[1,3]dioxolo[4,5-g]isoquinolin-6-ium chloride (117)



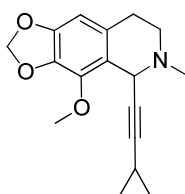
According to general procedure IX, **117** was obtained as a slightly yellow wax (8 mg, 13%). General procedure XIII using (*R*)-QUINAP yielded (*R*)-(+)-**117** (27 mg, 98%), $[\alpha]_{\text{D}}^{20} = +73^\circ$ ($c = 1.0$, CH_2Cl_2). Flash chromatography (gradient from 0 to 100% ethyl acetate in cyclohexane). $R_f = 0.31$ (petroleum ether/ethyl acetate, 2:1); $^1\text{H-NMR}$ (600 MHz, CD_3OD): δ = 3.04-3.07 (m, 1H, PhCH), 3.09 (s, 3H, NCH_3), 3.15-3.21 (m, 1H, PhCH), 3.49-3.53 (m, 1H, CHN), 3.68-3.73 (m, 1H, CHN), 3.75 (s, 6H, OMe), 4.10 (s, 3H, OMe), 5.65 (s, 1H, CH), 5.97 (s, 2H, O_2CH_2), 6.50 (s, 1H, CH_{ar}), 6.54 (t, 1H, $J = 2.6$ Hz, CH_{ar}), 6.61 (d, 2H, $J = 2.6$ Hz, CH_{ar}); $^{13}\text{C-NMR}$ (151 MHz, CD_3OD): δ = 26.6 (PhCH_2), 40.3 (NCH_3), 48.3 (CH_2N), 53.4 (CH), 56.1 (OMe), 60.6 (OMe), 80.6 (C_q alkyne), 90.8 (C_q alkyne), 103.2 (O_2CH_2), 103.6 (CH_{ar}), 103.8 (CH_{ar}), 110.9 (2CH_{ar}), 123.7 (C_q), 125.9 (C_q), 130.0 (C_q), 132.0 (C_q), 136.6 (C_q), 152.1 (C_q), 162.5 (2C_q); HRMS (ESI): $[\text{M}+\text{H}]^+$ calculated for $\text{C}_{22}\text{H}_{24}\text{O}_5\text{N}$ 382.16490, found 382.16548.

4-methoxy-5-({3-[2-(2-methoxyethoxy)ethoxy]phenyl}ethynyl)-6-methyl-5,6,7,8-tetrahydro-[1,3]dioxolo[4,5-g]isoquinolin-6-ium chloride (118)



According to general procedure IX, **118** was obtained as a slightly yellow wax (27 mg, 39%). Flash chromatography (gradient from 0 to 100% ethyl acetate in cyclohexane). $R_f = 0.33$ (petroleum ether/ethyl acetate, 1:1); $^1\text{H-NMR}$ (600 MHz, CD_3OD): $\delta = 3.06\text{-}3.09$ (m, 1H, PhCH), 3.14 (s, 3H, NCH_3), 3.18-3.27 (m, 1H, PhCH), 3.34 (OMe), 3.35-3.54 (m, 2H, CH_2), 3.56-3.60 (m, 1H, CHN), 3.65-3.67 (m, 2H, CH_2), 3.70-3.72 (m, 1H, CHN), 3.79-3.81 (m, 2H, CH_2), 4.10 (br s, 5H, OMe, CH_2), 5.72 (br s, 1H, CH), 5.97 (s, 2H, O_2CH_2), 6.50 (s, 1H, CH_{ar}), 7.00-7.07 (m, 3H, CH_{ar}), 7.25-7.28 (m, 1H, CH_{ar}); $^{13}\text{C-NMR}$ (151 MHz, CD_3OD): $\delta = 26.5$ (PhCH_2), 40.2 (NCH_3), 49.6 (CH_2N), 53.3 (CH), 59.1 (OMe), 60.5 (OMe), 68.8 (CH_2), 70.7 (CH_2), 71.5 (CH_2), 72.9 (CH_2), 89.9 (C_q alkyne), 91.0 (C_q alkyne), 103.1 (O_2CH_2), 103.7 (CH_{ar}), 117.7 (CH_{ar}), 118.8 (CH_{ar}), 123.1 (C_q), 125.6 (CH_{ar}), 130.8 (C_q), 130.9 (CH_{ar}), 136.7 (C_q), 139.9 (C_q), 141.0 (C_q), 152.0 (C_q) 160.2 (C_q); HRMS (ESI): $[\text{M}+\text{H}]^+$ calculated for $\text{C}_{25}\text{H}_{30}\text{O}_6\text{N}$ 440.20676, found 440.20642.

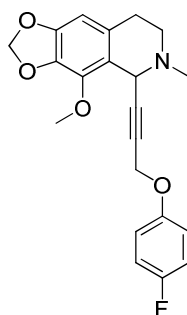
5-(Cyclopropylethynyl)-4-methoxy-6-methyl-5,6,7,8-tetrahydro-[1,3]dioxolo[4,5-g]isoquinoline (119)



According to general procedure IX, **119** was obtained as a colourless solid (6 mg, 16%). The product was purified *via* flash chromatography (petroleum ether/ethyl acetate, 2:1). $R_f = 0.33$ (petroleum ether/ethyl acetate, 1:1); m.p. 102-104 °C; $^1\text{H-NMR}$ (400 MHz, CDCl_3): $\delta = 0.60\text{-}0.63$ (m, 2H, CH_2), 0.68-0.72 (m, 2H, CH_2), 1.21-1.24 (m, 1H, CH), 2.46 (s, 3H, NCH_3), 2.56-2.65 (m, 2H, PhCH_2), 2.81-2.93 (m, 2H, CH_2N), 3.99 (s, 3H, OMe), 4.64 (s, 1H, CH), 5.86 (s, 2H, O_2CH_2), 6.29 (s, 1H, CH_{ar}); $^{13}\text{C-NMR}$ (101 MHz, CDCl_3): $\delta = -0.4$ (CH), 18.4 (2C, CH_2), 28.7 (PhCH_2), 42.9 (NCH_3), 46.4 (CH_2N), 50.6 (CH), 59.6 (OMe), 72.0 (C_q alkyne), 89.0 (C_q alkyne), 100.7 (O_2CH_2),

103.0 (CH_{ar}), 121.9 (C_q), 127.2 (C_q), 134.5 (C_q), 139.8 (C_q), 148.1 (C_q); HRMS (ESI): calculated for $[M+H]^+$ $C_{17}H_{20}O_3N$ 286.14377, found 286.14362.

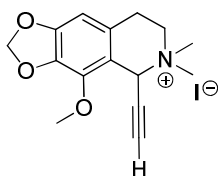
5-[3-(4-Fluorophenoxy)prop-1-ynyl]-4-methoxy-6-methyl-5,6,7,8-tetrahydro-[1,3]dioxolo[4,5-g]isoquinoline (120)



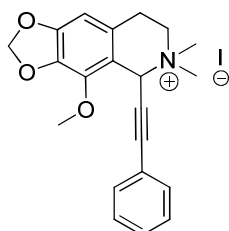
A suspension of cotarnine iodide **23** (100 mg, 0.29 mmol, 1 equiv) in THF (1 mL) was cooled to 0 °C. In a separate flask 1-fluoro-4-(prop-2-ynyloxy)benzene¹⁵⁴ (230 μ L, 1.73 mmol, 6 equiv) in THF (1.5 mL) was cooled to 0 °C and isopropyl magnesium chloride lithium chloride complex solution (1.3 M in THF, 1.33 mL, 1.73 mmol, 6 equiv) added dropwise. After 10 min stirring the reaction mixture was transferred to the cotarnine iodide/THF suspension. The resulting solution was stirred at 0 °C for 1h and then warmed to RT within 1h. The reaction was quenched by the addition of saturated aq. $NaHCO_3$ solution and extracted with diethyl ether (3 \times 20 mL). The combined organic fractions were dried with $MgSO_4$, filtered and the solvent was evaporated *in vacuo*. The residue was purified *via* flash chromatography (petroleum ether/ethyl acetate, 2:1) to give **120** as a slightly yellow solid (106 mg, 99%). R_f = 0.41 (petroleum ether/ethyl acetate, 1:1); m.p. 166-167 °C; 1H -NMR (400 MHz, $CDCl_3$): δ = 2.42 (s, 3H, NCH_3), 2.54-2.58 (m, 1H, $PhCH$), 2.61-2.65 (m, 1H, $PhCH$), 2.73-2.78 (m, 1H, CHN), 2.88-2.95 (m, 1H, CHN), 3.94 (s, 3H, OMe), 4.67 (d, 2H, J = 1.9, OCH_2), 4.71 (s, 1H, CH), 5.86 (s, 2H, O_2CH_2), 6.29 (s, 1H, CH_{ar}), 6.87-6.95 (m, 4H, CH_{ar}); ^{13}C -NMR (126 MHz, $CDCl_3$): δ = 28.6 ($PhCH_2$), 42.9 (NCH_3), 46.6 (CH), 50.7 (CH_2N), 57.1 (OCH_2), 59.4 (OMe), 80.2 (C_q alkyne), 85.0 (C_q alkyne), 100.7 (O_2CH_2), 102.8 (CH_{ar}), 115.6 (d, J = 22.5, $CH_{ar}-CF$), 116.5 (d, J = 7.5, CH_{ar}), 120.5 (C_q), 127.5 (C_q), 134.2 (C_q), 139.8 (C_q), 148.4 (C_q), 153.7 (C_q), 157.6 (d, J = 237.5, C_q-F); HRMS (ESI): $[M+H]^+$ calculated for $C_{21}H_{21}O_4NF$ 370.14491, found 370.14494.

General procedure X: quaternisation of tertiary tetrahydroisoquinolines

The corresponding tertiary amine was dissolved in dry acetonitrile (1 mL) and methyl iodide (40 equiv) was added dropwise. The reaction mixture was stirred overnight and the solvents were evaporated under reduced pressure to give the desired target compound.

5-Ethynyl-4-methoxy-6,6-dimethyl-5,6,7,8-tetrahydro[1,3]dioxolo[4,5-*g*]isoquinolin-6-ium iodide (121)

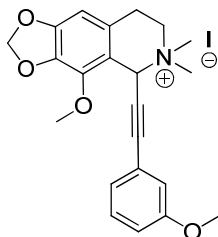
According to general procedure X, tertiary amine **106** (14.7 mg, 0.06 mmol, 1 equiv) yielded **121** as a colourless solid (159 mg, 88%). m.p. 232-233 °C; $^1\text{H-NMR}$ (400 MHz, DMSO-d_6): δ = 3.03 (s, 3H, NCH_3), 3.06-3.09 (m, 3H, NCH_3), 3.29 (s, 3H, NCH_3), 3.64-3.67 (m, 2H, CH_2N), 3.99 (s, 3H, OMe), 4.20 (d, 1H, J = 1.9, CH alkyne), 5.67 (s, 1H, CH), 6.04 (d, 2H, J = 0.8, O_2CH_2), 6.62 (s, 1H, CH_{ar}); $^{13}\text{C-NMR}$ (126 MHz, DMSO-d_6): δ = 23.1 (PhCH_2), 46.8 (NCH_3), 52.6 (NCH_3), 54.4 (CH_2N), 58.0 (CH), 59.6 (OMe), 75.7 (CH alkyne), 83.1 (C_q alkyne), 101.6 (O_2CH_2), 102.8 (CH_{ar}), 113.5 (C_q), 123.1 (C_q), 134.8 (C_q), 139.2 (C_q), 149.8 (C_q); HRMS (ESI): $[\text{M}]^+$ calculated for $\text{C}_{15}\text{H}_{18}\text{O}_3\text{N}$ 260.12812, found 260.12816.

4-Methoxy-6,6-dimethyl-5-(phenylethynyl)-5,6,7,8-tetrahydro[1,3]dioxolo[4,5-*g*]isoquinolin-6-ium iodide (122)

According to general procedure X, tertiary amine **107** (13 mg, 0.04 mmol, 1 equiv) yielded **122** as a colourless solid (22.7 mg, 99%). m.p. 113-114 °C; $^1\text{H NMR}$ (400 MHz, CD_3OD): δ = 3.18 (s, 3H, NCH_3), 3.20-3.26 (m, 2H, PhCH_2), 3.67-3.72 (m, 1H, CHN), 3.95-4.03 (m, 1H, CHN), 4.11 (s, 3H, OMe), 5.85 (s, 1H, CH), 5.99 (s, 2H, O_2CH_2), 6.54 (s, 1H, CH_{ar}), 7.34-7.42 (m, 3H, CH_{ar}), 7.47-7.49 (m, 2H, CH_{ar}); $^{13}\text{C-NMR}$ (126 MHz, CD_3OD): δ = 24.8 (PhCH_2), 48.2 (NCH_3), 54.2 (NCH_3), 56.7

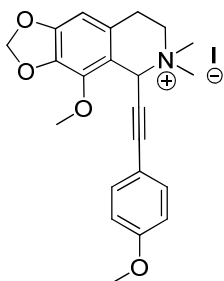
(CH₂N), 60.5 (OMe), 61.5 (CH), 81.2 (C_q alkyne), 93.0 (C_q alkyne), 103.2 (O₂CH₂), 103.8 (CH_{ar}), 115.0 (C_q), 121.9 (C_q), 124.1 (C_q), 129.8 (CH_{ar}), 131.0 (2C, CH_{ar}), 133.0 (2C, CH_{ar}), 136.7 (C_q), 141.3 (C_q), 152.3 (C_q); HRMS (ESI): [M]⁺ calculated for C₂₁H₂₂O₃N 336.15942, found 336.15954.

4-Methoxy-5-[(3-methoxyphenyl)ethynyl]-6,6-dimethyl-5,6,7,8-tetrahydro[1,3]dioxolo[4,5-g]isoquinolin-6-ium iodide (**123**)



According to general procedure X, tertiary amine **109** (15.4 mg, 0.04 mmol, 1 equiv) yielded **123** as a yellow solid (21.6 mg, 99%). m.p. 127-128 °C; ¹H-NMR (400 MHz, CD₃OD): δ = 3.18 (s, 3H, NCH₃), 3.20-3.25 (m, 2H, PhCH₂), 3.52 (s, 3H, NCH₃), 3.67-3.74 (m, 1H, CHN), 3.96-4.03 (m, 1H, CHN), 4.11 (s, 3H, OMe), 5.84 (s, 1H, CH), 5.99 (s, 2H, O₂CH₂), 6.54 (s, 1H, CH_{ar}), 6.97-7.06 (m, 3H, CH_{ar}), 7.27 (t, 1H, *J* = 8.0, CH_{ar}); ¹³C-NMR (126 MHz, CD₃OD): δ = 24.8 (PhCH₂), 48.2 (NCH₃), 54.3 (NCH₃), 56.0 (OMe), 56.7 (CH₂N), 60.6 (OMe), 61.5 (CH), 80.9 (C_q alkyne), 92.8 (C_q alkyne), 103.2 (O₂CH₂), 103.8 (CH_{ar}), 115.0 (C_q), 117.3 (CH_{ar}), 117.9 CH_{ar}), 122.8 (C_q), 124.1 (C_q), 125.4 (CH_{ar}), 130.9 (CH_{ar}), 136.7 (C_q), 141.2 (C_q), 152.2 (C_q), 162.1 (C_q); HRMS (ESI): [M]⁺ calculated for C₂₂H₂₄O₄N 366.16998, found 366.17008.

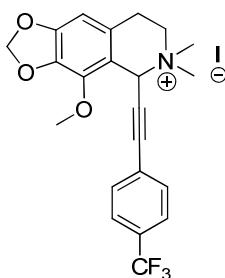
4-Methoxy-6,6-dimethyl-5-(phenylethynyl)-5,6,7,8-tetrahydro[1,3]dioxolo[4,5-g]isoquinolin-6-ium iodide (**124**)



According to general procedure X, tertiary amine **110** (13.5 mg, 0.04 mmol, 1 equiv) yielded **124** as a yellow solid (19 mg, 99%). m.p. 174-176 °C; ¹H-NMR (400 MHz, CD₃OD): δ = 3.17 (s, 3H, NCH₃), 3.19-3.27 (m, 2H, PhCH₂), 3.50 (s, 3H, NCH₃), 3.65-3.68 (m, 1H, CHN), 3.95-4.01 (m, 1H, CHN), 4.09 (s, 3H, OMe), 5.80 (s, 1H, CH), 5.98 (s, 2H, O₂CH₂), 6.53 (s, 1H, CH_{ar}), 6.91 (d, 2H, *J*

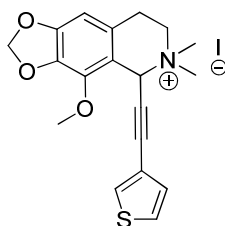
= 8.8, CH_{ar}), 7.41 (d, 2H, $J = 8.8$, CH_{ar}); ^{13}C -NMR (126 MHz, CD_3OD): $\delta = 24.8$ ($PhCH_2$), 48.1 (NCH_3), 54.2 (NCH_3), 55.9 (OMe), 56.5 (CH_2N), 60.5 (OMe), 61.7 (CH), 80.0 (C_q alkyne), 93.3 (C_q alkyne), 103.2 (O_2CH_2), 103.7 (CH_{ar}), 113.7 (C_q), 115.4 (C_q), 115.4 (2C, CH_{ar}), 124.0 (C_q), 134.7 (2C, CH_{ar}), 136.7 (C_q), 141.2 (C_q), 152.2 (C_q), 162.5 (C_q); HRMS (ESI): $[M]^+$ calculated for $C_{22}H_{24}O_4N$ 366.16998, found 366.17008.

4-Methoxy-6,6-dimethyl-5-[[4-(trifluoromethyl)phenyl]ethynyl]-5,6,7,8-tetrahydro[1,3]dioxolo[4,5-g]isoquinolin-6-ium iodide (125)



According to general procedure X, tertiary amine **111** (20.5 mg, 0.05 mmol, 1 equiv) yielded **125** as a yellow solid (28 mg, 99%). m.p. 141-142 °C; 1H -NMR (400 MHz, CD_3OD): $\delta = 3.21$ (s, 3H, NCH_3), 3.32-3.29 (m, 1H, $PhCH$), 3.40-3.43 (m, 1H, $PhCH$), 3.56 (s, 3H, NCH_3), 3.72-3.76 (m, 1H, CHN), 3.99-4.05 (m, 1H, CHN), 4.12 (s, 3H, OMe), 5.91 (s, 1H, CH), 5.99 (s, 2H, O_2CH_2), 6.55 (s, 1H, CH_{ar}), 7.67-7.75 (m, 4H, CH_{ar}); ^{13}C -NMR (126 MHz, CD_3OD): $\delta = 24.8$ ($PhCH_2$), 48.4 (NCH_3), 54.4 (NCH_3), 56.9 (CH_2N), 60.6 (OMe), 61.3 (CH), 83.6 (C_q alkyne), 91.2 (C_q alkyne), 103.2 (O_2CH_2), 103.8 (CH_{ar}), 114.5 (C_q), 124.3 (C_q), 126.6 (q, 2C, $J = 3.8$, CH_{ar}), 127.4 (q, $J = 270$, C_q - CF_3), 130.1 (C_q), 132.4 (q, 2C, $J = 32.4$, CH_{ar}), 133.7 (2C, CH_{ar}), 136.6 (C_q), 142.2 (C_q), 152.4 (C_q); HRMS (ESI): $[M]^+$ calculated for $C_{22}H_{21}O_3NF_3$ 404.14680, found 404.14614.

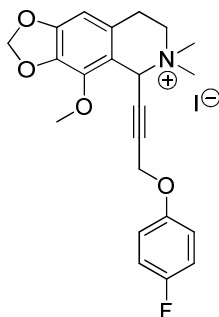
4-Methoxy-6,6-dimethyl-5-(thien-3-ylethynyl)-5,6,7,8-tetrahydro[1,3]dioxolo[4,5-g]isoquinolin-6-ium iodide (126)



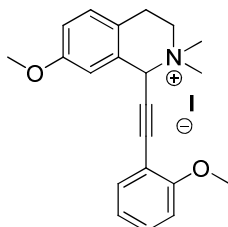
According to general procedure X, tertiary amine **112** (12.3 mg, 0.04 mmol, 1 equiv) yielded **126** as a yellow solid (17.6 mg, 99%). m.p. 157-158 °C; 1H -NMR (400 MHz, CD_3OD): $\delta = 3.17$ (s, 3H,

NCH_3), 3.18-3.27 (m, 2H, PhCH_2), 3.50 (s, 3H, NCH_3), 3.66-3.70 (m, 1H, CHN), 3.94-4.01 (m, 1H, CHN), 4.09 (s, 3H, OMe), 5.81 (s, 1H, CH), 5.99 (s, 2H, O_2CH_2), 6.54 (s, 1H, CH_{ar}), 7.16 (dd, 1H, $J_1 = 5.0$, $J_2 = 1.2$, CH_{ar}), 7.44 (dd, 1H, $J_1 = 5.0$, $J_2 = 3.1$, CH_{ar}), 7.76 (dd, 1H, $J_1 = 3.1$, $J_2 = 1.2$, CH_{ar}); ^{13}C -NMR (126 MHz, CD_3OD): $\delta = 24.8$ (PhCH_2), 48.2 (NCH_3), 54.2 (NCH_3), 56.6 (OMe), 56.6 (CH_2N), 60.5 (OMe), 61.6 (CH), 80.9 (C_q alkyne), 88.4 (C_q alkyne), 103.2 (O_2CH_2), 103.8 (CH_{ar}), 115.0 (C_q), 120.8 (C_q), 124.1 (C_q), 127.5 (CH_{ar}), 130.7 (CH_{ar}), 132.7 (CH_{ar}), 136.7 (C_q), 141.2 (C_q), 152.2 (C_q); HRMS (ESI): $[\text{M}]^+$ calculated for $\text{C}_{19}\text{H}_{20}\text{O}_3\text{NS}$ 342.11584, found 342.11586.

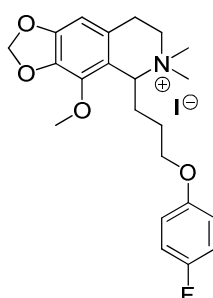
5-[3-(4-Fluorophenoxy)prop-1-ynyl]-4-methoxy-6,6-dimethyl-5,6,7,8-tetrahydro-[1,3]dioxolo [4,5-g]isoquinolin-6-ium iodide (127)



According to general procedure X, tertiary amine **120** (15 mg, 0.04 mmol, 1 equiv) yielded **127** as a slightly yellow solid (20.1 mg, 97%). m.p. 172-173 °C (decomposition); ^1H -NMR (400 MHz, DMSO-d_6): $\delta = 2.99$ (s, 3H, NCH_3), 3.03-3.07 (m, 2H, PhCH_2), 3.27 (s, 3H, NCH_3), 3.57-3.61 (m, 2H, CH_2N), 3.93 (s, 3H, OMe), 4.92 (d, 2H, $J = 1.5$, OCH_2), 5.70 (s, 1H, CH), 6.04 (s, 2H, O_2CH_2), 6.60 (s, 1H, CH_{ar}), 6.98-7.00 (m, 2H, CH_{ar}), 7.10-7.14 (m, 2H, CH_{ar}); ^{13}C -NMR (101 MHz, DMSO-d_6): $\delta = 23.2$ (PhCH_2), 46.8 (NCH_3), 52.5 (NCH_3), 54.4 (CH_2N), 56.1 (OCH_2), 58.2 (CH), 59.6 (OMe), 79.0 (C_q alkyne), 87.3 (C_q alkyne), 101.7 (O_2CH_2), 102.8 (CH_{ar}), 113.3 (C_q), 115.9 (d, 2C, $J = 23.0$, $\text{CH}_{\text{ar}}-\text{CF}$), 116.6 (d, 2C, $J = 9.0$, CH_{ar}), 123.2 (C_q), 134.8 (C_q), 139.2 (C_q), 149.8 (C_q), 153.1 (C_q), 157.6 (d, $J = 236.0$, C_q-F); HRMS (ESI): $[\text{M}]^+$ calculated for $\text{C}_{22}\text{H}_{23}\text{O}_4\text{NF}$ 384.16056, found 384.16108.

7-Methoxy-1-[(2-methoxyphenyl)ethynyl]-2,2-dimethyl-1,2,3,4-tetrahydroisoquinolinium iodide (128)

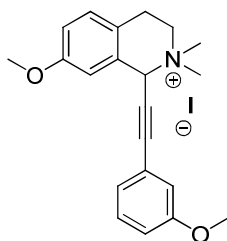
According to general procedure X, tertiary amine **97** (6 mg of the free amine, 0.02 mmol, 1 equiv) yielded **128** as a slightly yellow wax (8 mg, 93%). $^1\text{H-NMR}$ (600 MHz, CD_3OD): δ = 3.19-3.28 (m, 5H, NCH_3 , PhCH_2), 3.44 (s, 3H, NCH_3), 3.83 (s, 3H, OMe), 3.85-3.88 (m, 1H, CHN), 3.90 (s, 3H, OMe), 4.00-4.04 (m, 1H, CHN), 6.06 (s, 1H, CH), 6.96-6.99 (m, 1H, CH_{ar}), 7.03 (dd, 1H, $J_1 = 8.5$, $J_2 = 2.4$, CH_{ar}), 7.08 (d, 1H, $J = 8.5$, CH_{ar}), 7.21 (d, 1H, $J = 2.4$, CH_{ar}), 7.27 (d, 1H, $J = 8.5$, CH_{ar}), 7.43-7.45 (m, 1H, CH_{ar}), 7.5 (d, 1H, CH_{ar}); $^{13}\text{C-NMR}$ (151 MHz, CD_3OD): δ = 24.1 (PhCH_2), 47.1 (NCH_3), 53.0 (NCH_3), 56.0 (OMe), 56.5 (OMe), 60.3 (CH_2N), 67.4 (CH), 84.0 (C_q alkyne), 91.3 (C_q alkyne), 110.6 (C_q), 112.2 (CH_{ar}), 114.1 (CH_{ar}), 116.9 (CH_{ar}), 121.7 (CH_{ar}), 130.0 (2C_q), 131.5 (CH_{ar}), 132.0 (CH_{ar}), 134.2 (CH_{ar}), 160.7 ($\text{C}_q\text{-OMe}$), 162.5 ($\text{C}_q\text{-OMe}$); HRMS (ESI): $[\text{M}]^+$ calculated for $\text{C}_{21}\text{H}_{24}\text{O}_2\text{N}$ 322.18016, found 322.18024.

5-[3-(4-Fluorophenoxy)propyl]-4-methoxy-6,6-dimethyl-5,6,7,8-tetrahydro-[1,3]dioxolo[4,5-g]isoquinolin-6-ium iodide (244)

According to general procedure X, tertiary amine **133** (9 mg, 0.02 mmol, 1 equiv) yielded **245** as a slightly yellow solid (12.4 mg, 99%). m. p. 178-180 °C; $^1\text{H-NMR}$ (400 MHz, CD_3OD): δ = 1.82-1.99 (m, 3H, CH_2 , CH), 2.38-2.45 (m, 1H, CH), 3.06 (s, 3H, NCH_3), 3.13-3.16 (m, 2H, PhCH_2), 3.36 (s, 3H, NCH_3), 3.51-3.56 (m, 1H, CHN), 3.80-3.88 (m, 1H, CHN), 3.97 (t, 2H, $J = 5.8$, OCH_2), 4.05 (s, 3H, OMe), 4.72-4.73 (m, 1H, CH), 5.96 (d, 2H, $J = 2.5$, O_2CH_2), 6.49 (s, 1H, CH_{ar}), 6.85-6.89 (m, 2H, CH_{ar}), 6.95-6.99 (m, 2H, CH_{ar}); $^{13}\text{C-NMR}$ (101 MHz, CDCl_3): δ = 24.6 (PhCH_2), 28.1 (CH_2),

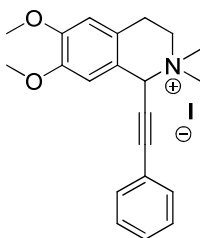
30.4 (CH₂), 51.6 (NCH₃), 53.1 (NCH₃), 55.0 (CH₂N), 60.2 (OMe), 68.8 (CH), 68.8 (OCH₂), 102.9 (O₂CH₂), 103.6 (CH_{ar}), 116.6 (d, 2C, *J* = 25.0, CH_{ar}-CF), 116.7 (d, 2C, *J* = 10.0, CH_{ar}), 118.0 (C_q), 124.2 (C_q), 136.1 (C_q), 141.2 (C_q), 151.6 (C_q), 156.4 (C_q), 158.7 (d, *J* = 236.0, C_q-F); HRMS (ESI): [M]⁺ calculated for C₂₂H₂₇O₄NF 388.19186, found 388.19228.

7-Methoxy-1-[(2-methoxyphenyl)ethynyl]-2,2-dimethyl-1,2,3,4-tetrahydroisoquinolinium iodide (**129**)



According to general procedure X, tertiary amine **98** (12.6 mg of the free amine, 0.04 mmol, 1 equiv) yielded **129** as a slightly yellow solid (14 mg, 76%). m.p. 139-141 °C; ¹H-NMR (400 MHz, CD₃OD): δ = 3.08-3.15 (m, 2H, PhCH₂), 3.18 (s, 6H, NCH₃), 3.69 (s, 3H, OMe), 3.70 (s, 3H, OMe), 3.73-3.78 (m, 1H, CHN), 3.89-3.95 (m, 1H, CHN), 5.98 (s, 1H, CH), 6.90-6.94 (m, 2H, CH_{ar}), 6.99 (d, 1H, *J* = 2.3, CH_{ar}), 7.03-7.06 (m, 2H, CH_{ar}), 7.16-7.23 (m, 2H, CH_{ar}); ¹³C-NMR (101 MHz, CD₃OD): δ = 24.1 (PhCH₂), 48.2 (NCH₃), 52.4 (NCH₃), 56.0 (2OMe), 59.9 (CH₂N), 66.8 (CH), 79.9 (C_q alkyne), 94.4 (C_q alkyne), 113.7 (CH_{ar}), 117.1 (CH_{ar}), 117.6 (CH_{ar}), 118.1 (CH_{ar}), 121.7 (C_q), 122.5 (C_q), 125.5 (CH_{ar}), 130.0 (C_q), 131.0 (CH_{ar}), 131.6 (CH_{ar}), 160.7 (C_q-OMe), 161.1 (C_q-OMe); HRMS (ESI): [M]⁺ calculated for C₂₁H₂₄O₂N 322.18016, found 322.18029.

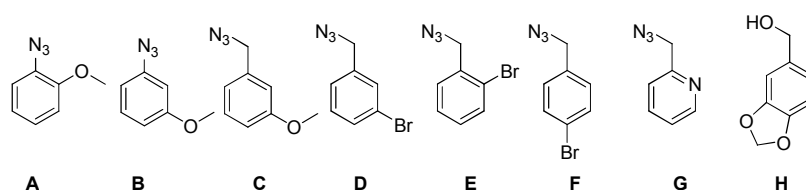
6,7-Dimethoxy-2,2-dimethyl-1-(phenylethynyl)-1,2,3,4-tetrahydroisoquinolinium iodide (**130**)



According to general procedure X, tertiary amine **82** (2.7 mg, 0.01 mmol, 1 equiv) yielded **130** as a slightly yellow solid (4 mg, 99%). m.p. 136-138 °C (decomposition); ¹H-NMR (600 MHz, CD₃OD): δ = 3.16-3.23 (m, 2H, PhCH₂), 3.29 (s, 3H, NCH₃), 3.39 (s, 3H, NCH₃), 3.78-3.83 (m, 1H, CHN), 3.84 (s, 3H, OMe), 3.86 (s, 3H, OMe), 3.97-4.01 (m, 1H, CHN), 5.95 (s, 1H, CH), 6.91 (s, 1H, CH_{ar}),

7.07 (s, 1H, CH_{ar}), 7.41-7.48 (m, 3H, CH_{ar}), 7.58-7.60 (m, 2H, CH_{ar}); ^{13}C -NMR (151 MHz, CD_3OD): δ = 24.5 ($PhCH_2$), 48.0 (NCH_3), 52.3 (NCH_3), 56.6 (OMe), 56.6 (OMe), 59.8 (CH_2N), 66.7 (CH), 80.4 (C_q alkyne), 94.4 (C_q alkyne), 111.7 (CH_{ar}), 112.8 (CH_{ar}), 120.7 (C_q), 121.6 (C_q), 122.6 (C_q), 129.9 (CH_{ar}), 131.3 (CH_{ar}), 133.2 (CH_{ar}), 150.4 (C_q -OMe), 151.8 (C_q -OMe); HRMS (ESI): $[M]^+$ calculated for $C_{21}H_{24}O_2N$ 322.18016, found 322.18023.

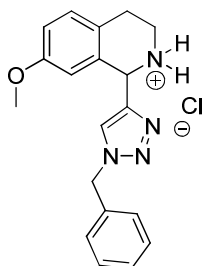
Preparation of azides



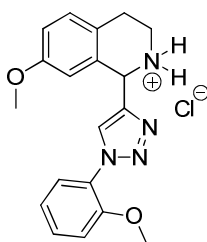
1-Azido-2-methoxybenzene (**A**) and 1-azido-3-methoxybenzene (**B**) were prepared from the corresponding aniline, dissolved in HCl solution (1 M) under addition of $NaNO_2$ and sodium azide.¹⁵⁵ Benzyl azides (**C-F**) were prepared from the corresponding benzyl bromide *via* substitution with sodium azide in DMSO.¹⁵⁶ 2-(Azidomethyl)pyridine (**G**) was obtained from 2-(chloromethyl)pyridine hydrochloride *via* azide substitution in water. (1,3-Benzodioxol-5-yl)methyl azide (**H**) was prepared from the corresponding alcohol *via* the benzyl tosylate.⁶⁹

General procedure XI: preparation of triazolyl-1,2,3,4-tetrahydroisoquinolinium chlorides

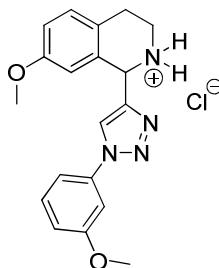
To a solution of alkyne **54** (1 equiv) in degassed ethanol (0.05 mmol alkyne in 1 mL) the corresponding azide (1.2 equiv) was added followed by a degassed solution of copper sulfate (1 M in water, 1.18 equiv) and sodium ascorbate (2M in water, 1.5 equiv). The reaction mixture was stirred at RT overnight. After conversion of the alkyne, the solvent was removed under reduced pressure, and the residue was purified by flash chromatography. The resulting material was subsequently dissolved in 5% HCl in methanol (1 mL) and stirred overnight. The solvents were removed *in vacuo* and the residue was washed several times with petroleum ether and diethyl ether to give the desired compound.

1-(1-Benzyl-1*H*-1,2,3-triazol-4-yl)-7-methoxy-1,2,3,4-tetrahydroisoquinolinium chloride (64)

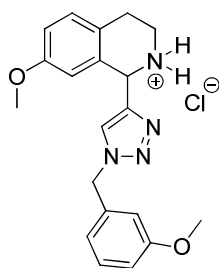
According to general procedure XI, triazole **64** was obtained as a colourless solid (18 mg, 64% over 2 steps). m.p. 214-216 °C; $^1\text{H-NMR}$ (400 MHz, CD_3OD): δ = 3.11-3.14 (m, 2H, PhCH_2), 3.46-3.60 (m, 2H, CH_2N), 3.66 (s, 3H, OMe), 5.63 (s, 2H, PhCH_2N), 5.95 (s, 1H, CH), 6.51 (d, 1H, J = 2.8, CH_{ar}), 6.91 (dd, 1H, J_1 = 8.5, J_2 = 2.8, CH_{ar}), 7.22 (d, 1H, J = 8.5, CH_{ar}), 7.35 (s, 5H, CH_{ar}), 8.10 (s, 1H, CH-triazole); $^{13}\text{C-NMR}$ (101 MHz, CD_3OD): δ = 25.3 (PhCH_2), 40.7 (CH_2N), 52.4 (CH), 55.1 (PhCH_2N), 55.8 (OMe), 113.1 (CH_{ar}), 116.4 (CH_{ar}), 124.7 (CH_{ar}), 126.7 (C_q), 129.3 (2C, CH_{ar}), 129.7 (CH_{ar}), 130.1 (2C, CH_{ar}), 131.6 (CH_{ar}), 132.0 (C_q), 136.6 (C_q), 145.2 (C_q), 160.1 ($\text{C}_q\text{-OMe}$); HRMS (ESI): $[\text{M}+\text{H}]^+$ calculated for $\text{C}_{19}\text{H}_{21}\text{ON}_4$ 321.17099, found 321.17107.

7-Methoxy-1-[1-(2-methoxyphenyl)-1*H*-1,2,3-triazol-4-yl]-1,2,3,4-tetrahydroisoquinolinium chloride (65)

According to general procedure XI, triazole **65** was obtained as a slightly yellow solid (24 mg, 63% over 2 steps). m.p. 233-235 °C; $^1\text{H-NMR}$ (400 MHz, CD_3OD): δ = 3.16-3.21 (m, 2H, PhCH_2), 3.53-3.60 (m, 1H, CHN), 3.66-3.70 (m, 1H, CHN), 3.72 (s, 3H, OMe), 3.89 (s, 3H, OMe), 6.06 (s, 1H, CH), 6.62 (d, 1H, J = 2.5, CH_{ar}), 6.95 (dd, 1H, J_1 = 8.7, J_2 = 2.5, CH_{ar}), 7.13-7.16 (m, 1H, CH_{ar}), 7.25-7.30 (m, 2H, CH_{ar}), 7.51-7.55 (m, 1H, CH_{ar}), 7.68 (dd, 1H, J_1 = 8.7, J_2 = 2.5, CH_{ar}), 8.61 (s, 1H, CH-triazole); $^{13}\text{C-NMR}$ (101 MHz, CD_3OD): δ = 25.4 (PhCH_2), 40.9 (CH_2N), 52.5 (CH), 55.9 (OMe), 56.7 (OMe), 113.3 (CH_{ar}), 113.8 (CH_{ar}), 116.4 (CH_{ar}), 122.2 (CH_{ar}), 124.8 (C_q), 126.7 (CH_{ar}), 128.6 (CH_{ar}), 131.6 (CH_{ar}), 132.0 (C_q), 132.3 (CH_{ar}), 144.5 (C_q), 153.1 ($\text{C}_q\text{-OMe}$), 160.2 ($\text{C}_q\text{-OMe}$); HRMS (ESI): $[\text{M}+\text{H}]^+$ calculated for $\text{C}_{19}\text{H}_{21}\text{O}_2\text{N}_4$ 337.16590, found 337.16599.

7-Methoxy-1-[1-(3-methoxyphenyl)-1*H*-1,2,3-triazol-4-yl]-1,2,3,4-tetrahydroisoquinolinium chloride (66)

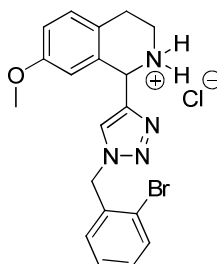
According to general procedure XI, triazole **66** was obtained as a yellow solid (23 mg, 54% over 2 steps). m.p. 227-229 °C; ¹H-NMR (400 MHz, CD₃OD): δ = 3.16-3.19 (m, 2H, PhCH₂), 3.53-3.56 (m, 1H, CHN), 3.63-3.69 (m, 1H, CHN), 3.71 (s, 3H, OMe), 3.87 (s, 3H, OMe), 6.06 (s, 1H, CH), 6.65 (d, 1H, *J* = 2.3, CH_{ar}), 6.95 (dd, 1H, *J*₁ = 8.6, *J*₂ = 2.3, CH_{ar}), 7.06 (dd, 1H, *J*₁ = 8.2, *J*₂ = 1.3, CH_{ar}), 7.25 (d, 1H, *J* = 8.6, CH_{ar}), 7.40-7.48 (m, 3H, CH_{ar}), 8.61 (s, 1H, CH_{ar}); ¹³C-NMR (101 MHz, CD₃OD): δ = 25.3 (PhCH₂), 40.6 (CH₂N), 52.4 (CH), 55.9 (OMe), 56.2 (OMe), 107.5 (CH_{ar}), 113.4 (CH_{ar}), 113.6 (CH_{ar}), 116.0 (CH_{ar}), 116.5 (CH_{ar}), 124.7 (CH_{ar}), 125.0 (C_q), 131.6 (CH_{ar}), 131.8 (C_q), 131.9 (CH_{ar}), 139.1 (C_q), 145.6 (C_q), 160.2 (C_q-OMe), 162.3 (C_q-OMe); HRMS (ESI): [M+H]⁺ calculated for C₁₉H₂₁O₂N₄ 337.16590, found 337.16598.

7-Methoxy-1-[1-(4-methoxybenzyl)-1*H*-1,2,3-triazol-4-yl]-1,2,3,4-tetrahydroisoquinolinium chloride (67)

According to general procedure XI, triazole **67** was obtained as a colourless solid (27 mg, 71% over 2 steps). m.p. 198-200 °C; ¹H-NMR (400 MHz, CD₃OD): δ = 3.08-3.17 (m, 2H, PhCH₂), 3.47-3.52 (m, 1H, CHN), 3.54-3.59 (m, 1H, CHN), 3.67 (s, 3H, OMe), 3.76 (s, 3H, OMe), 5.59 (s, 2H, PhCH₂N), 5.94 (s, 1H, CH), 6.50 (d, 1H, *J* = 2.3, CH_{ar}), 6.88-6.92 (m, 4H, CH_{ar}), 7.22 (d, 1H, *J* = 8.8, CH_{ar}), 7.25-7.26 (m, 1H, CH_{ar}), 8.07 (s, 1H, CH-triazole); ¹³C-NMR (126 MHz, CD₃OD): δ = 25.3 (PhCH₂), 40.8 (CH₂N), 52.5 (CH), 55.0 (PhCH₂N), 55.8 (OMe), 113.1 (CH_{ar}), 114.9 (CH_{ar}), 115.0 (CH_{ar}), 116.4 (CH_{ar}), 121.3 (CH_{ar}), 124.7 (C_q), 126.7 (C_q), 131.2 (CH_{ar}), 131.6 (CH_{ar}), 132.0

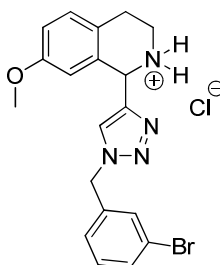
(CH_{ar}), 137.9 (C_q), 145.2 (C_q), 160.1 (C_q -OMe), 161.6 (C_q -OMe); HRMS (ESI): $[M+H]^+$ calculated for $C_{20}H_{23}O_2N_4$ 351.18155, found 351.18152.

1-[1-(2-Bromobenzyl)-1*H*-1,2,3-triazol-4-yl]-7-methoxy-1,2,3,4-tetrahydroisoquinolinium chloride (68)



According to general procedure XI, triazole **68** was obtained as a colourless solid (24 mg, 73% over 2 steps). m.p. 246-248 °C; 1H -NMR (400 MHz, CD_3OD): δ = 3.09-3.16 (m, 2H, $PhCH_2$), 3.48-3.53 (m, 1H, CHN), 3.56-3.61 (m, 1H, CHN), 3.68 (s, 3H, OMe), 5.76 (s, 2H, $PhCH_2N$), 5.96 (s, 1H, CH), 6.52 (s, 1H, CH_{ar}), 6.92 (dd, 1H, $J_1 = 8.2$, $J_2 = 2.1$, CH_{ar}), 7.22 (d, 1H, $J = 8.2$, CH_{ar}), 7.28-7.34 (m, 2H, CH_{ar}), 7.37-7.40 (m, 1H, CH_{ar}), 7.65 (d, 1H, $J = 8.2$, CH_{ar}), 8.04 (s, 1H, CH -triazole); ^{13}C -NMR (126 MHz, CD_3OD): δ = 25.3 ($PhCH_2$), 40.8 (CH_2N), 52.5 (CH), 55.2 ($PhCH_2N$), 55.8 (OMe), 113.1 (CH_{ar}), 116.5 (CH_{ar}), 124.7 (C_q), 124.7 (C_q), 127.1 (CH_{ar}), 129.4 (CH_{ar}), 131.6 (CH_{ar}), 131.8 (CH_{ar}), 132.0 (C_q), 132.2 (CH_{ar}), 134.5 (CH_{ar}), 135.5 (2C, C_q), 160.2 (C_q -OMe); HRMS (ESI): $[M+H]^+$ calculated for $C_{19}H_{20}ON_4Br$ 399.08150, found 399.08109.

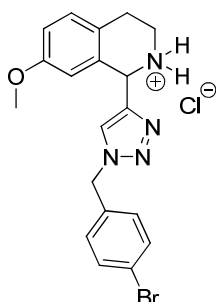
1-[1-(3-Bromobenzyl)-1*H*-1,2,3-triazol-4-yl]-7-methoxy-1,2,3,4-tetrahydroisoquinolinium chloride (69)



According to general procedure XI, triazole **69** was obtained as a colourless solid (31 mg, 75% over 2 steps). m.p. 245-247 °C; 1H -NMR (400 MHz, CD_3OD): δ = 3.11-3.14 (m, 2H, $PhCH_2$), 3.48-3.57 (m, 2H, CH_2N), 3.68 (s, 3H, OMe), 5.63 (s, 2H, $PhCH_2N$), 5.96 (s, 1H, CH), 6.54 (d, 1H, $J = 2.5$, CH_{ar}), 6.93 (dd, 1H, $J_1 = 8.5$, $J_2 = 2.5$, CH_{ar}), 7.23 (d, 1H, $J = 8.5$, CH_{ar}), 7.27-7.35 (m, 2H,

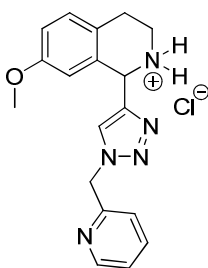
CH_{ar}), 7.50-7.52 (m, 2H, CH_{ar}), 8.11 (s, 1H, CH -triazole); ^{13}C -NMR (101 MHz, CD_3OD): δ = 23.8 ($PhCH_2$), 39.2 (CH_2N), 50.9 (CH), 52.8 ($PhCH_2N$), 54.3 (OMe), 111.6 (CH_{ar}), 115.0 (CH_{ar}), 122.3 (C_q), 123.1 (C_q), 125.4 (CH_{ar}), 126.6 (CH_{ar}), 130.1 (CH_{ar}), 130.4 (CH_{ar}), 130.4 (C_q), 130.7 (CH_{ar}), 131.3 (CH_{ar}), 137.6 (2C, C_q), 158.7 (C_q -OMe); HRMS (ESI): $[M+H]^+$ calculated for $C_{19}H_{20}ON_4Br$ 399.08150, found 399.08120.

1-[1-(4-Bromobenzyl)-1*H*-1,2,3-triazol-4-yl]-7-methoxy-1,2,3,4-tetrahydroisoquinolinium chloride (70)



According to general procedure XI, triazole **70** was obtained as a colourless solid (31 mg, 60% over 2 steps). m.p. 250-252 °C; 1H -NMR (400 MHz, CD_3OD): δ = 3.10-3.14 (m, 2H, $PhCH_2$), 3.47-3.56 (m, 2H, CH_2N), 3.68 (s, 3H, OMe), 5.60 (s, 2H, $PhCH_2N$), 5.94 (s, 1H, CH), 6.53 (d, 1H, J = 2.3, CH_{ar}), 6.91-6.94 (m, 1H, CH_{ar}), 7.22 (d, 1H, J = 8.5, CH_{ar}), 7.28 (d, 2H, J = 8.3, CH_{ar}), 7.53 (d, 2H, J = 8.3, CH_{ar}), 8.10 (s, 1H, CH -triazole); ^{13}C -NMR (101 MHz, CD_3OD): δ = 25.3 ($PhCH_2$), 40.6 (CH_2N), 52.4 (CH), 54.4 ($PhCH_2N$), 55.8 (OMe), 113.2 (CH_{ar}), 116.4 (CH_{ar}), 123.7 (C_q), 124.6 (C_q), 126.1 (C_q), 128.5 (CH_{ar}), 131.2 (2C, CH_{ar}), 131.6 (CH_{ar}), 133.2 (2C, CH_{ar}), 135.9 (C_q), 160.1 (C_q -OMe); HRMS (ESI): $[M+H]^+$ calculated for $C_{19}H_{20}ON_4Br$ 399.08150, found 399.08114.

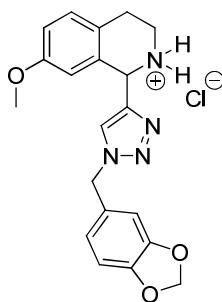
7-Methoxy-1-[1-(pyridin-2-ylmethyl)-1*H*-1,2,3-triazol-4-yl]-1,2,3,4-tetrahydroisoquinolinium chloride (71)



According to general procedure XI, triazole **71** was obtained as a colourless solid (24 mg, 64% over 2 steps). m.p. 107-109 °C; 1H -NMR (400 MHz, CD_3OD): δ = 2.98-3.02 (m, 2H, $PhCH_2$), 3.35-

3.40 (m, 1H, CHN), 3.41-3.49 (m, 1H, CHN), 3.56 (s, 3H, OMe), 5.90 (s, 1H, CH), 6.03 (s, 2H, PhCH₂N), 6.48 (d, 1H, *J* = 2.3, CH_{ar}), 6.78 (dd, 1H, *J*₁ = 8.8, *J*₂ = 2.3, CH_{ar}), 7.09 (d, 1H, *J* = 8.8, CH_{ar}), 7.82 (d, 1H, *J* = 8.0, CH_{ar}), 7.94-7.97 (m, 1H, CH_{ar}), 8.24 (s, 1H, CH-triazole), 8.50-8.53 (m, 1H, CH_{ar}), 8.77 (d, 1H, *J* = 5.7, CH_{ar}); ¹³C-NMR (101 MHz, CD₃OD): δ = 25.3 (PhCH₂), 40.6 (CH₂N), 51.3 (PhCH₂N), 52.2 (CH), 55.9 (OMe), 113.5 (CH_{ar}), 116.3 (CH_{ar}), 124.8 (C_q), 128.4 (CH_{ar}), 128.4 (CH_{ar}), 128.5 (CH_{ar}), 131.6 (CH_{ar}), 131.7 (C_q), 143.6 (CH_{ar}), 145.5 (CH_{ar}), 149.1 (C_q), 150.4 (C_q), 160.1 (C_q-OMe); HRMS (ESI): [M+H]⁺ calculated for C₁₈H₂₀ON₅ 322.16624, found 322.16632.

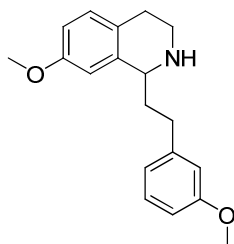
1-[1-(1,3-Benzodioxol-5-ylmethyl)-1*H*-1,2,3-triazol-4-yl]-7-methoxy-1,2,3,4-tetrahydroisoquinolinium chloride (72)



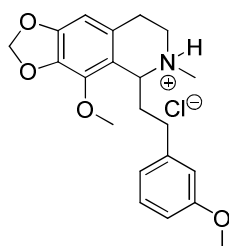
According to general procedure XI, triazole **72** was obtained as a colourless solid (26 mg, 75% over 2 steps). m.p. 229-231 °C; ¹H-NMR (400 MHz, CD₃OD): δ = 2.92-2.98 (m, 2H, PhCH₂), 3.26-3.33 (m, 1H, CHN), 3.35-3.41 (m, 1H, CHN), 3.47 (s, 3H, OMe), 5.33 (s, 2H, PhCH₂N), 5.73 (s, 2H, O₂CH₂), 5.76 (s, 1H, CH), 6.31 (d, 1H, *J* = 1.9, CH_{ar}), 6.60 (d, 1H, *J* = 8.0, CH_{ar}), 6.65 (s, 1H, CH_{ar}), 6.69-6.72 (m, 2H, CH_{ar}), 7.02 (d, 1H, *J* = 8.4, CH_{ar}), 7.89 (s, 1H, CH-triazole); ¹³C-NMR (126 MHz, CD₃OD): δ = 25.3 (PhCH₂), 40.7 (CH₂N), 52.4 (CH), 55.0 (OMe), 55.8 (PhCH₂N), 102.8 (O₂CH₂), 109.4 (CH_{ar}), 109.6 (CH_{ar}), 113.1 (CH_{ar}), 116.5 (CH_{ar}), 123.3 (CH_{ar}), 124.7 (C_q), 126.5 (CH_{ar}), 130.1 (C_q), 131.5 (CH_{ar}), 132.0 (CH_{ar}), 145.1 (C_q), 149.4 (C_q-OCH₂), 149.6 (C_q-OCH₂), 160.1 (C_q-OMe); HRMS (ESI): [M+H]⁺ calculated for C₂₀H₂₁O₃N₄ 365.16082, found 365.16085.

General procedure XII: reduction of alkynylated tetrahydroisoquinolines

To a solution of the corresponding alkynylated tetrahydroisoquinoline (1 equiv) in ethyl acetate (20 mL), catalytic amounts of K₂CO₃ and palladium on carbon were added. The reaction mixture was stirred under a balloon of hydrogen overnight. The reaction mixture was filtered over Cellite and the organic solvents were removed *in vacuo*. The residue was purified *via* flash chromatography to give the target compound. Most of the amines were then converted to the corresponding HCl-salt by addition of HCl in diethyl ether (1 M).

7-Methoxy-1-(3-methoxyphenethyl)-1,2,3,4-tetrahydroisoquinoline (131)

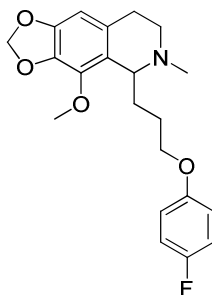
According to general procedure XII, alkynylated tetrahydroisoquinoline **77** (10 mg, 0.03 mmol, 1 equiv) yielded **131** as a colourless oil (9.6 mg, 95%). Flash chromatography (acetone). $R_f = 0.15$ (acetone); $^1\text{H-NMR}$ (400 MHz, CD_3OD): $\delta = 2.08\text{--}2.18$ (m, 1H, CH_2), 2.19–2.24 (m, 1H, CH_2), 2.69–2.89 (m, 4H, PhCH_2), 3.03–3.07 (m, 1H, CHN), 3.32–3.35 (m, 1H, CHN), 3.74 (s, 3H, OMe), 3.77 (s, 3H, OMe), 4.12–4.14 (m, 1H, CH), 6.68 (d, 1H, $J = 2.6$, CH_{ar}), 6.74–6.77 (m, 2H, CH_{ar}), 6.81–6.83 (m, 2H, CH_{ar}), 7.04 (d, 1H, $J = 8.5$, CH_{ar}), 7.18–7.21 (m, 1H, CH_{ar}); $^{13}\text{C-NMR}$ (101 MHz, CD_3OD): $\delta = 28.1$ (PhCH_2), 33.1 (PhCH_2), 38.4 (CH_2), 41.4 (CH_2N), 55.6 (OMe), 55.7 (OMe), 56.5 (CH), 112.3 (CH_{ar}), 112.5 (CH_{ar}), 114.2 (CH_{ar}), 115.2 (CH_{ar}), 121.8 (CH_{ar}), 126.9 (C_q), 130.6 (C_q), 131.2 (C_q), 138.3 (C_q), 144.4 (C_q), 159.6 ($\text{C}_q\text{-OMe}$), 161.4 ($\text{C}_q\text{-OMe}$); HRMS (ESI): $[\text{M}+\text{H}]^+$ calculated for $\text{C}_{19}\text{H}_{24}\text{O}_2\text{N}$ 298.18016, found 298.18017.

4-methoxy-5-[2-(3-methoxyphenyl)ethyl]-6-methyl-5,6,7,8-tetrahydro[1,3]dioxolo[4,5-g]isoquinolin-6-ium chloride (132)

According to general procedure XII, alkynylated tetrahydroisoquinoline **109** (40 mg, 0.11 mmol, 1 equiv) yielded **132** converted to the HCl-salt as a colourless wax (24 mg, 54%). Flash chromatography (cyclohexane/ethyl acetate, gradient from 0 to 100% ethyl acetate). $R_f = 0.33$ (petroleum ether/ethyl acetate, 1:2); $^1\text{H-NMR}$ (500 MHz, CDCl_3): $\delta = 2.00\text{--}2.37$ (m, 2H, CH_2), 2.77 (d, 3H, $J = 8.5$, NCH_3), 2.88–3.12 (m, 4H, 2PhCH_2), 3.28–3.30 (m, 1H, CHN), 3.64–3.66 (m, 1H, CHN), 3.79 (s, 3H, OMe), 3.96 (s, 3H, OMe), 4.23–4.25 (m, 1H, CH), 5.90 (s, 2H, O_2CH_2), 6.33 (s, 1H, CH_{ar}), 6.70–6.72 (m, 1H, CH_{ar}), 6.91–6.92 (m, 2H, CH_{ar}), 7.15–7.19 (m, 1H, CH_{ar}); $^{13}\text{C-NMR}$ (126 MHz, CDCl_3): $\delta = 22.0$ (PhCH_2), 32.4 (PhCH_2), 36.0 (CH_2), 40.9 (NCH_3), 44.6 (CH_2N), 55.3

(OMe), 59.2 (OMe), 59.9 (CH), 101.2 (CH_{ar}), 102.2 (CH_{ar}), 111.9 (CH_{ar}), 114.3 (CH_{ar}), 115.7 (C_q), 121.1 (CH_{ar}), 123.6 (C_q), 129.3 (CH_{ar}), 134.5 (C_q), 140.0 (C_q), 141.9 (C_q), 149.6 (C_q-OMe), 159.7 (C_q-OMe); HRMS (ESI): [M+H]⁺ calculated for C₂₁H₂₆O₄N 356.18563, found 356.18575.

5-[3-(4-Fluorophenoxy)propyl]-4-methoxy-6-methyl-5,6,7,8-tetrahydro-[1,3]dioxolo[4,5-g]isoquinoline (**133**)



According to general procedure XII, alkynylated tetrahydroisoquinoline **120** (13 mg, 0.04 mmol, 1 equiv) yielded **133** as a colourless oil (12 mg, 91%). Flash chromatography (petroleum ether/ethyl acetate, 1:2). R_f = 0.33 (acetone); ¹H-NMR (400 MHz, CDCl₃): δ = 1.71-1.77 (m, 2H, CH₂), 1.88-1.93 (m, 2H, CH₂), 2.43 (s, 3H, NCH₃), 2.44-2.47 (m, 1H, 3.03-3.07, PhCH), 2.71-2.86 (m, 2H, PhCH, CHN), 3.14-3.21 (m, 1H, CHN), 3.67-3.70 (m, 1H, CH), 3.91-3.94 (m, 2H, OCH₂), 3.95 (s, 3H, OMe), 5.84 (dd, 2H, J₁ = 6.8, J₂ = 1.4, O₂CH₂), 6.28 (s, 1H, CH_{ar}), 6.79-6.82 (m, 2H, CH_{ar}), 6.91-6.96 (m, 2H, CH_{ar}); ¹³C-NMR (101 MHz, CDCl₃): δ = 23.4 (PhCH₂), 26.7 (CH₂), 31.0 (CH₂), 42.1 (NCH₃), 44.5 (CH₂N), 58.4 (CH), 59.2 (OMe), 68.6 (OCH₂), 100.4 (O₂CH₂), 102.6 (CH_{ar}), 115.4 (d, 2C, J = 7.0, CH_{ar}), 115.6 (d, 2C, J = 23.0, CH_{ar}-CF), 122.7 (C_q), 127.5 (C_q), 134.1 (C_q), 140.5 (C_q), 147.5 (C_q), 155.3 (C_q), 157.0 (d, J = 236.0, C_q-F); HRMS (ESI): [M+H]⁺ calculated for C₂₁H₂₃O₄NF 374.17621, found 374.17630.

General procedure XIII: copper-catalysed alkylation

By analogy to the literature⁷⁶ a reaction tube was charged with cotarnine iodide (25 mg, 0.07 mmol, 1 equiv) the chiral ligand (3.96 μmol, 0.055 equiv), CuBr (0.52 mg, 3.6 μmol, 0.05 equiv) and a stirbar before being sealed and purged with argon, followed by addition of dichloromethane (1.7 mL) and the corresponding acetylene (0.72 mmol, 10 equiv). The solution was cooled to -78 °C before the addition of triethylamine (10 μL, 0.07 mmol, 1 equiv). The solution was placed in a cooling bath, where it was warmed to -55 °C and stirred for 48h. The solvents were evaporated and the residue was purified *via* flash chromatography to give the desired compound.

4-Methoxy-6-methyl-5-(phenylethynyl)-5,6,7,8-tetrahydro[1,3]dioxolo[4,5-g]isoquinoline (107)

Using the general procedure for the alkynylation of cotarnine iodide (general procedure XIII), different ligands were screened for the synthesis of **107** using phenylacetylene. The residue was purified *via* flash chromatography (petroleum ether/ethyl acetate, 3:1) to give the desired compound as a slightly yellow oil. Product ratio was determined by HPLC, Chiralpak IC column, 40% DCM/EtOH (100:2) in hexanes, 0.5 mL/min, 254 nm (**Table 19**).

Table 19: Ligand screening for the synthesis of 107 using general procedure XIII.

Ligand	yield [%]	t _R [min]	area [mAU·s]	t _R [min]	area [mAU·s]	ee [%]
136	99	6.38	5502.8 (49%)	12.20	5723.4 (51%)	2
137	25	5.65	1.62·10 ⁴ (52%)	11.16	1.48·10 ⁴ (48%)	4
138	56	7.21	4265.3 (48%)	13.00	4671.0 (52%)	4
139	99	7.28	4994.2 (51%)	13.11	4711.8 (49%)	2
140	15	5.72	1.09·10 ⁴ (56%)	11.48	8642.1 (44%)	12
141	26	5.90	1.01·10 ⁴ (45%)	11.60	1.24·10 ⁴ (55%)	10
142	99	7.67	3282.4 (50%)	13.48	3269.4 (50%)	0
Josiphos (143)	42	5.76	2.49·10 ⁴ (55%)	11.54	2.05·10 ⁴ (45%)	10
(<i>R</i>)-QuinoxP [®] (144)	99	6.99	2787.5 (25%)	12.36	8187.9 (75%)	50
145	41	4.85	1.93·10 ⁴ (47%)	10.59	2.16·10 ⁴ (53%)	6
(<i>R</i>)-Phanephos	99	6.85	6160.1 (41%)	12.45	8999.3 (59%)	18
147	52	5.08	1.92·10 ⁴ (54%)	10.94	1.63·10 ⁴ (46%)	8
(<i>R</i>)-BINAP (148)	99	6.91	1922.2 (25%)	12.37	5719.9 (75%)	50
(<i>R</i>)-ToIBINAP (149)	73	5.09	1.90·10 ⁴ (58%)	11.12	1.37·10 ⁴ (42%)	16
(<i>R</i>)-XylBINAP (150)	61	5.22	1.20·10 ⁴ (61%)	11.3	7586.5 (39%)	22
(<i>R</i>)-MonoPhos (151)	53	5.34	9371.9 (52%)	11.58	8803.8 (48%)	4
(<i>S</i>)-QUINAP* (152)	99	12.90	4.46·10 ⁴ (99.2%)	39.74	345.9 (0.8%)	98

* measured at 30% DCM/EtOH (100:2) in hexanes, 0.5 mL/min, 254 nm.

5-[3-(4-Fluorophenoxy)prop-1-ynyl]-4-methoxy-6-methyl-5,6,7,8-tetrahydro-[1,3]dioxolo [4,5-*g*]isoquinoline (120)

Using the general procedure for the alkylation of cotarnine iodide, different ligands were screened for the synthesis of **120** using 1-fluoro-4-(prop-2-ynoxy)benzene.¹⁵⁴ The residue was purified *via* flash chromatography (petroleum ether/ethyl acetate, 2:1) to give the desired target compound as slightly yellow oil. Product ratio was determined by HPLC, Chiralpak IC column, 50% DCM/EtOH (100:2) in hexanes, 0.5 mL/min, 254 nm.

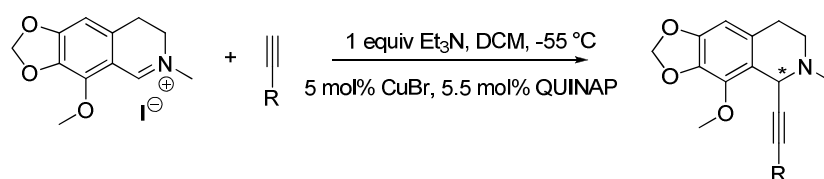
Table 20: Synthesis of 120 using general procedure XIII with QUINAP as chiral ligand.

Ligand	yield [%]	t_R^(major) [min]	area [mAU·s]	t_R^(minor) [min]	area [mAU·s]	ee [%]
(<i>R</i>)-BINAP	16	9.11	409.5 (43%)	17.87	532.8 (57%)	14
(<i>R</i>)-QuinoxP	46	9.11	402.5 (45%)	17.90	488.3 (55%)	10
(<i>R</i>)-ToIBINAP	40	8.80	857.9 (48%)	17.39	916.7 (52%)	4
(<i>R</i>)-XyIBINAP	30	8.82	823.9 (39%)	17.31	1264.5 (61%)	22
(<i>S</i>)-QUINAP	83	10.10	995.36 (81.3%)	19.42	228.4 (18.7%)	63

Alkynylation using various alkynes

The general procedure XIII described above was used to synthesize various alkynylated cotarnine derivatives in an enantioselective fashion. Product ratio was determined by HPLC, Chiralpak IC column, 10% EtOH in hexanes, 0.5 mL/min, 254 nm.

Table 21: Alkynylation of cotarnine iodide using general procedure XIII with QUINAP as chiral ligand.



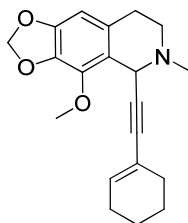
R (compound ID)	yield [%]	$t_R^{(major)}$ [min]	area [mAU·s]	$t_R^{(minor)}$ [min]	area [mAU·s]	ee [%]	$[\alpha]_D^{20}$ (CH ₂ Cl ₂ , c=1.0)
Phenyl (S)-107*	99	12.90	4.5 · 10 ⁴ (99.2%)	39.74	345.9 (0.8%)	98	-95.0°
3-OMePh (S)-109	92	16.10	1.1 · 10 ⁵ (99.3%)	31.01	767.7 (0.7%)	99	-98.8°
4-OMePh (S)-110	88	20.24	7.2 · 10 ⁴ (99.4%)	39.33	469.42 (0.6%)	99	-98.1°
4-CF ₃ Ph (S)-111	95	10.43	4.9 · 10 ⁴ (98.6%)	15.25	671.6 (1.4%)	97	-86.3°
3-Thiophene (S)-112	99	14.74	8.6 · 10 ⁴ (99.4%)	28.08	559.6 (0.6%)	99	-107.3°
Cyclopropane (S)-119***	75	15.13	1.6 · 10 ⁵ (99.3%)	32.59	1216.15 (0.7%)	99	-56.9°
CH ₂ O-(4-F-Ph) (S)-120**	83	10.10	995.36 (81.3%)	19.42	228.4 (18.7%)	63	-33.0°
1-Cyclohexene (S)-161	58	13.77	2.5 · 10 ⁴ (98.4%)	25.64	403.1 (1.6%)	97	-78.1°

* measured at 30% DCM/EtOH (100:2) in hexanes, 0.5 ml/min, 254 nm.

** measured at 50% DCM/EtOH (100:2) in hexanes, 0.5 ml/min, 254 nm.

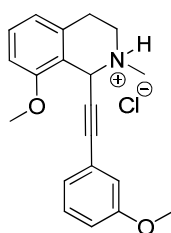
*** product ratio determined at 210 nm.

**5-(Cyclohexenylethynyl)-4-methoxy-6-methyl-5,6,7,8-tetrahydro-[1,3]dioxolo
[4,5-g]isoquinoline (161)**



According to general procedure XIII using (*S*)-QUINAP, (*S*)-**161** was obtained as a colourless oil (13.5 mg, 58%). Flash chromatography (petroleum ether/ethyl acetate, 3:1). $R_f = 0.42$ (petroleum ether/ethyl acetate, 2:1); $[\alpha]_D^{20} = -78.1^\circ$ ($c = 1.0$, CH_2Cl_2); $^1\text{H-NMR}$ (400 MHz, CDCl_3): $\delta = 1.52$ - 1.60 (m, 2H, CH_2), 2.03 - 2.10 (m, 2H, CH_2), 2.51 (s, 3H, NCH_3), 2.57 - 2.69 (m, 2H, PhCH_2), 2.87 - 2.97 (m, 2H, CH_2N), 4.00 (s, 3H, OMe), 4.82 (s, 1H, CH), 5.86 (s, 2H, O_2CH_2), 6.01 - 6.05 (m, 1H, CH), 6.30 (s, 1H, CH_{ar}); $^{13}\text{C-NMR}$ (101 MHz, CDCl_3): $\delta = 21.5$ (CH_2), 22.3 (CH_2), 25.5 (CH_2), 28.7 (CH_2), 29.6 (CH_2), 28.7 (PhCH_2), 43.0 (NCH_3), 46.6 (CH_2N), 51.0 (CH), 59.6 (OMe), 83.5 (C_q alkyne), 87.6 (C_q alkyne), 100.7 (O_2CH_2), 103.0 (CH_{ar}), 120.5 (C_q), 121.6 (C_q), 127.2 (C_q), 134.0 (CH alkene), 134.6 (C_q), 139.9 (C_q), 148.2 (C_q); HRMS (ESI): calculated for $[\text{M}+\text{H}]^+$ $\text{C}_{20}\text{H}_{24}\text{O}_3\text{N}$ 326.17507, found 326.17501.

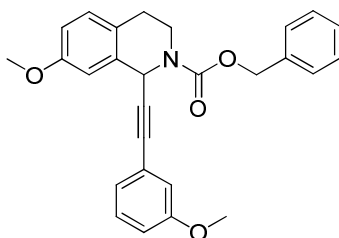
8-Methoxy-1-((3-methoxyphenyl)ethynyl)-2-methyl-1,2,3,4-tetrahydroisoquinolinium chloride (160)



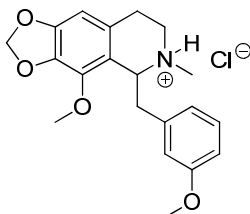
According to general procedure XIII using (*S*)-QUINAP and 8-methoxy-2-methyl-3,4-dihydroisoquinolinium iodide (158)¹⁵⁷ followed by conversion to the HCl-salt by addition of HCl in diethylether (1 M), afforded (*S*)-(-)-**160** as a slightly yellow solid (34 mg, 99%). Flash chromatography (gradient from 0 to 100% ethyl acetate in cyclohexane); $R_f = 0.37$ (petroleum ether/ethyl acetate, 1:1); $[\alpha]_D^{20} = -5^\circ$ ($c = 1.0$, CH_2Cl_2); m.p. 52 - 54°C ; $^1\text{H-NMR}$ (600 MHz, CD_3OD): $\delta = 3.09$ (s, 3H, NCH_3), 3.11 - 3.16 (m, 2H, PhCH_2), 3.50 - 3.60 (m, 2H, CH_2N), 3.74 (s, 3H, OMe), 3.91 (s, 3H, OMe), 5.72 (s, 1H, CH), 6.88 - 7.00 (m, 5H, CH_{ar}), 7.23 - 7.34 (m, 2H, CH_{ar}); $^{13}\text{C-NMR}$ (111 MHz, CD_3OD): $\delta = 26.1$ (PhCH_2), 41.6 (NCH_3), 48.3 (CH_2N), 53.1 (CH), 55.8 (OMe), 56.5

(OMe), 79.2 (C_q alkyne), 90.7 (C_q alkyne), 110.2 (CH_{ar}), 116.8 (CH_{ar}), 117.9 (CH_{ar}), 119.6 (C_q), 122.1 (CH_{ar}), 123.2 (C_q), 125.3 (CH_{ar}), 130.8 (CH_{ar}), 131.2 (CH_{ar}), 132.4 (C_q), 157.4 (C_q-OMe), 161.0 (C_q-OMe); HRMS (ESI): [M+H]⁺ calculated for C₂₀H₂₂O₂N 308.16451, found 308.16453.

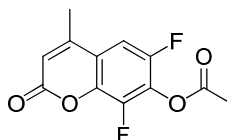
Benzyl 7-methoxy-1-[(3-methoxyphenyl)ethynyl]-3,4-dihydroisoquinoline-2(1*H*)-carboxylate (159)



General procedure XIII was slightly modified as follows. 7-Methoxy-3,4-dihydroisoquinoline (**58**) (19 mg, 0.12 mmol, 1 equiv) was dissolved in DCM (1 mL), cooled to 0 °C and benzyl chloroformate (19 μL, 0.13 mmol, 1.1 equiv) was added dropwise. The reaction mixture was stirred for 2h. Then (*R*)-QUINAP (2.85 mg, 6.5 μmol, 0.055 equiv) and CuBr (0.85 mg, 5.9 μmol, 0.05 equiv) were added, followed by DCM (0.7 mL) and 3-ethynylanisole (150 μL, 1.18 mmol, 10 equiv). The solution was cooled to -78 °C in a dry ice/acetone bath before the addition of triethylamine (16 μL, 0.12 mmol, 1 equiv). The solution was placed in a cooling bath, where it was warmed to -55 °C and stirred for 48h. The reaction was worked up by the addition of saturated NH₄Cl (aq.) and extracted with diethyl ether. The combined organic extracts were washed with brine, dried with MgSO₄ and the solvents evaporated in vacuo. The residue was purified via flash chromatography (petroleum ether/ethyl acetate = 9:1) to give **159** as a yellow oil (17 mg, 34%). R_f = 0.39 (petroleum ether/ethyl acetate, 3:1); [α]_D²⁰ = 0° (c = 1.0, CH₂Cl₂); ¹H-NMR (400 MHz, CDCl₃): δ = 2.75-2.94 (m, 2H, PhCH₂), 3.45-3.58 (m, 1H, CHN), 3.77 (s, 3H, OMe), 3.79 (s, 3H, OMe), 4.14-4.34 (m, 1H, CHN), 5.17-5.33 (m, 2H, Cbz-CH₂), 6.08-6.21 (m, 1H, CH), 6.78-7.19 (m, 7H, CH_{ar}), 7.33-7.41 (m, 5H, Cbz-CH_{ar}); ¹³C-NMR (101 MHz, CDCl₃): δ = 27.6 (PhCH₂), 39.0 (CH₂N), 47.5 (CH), 55.3 (OMe), 55.4 (OMe), 67.5 (Cbz-CH₂), 83.2 (C_q-alkyne), 88.0 (C_q-alkyne), 112.0 (CH_{ar}), 114.0 (CH_{ar}), 115.0 (CH_{ar}), 116.5 (CH_{ar}), 123.6 (C_q), 124.4 (CH_{ar}), 127.9 (CH_{ar}), 128.0 (CH_{ar}), 128.5 (CH_{ar}), 128.6 (C_q), 129.2 (CH_{ar}), 130.0 (CH_{ar}), 134.6 (C_q), 136.5 (C_q), 154.1 (C_q), 158.4 (C_q-OMe), 159.1 (C_q-OMe); HRMS (ESI): calculated for [M-H]⁺ C₂₇H₂₅NO₄ 428.18563, found 428.18541.

4-methoxy-5-(3-methoxybenzyl)-6-methyl-5,6,7,8-tetrahydro[1,3]dioxolo[4,5-g]isoquinolin-6-ium chloride (246)

A suspension of cotarnine iodide **23** (50 mg, 0.14 mmol, 1 equiv) in THF (1 mL) was cooled to 0 °C. Then 3-methoxybenzylmagnesium chloride (0.25 M in THF, 1.7 mL, 0.43 mmol, 3 equiv) was added dropwise. The resulting solution was stirred at 0 °C for 1h and then warmed to RT within 1h. The reaction was quenched by addition of methanol and the solvents were evaporated *in vacuo*. The residue was purified *via* flash chromatography (cyclohexane/ethyl acetate, gradient from 0 to 100% ethyl acetate) and the target compound converted to the HCl-salt by addition of HCl in diethylether (1 M) to give **247** as a slightly yellow wax (23 mg, 42%). $R_f = 0.26$ (petroleum ether/ethyl acetate, 1:1); $^1\text{H-NMR}$ (500 MHz, CDCl_3): $\delta = 2.70$ (s, 3H, NCH_3), 2.84-3.27 (m, 4H, PhCH_2), 3.53-3.69 (m, 2H, CH_2N), 3.73 (s, 3H, OMe), 3.75 (s, 3H, OMe), 4.62 (bs, 1H, CH), 5.91 (s, 2H, O_2CH_2), 6.33 (s, 1H, CH_{ar}), 6.74-6.82 (m, 3H, CH_{ar}), 7.12-7.15 (m, 1H, CH_{ar}), 12.52 (bs, 1H, NH); $^{13}\text{C-NMR}$ (126 MHz, CDCl_3): $\delta = 29.7$ (PhCH_2), 40.1 (PhCH_2), 42.3 (NCH_3), 46.5 (CH_2N), 55.4 (OMe), 59.0 (OMe), 61.7 (CH), 101.1 (O_2CH_2), 102.2 (CH_{ar}), 113.4 (CH_{ar}), 115.0 (CH_{ar}), 122.2 (CH_{ar}), 124.7 (C_q), 129.4 (CH_{ar}), 134.3 (C_q), 137.5 (2C_q), 140.2 (C_q), 149.7 (C_q), 159.6 (C_q); HRMS (ESI): $[\text{M}+\text{H}]^+$ calculated for $\text{C}_{20}\text{H}_{24}\text{O}_4\text{N}$ 342.16998, found 342.17004.

6,8-Difluoro-4-methylumbelliferol acetate (221, DiFMUA)

6,8-difluoro-4-methylumbelliferol (**222**, DiFMU)¹⁴⁹ (100 mg, 0.47 mmol, 1 equiv) was dissolved in dichloromethane (5 ml), triethylamine (99 μl , 0.71 mmol, 1.5 equiv) was added followed by acetylchloride. The reaction mixture was stirred at RT overnight. Solvents were evaporated and the product was purified *via* flash chromatography to give a colourless solid (78 mg, 65%). m.p. 129-131 °C; $R_f = 0.39$ (petroleum ether/ethyl acetate, 3:1); $^1\text{H-NMR}$ (400 MHz, DMSO-d_6): $\delta = 2.41$ (s, 3H, COCH_3), 2.46 (s, 3H, CH_3), 6.55 (s, 3H, CH), 7.75 (dd, 1H, $J_1 = 10.5$, $J_2 = 2.3$, CH_{ar}); $^{13}\text{C-NMR}$ (101 MHz, DMSO-d_6): $\delta = 18.3$ (CH_3), 19.8 (COCH_3), 107.2 (d, $J = 4$, CH_{ar}), 115.7 (CH), 118.5-

118.6 (m, C_q), 128.7 (dd, $J_1 = 18$, $J_2 = 13$, C_q), 138.7 (dd, $J_1 = 10$, $J_2 = 3$, C_q), 141.8 (dd, $J_1 = 253$, $J_2 = 5$, C_q), 150.0 (dd, $J_1 = 242$, $J_2 = 4$, C_q), 152.3-152.4 (m, C_q), 157.9 (CO), 167.2 (CO); HRMS (ESI): calculated for [M+H]⁺ C₁₂H₉O₄F₂ 255.04634, found 255.04658.

6 Tetrahydroisoquinoline Compound Library

The following 103 compounds were tested on microtubule inhibition: **21, 23, 61, 62, 63, 74, 75, (S)-75, (R)-75, 76, 77, (S)-77, (R)-77, 78, 79, (S)-79, (R)-79, 64, 65, 66, 68, 69, 70, 72, 81, 82, (S)-82, (R)-82, 83, 84, (S)-84, (R)-84, 85, 86, 87, 88, 89, 90, 91, 92, 93, 94, 95, 96, 97, 98, (S)-98, (R)-98, 99, 100, 101, 102, 103, 104, (R)-104, 105, 106, 107, (S)-107, (R)-107, 108, 109, (S)-109, (R)-109, 110, 111, 112, 113, 114, 115, 116, 117, 118, 119, (S)-119, 120, (S)-120, (R)-120, 121, (S)-122, (R)-122, 123, 124, 126, 127, (S)-127, (R)-127, 128, 129, (S)-129, (R)-129, 130, 132, (S)-161, 162, 246, 322, 323, 324, 325, 326, 327.**

VI References

1. Dobson, C. M. *Nature* **2004**, *432*, 824-828.
2. Kaiser, M.; Wetzel, S.; Kumar, K.; Waldmann, H. *Cell. Mol. Life Sci.* **2008**, *65*, 1186-1201.
3. Spring, D. R. *Chem. Soc. Rev.* **2005**, *34*, 472-82.
4. Wilk, W.; Zimmermann, T. J.; Kaiser, M.; Waldmann, H. *Biol. Chem.* **2010**, *391*, 491-497.
5. Lipinski, C.; Hopkins, A. *Nature* **2004**, *432*, 855-861.
6. Osada, H. *Biosci., Biotechnol., Biochem.* **2010**, *74*, 1135-1140.
7. Kanoh, N.; Kumashiro, S.; Simizu, S.; Kondoh, Y.; Hatakeyama, S.; Tashiro, H.; Osada, H. *Angew. Chem. Int. Ed.* **2003**, *42*, 5584-5587.
8. Newman, D. J.; Cragg, G. M. *J. Nat. Prod.* **2007**, *70*, 461-477.
9. Cragg, G. M.; Newman, D. J. *Pure Appl. Chem.* **2005**, *77*, 7-24.
10. Fallarino, M. *HerbalGram* **1994**, *31*, 38-44.
11. Sertürner, F. W. *J. Pharmacie* **1805**, *13*, 234-236.
12. Buss, A. D.; Waigh, R. D. In *Burgers Medicinal Chemistry and Drug Discovery*; Wolff, M. E. Ed.; John Wiley: New York, USA, 1995; pp. 983-1033.
13. Tan, C.; Tasaka, H.; Yu, K. P.; Murphy, M. L.; Karnofsky, D. A. *Cancer* **1967**, *20*, 333-353.
14. Stob, M.; Baldwin, R. S.; Tuite, J.; Andrews, F. N.; Gillette, K. G. *Nature* **1962**, *196*, 1318.
15. Bennett, J. W.; Klich, M. *Clin. Microbiol. Rev.* **2003**, *16*, 497-516.

16. Mayer, A. M.; Glaser, K. B.; Cuevas, C.; Jacobs, R. S.; Kem, W.; Little, R. D.; McIntosh, J. M.; Newman, D. J.; Potts, B. C.; Shuster, D. E. *Trends Pharmacol. Sci.* **2010**, *31*, 255-265.
17. Gunasekera, S. P.; Gunasekera, M.; Longley, R. E.; Schulte, G. K. *J. Org. Chem.* **1990**, *55*, 4912-4915.
18. Paterson, I. I.; Florence, G. J.; Gerlach, K.; Scott, J. P. *Angew. Chem. Int. Ed.* **2000**, *39*, 377-380.
19. Smith, J. M. *Nature* **1970**, *225*, 563-564.
20. Schreiber, S. L. *Science* **2000**, *287*, 1964-1969.
21. Bon, R. S.; Waldmann, H. *Acc. Chem. Res.* **2010**, *43*, 1103-1114.
22. Nören-Müller, A.; Reis-Correa Jr., I.; Prinz, H.; Rosenbaum, C.; Saxena, K.; Schwalbe, H. J.; Vestweber, D.; Cagna, G.; Schunk, S.; Schwarz, O.; Schiewe, H.; Waldmann, H. *Proc. Natl. Acad. Sci. USA* **2006**, *103*, 10606-10611.
23. Altmann, K.-H. *Chem. Biol.* **2007**, *14*, 347-349.
24. Koch, M. A.; Schuffenhauer, A.; Scheck, M.; Wetzel, S.; Casaulta, M.; Odermatt, A.; Ertl, P.; Waldmann, H. *Proc. Natl. Acad. Sci. USA* **2005**, *102*, 17272-17277.
25. Dekker, F. J.; Koch, M. A.; Waldmann, H. *Curr. Opin. Chem. Biol.* **2005**, *9*, 232-239.
26. Wetzel, S.; Klein, K.; Renner, S.; Rauh, D.; Oprea, T. I.; Mutzel, P.; Waldmann, H. *Nat. Chem. Biol.* **2009**, *5*, 581-583.
27. Renner, S.; van Otterlo, W. A. L.; Dominguez Seoane, M.; Mocklinghoff, S.; Hofmann, B.; Wetzel, S.; Schuffenhauer, A.; Ertl, P.; Oprea, T. I.; Steinhilber, D.; Brunsveld, L.; Rauh, D.; Waldmann, H. *Nat. Chem. Biol.* **2009**, *5*, 585-592.
28. Mocklinghoff, S.; van Otterlo, W. A.; Rose, R.; Fuchs, S.; Zimmermann, T. J.; Dominguez Seoane, M.; Waldmann, H.; Ottmann, C.; Brunsveld, L. *J. Med. Chem.* **2011**, *54*, 2005-11.

29. Koch, M. A.; Waldmann, H. *Drug Discov. Today* **2005**, *10*, 471-83.
30. Koch, M. A.; Wittenberg, L.-O.; Basu, S.; Jeyaraj, D. A.; Gourzoulidou, E.; Reinecke, K.; Odermatt, A.; Waldmann, H. *Proc. Natl. Acad. Sci. USA* **2004**, *101*, 16721-16726.
31. Scheck, M.; Koch, M. A.; Waldmann, H. *Tetrahedron* **2008**, *64*, 4792-4802.
32. McArdle, B. M.; Campitelli, M. R.; Quinn, R. J. *J. Nat. Prod.* **2006**, *69*, 14-17.
33. McArdle, B. M.; Quinn, R. J. *Chembiochem* **2007**, *8*, 788-798.
34. Zimmermann, T. J.; Niesen, F. H.; Pilka, E. S.; Knapp, S.; Oppermann, U.; Maier, M. E. *Bioorg. Med. Chem.* **2009**, *17*, 530-536.
35. Forrest, G. L.; Gonzalez, B.; Tseng, W.; Li, X.; Mann, J. *Cancer Res.* **2000**, *60*, 5158-5164.
36. Olson, L. E.; Bedja, D.; Alvey, S. J.; Cardounel, A. J.; Gabrielson, K. L.; Reeves, R. H. *Cancer Res.* **2003**, *63*, 6602-6606.
37. Rink, C.; Sasse, F.; Zubriene, A.; Matulis, D.; Maier, M. E. *Chem. Eur. J.* **2010**, *16*, 14469-14478.
38. Ugele, M.; Sasse, F.; Knapp, S.; Fedorov, O.; Zubriene, A.; Matulis, D.; Maier, M. E. *ChemBioChem* **2009**, *10*, 2203-2212.
39. Corrêa, I. R. J.; Nören-Müller, A.; Ambrosi, H.-D.; Jakupovic, S.; Saxena, K.; Schwalbe, H.; Kaiser, M.; Waldmann, H. *Chem. Asian. J.* **2007**, *2*, 1109-1126.
40. Nören-Müller, A.; Wilk, W.; Saxena, K.; Schwalbe, H.; Kaiser, M.; Waldmann, H. *Angew. Chem. Int. Ed.* **2008**, *47*, 5973-5977.
41. Stahl, P.; Kissau, L.; Mazitschek, R.; Giannis, A.; Waldmann, H. *Angew. Chem. Int. Ed.* **2002**, *41*, 1174-1178.
42. Stahl, P.; Kissau, L.; Mazitschek, R.; Huwe, A.; Furet, P.; Giannis, A.; Waldmann, H. *J. Am. Chem. Soc.* **2001**, *123*, 11586-11593.

43. Crozier, A.; Clifford, M. N.; Ashihara, H. *Plant Secondary Metabolites*; Blackwell, 2006.
44. Dewick, P. M. *Medicinal Natural Products*, 3 ed.; Wiley, 2009.
45. Rinehart, K. L.; Holt, T. G.; Fregeau, N. L.; Stroh, J. G.; Keifer, P. A.; Sun, F.; Li, L. H.; Martin, D. G. *J. Org. Chem.* **1990**, *55*, 4512-4515.
46. Wright, A. E.; Forleo, D. A.; Gunawardana, G. P.; Gunasekera, S. P.; Koehn, F. E.; Mcconnell, O. J. *J. Org. Chem.* **1990**, *55*, 4508-4512.
47. Pathak, R.; Naicker, P.; Thompson, W. A.; Fernandes, M. A.; de Koning, C. B.; van Otterlo, W. A. L. *Eur. J. Org. Chem.* **2007**, 5337-5345.
48. van Otterlo, W. A. L.; Pathak, R.; de Koning, C. B.; Fernandes, M. A. *Tetrahedron Lett.* **2004**, *45*, 9561-9563.
49. Ishiwata, K.; Koyanagi, Y.; Abe, K.; Kawamura, K.; Taguchi, K.; Saitoh, T.; Toda, J.; Senda, M.; Sano, T. *J. Neurochem.* **2001**, *79*, 868-876.
50. Kamei, J. *Pulm. Pharmacol.* **1996**, *9*, 349-356.
51. Ye, K.; Ke, Y.; Keshava, N.; Shanks, J.; Kapp, J. A.; Tekmal, R. R.; Petros, J.; Joshi, H. C. *Proc. Natl. Acad. Sci. USA* **1998**, *95*, 1601-1606.
52. Aneja, R.; Karna, P.; Rida, P. C. G.; Pannu, V.; Gupta, K. K.; Dalton, W. B.; Joshi, H.; Yang, V. W.; Zhou, J. *Cell Death Differ.* **2011**, *18*, 632-644.
53. Aneja, R.; Miyagi, T.; Karna, P.; Ezell, T.; Shukla, D.; Gupta, M. V.; Yates, C.; Chinni, S. R.; Zhau, H. Y.; Chung, L. W. K.; Joshi, H. C. *Eur. J. Cancer* **2010**, *46*, 1668-1678.
54. Kingston, D. G. I. *J. Nat. Prod.* **2009**, *72*, 507-515.
55. Ni, J.; Xiao, H.; Weng, L.; Wei, X.; Xu, Y. *Tetrahedron* **2011**, *67*, 5162-5167.
56. Salway, A. H. *J. Chem. Soc., Trans.* **1910**, *97*, 1208-1219.

57. Perkin, W. H.; Robinson, R. *J. Chem. Soc., Trans.* **1911**, 99, 775-792.
58. Dumontet, C.; Jordan, M. A. *Nat. Rev. Drug. Discov.* **2010**, 9, 587-587.
59. Risinger, A. L.; Giles, F. J.; Mooberry, S. L. *Cancer Treat. Rev.* **2009**, 35, 255-61.
60. Jordan, M. A.; Kamath, K. *Curr. Cancer Drug Targets* **2007**, 7, 730-742.
61. Giannakakou, P.; Sackett, D.; Fojo, T. *J. Natl. Cancer.* **2000**, 92, 182-183.
62. Johnson, T. *CRC Ethnobotany Desk Reference*; CRC Press: Boca Raton, FL, 1999.
63. Pasquier, E.; Kavallaris, M. *IUBMB Life* **2008**, 60, 165-170.
64. Perez, E. A. *Mol. Cancer Ther.* **2009**, 8, 2086-2095.
65. Gerding-Reimers, C. Dissertation, TU Dortmund, 2011.
66. Decker, M. *Eur. J. Med. Chem.* **2005**, 40, 305-313.
67. Wang, X.-j.; Tan, J.; Grozinger, K. *Tetrahedron Lett.* **1998**, 39, 6609-6612.
68. Yamaguchi, M.; Hirao, I. *Tetrahedron Lett.* **1983**, 24, 1719-1722.
69. Ritschel, J.; Sasse, F.; Maier, M. E. *Eur. J. Org. Chem.* **2007**, 78-87.
70. Kenkichi, S. *J. Organomet. Chem.* **2002**, 653, 46-49.
71. Rostovtsev, V. V.; Green, L. G.; Fokin, V. V.; Sharpless, K. B. *Angew. Chem. Int. Ed.* **2002**, 41, 2596-2599.
72. Williams, E.; Elliot, M. C. *Org. Biomol. Chem.* **2003**, 1, 3038-3047.
73. Werner, F.; Blank, N.; Opatz, T. *Eur. J. Org. Chem.* **2007**, 3911-3915.
74. Soriano, M. D. P. C.; Shankaraiah, N.; Santos, L. S. *Tetrahedron Lett.* **2010**, 51, 1770-1773.

75. Jahangir; MacLean, D. B.; Brook, M. A.; Holland, H. L. *J. Chem. Soc., Chem. Commun.* **1986**, 1608-1609.
76. Taylor, A. M.; Schreiber, S. L. *Org. Lett.* **2006**, *8*, 143-146.
77. Gommermann, N.; Koradin, C.; Polborn, K.; Knochel, P. *Angew. Chem. Int. Ed.* **2003**, *42*, 5763-5766.
78. Koradin, C.; Gommermann, N.; Polborn, K.; Knochel, P. *Chemistry* **2003**, *9*, 2797-2811.
79. Koradin, C.; Polborn, K.; Knochel, P. *Angew. Chem. Int. Ed.* **2002**, *41*, 2535-2538.
80. MarvinSketch. Version 5.7.0, ChemAxon.
81. Moll, A.; Hildebrandt, A.; Lenhof, H. P.; Kohlbacher, O. *J. Comput. Aided. Mol. Des.* **2005**, *19*, 791-800.
82. Moll, A.; Hildebrandt, A.; Lenhof, H. P.; Kohlbacher, O. *Bioinformatics* **2006**, *22*, 365-366.
83. Bonne, D.; Heusele, C.; Simon, C.; Pantaloni, D. *J. Biol. Chem.* **1985**, *260*, 2819-2825.
84. Alisaraie, L.; Tuszynski, J. A. *Chem. Biol. Drug Des.* **2011**, *78*, 535-546.
85. Naik, P. K.; Santoshi, S.; Rai, A.; Joshi, H. C. *J. Mol. Grap. Model* **2011**, *29*, 947-55.
86. Uttamchandani, M.; Walsh, D. P.; Yao, S. Q.; Chang, Y. T. *Curr. Opin. Chem. Biol.* **2005**, *9*, 4-13.
87. MacBeath, G.; Koehler, A. N.; Schreiber, S. L. *J. Am. Chem. Soc.* **1999**, *121*, 7967-7968.
88. Kanoh, N.; Honda, K.; Simizu, S.; Muroi, M.; Osada, H. *Angew. Chem. Int. Ed.* **2005**, *44*, 3559-3562.

89. Kanoh, N.; Asami, A.; Kawatani, M.; Honda, K.; Kumashiro, S.; Takayama, H.; Simizu, S.; Amemiya, T.; Kondoh, Y.; Hatakeyama, S.; Tsuganezawa, K.; Utata, R.; Tanaka, A.; Yokoyama, S.; Tashiro, H.; Osada, H. *Chem. Asian J.* **2006**, *1*, 789-797.
90. Miyazaki, I.; Simizu, S.; Ichimiya, H.; Kawatani, M.; Osada, H. *Biosci., Biotechnol., Biochem.* **2008**, *72*, 2739-2749.
91. Hagiwara, K.; Kondoh, Y.; Ueda, A.; Yamada, K.; Goto, H.; Watanabe, T.; Nakata, T.; Osada, H.; Aida, Y. *Biochem. Biophys. Res. Commun.* **2010**, *394*, 721-727.
92. Saito, A.; Kawai, K.; Takayama, H.; Sudo, T.; Osada, H. *Chem. Asian J.* **2008**, *3*, 1607-1612.
93. Kanoh, N.; Kyo, M.; Inamori, K.; Ando, A.; Asami, A.; Nakao, A.; Osada, H. *Anal. Chem.* **2006**, *78*, 2226-2230.
94. Sigal, G. B.; Bamdad, C.; Barberis, A.; Strominger, J.; Whitesides, G. M. *Anal. Chem.* **1996**, *68*, 490-497.
95. Thery-Merland, F.; Méthivier, C.; Pasquinet, E.; Hairault, L.; Pradier, C. M. *Sensors and Actuators B: Chemical* **2006**, *114*, 223-228.
96. Ellis, R. W.; Defeo, D.; Shih, T. Y.; Gonda, M. A.; Young, H. A.; Tsuchida, N.; Lowy, D. R.; Scolnick, E. M. *Nature* **1981**, *292*, 506-511.
97. Parada, L. F.; Tabin, C. J.; Shih, C.; Weinberg, R. A. *Nature* **1982**, *297*, 474-478.
98. Ireland, C. M. *Cancer Res.* **1989**, *49*, 5530-5533.
99. Waldmann, H.; Wittinghofer, A. *Angew. Chem. Int. Ed.* **2000**, *39*, 4192-4214.
100. Downward, J. *Nat. Rev. Cancer* **2003**, *3*, 11-22.
101. Burgering, B. M. T.; Bos, J. L. *Trends Biochem. Sci.* **1995**, *20*, 18-22.
102. Scheffzek, K.; Ahmadian, M. R.; Kabsch, W.; Wiesmuller, L.; Lautwein, A.; Schmitz, F.; Wittinghofer, A. *Science* **1997**, *277*, 333-338.

103. Rocks, O.; Peyker, A.; Bastiaens, P. I. H. *Curr. Opin. Cell Biol.* **2006**, *18*, 351-357.
104. Bijlmakers, M.-J.; Marsh, M. *Trends Cell Biol.* **2003**, *32*, 32-42.
105. Linder, M. E.; Deschenes, R. J. *Nat. Rev. Mol. Cell Biol.* **2007**, *8*, 74-84.
106. Greaves, J.; Chamberlain, L. H. *J. Cell Biol.* **2007**, *176*, 249-254.
107. Rocks, O.; Peyker, A.; Kahms, M.; Verveer, P. J.; Koerner, C.; Lumbierres, M.; Kuhlmann, J.; Waldmann, H.; Wittinghofer, A.; Bastiaens, P. I. H. *Science* **2005**, *307*, 1746-1751.
108. Camp, L. A.; Hofmann, S. L. *J. Biol. Chem.* **1993**, *268*, 22566-22574.
109. Camp, L. A.; Verkruyse, L. A.; Afendis, S. J.; Slaughter, C. A.; Hofmann, S. L. *J. Biol. Chem.* **1994**, *269*, 23212-23219.
110. Verkruyse, L. A.; Hofmann, S. L. *J. Biol. Chem.* **1996**, *271*, 15831-15836.
111. Hellsten, E.; Vesa, J.; Olkkonen, V. M.; Jalanko, A.; Peltonen, L. *EMBO J.* **1996**, *15*, 5240-5245.
112. Schriener, J. E.; Yi, W.; Hofmann, S. L. *Genomics* **1996**, *34*, 317-322.
113. Devedjiev, Y.; Dauter, Z.; Kuznetsov, S. R.; Jones, T. L. Z.; Derewenda, Z. S. *Structure (London)* **2000**, *8*, 1137-1146.
114. Duncan, J. A.; Gilman, A. G. *J. Biol. Chem.* **1998**, *273*, 15830-15837.
115. Wang, A.; Deems, R. A.; Dennis, E. A. *J. Biol. Chem.* **1997**, *272*, 12723-12729.
116. Sugimoto, H.; Hayashi, H.; Yamashita, S. *J. Biol. Chem.* **1996**, *271*, 7705-7711.
117. Wang, A.; Loo, R.; Chen, Z.; Dennis, E. A. *J. Biol. Chem.* **1997**, *272*, 22030-22036.
118. Bolen, A. L.; Naren, A. P.; Yarlagadda, S.; Beranova-Giorgianni, S.; Chen, L.; Norman, D.; Baker, D. L.; Rowland, M. M.; Best, M. D.; Sano, T.; Tsukahara, T.; Liliom, K.; Igarashi, Y.; Tigyi, G. *J. Lipid Res.* **2011**, *52*, 958-70.

119. Duncan, J. A. *J. Biol. Chem.* **2002**, *277*, 31740-31752.
120. Flaumenhaft, R.; Rozenvayn, N.; Feng, D.; Dvorak, A. M. *Blood* **2007**, *110*, 1492-14501.
121. Satou, M.; Nishi, Y.; Yoh, J.; Hattori, Y.; Sugimoto, H. *Endocrinology* **2010**, *151*, 4765-4775.
122. Sim, D. S.; Dilks, J. R.; Flaumenhaft, R. *Arterioscler. Thromb. Vasc. Biol.* **2007**, *27*, 1478-1485.
123. Yeh, D. C.; Duncan, J. A.; Yamashita, S.; Michel, T. *J. Biol. Chem.* **1999**, *274*, 33148-33154.
124. Rocks, O.; Gerauer, M.; Vartak, N.; Koch, S.; Huang, Z.-P.; Pechlivanis, M.; Kuhlmann, J.; Brunsveld, L.; Chandra, A.; Ellinger, B.; Waldmann, H.; Bastiaens, P. I. H. *Cell* **2010**, *141*, 458-471.
125. Salaun, C.; Greaves, J.; Chamberlain, L. H. *J. Cell. Biol.* **2010**, *191*, 1229-1238.
126. Dietzen, D. J.; Hastings, W. R.; Lublin, D. M. *J. Biol. Chem.* **1995**, *270*, 6838-6942.
127. Sunaga, H.; Sugimoto, H.; Nagamachi, Y.; Yamashita, S. *Biochem. J.* **1995**, *308*, 551-557.
128. Toyoda, T.; Sugimoto, H.; Yamashita, S. *Biochim. Biophys. Acta* **1999**, *1437*, 182-193.
129. Tomatis, V. M.; Trenchi, A.; Gomez, G. A.; Daniotti, J. L. *PLoS One* **2010**, *5*, e15045.
130. Deck, P.; Pendzialek, D.; Biel, M.; Wagner, M.; Popkirova, B.; Ludolph, B.; Kragol, G.; Kuhlmann, J.; Giannis, A.; Waldmann, H. *Angew. Chem. Int. Ed.* **2005**, *44*, 4975-4980.
131. Biel, M.; Deck, P.; Athanassios, G.; Waldmann, H. *Chem. Eur. J.* **2006**, *12*, 4121-4143.

132. Dekker, F. J.; Rocks, O.; Vartak, N.; Menninger, S.; Hedberg, C.; Balamurugan, R.; Wetzel, S.; Renner, S.; Gerauer, M.; Scholermann, B.; Rusch, M.; Kramer, J. W.; Rauh, D.; Coates, G. W.; Brunsveld, L.; Bastiaens, P. I.; Waldmann, H. *Nat. Chem. Biol.* **2010**, *6*, 449-456.
133. Fischer, M.; Pleiss, J. *Nucl. Acid Res.* **2003**, *31*, 319-321.
134. Burger, M.; Zimmermann, T. J.; Kondoh, Y.; Stege, P.; Watanabe, N.; Osada, H.; Waldmann, H.; Vetter, I. R. *J. Lipid. Res.* **2012**, *53*, 43-50.
135. Steinberg, G. R.; Kemp, B. E.; Watt, M. J. *Am. J. Physiol. Endocrinol. Metab.* **2007**, *293*, E958-964.
136. Benjamin, A. M.; Suchindran, S.; Pearce, K.; Rowell, J.; Lien, L. F.; Guyton, J. R.; McCarthy, J. J. *J. Obes.* **2011**, 1-8.
137. Heid, I. M.; Jackson, A. U.; Randall, J. C.; Winkler, T. W. *et al. Nat. Genet.* **2010**, *42*, 949-960.
138. Lindgren, C. M.; Heid, I. M.; Randall, J. C.; Lamina, C. *et al. PLoS Genet* **2009**, *5*, e1000508.
139. Speliotes, E. K.; Yerges-Armstrong, L. M.; Wu, J.; Hernaez, R.; Kim, L. J.; Palmer, C. D.; Gudnason, V.; Eiriksdottir, G.; Garcia, M. E.; Launer, L. J.; Nalls, M. A.; Clark, J. M.; Mitchell, B. D.; Shuldiner, A. R.; Butler, J. L.; Tomas, M.; Hoffmann, U.; Hwang, S. J.; Massaro, J. M.; O'Donnell, C. J.; Sahani, D. V.; Salomaa, V.; Schadt, E. E.; Schwartz, S. M.; Siscovick, D. S.; Voight, B. F.; Carr, J. J.; Feitosa, M. F.; Harris, T. B.; Fox, C. S.; Smith, A. V.; Kao, W. H.; Hirschhorn, J. N.; Borecki, I. B. *PLoS Genet.* **2011**, *7*, e1001324.
140. Rusch, M.; Zimmermann, T. J.; Bürger, M.; Dekker, F. J.; Görmer, K.; Triola, G.; Brockmeyer, A.; Janning, P.; Böttcher, T.; Sieber, S. A.; Vetter, I. R.; Hedberg, C.; Waldmann, H. *Angew. Chem. Int. Ed.* **2011**, *50*, 9838-9842.
141. Tomiki, T.; Saito, T.; Ueki, M.; Konno, H.; Asaoka, T.; Suzuki, R.; Uramoto, M.; Kakeya, H.; Osada, H. *J. Comp. Aid. Chem.* **2006**, *7*, 157-162.

142. Hedberg, C.; Dekker, F. J.; Rusch, M.; Renner, S.; Wetzels, S.; Vartak, N.; Gerding-Reimers, C.; Bon, R. S.; Bastiaens, P. I.; Waldmann, H. *Angew. Chem. Int. Ed.* **2011**, *50*, 9832-9837.
143. Suzuki, A. Z.; Ozaki, S.; Goto, J.; Mikoshiba, K. *Bioorg. Med. Chem. Lett.* **2010**, *20*, 1395-1398.
144. Garner, C. W. *J. Biol. Chem.* **1980**, *255*, 5064-5068.
145. Bonvini, P.; Zorzi, E.; Basso, G.; Rosolen, A. *Leukemia* **2007**, *21*, 838-842.
146. Kansy, M.; Senner, F.; Gubernator, K. *J. Med. Chem.* **1998**, *41*, 1007-1010.
147. Devedjiev, Y.; Dauter, Z.; Kuznetsov, S. R.; Jones, T. L.; Derewenda, Z. S. *Structure* **2000**, *8*, 1137-46.
148. Görmer, K.; Bürger, M.; Kruijtzter, J. A. W.; Vetter, I. R.; Vartak, N.; Brunsveld, L.; Bastiaens, P.; Triola, G.; Liskamp, R. M. J.; Waldmann, H. *manuscript submitted* **2011**.
149. Sun, W.-C.; Gee, K. R.; Haugland, R. P. *Bioorg. Med. Chem. Lett.* **1998**, *8*, 3107-3110.
150. Ortwine, D. F.; Malone, T. C.; Bigge, C. F.; Drummond, J. T.; Humblet, C.; Johnson, G.; Pinter, G. W. *J. Med. Chem.* **1992**, *35*, 1345-1370.
151. Sall, D. J.; Grunewald, G. L. *J. Med. Chem.* **1987**, *30*, 2208-2216.
152. Chern, M.-S.; Li, W.-R. *Tetrahedron Lett.* **2004**, *45*, 8323-8326.
153. Williams, G. D.; Pike, R. A.; Wade, C. E.; Wills, M. *Org. Lett.* **2003**, *5*, 4227-4230.
154. Luo, F. T.; Ko, S. L.; Liu, L. J.; Chen, H. *Heterocycles* **2000**, *53*, 2055-2066.
155. Hu, M.; Li, J.; Q. Yao, S. *Org. Lett.* **2008**, *10*, 5529-5531.
156. Mayer, T.; Maier, M. E. *Eur. J. Org. Chem.* **2007**, 4711-4720.

157. Schlosser, M.; Simig, G. *Tetrahedron Lett.* **1991**, 32, 1965-1966.

VII Summary

The presented work deals with two major aspects of chemical biology: chemical synthesis and application of protein-based test systems. In the first part, the synthesis of a compound collection based on the tetrahydroisoquinoline skeleton is described and is followed by a second part that details the use of small molecule microarrays as a tool for the identification of high-affinity ligand-protein interactions.

BIOS of a tetrahydroisoquinoline-based compound library

Using the principles of biology-oriented synthesis a library of alkynylated tetrahydroisoquinolines was synthesised. This library was based on the biologically prevalidated core scaffold of tetrahydroisoquinoline (THIQ), a structural backbone occurring in various natural products of diverse origin, exerting numerous biological effects. A prominent member of the THIQ-family is the natural product noscapine (**21**) that has recently drawn a lot of interest to its anti-cancer effect. The significant *in vivo* antitumor activity coupled with its minimal toxicity render noscapine an interesting THIQ-based lead compound that entered clinical phase trials. To resemble the structural rigidity of noscapine, alkynylated THIQs were synthesised where the meconine residue was replaced by an alkyne (**Figure 66**).

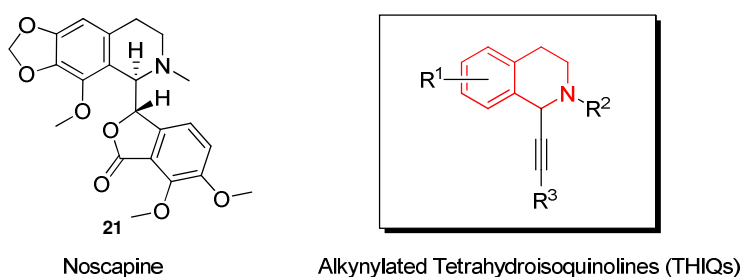
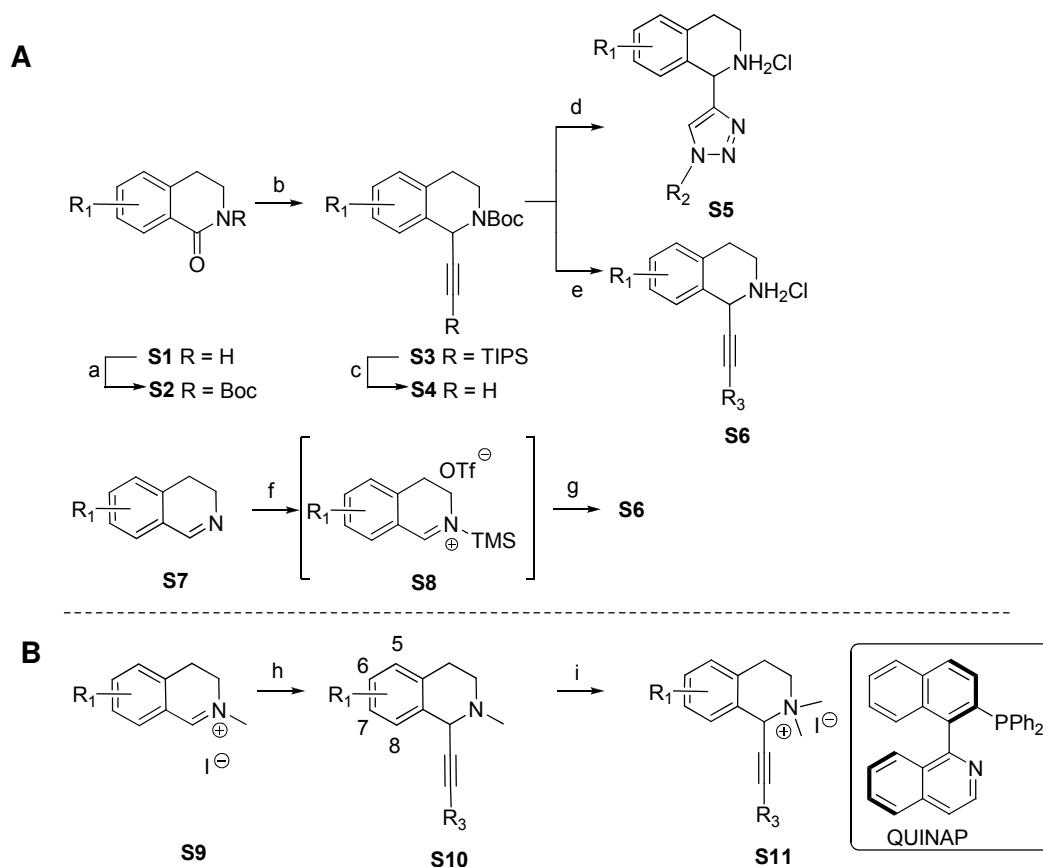


Figure 66: Parent natural compound noscapine (**21**) and outlined collection of alkynylated tetrahydroisoquinolines (THIQs). The THIQ core is highlighted in red.

The synthesis of secondary THIQs **S5** and **S6** (A, **Scheme 1**) started from various phenylethylamines that were cyclized to result in the corresponding lactams (**S1**). After Boc-protection these lactams (**S2**) were alkynylated using boron acetylides in a one-pot protocol. On the basis of the fully protected THIQ core **S3** various modifications were possible. Library generations however, focused on triazole derivatives generated by click chemistry (**S5**) and diverse alkynylated THIQs available *via* Sonogashira coupling (**S6**). As the one-pot alkynylation reaction proved to be challenging, especially for electron rich dimethoxy lactams, an alternative approach

via the alkylation of TMS-triflate precipitated imines (**S8**) was developed. In most cases this approach resulted in enhanced yields for the synthesis of electron rich alkynylated THIQs. Together with the lactam alkylation a very efficient methodology platform was established in order to access numerous secondary THIQs, that are challenging to obtain otherwise.

A sub-library of tertiary and quaternary THIQs (B, **Scheme 1**) was synthesised by derivatization of substituted 2-methyl-3,4-dihydroisoquinolinium iodides (**S9**). Besides synthetic compounds, the natural product cotarnine **23** ($R^1 = 6,7\text{-OCH}_2\text{O}$, 8-OMe) was used. To this end, diverse alkynes were deprotonated with $i\text{PrMgCl}$ and added to the iminium ion to yield *N*-methylated analogues **S10** which were additionally converted into quaternary ammonium salts **S11** (**Scheme 1**).



Scheme 1: Synthesis of a focused library of alkynylated tetrahydroisoquinolines. A) Synthesis of secondary THIQs. a) 1. NaH or DMAP/ Et_3N ; 2. Boc_2O , 57-89%; b) 1. TIPS-acetylene, $n\text{-BuLi}$, $\text{BF}_3 \cdot \text{Et}_2\text{O}$, -78°C , 2. DIBAL-H, 17-73%; c) TBAF, THF, 0°C , 86-88%; d) $\text{Pd}(\text{PPh}_3)_4$, CuI, Et_3N , THF, RT, R_2I , then HCl/MeOH, 15-95%; e) CuSO_4 , Na-ascorbate, EtOH/ H_2O , R^2N_3 , then HCl/MeOH, 54-75%. f) TMS-OTf, THF, 0°C , 2h. g) $i\text{PrMgCl}$, R^3 -alkyne, THF, 0°C , 31-90%. B) Synthesis of tertiary and quaternary THIQs. h) $i\text{PrMgCl}$, R^3 -alkyne, THF, 0°C , 13-99% or $\text{CuBr}/\text{QUINAP}$, R^3 -alkyne, Et_3N , CH_2Cl_2 , -55°C , i) MeI, acetonitrile, 99%. DMAP = 4-dimethylaminopyridine, Boc_2O = di-*tert*-butyl dicarbonate, TIPS = triisopropylsilyl, $n\text{-BuLi}$ = *n*-Butyllithium, DIBAL-H = diisobutylaluminium hydride, TBAF = tetrabutylammonium fluoride, TMS = trimethylsilyl, OTf = triflate.

In order to obtain enantiomerically pure, or highly enantio-enriched analogues, further investigations concentrated on CuBr-catalysed enantioselective alkynylation reactions of iminium salts (**S9**). Extensive ligand screening efforts led to a very efficient method (CuBr/QUINAP) giving high *ee* and almost quantitative yields. The absolute stereochemistry of the obtained alkynylated THIQs could be assigned in analogy to reports published by Taylor and Schreiber (Org. Lett. **2006**, 8, 143-146).

A library of 103 THIQ derivatives was screened for phenotypic changes associated with microtubule cytoskeleton and mitotic arrest in BSC-1 and HeLa cells. Several compounds induced phenotypic changes, such as accumulation of round-shaped cells with condensed DNA, which is indicative of mitotic arrest (**Figure 67**). Quite interestingly, only compounds closely related to the natural product noscapine were identified. In contrast to noscapine that contains two stereocenters, the identified compounds comprised only one stereocenter with the same (*R*)-stereochemistry at the carbon in the α position to the nitrogen. Compounds being more potent than noscapine were obtained, e.g. (*R*)-**109**. As new microtubule inhibitors due to tumor resistance are in urgent need, these structurally related, simplified small molecules could be of great interest.

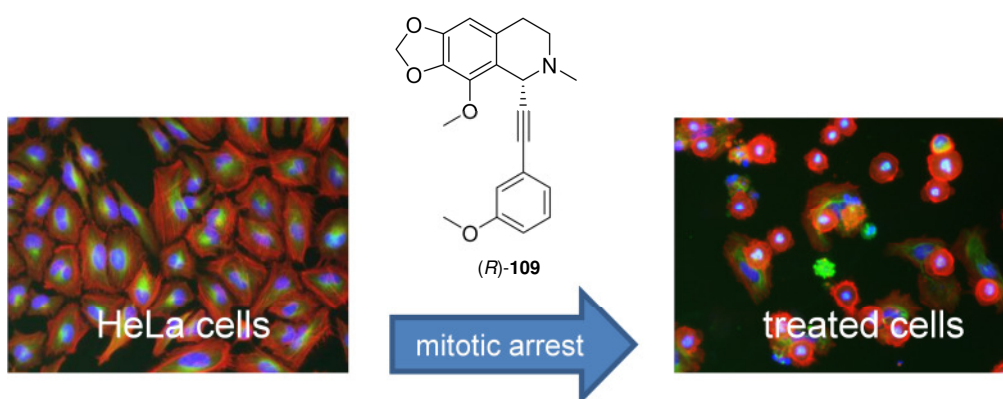


Figure 67: Schematic representation of cell-based phenotypic screening. Human cancer cells (HeLa cells) were incubated with alkynylated THIQs and checked for phenotypic changes like mitotic arrest.

Small molecule microarray screening as tool in chemical biology

Screening is a systematic test procedure to identify certain properties of the test objects. In the context of chemical biology, screening experiments are performed to investigate the perturbation of whole cells, cellular networks or isolated biochemical assay systems by small molecules of synthetic or natural origin. Ultimately, the interplay of a specific small molecule probe with a protein is analysed. Over the years Osada *et al.* (RIKEN Advanced Science Institute, Japan) have developed various techniques for the direct study of ligand-protein interactions by immobilizing small molecules. After incubation of proteins with immobilized probes and subsequent washing, the proteins with high binding affinity for the corresponding small molecule probes "stick" to the surface. In the case of the small molecule microarrays on glass arrays, bound protein is detected with antibodies or fluorescent markers. If surface plasmon resonance (SPR) is used to detect the protein bound to a SPR-chip, the change of the total reflection angle of polarized light on a gold surface is recorded. However, small molecule microarray binders do not necessarily yield enzyme inhibitors, as only the binding is detected with this method.

For the preparation of such microarrays, high-precision automated spotting robots are used to produce spots with the diameters of about 100 μm on the glass slides. The main feature of the microarray technology is the highly efficient and fast data analysis, as thousands of compounds can be spotted on a single glass slide. The key feature of the small molecule microarray technology is the functional group independent immobilization. In a classical approach, the functional groups that allow for chemical immobilization without affecting the protein-ligand interaction need to be introduced into the small molecule probe. This usually requires elaborate structure-activity relationship studies. Osada *et al.* developed an immobilization strategy where glass or gold surfaces were coated with photo-activatable molecules that generate carbenes upon UV-irradiation. The resulting statistical immobilization renders chemical modification of probes unnecessary. Even complex natural products can be immobilized using this protocol (B, **Figure 68**).

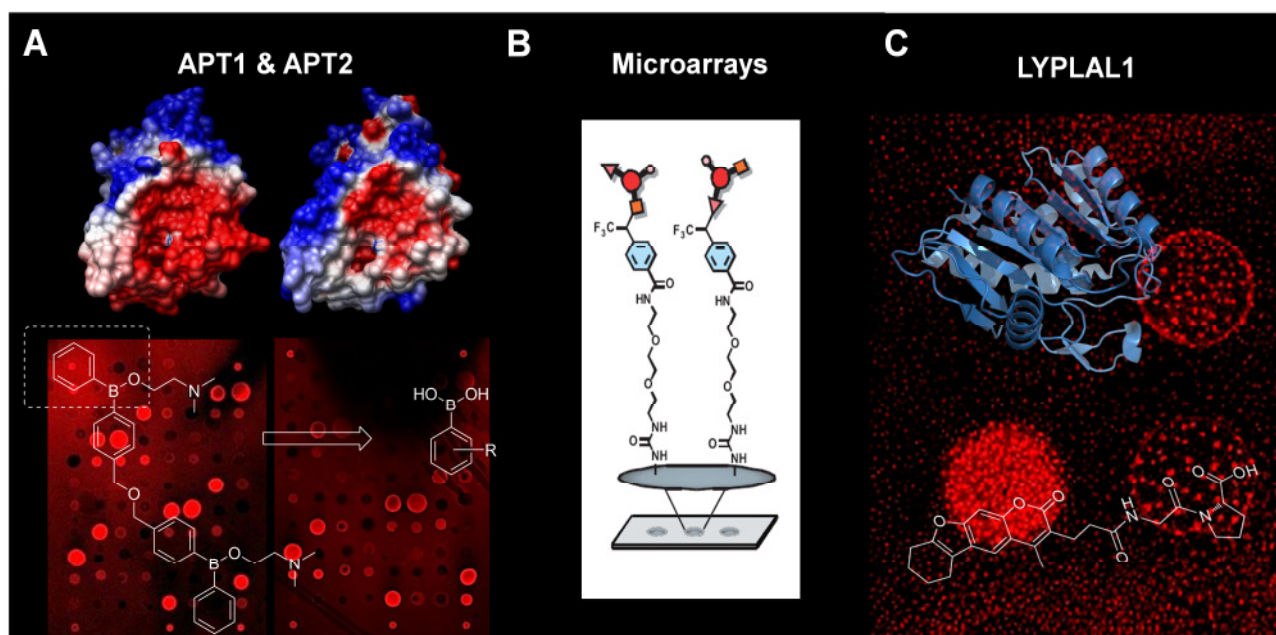


Figure 68: Schematic representation of small molecule microarray technology. A) Crystal structure of human APT1 and 2. Background: binding profile for both proteins, proteins binding to small molecule array were visualized using a fluorescently labelled antibody. Foreground: borinic acid microarray binder and derived boronate esters. B) Representation of small molecules immobilized on glass array. C) LYPLAL1 crystal structure. Background: binding profile. Foreground: small molecule LYPLAL1 inhibitor.

Three proteins with high sequence and structure match were selected as the target proteins for evaluation of the microarray screening technology. Acyl protein thioesterase 1 (APT1), APT2 and lysophospholipase-like 1 (LYPLAL1) protein are part of the α/β hydrolase family. APT1 was identified as the key protein in the control of the Ras-cycle, a dynamic de- and repalmitoylation cycle that is responsible for the correct localization and function of this oncogene. The inhibition of APT1 is regarded as a new strategy for the treatment of cancers caused by Ras mutations. The isoenzyme APT2 was recently identified by pull-down experiments using known covalent APT1 β -lactone inhibitors and its biological functions remain unclear. Despite the fact that APT2 is closely related to LYPLAL1 and APT1, not much is known about this protein. However, various recent literature reports suggest its involvement in obesity. Using a library of immobilized small molecules from the RIKEN institute (NPDepo), all three proteins could be fingerprinted, generating binding profiles for the three related proteins (A and C, **Figure 68**). As already implicated by the sequence and structural homology of APT1 and APT2, a virtually identical binding profile was observed. However, these profiles differed significantly from the binding profile of LYPLAL1.

For APT1 and APT2, borinic acids and boronate esters could be identified as the high-affinity binders and potent inhibitors in a functional enzymatic assay (A, **Figure 68**). Lineweaver-Burk analysis showed a competitive inhibition of both enzymes, which suggests a coordination of the

boron atom to the serine within the active site. Inspired by the activity of boron-containing substances, simple phenylboronic acids were tested for their inhibitory potency and nanomolar, non-toxic and cell-permeable inhibitors, particularly of APT2, were indentified. Co-crystallization of inhibitors with APT1 or APT2 were not successful, as both proteins crystallised as dimers. The search for a crystallographic model system led to the yeast APT1 that crystallised as a monomer. The high sequence homology with human APT1 and its capability to depalmitoylate N-Ras renders yeast APT1 a suitable crystallographic model system. Subsequently, several boronic acids were co-crystallised with yeast APT1 and showed the expected binding to the serine residue of the catalytic triad.

In order to validate the LYPLAL1 array binders, a functional enzymatic assay had to be developed. Based on a thorough analysis of the crystal structure, several substrates were tested. In contrast to APT1 and APT2, LYPLAL1 did not tolerate long hydrophobic substrates and, contrary to the literature speculations, LYPLAL1 did not exhibit detectable phospholipase activity. A study using 4-nitrophenyl esters of different chain length as substrates, showed the preference for short chain length. The functional enzyme assay could confirm microarray binders as the first known LYPLAL1 inhibitors (C, **Figure 68**).

VIII Zusammenfassung

Die vorliegende Arbeit beschäftigt sich mit zwei Grundpfeilern der chemischen Biologie: Mit der Synthese- und Methodenentwicklung zur Synthese einer Substanzkollektion auf Basis des Tetrahydroisochinolin-Grundgerüsts sowie mit der Anwendung von Mikroarrays mit immobilisierten niedermolekularen Sonden als Werkzeug zum Auffinden von hoch-affinen Ligand-Protein-Wechselwirkungen.

BIOS einer Substanzkollektion auf Basis des Tetrahydroisochinolin-Grundgerüsts

Unter Anwendung der Prinzipien der Biologie-orientierten Synthese wurde eine Substanzbibliothek von alkinilierten Tetrahydroisochinolinen (THIQs) dargestellt. Diese Substanz-Kollektion basiert auf dem biologisch prävalidierten Grundgerüst der Tetrahydroisochinoline, das ein häufig in Naturstoffen anzutreffendes Motiv ist. Inspiriert durch das natürlich vorkommende Tetrahydroisochinolin Noscapin (**21**), das besonders durch seine niedrige Toxizität kombiniert mit seiner Fähigkeit Krebszellen durch die Störung der Mikrotubulidynamik in den Zelltod zu führen attraktiv erscheint, wurde eine Substanzkollektion unter Beibehaltung des Noscapin-THIQ-Grundgerüsts und Variation der Substituenten in α -Position des Stickstoffs erstellt (**Abbildung 1**).

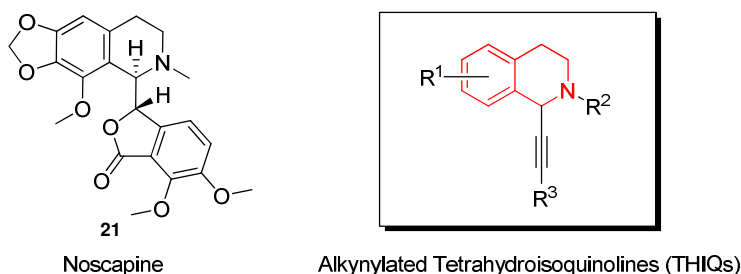
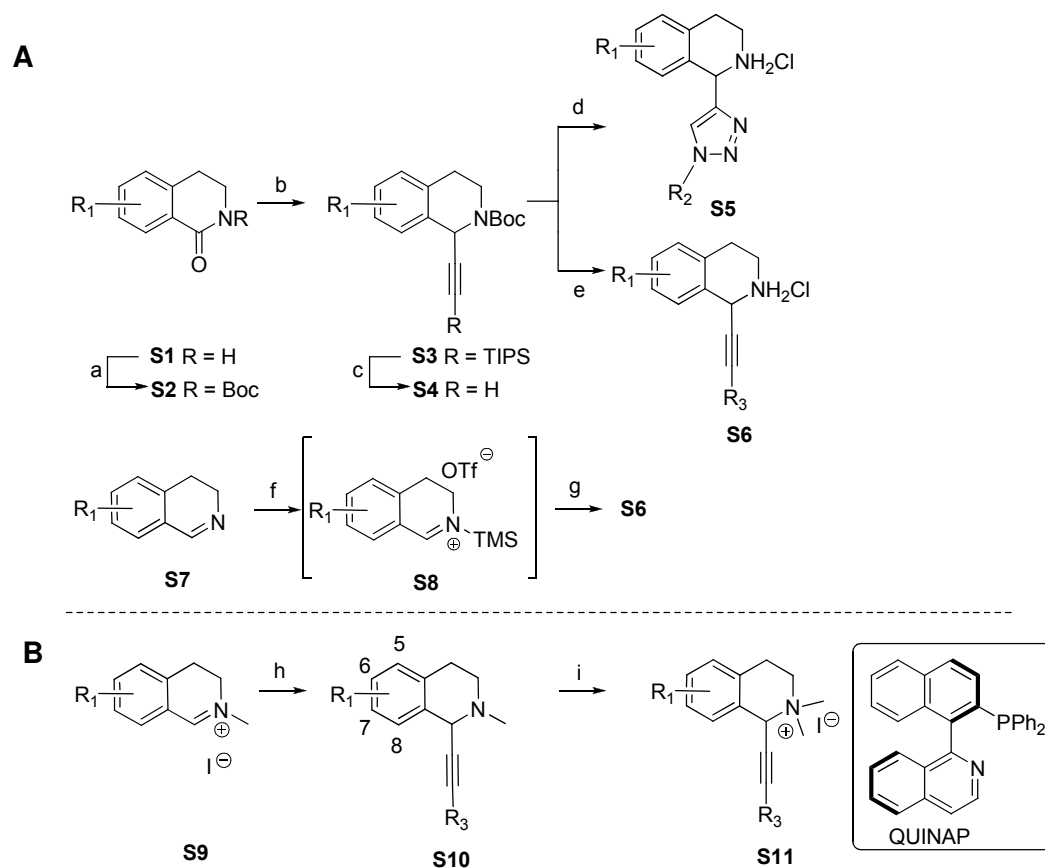


Abbildung 1: Naturstoff Noscapin (**21**) und synthetisierte Substanzkollektion alkinilierter Tetrahydroisochinoline (THIQs). Das THIQ-Grundgerüst ist in rot hervorgehoben.

Die Synthese der sekundären Tetrahydroisochinoline **S5** und **S6** (A, **Schema 1**) erfolgte ausgehend von verschiedenen Phenylethylaminen, die mittels Bischler-Napieralski-Cyclisierung zu den entsprechenden Lactamen (**S2**) umgesetzt wurden. Nach Boc-Schützung (**S2**) wurde eine Eintopf-Lactam-Alkinilierung unter Verwendung von Bor-Acetylen und anschließender Reduktion durchgeführt. Auf Basis des geschützten Tetrahydroisochinolin-Grundgerüsts **S4** waren zahlreiche Modifikationen möglich. Zur Diversifizierung der Substanzkollektion wurden zum einen Triazole mittels Click-Chemie (**S5**) synthetisiert und zum anderen diverse alkinilierte Tetrahydroisochinoline unter Verwendung der Sonogashira-Kupplung (**S6**) hergestellt. Da die Eintopf-Alkinilierung für

elektronenreiche Dimethoxylactame nur in niedrigen Ausbeuten funktionierte, wurde ein zweiter Zugang durch die Alkinilierung von mit TMS-Triflat ausgefällten Iminen (**S8**) entwickelt. In den meisten Fällen konnten über diese Route höhere Ausbeuten bei der Synthese elektronenreicher Tetrahydroisochinoline erzielt werden. Zusammen mit der Lactam-Alkinilierung konnte so ein effizienter Zugang zu zahlreichen sekundären Tetrahydroisochinolininen geschaffen werden. Eine weitere Kollektion tertiärer und quaternärer Tetrahydroisochinoline (B, **Schema 1**) wurde mittels Derivatisierung substituierter 2-Methyl-3,4-dihydroisochinoliniumiodid (**S9**) synthetisiert. Neben synthetischen Iminiumsalze wurde auch das Naturstoffderivat Cotarnin **23** ($R^1 = 6,7\text{-OCH}_2\text{O}$, 8-OMe) verwendet. Um *N*-methylierte Analoga **S10** zu erhalten, wurden diverse Alkine nach Deprotonierung mit *i*PrMgCl zu dem entsprechenden Iminiumsalz gegeben. Eine Quaternisierung erfolgte anschließend über die Reaktion mit Methyljodid (**S11**).



Schema 1: Synthese einer Substanzkollektion alkinilierter Tetrahydroisochinoline. **A)** Synthese sekundärer Tetrahydroisochinoline. a) 1. NaH oder DMAP/Et₃N; 2. Boc₂O, 57-89%; b) 1. TIPS-Acetylen, *n*-BuLi, BF₃·Et₂O, -78 °C, 2. DIBAL-H, 17-73%; c) TBAF, THF, 0 °C, 86-88%; d) Pd(PPh₃)₄, CuI, Et₃N, THF, RT, R₂I, dann HCl/MeOH, 15-95%; e) CuSO₄, Na-Ascorbat, EtOH/H₂O, R²N₃, dann HCl/MeOH, 54-75%. f) TMS-OTf, THF, 0 °C, 2h. g) *i*PrMgCl, R³-Alkin, THF, 0 °C, 31-90%. **B)** Synthese tertiärer und quaternärer Tetrahydroisochinoline. h) *i*PrMgCl, R³-Alkin, THF, 0 °C, 13-99% oder CuBr/QUINAP, R³-Alkin, Et₃N, CH₂Cl₂, -55 °C, i) MeI, Acetonitril, 99%. DMAP = 4-Dimethylaminopyridin, Boc₂O = di-*tert*-Butyldicarbonat, TIPS = Triisopropylsilyl, *n*-BuLi = *n*-Butyllithium, DIBAL-H = Diisobutylaluminiumhydrid, TBAF = Tetrabutylammoniumfluorid, TMS = Trimethylsilyl, OTf = Triflat.

Um enantiomerenreine Tetrahydroisochinoline zu erhalten, wurde eine kupferkatalysierte enantioselektive Alkinilierungsreaktion von Iminiumsalzen (**S9**) untersucht. Nach intensivem Liganden-Screening konnte mit CuBr/QUINAP eine sehr gute Alkinilierungsmethode gefunden werden, die mit hohen Ausbeuten und ee's funktioniert. Die absolute Konfiguration der alkinilierten Tetrahydroisochinoline konnte in Analogie zu den Publikationen von Taylor und Schreiber bestimmt werden (Org. Lett. **2006**, 8, 143-146).

Die Substanzkolektion von 103 Tetrahydroisochinolin-Derivaten wurde auf phänotypische Änderungen in BSC-1 und HeLa-Zelllinien getestet. Alkinilierte Tetrahydroisochinoline zeigten eine sehr effektive Hemmung der Tubulinpolymerisation und verursachten Apoptose in HeLa-Zellen (**Abbildung 2**). Interessanterweise konnten ausschließlich mit Noscaphin verwandte Strukturen als Hits identifiziert werden. Während Noscaphin über zwei Stereozentren verfügt, wiesen die aktiven Substanzen lediglich ein Stereozentrum mit gleicher (*R*)-Konfiguration wie im Naturstoff in der α -Position zum Stickstoff auf. Letztlich konnte ein Tetrahydroisochinolinderivat (*R*)-**109** identifiziert werden, das sowohl *in vitro* als auch *in vivo* stärker die Tubulin-Polymerisation inhibiert als der zugrunde liegende Naturstoff.

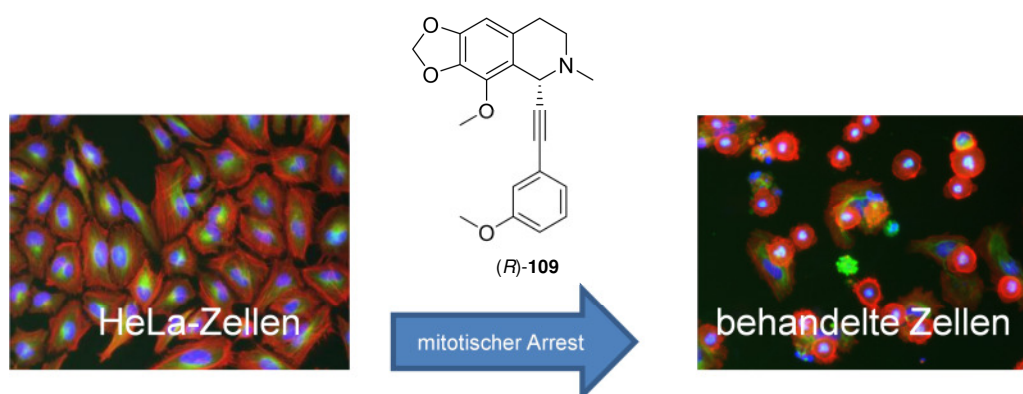


Abbildung 2: Schematische Darstellung des phänotypischen Screenings. Humane Krebszellen (HeLa) wurden mit alkinilierten Tetrahydroisochinolin-Derivaten inkubiert und auf phänotypische Änderungen hin untersucht.

Mikroarrays mit immobilisierten niedermolekularen Sonden als Werkzeuge in der chemischen Biologie

In der chemischen Biologie werden Screeningverfahren angewendet, um die Beeinflussung von ganzen Zellen, Zellverbänden oder isolierten biochemischen Testsystemen durch niedermolekulare Sonden synthetischen oder natürlichen Ursprungs zu untersuchen. Letztlich werden so die Wechselwirkungen einer bestimmten niedermolekularen Sonde mit einem Protein untersucht. Osada (RIKEN Advanced Science Institute, Japan) entwickelte über die Jahre verschiedene Techniken für die direkte Untersuchung dieser Ligand-Protein-Wechselwirkungen durch die Immobilisierung niedermolekularer Moleküle. Nach Inkubation von Proteinen mit immobilisierten Sonden und folgenden Waschvorgängen bleiben komplementäre Proteine mit hoher Bindungsaffinität an den entsprechenden Sonden „kleben“. Die Detektion von gebundenem Protein erfolgt bei Immobilisierung auf Glasoberflächen mit Antikörpern oder Fluoreszenzmarkern oder im Fall von Oberflächenplasmonenresonanz durch die Änderung des Totalreflexionswinkels von polarisiertem Licht an einer Goldoberfläche. Nicht zwangsläufig führen jedoch Protein-Binder auch zu Protein-Inhibitoren, da in dieser Methode keine Aussage über eine das Enzym hemmende Sonden-Protein-Wechselwirkung getroffen wird.

Zur Herstellung dieser Mikroarrays werden Hochpräzisions-Spotter eingesetzt, um Substanzen als Spots mit Durchmesser von ca. 100 µm auf Glasplatten aufzubringen. Hauptmerkmal dieser Mikroarraytechnologie ist die hocheffiziente und schnelle Datenanalyse. Einzigartig wird diese Methode durch die verwendete Immobilisierungstechnik. Klassischerweise müssen für das Anbringen funktioneller Gruppen, die eine chemische Immobilisierung ermöglichen ohne die Sonde-Protein Wechselwirkung zu beeinflussen, aufwändige Struktur-Aktivitätsbeziehungen durchgeführt werden. Die von Osada entwickelte Immobilisierungsmethode ist von funktionellen Gruppen unabhängig. Die Verwendung von beschichteten Glasplatten mit photoaktivierbaren Carbenen ermöglicht eine statistische Immobilisierung und macht folglich eine vorherige chemische Modifikation der Sonden unnötig. So können selbst komplexe Naturstoffe auf Glas- oder Goldoberflächen immobilisiert werden (B, **Abbildung 3**).

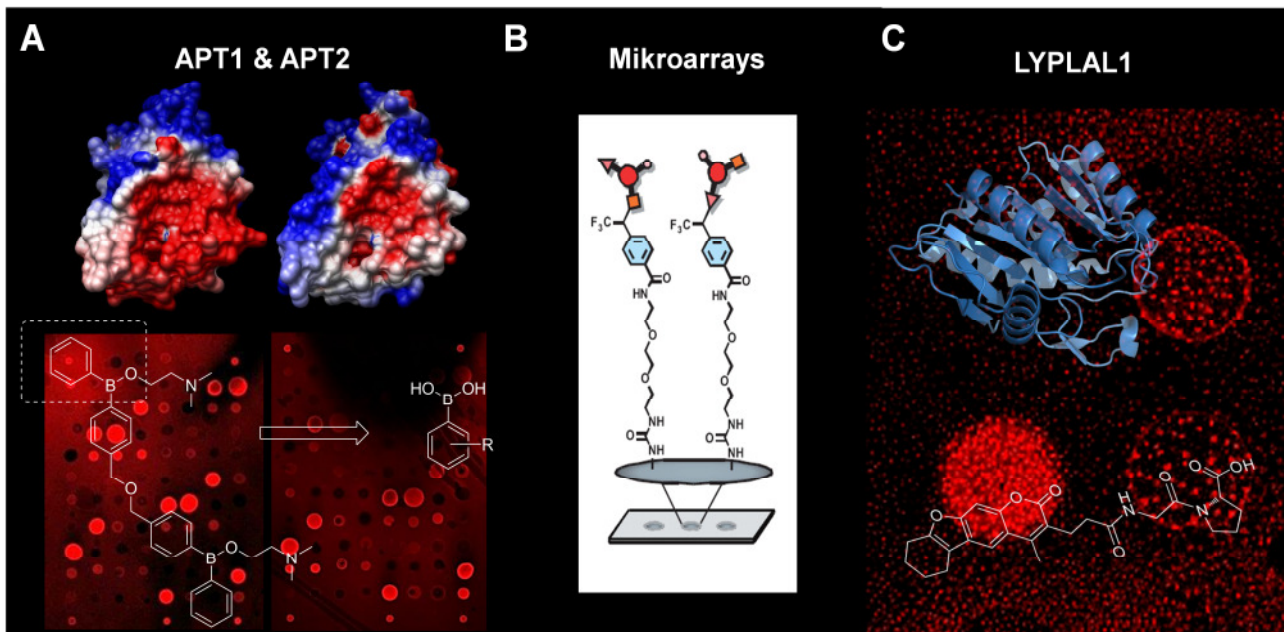


Abbildung 3: Schematische Darstellung des Mikroarray Screenings. A) Kristallstrukturen von humanem APT1 und 2. Hintergrund: Bindeprofil für beide Proteine. Proteine die an immobilisierte Sonden binden wurden mittels fluoreszenzmarkierten Antikörpern sichtbar gemacht. Vordergrund: Borinatester- und abgeleitete Boronsäure-Mikroarraybinder. B) Darstellung eines Mikroarrays mit immobilisierten niedermolekularen Sonden. C) Kristallstruktur von humanem LYPLAL1. Hintergrund: Bindeprofil. Vordergrund: Identifizierter LYPLAL1-Inhibitor.

Als Zielproteine für die Evaluierung des Mikroarrayscreenings wurden drei Proteine mit hoher Sequenz- und Strukturübereinstimmung gewählt. Acyl protein thioesterase 1 (APT1), APT2 und Lysophospholipase-like 1 (LYPLAL1) Protein sind Teil der α/β -Hydrolase Familie. APT1 wurde als wesentliches Protein bei der Steuerung des Ras-Zyklus identifiziert, eines dynamischen De- und Repalmitoylierungskreislaufes, der für die korrekte Lokalisierung und Funktion dieses Onkogens verantwortlich ist. Die Inhibition von APT1 wird als neue Strategie zur Behandlung von durch Ras-Mutationen verursachten Krebsarten angesehen. Erst kürzlich wurde durch Pulldown-Experimente mit als APT1 bekannten kovalenten β -Laktoninhibitoren APT2 als Isoenzym identifiziert. Dessen biologische Funktion ist jedoch noch weitgehend unklar. Über LYPLAL1 ist trotz großer Verwandtschaft zu APT1 außer zahlreichen Hinweisen über eine Beteiligung an Fettleibigkeit ebenfalls nichts bekannt. Durch Mikroarray-Screeningexperimente mit der Substanzbibliothek des RIKEN Instituts (NPDepo) konnte ein „chemischer Fingerabdruck“ mit charakteristischen Bindeprofilen für die drei verwandten Proteine erzeugt werden (A und C, **Abbildung 3**). Wie bereits Sequenz- und Strukturhomologie von APT1 und APT2 nahelegten, wurde auch ein nahezu identisches Bindeprofil festgestellt. Deutlich davon unterschied sich jedoch das Profil von LYPLAL1.

Für APT1 und APT2 konnten Borinsäuren bzw. Borinatester im Mikroarray als hochaffine Proteinbinder und in einem funktionalen enzymatischen Assay als potente Inhibitoren identifiziert werden (A, **Abbildung 3**). Mittels Lineweaver-Burk Analyse konnte eine kompetitive Inhibition der beiden Enzyme gezeigt werden, die eine Koordination des Boratoms an das Serin der aktiven Tasche nahelegt. Inspiriert durch die Aktivität der borhaltigen Substanzen, wurden einfache Phenylboronsäuren auf ihre Inhibitionseigenschaft hin überprüft. Tatsächlich konnten insbesondere für APT2 Inhibitoren im nanomolaren Bereich gefunden werden, die sowohl nicht toxisch als auch zellgängig waren. Kokristallisationen mit APT1 oder APT2 Inhibitoren waren nicht erfolgreich, da beide Proteine als Dimer kristallisierten. Die Suche nach einem kristallographischen Modellsystem führte schließlich zum als Monomer kristallisierenden APT1 aus Hefe, das hohe Sequenzhomologie mit humanem APT1 aufweist und ebenso in der Lage ist N-Ras zu depalmitoylieren. Einige Boronsäuren konnten kristallisiert werden und zeigten die erwartete Bindung an das Serin der katalytischen Triade.

Für LYPLAL1 musste zuerst ein funktioneller Assay entwickelt werden, um die identifizierten Mikroarray-Binder zu validieren. Basierend auf einer genauen Analyse der Kristallstruktur wurden zahlreiche Substrate getestet. Im Gegensatz zu APT1 und APT2 setzt LYPLAL1 keine langen, hydrophoben Substrate um und entgegen den in der Literatur geäußerten Vermutungen ist LYPLAL1 auch keine Phospholipase. Eine Studie mit 4-Nitrophenylestern unterschiedlicher Kettenlänge zeigte die Bevorzugung kurzer Substrate. Im funktionalen Enzymassay konnten Mikroarray-Binder als Inhibitoren von LYPLAL1 identifiziert werden (C, **Abbildung 3**).

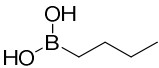
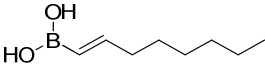
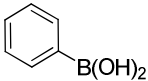
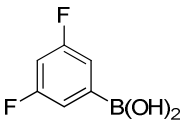
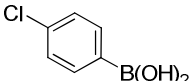
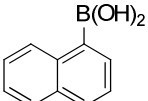
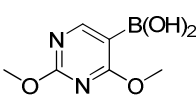
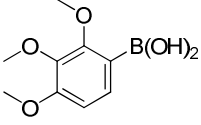
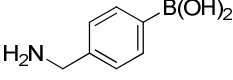
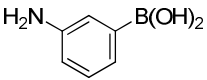
IX Appendix

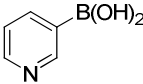
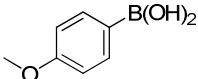
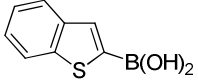
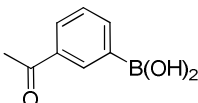
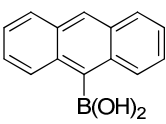
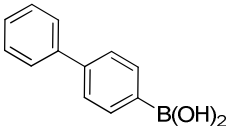
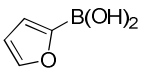
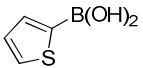
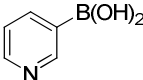
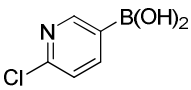
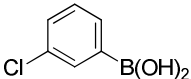
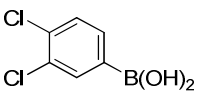
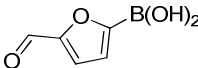
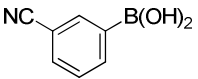
Boronic acids

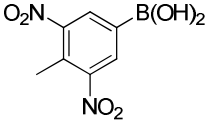
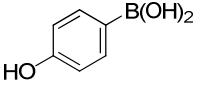
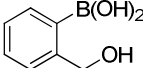
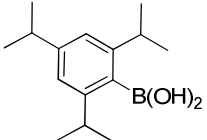
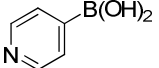
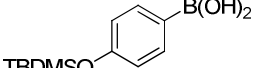
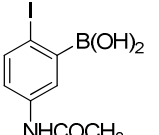
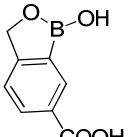
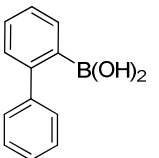
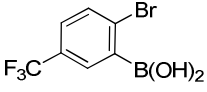
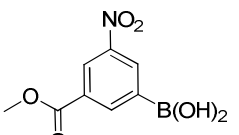
Boronic acids are of commercial and synthetic origin (kindly provided by Prof. Dr. Dennis Hall).

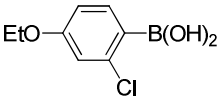
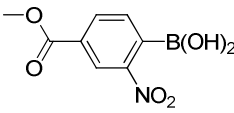
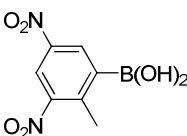
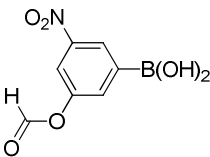
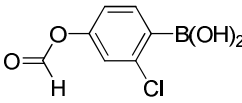
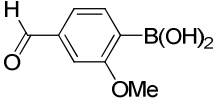
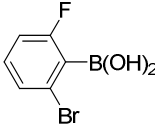
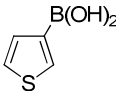
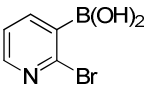
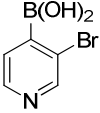
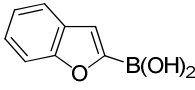
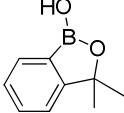
For APT1 IC_{50} values were determined for compounds showing more than 80% inhibition at 50 μ M.

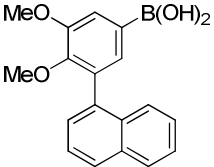
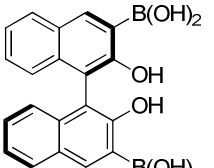
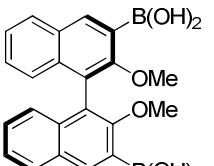
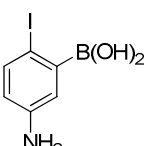
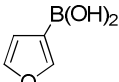
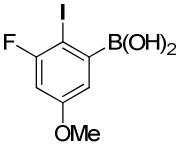
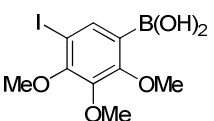
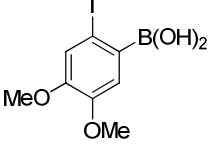
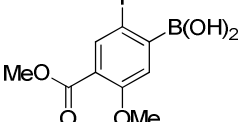
For APT2 IC_{50} values were determined for compounds showing more than 99% inhibition at 50 μ M.

Cpd	ID	Structure	IC_{50} [μ M] APT1	IC_{50} [μ M] APT2
248	BA01		> 50	> 50
249	BA02		> 50	n. d.
250	BA03		14.7 ± 1.6	25.1 ± 1.41
190	BA04		0.51 ± 0.03	1.97 ± 0.10
251	BA05		4.6 ± 0.4	4.18 ± 0.77
252	BA06		> 50	n. d.
253	BA07		> 50	n. d.
254	BA08		> 50	> 50
255	BA09		n. d.	n. d.
256	BA10		n. d.	n. d.

Cpd	ID	Structure	IC ₅₀ [μM] APT1	IC ₅₀ [μM] APT2
257	BA11		> 50	n. d.
258	BA12		> 50	n. d.
259	BA13		2.3 ± 0.1	0.529 ± 0.133
260	BA14		3.9 ± 1.0	2.87 ± 0.63
261	BA15		> 50	n. d.
262	BA16		16.9 ± 1.5	3.55 ± 0.40
263	BA18		> 50	n. d.
264	BA19		> 50	n. d.
265	BA20		> 50	n. d.
266	BA21		17.2 ± 1.9	n. d.
191	BA22		1.4 ± 0.1	0.418 ± 0.013
192	BA23		1.1 ± 0.2	0.138 ± 0.013
267	BA24		n. d.	n. d.
268	BA25		> 50	> 50

Cpd	ID	Structure	IC ₅₀ [μM] APT1	IC ₅₀ [μM] APT2
269	BA26		> 50	n. d.
270	BA27		> 50	n. d.
271	BA28		> 50	> 50
272	BA29		> 50	> 50
273	BA30		n. d.	n. d.
274	BA31		> 50	n. d.
275	BA33		n. d.	n. d.
276	BA34		> 50	> 50
277	BA35		> 50	> 50
278	BA36		6.3 ± 0.5	2.16 ± 0.17
279	BA37		3.7 ± 0.4	2.95 ± 0.15

Cpd	ID	Structure	IC ₅₀ [μM] APT1	IC ₅₀ [μM] APT2
280	BA38		25.0 ± 2.1	n. d.
281	BA39		> 50	n. d.
282	BA40		> 50	n. d.
283	BA41		> 50	n. d.
284	BA42		> 50	> 50
285	BA43		n. d.	n. d.
286	BA44		> 50	n. d.
287	BA45		n. d.	n. d.
288	BA46		n. d.	n. d.
289	BA47		> 50	n. d.
290	BA49		13.5 ± 1.4	11.3 ± 4.0
291	BA50		> 50	> 50

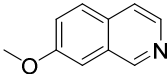
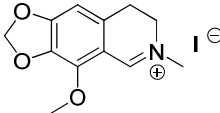
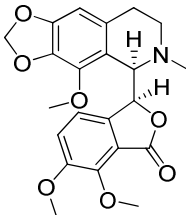
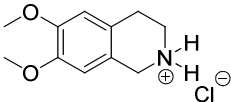
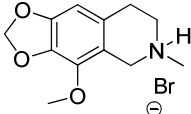
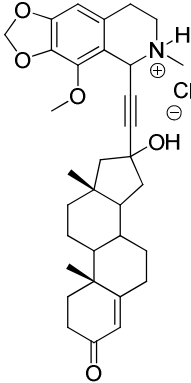
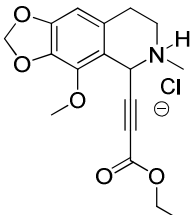
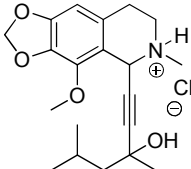
Cpd	ID	Structure	IC ₅₀ [μM] APT1	IC ₅₀ [μM] APT2
292	BA51		> 50	n. d.
293	BA52		> 50	> 50
294	BA53		> 50	n. d.
295	BA54		> 50	n. d.
296	BA55		> 50	> 50
297	BA56		16.9 ± 1.5	n. d.
298	BA57		> 50	n. d.
299	BA58		> 50	n. d.
300	BA59		n. d.	n. d.

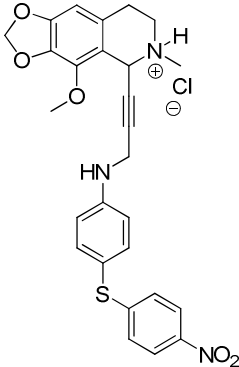
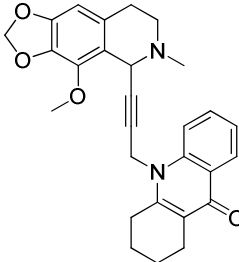
Cpd	ID	Structure	IC ₅₀ [μM] APT1	IC ₅₀ [μM] APT2
301	BA60		> 50	n. d.
302	BA61		> 50	> 50
303	BA62		10.2 ± 1.0	1.98 ± 0.09
304	BA63		> 50	n. d.
305	BA64		> 50	> 50
306	BA65		22.6 ± 2.6	n. d.
307	BA66		> 50	n. d.
308	BA68		> 50	> 50
309	BA69		> 50	> 50
310	BA70		> 50	n. d.

Cpd	ID	Structure	IC ₅₀ [μM] APT1	IC ₅₀ [μM] APT2
311	BA71		n. d.	n. d.
312	BA72		> 50	> 50
313	BA73		n. d.	n. d.
314	BA74		3.2 ± 0.2	0.238 ± 0.025
315	BA75		n. d.	n. d.
316	BA76		n. d.	> 50
317	BA77		> 50	> 50

Commercial THIQs and Derivatives

Cpd	ID	Structure
318	6,7-Dihydroxy-3,4-dihydroisoquinoline (DDIQ)	
319	7-Hydroxy-6-methoxy-3,4-dihydroisoquinoline (7-HDIQ)	
320	6,7-Dimethoxyisoquinoline (6,7-DIQ)	

321	7-Monomethoxyisoquinoline (7-MIQ)	
23	Cotarnine	
21	Noscapine	
162	6,7-Dimethoxy-1,2,3,4-tetrahydroisoquinolinium chloride (DHTHIQ)	
322	MIC1501014	
323	IBS_STOCK1N-30368	
324	IBS_STOCK1N-31232	
325	IBS_STOCK1N-31719	

326	IBS_STOCK1N-32001	 <p>The chemical structure of IBS_STOCK1N-32001 consists of a 2,3-dihydrobenzofuran core. The benzene ring of the core is substituted with a methoxy group (-OCH₃) at the 6-position and a propargyl group (-C≡CH) at the 4-position. The nitrogen atom of the dihydrofuran ring is protonated (N⁺-H) and is associated with a chloride counterion (Cl⁻). The propargyl group is further substituted with a secondary amine (-NH-) which is connected to a para-substituted phenyl ring. This phenyl ring is in turn connected via a sulfur atom to another para-substituted phenyl ring, which bears a nitro group (-NO₂) at the para position.</p>
327	IBS_STOCK1N-40298	 <p>The chemical structure of IBS_STOCK1N-40298 features a 2,3-dihydrobenzofuran core. The benzene ring of the core is substituted with a methoxy group (-OCH₃) at the 6-position and a propargyl group (-C≡CH) at the 4-position. The nitrogen atom of the dihydrofuran ring is substituted with a methyl group (-CH₃). The propargyl group is substituted with a nitrogen atom that is part of a bicyclic system. This nitrogen is bonded to a cyclohexane ring and a benzene ring. The benzene ring is substituted with a carbonyl group (-C(=O)-) at the ortho position relative to the nitrogen.</p>

X Curriculum Vitae

NAME Tobias Joachim Zimmermann
DATE OF BIRTH 05/02/1983
PLACE OF BIRTH Riedlingen/Württemberg

EDUCATION

07/2008 – present **Doktoral Studies**
Max Planck Institute of Molecular Physiology, Dortmund
Supervisor: Prof. Dr. H. Waldmann

08/2010 – 11/2010 **Research Visit**
RIKEN Advanced Science Institute, Tokyo, Japan
Supervisor: Prof. Dr. H. Osada

10/2007 – 03/2008 **Diploma Thesis**
University of Tuebingen/University of Oxford, UK
Supervisor: Prof. Dr. M. Maier

07/2005 – 01/2006 **Visiting Student & Researcher**
University of Melbourne, Australia

10/2003 – 03/2008 **Undergraduate & Graduate Studies, Chemistry**
University of Tuebingen

07/1994 – 07/2002 **High School Diploma**
Kreisgymnasium Riedlingen

SCHOLARSHIPS

07/2008 – present **Doctoral studies:**

- International Max-Planck Research School in Chemical Biology
- Kekulé-Scholarship, Fonds der Chemischen Industrie e.V.

10/2007 – 03/2008 **Diploma thesis:**
Bayer Science & Education Foundation (research scholarship Oxford)

10/2003 – 03/2008 **Undergraduate & Graduate Studies:**

- German National Academic Foundation
- Fonds der Chemischen Industrie e.V.

PUBLICATIONS

M. Burger*, **T. J. Zimmermann***, Y. Kondoh, P. Stege, N. Watanabe, H. Osada, H. Waldmann, I. R. Vetter, "Crystal structure of the predicted phospholipase LYPLAL1 reveals unexpected functional plasticity in spite of close relationship to acyl protein thioesterases" *J. Lipid. Res.* **2012**, *53*, 43-50. *equal contribution.

M. Rusch, **T. J. Zimmermann**, M. Bürger, F. J. Dekker, K. Görmer, G. Triola, A. Brockmeyer, P. Janning, T. Böttcher, S. A. Sieber, I. R. Vetter, C. Hedberg, H. Waldmann, "Identification of Acyl Protein Thioesterases 1 and 2 as the Cellular Targets of the Ras-Signalling Modulators Palmostatin B and M" *Angew. Chem. Int. Ed.* **2011**, *50*, 9838-9842.

S. Mocklinghoff, W. A. L. van Otterlo, R. Rose, S. Fuchs, **T. J. Zimmermann**, S. M. Dominguez, H. Waldmann, C. Ottmann, L. Brunsveld, "Design and Evaluation of Fragment-Like Estrogen Receptor Tetrahydroisoquinoline Ligands from a Scaffold-Detection Approach" *J. Med. Chem.* **2011**, *54*, 2005-2011.

W. Wilk*, **T. J. Zimmermann***, M. Kaiser, H. Waldmann, "Principles, Implementation, and Application of Biology-Oriented Synthesis (BIOS)" *Biol. Chem.* **2010**, *391*, 491-497. *equal contribution.

T. J. Zimmermann, F. H. Niesen, E. S. Pilka, S. Knapp, U. Oppermann, M. E. Maier, "Discovery of a Potent and Selective Inhibitor for Human Carbonyl Reductase 1 from Propionate Scanning Applied to the Macrolide Zearalenone" *Bioorg. Med. Chem.* **2009**, *17*, 530-536.

J. L. Xie, B. F. Abrahams, **T. J. Zimmermann**, A. Mukherjee, A. G. Wedd, "Ferrocene Mono- and Di-Sulfonates as Building Blocks in Hydrogen-Bonded Networks" *Aust. J. Chem.* **2007**, *60*, 578-582.